UNIVERSITY OF LIVERPOOL

DIABETES AND OBESITY: EVIDENCE FOR A CARDIOMYOPATHY

Thesis submitted in accordance with the requirements of the University of Liverpool by

Reza Ashrafi

August 2016

Abstract

Introduction: Obesity and type 2 diabetes are leading causes of cardiovascular morbidity and mortality most commonly through accelerated atherosclerotic disease. Researchers have recognised clearly that there is a cardiac pathological process that is over and beyond any damage secondary to accelerated atherosclerosis or associated hypertension. There has been much research into the histological, genetic and functional changes that may underpin these specific processes; these demonstrate structural hypertrophic and fibrotic changes accompanied by changes in energy metabolism, nervous control, contractile performance and electrical conduction. To date, there is very little in the way of comparative study between animal diabetes and obesity models or of cardiac gene expression in the human type 2 diabetes phenotype, which in many individuals comprises both diabetes and obesity.

Aim: To investigate cardiac genetic expression of proteins and ion channels in obesity and diabetes to identify changes underpinning the pathological processes and to characterise features common to both conditions, specifically features that may affect contractile performance and secondly, changes that may lead to increased arrhythmogenesis.

Methods: A streptozocin rat model of type 1 diabetes was compared with a high fat diet rat model of obesity and finally a human group with type 2 diabetes to understand the gene expression changes in the left ventricle characterising the obesity and diabetic cardiomyopathy. Gene expression of left ventricle tissue was measured using qPCR and compared to a control group; followed by mathematical modelling to predict changes in the cardiac action potential. This was used to investigate specific changes to each condition and common changes between the groups to identify if there was a common genotype and action potential phenotype.

In addition, echocardiography, the standard ECG and the signal averaged ECG were used to assess the human study group for early signs of cardiac dysfunction related to diabetes.

Results: All three groups had gene expression changes likely to lead to action potential prolongation and higher rates of arrhythmias, with ERG (Human Ether Related a Go-Go) mRNA reduced in all 3 study groups responsible for $I_{K,r}$. AP modelling, suggested that the likely functional change of the gene expression alterations would be to cause AP prolongation and in the human study, early-after depolarizations at the endocardial level.

As part of the confirmatory process for one of the more unexpected gene changes, up-regulation in HCN4 gene expression in the obese rats was associated with a significant increase in HCN4 protein immunofluorescence in the ventricles.

In addition, the human type 2 diabetes group had evidence of reduced ventricular contractile function, atrial changes and strain rate changes suggestive of myocardial fibrosis. No significant alterations were noted in the signal averaged ECG between groups but as has been seen in other studies, QT prolongation was found in the type 2 diabetes group.

Conclusion: Diabetes and obesity lead to changes in cardiac gene expression that when modelled will prolong the action potential, possibly as a compensatory mechanism to maintain contractile function at the expense of an arrhythmogenic phenotype.

Acknowledgements

I would like to thank my supervisors on this project for all their help and advice, Professor John Wilding, Dr Gershan Davis and Professor George Hart.

I would also like to thank Professor Mark Boyett, who despite me not being one of his students, allowed me free use of the laboratory in the University of Manchester and provided invaluable advice and help at every turn.

My thanks to Dr Lucy Pickavance and Dr Marianne Yon at the University of Liverpool for providing the animals for the obesity part of my study and Dr Natalie Gardiner at the University of Manchester for providing animals for the STZ experiment.

At the laboratory in Manchester, my thanks go to Dr Yanni-Gerges for instruction in all the experimental techniques used in this study.

I would also like to acknowledge the work of Professor Henngui Zhang and Dr Kun Jian, who very kindly performed the mathematical AP modelling calculations and AP curve generation quoted in this study.

Finally, my thanks to the surgical team at Liverpool Heart and Chest hospital, Mr Pullan, Mr Oo, Mr Modi, Mr Kuduvalli and most importantly the patients.

List of Figures

19. Expression of mRNA for intracellular Ca^{2+} handling proteins in the left ventricle of the control and STZ groups for each section of the myocardium
20. Expression of mRNA for Cl^- channels, ATPases and Cx43 in the left ventricle of the control and STZ groups for each section of the myocardium
21. Cardiac energy production gene expression in the left ventricle of the control and STZ groups for each section of the myocardium
22. Cardiac neuronal gene expression in the left ventricle of the control and STZ groups for each section of the myocardium
23. Expression of mRNA for major ion channels active during the action potential in the left ventricle of the control and HFD groups
24. Expression of mRNA for major ion channels active during diastole in the left ventricle of the control and HFD group
25. Expression of mRNA for major Ca2+-handling molecules in the left ventricle of the control and HFD groups
26. Expression of mRNA for Cl- channels, α-subunits of the Na^+-K^+ pump and the gap junction Cx43 in the left ventricle of the control and HFD groups
27. Expression of mRNA for important cardiac energy production genes in the left ventricle of the control and HFD groups
28. Expression of mRNA for major Ca^{2+} handling molecules in the left ventricle of the control and HFD groups.
29. Immunofluorescent Expression of HCN4 protein in the left ventricle of the control and HFD groups
30. Simulated rat ventricular endocardial and epicardial action potentials and underlying ionic currents and intracellular Ca^{2+} concentration in control and HFD groups
31. Simulated rat ventricular endocardial and epicardial action potentials in control and HFD groups with each of the remodelled ion channels/ionic currents modified singularly
32. Measurements from the signal averaged ECG for the diabetes and control groups
33. Intra- and inter-observer variability of standard echocardiographic measurements

34. Inter- and intra-observer variability of speckle derived longitudinal and circumferential stain
35. Atrial function assessed using echocardiography
36. Bland-Altman comparison of longitudinal and circumferential strain using TVI and speckle tracking
37. 2D Speckle derived measurements of strain in the longitudinal, circumferential and radial vectors
38. Expression of mRNA for major ion channels active during the action potential in the left ventricle of the control and diabetes groups
39. Expression of mRNA for major ion channels active during diastole in the left ventricle of the control and diabetes groups
40. Expression of mRNA for cardiac Ca^{2+} handling proteins in the left ventricle of the control and diabetes groups
41. Expression of mRNA for Cl^- channels, α-subunits of the Na^+-K^+ pump and the gap junctions Cx43/Cx40 in the left ventricle of the control and diabetes groups
42. Expression of mRNA for important cardiac energy production genes in the left ventricle of the control and diabetes groups
43. Expression of mRNA for important cardiac neuronal genes in the left ventricle of the control and diabetes groups
44. Simulated human ventricular endocardial and epicardial action potentials and underlying ionic currents and intracellular Ca^{2+} concentration in control and diabetes groups
45. Simulated human ventricular endocardial and epicardial action potentials in control and diabetes groups with each of the remodelled ion channels/ionic currents modified singularly

List of Tables

Abbreviations

ACEi-Angiotensin Converting Enzyme Inhibitor	**iNOS**-Inducible Nitric Oxide Synthetase
ACh-Acetylcholine	**IRS**-Insulin Receptor Substrate-1
AF-Atrial Fibrillation	**JAK2**-Janus Kinase 2
AGEs-Advanced Glycosylation End Products	**K^+**-Potassium
AKT-Protein Kinase B	**LA**-Left Atrium
ANO1-Anoctamin 1	**LAEI**-Left Atrial Expansion Index
ANOVA-Analysis of Variance	**LAPEF**-Left Atrial Passive Emptying Fraction
AP-Action Potential	**LAAEF**-Left Atrial Active Emptying Fraction
APD-Action Potential Duration	**L-DOPA**-L-3,4-dihydroxyphenylalanine
ADP-Adenosine Diphosphate	**LV**-Left Ventricle
ATP-Adenosine Triphosphate	**LVH**-Left Ventricular Hypertrophy
ARB-Angiotensin Receptor II blocker	**MIBG**-Metaiodobenzylguanidine
BA-Bland-Altman	**Mitral E**-Mitral Early Diastolic Velocity
BEST 1-3-Bestrophin 1-3	**Mitral E**-Mitral Late Diastolic Velocity
BMI-Body Mass Index	**Mitral e'**- Mitral annular early diastolic velocity
BRDU-5-bromo-2-deoxyuridine	**M-Mode**-Motion Modulation
bSA-Bovine Serum Albumin	**mRNA**-Messenger RNA
BSA-Body Surface Area	**MRI**-Magnetic Resonance Imaging
Ca^{2+}-Calcium	**MT-ATP-6+8**-Mitochondrially Encoded ATP Synthase 6 + 8
CACNA1 C+D-L-type Voltage-Gated Ca^{2+} Channels Alpha Subunits 1c + 1d	**mV02**-Myocardial Oxygen Consumption
CAN-Cardiac Autonomic Neuropathy	**Na^+**-Sodium
cDNA-Complementary DNA	**NADPH**-Nicotinamide Adenine Dinucleotide Phosphate
CI-Confidence Interval	**NOX1**-Nicotinamide Adenine Dinucleotide Phosphate Oxidase 1
Cl^--Chloride	**NCBI**-National centre for Biotechnology Information
CLCN 1-3-Cl^- Channel 1-3	**NCX1**-Na^+-Ca^{2+} Exchanger
CPT-I-Carnitine Palmitoyltransferase I	**NGF**-Nerve Growth factor
C_t-Threshold Cycle	**OCT**-Optimal Cutting Temperature Compound
DAD-Delayed After Depolarization	**qPCR**-Quantitative Polymerase Chain Reaction
DNA-Deoxyribonucleic Acid	**QTc**-Corrected QT interval
EAD-Early After Depolarization	**PBS**- Phosphate Buffered Saline
ECC-Excitation-Contraction Coupling	**PCR**-Polymerase Chain Reaction
ERG-Human Ether Related a Go-Go	**PCr**-Phosphocreatine

FA-Fatty Acid	**PI3K-**Phosphatidylinositol-3 kinase
FATP-Fatty Acid Transport Protein	**PKC-**Protein Kinase C
FFA-Free Fatty Acid	**PPARα-**Peroxisome Proliferator Activated Receptor-Alpha
FPS-Frames per Second	**RAAS-**Renin Angiotensin System
GJA 1+5-Gap Junction Alpha 1 + 5	**RAGEs-**Receptors of AGEs
GLUT-4-Glucose Transporter 4	**rHOA-**Ras Homolog Gene Family, Member A
Hb-Haemoglobin	**RNA-**Ribonucleic Acid
HCN1-4-Hyperpolarization Activated Cyclic Nucleotide-Gated K^+ Channel 1-4	**ROCK-**Rho-Associated Protein Kinase
ECG- Electrocardiogram	**ROI-**Region of Interest
ECHO-Echocardiogram	**ROS-**Reactive Oxygen Species
ERG-Human Ether Related a Go-Go	**RPM-**Revolutions per minute
HSD- Honestly Significant Difference	**RT-PCR-**Real Time Polymerase Chain Reaction
I_{Ca-L}-Long lasting Ca^{2+} Current	**RYR2-**Ryanodine 2
I_F - Funny Current	**SAECG-**Signal Averaged ECG
$I_{K'1}$-Inward K^+ Rectifying Current	**SCN5α-**Na^+ Channel, Voltage-Gated Type Vα
$I_{K,r}$-Rapid delayed K^+ Rectifying Current	**STAT3-** Signal transducer and activator of transcription 3
$I_{K,s}$-Slowly Activating K^+ Rectifying Current	**STI-**Speckle Tracking Imaging
$I_{K,ss}$-Ultrafast K^+ Rectifying Current	**STZ-**Strepotozocin
$I_{K,ACh}$-Inward K^+ Rectifying Current	**TGFβ-**Transforming Growth Factor β
$I_{K,r}$-Rapid delayed K^+ Rectifying Current	**TNFα-** Tumour Necrosis α
I_{Na}-Primary Na^+ Current	**TDR-**Transmural Dispersion of Repolarization
I_{NaCa}-Na^+/Ca^{2+} Exchanger current	**TTYH-1-3-**Tweety Homolog 1-3
I_{Na-L}-Late Na^+ Current	**TVI-**Tissue Doppler Imaging
$I_{to,\ f+s}$-Transient Outward Current- fast + slow	**UK-**United Kingdom
IF-Immunofluorescence	**WMSI-**Wall Motion Scoring Index

Contents

1. Introduction

Diabetes and obesity are two of the leading health challenges in medicine across the world and specifically in cardiovascular medicine. They remain contributing factors to atherosclerotic disease which remains the number one killer in the western world [1]. The prevalence of diabetes and obesity across the world has increased significantly over the years with some areas of the UK reporting a near 50% increase in diabetes prevalence over only a decade[2] with similar rapid rises reported in obesity defined as a body mass index (BMI) greater than 30kg/m^2[3].

These epidemiological changes have led people to look at the effects that diabetes and obesity have on the heart beyond the well-recognised pathophysiological processes associated with atherosclerosis and hypertension; increasingly a specific pathological process is recognised for each entity with some degree of overlap. In 1972, Rubler and co-workers first described a diabetic cardiomyopathy in 4 patients with diabetes presenting with clinical heart failure in the absence of hypertension, coronary or structural heart disease[4]. As a result of this and further work on cardiomyopathic process and heart failure symptoms in the presence of diabetes and obesity, most authors now define a diabetic or obesity related cardiomyopathy as:

Symptoms of heart failure or evidence of cardiac impairment in the presence respectively of diabetes or obesity without concomitant hypertension, structural or atherosclerotic heart disease[5].

This cardiomyopathy can present with impairment of contractile performance, arrhythmogenic complications or a combination of both.

Before advanced imaging and specialised laboratory testing, the cardiomyopathic effect of diabetes alone was illustrated by UK studies revealing an estimated prevalence of diabetes of 4.3 percent but a disproportionate prevalence of diabetes in people with congestive heart failure quoted at between 20 and 35 percent reflecting the earlier work in Framingham[6].

In Figure 1 shown below is a graph illustrating the prevalence of diabetes in several large scale unselected heart failure trials in both ischaemic and non-ischaemic heart failure

in the over 65s, which shows prevalence levels much higher than the prevalence in the general population.

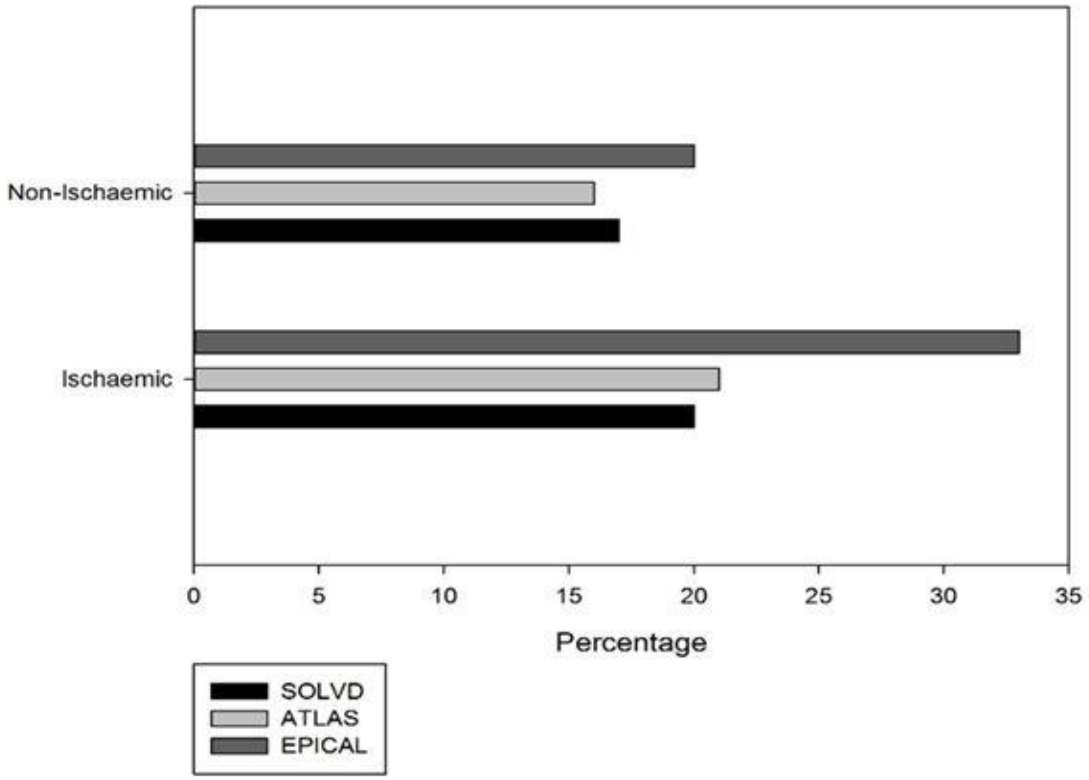

Figure 1: Prevalence of diabetes in patients in several large scale commercial drug trials for heart failure treatment showing a high percentage of patients with ischaemic and non-ischaemic heart failure drawn from Bauters et al.[7]

Similarly, with obese subjects, researchers noticed that the likelihood of developing heart failure was much higher even when adjusted for traditional risk factors such as smoking or age than in non-obese subjects as shown below in Figure 2[8].

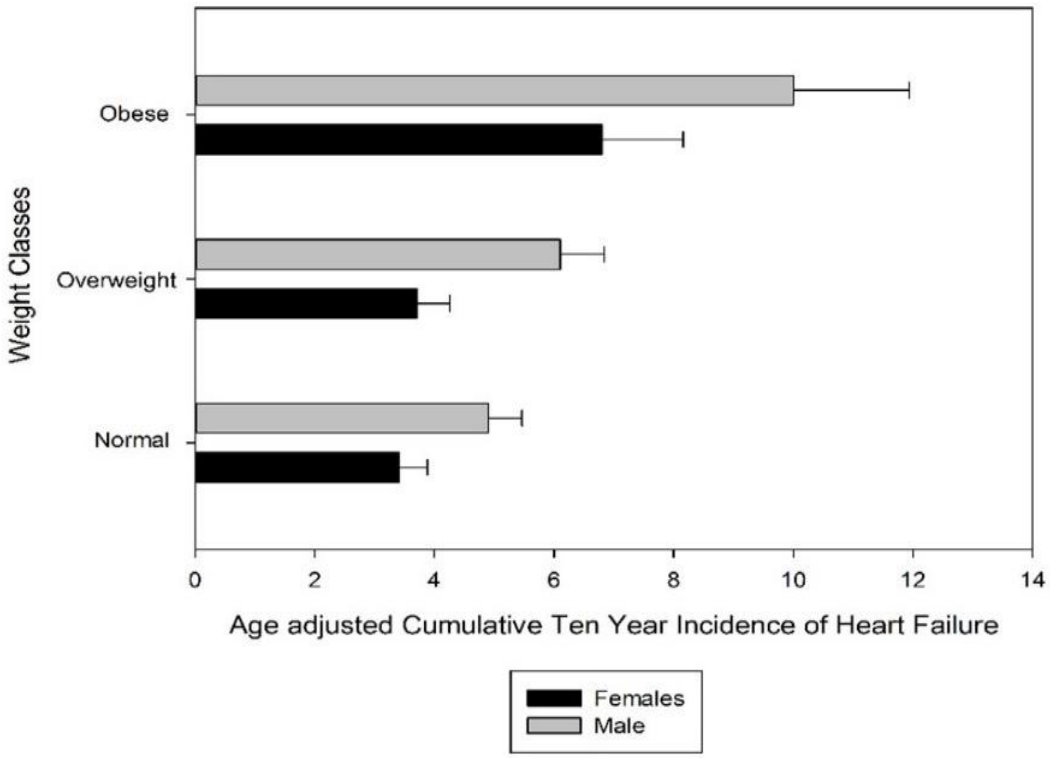

Figure 2: Age adjusted cumulative incidence of heart failure for increasing weight bands over 10 years showing a marked increase for obese individuals compared to normal weight controls drawn from Kenchaiah et al.[8]

What has become more evident in recent years is that as imaging has improved more people with diabetes and obesity have been found to have signs of cardiac dysfunction even at a preclinical/asymptomatic stage. The most common method of imaging the heart in routine clinical practice is echocardiography and in many departments the performance of the left ventricle (LV) as a pump is most commonly assessed and reported using the Simpson's biplane ejection fraction[9]. Using echocardiography, children with type 1 diabetes have been found to have subtle changes suggestive of cardiac impairment including impaired myocardial relaxation patterns, a phenomenon that was previously confirmed in adult diabetes studies in patients with heart failure clinically and a normal ventricular ejection fraction[10]. In obese patients similar subclinical changes can be seen in cardiac performance and can be picked up using more detailed imaging techniques and these

patients also are often found to have a normal ejection fraction[11]. These findings would suggest that obesity and diabetes affect cardiac function at least initially in a fairly subtle manner.

Once clinical heart failure symptoms occur even with a preserved ejection fraction as can be seen in many patients with diabetes and obesity there is a significant increase in mortality[12]. While contractile performance is a major area of concern for many clinicians the rate of cardiac rhythm disturbances as part of the cardiomyopathic process is increased in patients with diabetes[13, 14] and obesity[15] compared to matched controls.

This epidemiological evidence supports the hypothesis that there is a specific cardiomyopathic process in diabetes and obesity and the scale of the potential problem merits further assessment.

Reviewed below is the current pathological understanding of the subject and a short summary of left ventricular structure and action potential organisation pertinent to this study.

1.1. Left ventricular structure

The left ventricle is not a homogenous structure from outer to inner or from base to apex and this is important whenever measurements are made of its function, tissue character or gene expression. From inner to outer, the left ventricle is made up of three distinct muscle layers, the endocardium, mid-myocardium and epicardium.

The endocardium has fibres that run longitudinally, the mid-myocardium as the largest layer has circumferential running fibres and the epicardium at 45 degrees to the myocardium running spirally[16]. The relationship of muscle fibres is shown in Figure 3 below:

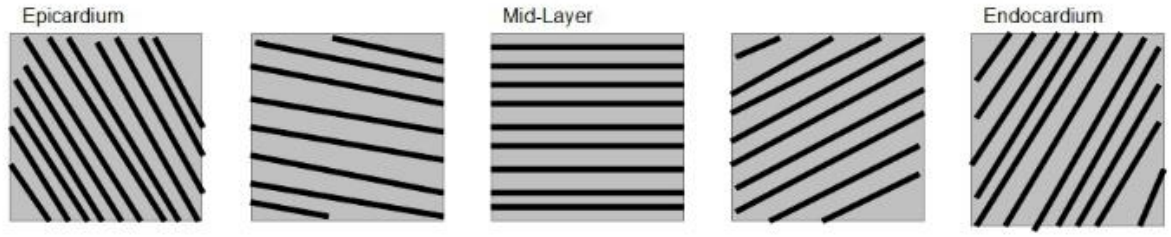

Figure 3: LV fibre orientation topographically from epicardium to endocardium, reflecting the changing orientation of fibres adaptive to changing mechanical and electrical stress drawn from Trew et al.[17]

This is important because as layers differ in orientation from epicardium to endocardium and also in terms of their location from apex to base, they experience differing amounts of mechanical strain. As a result, there are differences in the fibre properties and their metabolic actions and therefore the genes that encode for these properties.

Each of these layers contributes to myocardial performance but the mid-myocardium provides the largest amount of contractile force as the largest layer. The myocardium traditionally has been the easiest layer to assess echocardiographically as it is responsible for the classic lateral contraction picture seen in the apical 4-chamber view and is best represented using the Simpson's method.

1.2. Cardiac action potential

Generation of the action potential (AP), is caused by a change in the electrochemical gradient across the sarcolemma which occurs through conductance of ions through channels. These channels characteristically have α and β subunits, α subunits normally represent the pore element of the channel and the β subunits accessory structures. Movement of ions across the sarcolemma, can be passive or active but in the passive state, where the electrochemical gradient is responsible for generating ion movement, current amplitude is expressed as:

Current amplitude=membrane potential x channel conductivity[18]

Although for many channels in the body, this equation implies a linear relationship however for many cardiac channels conductivity is different at different membrane potentials, for example with the inward rectifier K^+ rectifying current, $I_{K,1}$ which generates an outward current at more negative membrane potentials[18]. Figure 4 summarises the movement in and out of the major ions involved in the cardiac ventricular action potential in humans.

The cardiac action potential has distinct phases, initially, at rest (phase 4) there is comparatively high intracellular K^+, maintaining a resting potential of approximately -96 mV. This state is maintained by the $I_{K,1}$ current and by an amount of constant active ion transport of Na^+/K^+ via ATPase driven active exchangers.

In response to a pacemaker stimulus, there is opening of the fast Na^+ channels and a massive influx of positive Na^+ ions, seen in the diagram below as phase 0, which is normally initiated by the depolarization of a nearby cell. $I_{Na,}$ the main cardiac Na^+ current responsible for phase 0, at normal negative phase 4 membrane potentials will be generated by the opening of all the $Na_v1.5$ channels at a conduction velocity of 1 m/s. The all-or-none principle of Na^+ channel opening does not apply in disease states and at a higher resting potential not all channels will be activated, potentially being arrhythmogenic[19]. As the membrane potential rises rapidly due to Na^+ influx, there is closure of the fast Na^+ channels and K^+ and Cl^- efflux (via the I_{to} current), leading to a small drop in voltage, seen as phase 1, classically in sub-epicardial cells. The I_{to} current, can be both a fast and slow current- $I_{to\text{-}F}$ or $I_{to\text{-}s}$ respectively and is generated by Ca^{2+}-dependent Cl^- channels and K^+ channels ($K_v4.3$- $I_{to\text{-}f}$,$K_v1.5$- $I_{to\text{-}s}$ and to some degree $K_v1.4$ $I_{to\text{-}s}$)[19].

Next, is the longest phase, the plateau phase where the L-type channels- $Ca_v1.2$ ($I_{Ca\text{-}L}$ current-which begin to open at -10mV (during phase 0) allowing initially a small influx of extracellular Ca^{2+} ions and due to voltage changes there is also an efflux of intracellular K^+ ions using the $I_{K,1,}$ I_{to} and $I_{K,r}$. In this phase the initially small amount Ca^{2+} ions influx which began in phase 0 increases and is balanced by K^+ via the channels mentioned above, which helps to create the long plateau in membrane voltage. This inward current of Ca^{2+} allows for

activation of sarcoplasmic Ca^{2+} channels (RYR2) which when activated allow for Ca^{2+} release and excitation and contraction coupling. In the background, due to the more positive membrane potential, the forward mode of $Na^{+}Ca^{2+}$ Exchanger (NCX1) is favoured with exit of Na^{+} for Ca^{2+} which helps to maintain the plateau phase, this current is termed the I_{NaCa} current.

Finally, there is repolarization, when the Ca^{2+} channels close and K^{+} rectifying channels stay open allowing exit of K^{+}, till the membrane potential reaches approximately -80mV at which point only the inward rectifying K^{+} channel stays open, keeping the intracellular K^{+} concentration constant (phase 3 then 4).

Important in this phase of repolarization, is the concept of equilibrium potential of K^{+}, which is calculated using the simplified Nernst equation, which is shown below for K^{+}:

$$-61.5 \log K^{+} \text{ intracellular} / K^{+} \text{ extracellular}$$

This gives an equilibrium potential of K^{+} of -96mV and this very negative equilibrium potential means that continuous K^{+} is required for a prolonged period to allow the cell to come back to a period of equilibrium prior to the next action potential and the separate K^{+} channels involved are discussed below.

In the mid-myocardium, K^{+} currents, can be broadly broken down in to two main groups; voltage gated ($I_{to,}$ $I_{K,ss}$ $I_{K,r}$ and $I_{K,s}$) and rectifying currents ($I_{K,1}$ and $I_{K,ACh}$). $I_{K,ss}$ $I_{K,r}$ and $I_{K,s}$ are slowly activating rectifying channels that are active during phases 2 and 4 of the AP and control repolarization. The $I_{K,r}$ current, created by the ERG channel, is a pivotal channel in the repolarization process being slowly activated and rapidly inactivated, beginning during initial depolarization but accelerating in phase 2 as the membrane potential drops, creating a large outward K^{+} current before closing quickly as K^{+} concentrations drop at the extracellular mouth of the channel. The next most important current in repolarization is $I_{K,s}$ which, as a slow rectifying current created by the K_vLQT1 channel, creates an outward K^{+} current but unlike ERG as the membrane potential becomes more negative, K_vLQT1 channels become inactivated slowly. $I_{K,s}$ has two important features that are different to the other voltage gated channels, firstly that its expression is markedly reduced in the mid-myocardial

layer giving rise to the prolonged APD in the mid-myocardial layer and it is increased at higher heart rates helping to shorten the APD as the heart rate increases. The last of the voltage gated currents considered here is $I_{K,ss}$ (also known as I_{Kur}) which is an ultrafast voltage gated K^+ rectifying current which is quickly activated but slowly inactivated and mainly found in the atria but has been shown in some studies to be found in the ventricle[20]. $I_{K,ACh}$ is a rectifying current that is activated by acetylcholine release from the vagal nerve and is best understood in terms of its role in the atria and conduction tissues where it helps regulate heart rate by shortening the action potential and delaying phase 4 depolarization, which causes firing of the sino-atrial node.

A summary of the cardiac ventricular AP and ion movement is shown below in Figure 4:

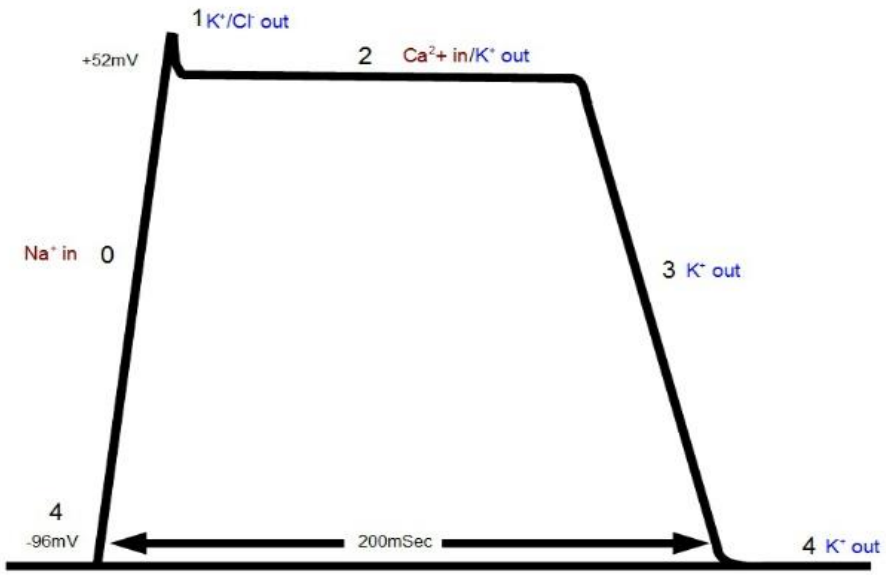

Figure 4: The cardiac ventricular action potential and major ion movements in/out

In addition to these main currents, there are several other proteins/currents that are important in the action potential of the ventricle. Firstly, is the role of gap junction proteins which help transmit depolarization from one cell to the next cell on in ordered and regulated manner and secondly, the hyperpolarization activated cyclic nucleotide-gated K^+ channels (HCNs) which primarily are responsible for phase 4 depolarization in the pacemaker regions of the heart. It does not occur in the normal ventricular myocyte AP, but

is important in the foetal/neo-natal phenotype[21] and generation of the I_F current. While HCNs are predominantly seen only in specialist pacemaker and conduction tissue in the heart, studies have shown that there is low level ventricular expression and especially in disease states may generate ectopic beats and higher resting heart rates[22].

As mechanical orientation changes spatially across the left ventricle, so does the cardiac electrical activity (pacemaker cells and specialist conduction cells are not considered here), which stimulates myocyte muscle contraction. Initial electrical depolarization begins in the endocardial layer and this charge spreads towards the epicardial layer before repolarization spreads in reverse through the wall before the next sequence. This is borne out in the fact, that the endocardial action potential duration (APD) is much longer than the epicaridal APD (shown below in Figure 5), so as to prevent re-excitation before the epicardium and mid-myocardium have repolarized and are ready for the next beat. This physiological development is protective as it acts to prevent re-excitation ventricular arrhythmias and is largely controlled through a transmural gradient in re-polarising potassium channels which control the rate of repolarization and thus action potential duration[23].

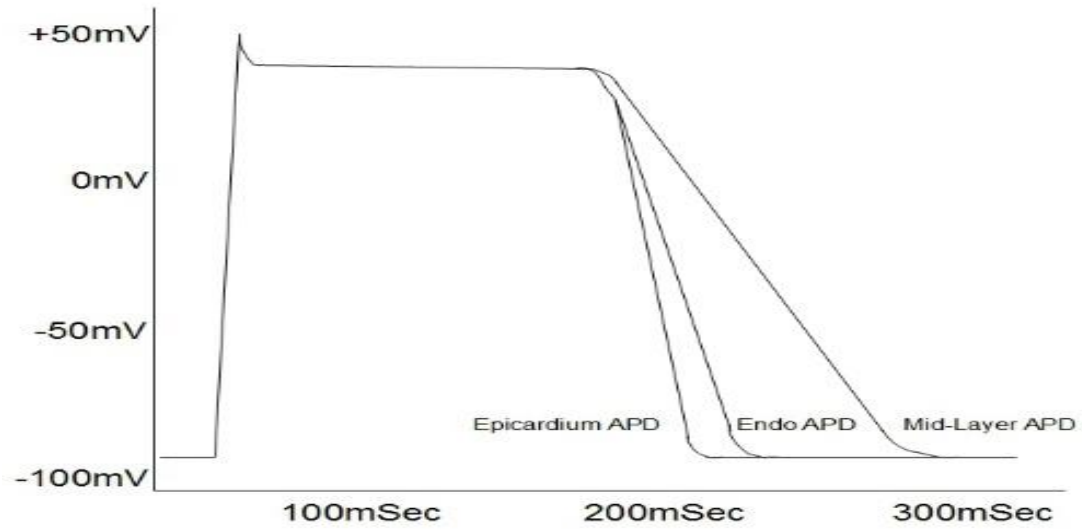

Figure 5: Illustrations of the comparative action potential duration of the left ventricle wall, showing the longest APD for the mid-myocardial layer drawn from Colli Franzone et al.[24]

Importantly when it comes to the generation of arrhythmias, is the principle of refractoriness, whereby the cell after being depolarized cannot then be depolarized a second time and this is due to closure of the $Na_v1.5$ channels, which is the principle depolarizing current in the human heart. This refractory period can either be absolute or relative, i.e. no depolarization at all possible or in the right circumstances depolarization is possible but does not occur normally. In the human ventricular myocyte, the absolute refractory period is from phase 1-2, due to Ca^{2+} influx and the relative refractory period is from late in phase 2 to phase 4.

The roles of the main ion channels in relation to the human ventricular AP are summarised below in Table 1:

Ion channel	**Current**	**Main AP phase of action**	**Ion movement**	**Physiological role**
$Na_v1.5$	I_{Na}	0	Na^+ influx	Cell depolarization
$K_v1.5$, $K_v1.4$, $K_v4.3$	I_{to}	1-2	K^+ efflux	K^+ efflux to balance Ca^{2+} influx and maintain plateau
$Ca_v1.2$	$I_{Ca\text{-}L}$	2	Ca^{2+} influx	Ca^{2+} influx to allow for excitation/contraction
K_vLQT1	$I_{K,s}$	2-4	K^+ efflux	Abbreviation of the plateau phase and repolarization
ERG	$I_{K,r}$	2-4	K^+ efflux	Abbreviation of the plateau phase and repolarization
$K_{ir}2.1$	$I_{K,1}$	4	K^+ efflux	Setting of the resting membrane potential

Table 1: A summary of the roles of the main ion channels in the human ventricular AP

1.3. The cardiac action potential: ion channels and arrhythmogenesis

Arrhythmia generation in the heart considered only at a ventricular level can be thought of as falling into two main categories, abnormal impulse formation and abnormal impulse conduction and then these two categories can be then further subdivided.

Firstly, abnormal impulse formation, which is broadly seen in clinical and scientific practice as either increased altered automaticity or triggered activity. Altered automaticity normally is most commonly seen in atrial or pacemaker cell generated arrhythmias but at a ventricular level is also important where abnormal foci may develop increased automaticity in settings with increased sympathetic stimulation, classically seen with VT in ischaemia/reperfusion[25].

The most important type of abnormal impulse formation from the perspective of this study, is that of triggered activity where an abnormal impulse is generated during or after an existing action potential that reaches a threshold potential causing an after-depolarization and a new AP. These can be either early- (EAD) or delayed after depolarization (DAD) depending on whether they occur in phase 2/3 or after repolarization is finished respectively, shown below in Figure 6:

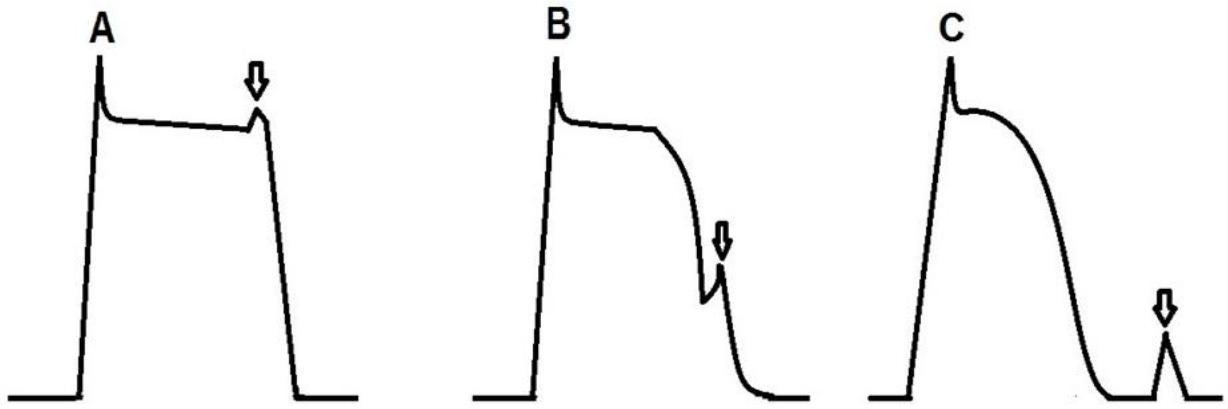

Figure 6: Ventricular AP's with arrowed depolarizations. **A**, an early after depolarization occurring late in phase 2, **B**, an early after depolarization occurring in phase 3 but before

the completion of repolarization and **C**, a delayed after depolarization in phase 4 with repolarization complete. Drawn from Gaztanaga et al.[26]

Firstly, the early after depolarization, this is caused predominantly by re-activation of the $I_{Ca\text{-}L}$ current which occurs during the end of phase 2, when there is AP repolarization and the membrane potential drops, $I_{Ca\text{-}L}$ can enter a window phase of 0 to-30mV (overlap between steady inactivation and activation) where the channel can re-open creating a new inward current and when large enough an EAD [23]. In normal circumstances during the end of phase 2 to phase 3 there is high K^+ conductance via $I_{K,r}$ and $I_{K,s}$ creating a high and fast outward current which repolarises and does not allow $I_{Ca\text{-}L}$ to self-amplify and create an EAD[27]. Multiple conditions exist where $I_{K,r}$ and $I_{K,s}$ may be reduced or have their function impaired including drug treatment with erythromycin, low Mg^{2+} levels and hypoxia. EADs tend also to be seen in bradycardic situations as the channels $I_{K,r}$ and $I_{K,s}$ are in more deeply closed states[27].

The second important current, involved in EAD formation is the I_{NaCa} current which helps to create EADs in tandem with $I_{Ca\text{-}L}$ by two main mechanisms, firstly when there is high and dyssynchronous Ca^{2+} release this stimulates NCX1s forward activity and generation of an inward current, prolonging the AP and allowing enough time for $I_{Ca\text{-}L}$ to reactivate which then increases Ca^{2+} forming a positive feedback loop and EADs. The second method, is conditions such as heart failure where there is increased NCX1 levels, as the AP repolarises, there is increased NCX1 forward activity and generation of a current to oppose outward repolarization, prolonging the AP, which may create enough time for $I_{Ca\text{-}L}$ to reactivate. Both mechanisms, lead to AP prolongation and are common in inherited channelopathies but the EAD can only form a clinical arrhythmia if the EAD can be transmitted to enough neighbouring myocytes to interrupt repolarization and form a waveform.

DADs predominantly occur as a result of oscillations in Ca^{2+} levels in late phase 3 or phase 4 predominantly thought by many groups to stem from an inability of the sarcoplasmic reticulum to store the Ca^{2+} which, when released in an oscillatory fashion can then stimulate NCX1 to create a late inward Na^{2+} current, I_{Ti} and this can then lead to a DAD and an abnormal AP. This situation can occur as a result of abnormalities in the ryanodine

receptor, which controls SR Ca^{2+} release, digoxin toxicity, catecholamine related arrhythmias and AP prolongation as it allows excess Ca^{2+} influx[28].

This study has focussed on the effects of obesity and diabetes and the experimental groups involved are not likely to have structural ventricular abnormalities likely to cause conduction block. This is an important point as when discussing arrhythmia generation secondary to abnormal impulse conduction, we are reviewing functional impulse conduction abnormalities due to alterations in current/channel function.

Abnormal impulse conduction occurs when heterogeneous expression of ion channels lead to conduction slowing or block allowing a waveform to return[29] or a unidirectional conduction block preventing waveform dissipation[23] which then can re-enter a non-depolarised area forming a circuit. This can be seen with loss of gap junction proteins and in Brugada syndrome with loss of I_{Na} particularly in the epicardium leading to late phase 2 re-entry[30].

After consideration of ionic generation of arrhythmias and based on the structure of the LV discussed earlier, it is important to note that there is a transmural gradient of ion channels. Specifically, a gradient from epicardium to endocardium exists predominantly of rectifying K^+ channels and if this fine balance is lost, there is increased conduction block and re-entrant arrhythmias[31]. Also, transmural heterogeneity, away from the normal smooth gradient may lead, in combination with normal beat to beat AP alternans, to an increase in arrhythmogenic potential as seen in animal models[32].

Much of what is known about the ion currents and channels discussed in this section comes from work on inherited cardiac conditions and a selection of the genes/currents and conditions are described below in Table 2:

Condition	Occurrence	Gene	Protein	Function	Current Change
Long QT 1	42-54%	KCNQ1	K_vLQT1	$I_{K,s}$ current	$I_{K,s}$ decrease
Long QT 2	35-45%	KCNH2	ERG	$I_{K,r}$ current	$I_{K,r}$ decrease
Long QT 3	<8%	SCN5A	Na_v1.5	I_{Na} current	I_{Na} decrease
Long QT 4	<1%	ANK2	Ankyrin-B	Adaptor	None
Long QT 5	<1%	KCNE1	MinK	B-subunit $I_{K,s}$	$I_{K,s}$ decrease
Long QT 6	<1%	KCNE2	MiRP1	B-subunit $I_{K,r}$	$I_{K,r}$ decrease
Long QT 7	<1%	KCNJ2	K_{ir}2.1	$I_{K,1}$ current	$I_{K,1}$ decrease
Long QT 8	<1%	CACNA1C	Ca_v1.2	$I_{Ca\text{-}L}$ current	$I_{Ca\text{-}L}$ increase
Short QT 1	Rare	KCNH2	ERG	$I_{K,r}$ current	$I_{K,r}$ increase
Short QT 2	Rare	KCNQ1	K_vLQT1	$I_{K,s}$ current	$I_{K,s}$ increase
Short QT 3	Rare	KCNJ2	K_{ir}2.1	$I_{K,1}$ current	$I_{K,1}$ increase
Brugada	10-30%	SCN5A	Na_v1.5	I_{Na} current	I_{Na} decrease
Brugada	<8.5%	CACNA1C	Ca_v1.2	$I_{Ca\text{-}L}$ current	$I_{Ca\text{-}L}$ decrease
Familial AF	Family linkage	KCNE3	MiRP2	B-subunit $I_{to\text{-}f}$	$I_{to\text{-}f}$ increase
Familial AF	Family linkage	KCNA5	K_v1.5	$I_{K,ss}$ current	$I_{K,ss}$ increase
Familial AF	Family linkage	KCNH2	ERG	$I_{K,r}$ current	$I_{K,r}$ increase
Familial AF	Family linkage	KCNH2	MiRP1	B-subunit $I_{K,r}$	$I_{K,r}$ increase
Familial AF	Family linkage	KCNQ1	K_vLQT1	$I_{K,s}$ current	$I_{K,s}$ increase
Familial AF	Family linkage	KCNJ2	K_{ir}2.1	$I_{K,1}$ current	$I_{K,1}$ increase

Table 2: A summary of inherited cardiac rhythm disorders and their gene and ion current basis drawn from Amin et al.[18]

Using this information and the earlier review of the AP phases a summary of AP phase and currents and the most common arrhythmia generation mechanisms is presented in Table 3[33]:

Arrhythmia mechanism	AP Phase	Channel	Current change
Reduced conduction propagation leading to functional block and re-entry	0	$Na_v1.5$	I_{Na} - decrease
Creation of a transmural repolarization gradient leading to triggered activity with phase 2 re-entry	1-2	$K_v1.5, K_v1.4, K_v4.3$	I_{to} - increase
Prolongation of the AP leading to triggered activity with EADs	2	$Na_v1.5$	I_{Na} - increase
		$Ca_v1.2$	$I_{Ca\text{-}L}$ - increase
		NCX1	I_{Ti} - increase
		ERG	$I_{K,r}$ - decrease
		K_vLQT1	$I_{K,s}$ - decrease
		$K_{ir}2.1$	$I_{K,1}$ - decrease
Prolongation of the AP leading to triggered activity with EADs	3	$Na_v1.5$	I_{Na} - increase
		$Ca_v1.2$NCX1	$I_{Ca\text{-}L}$ - increase
		ERG	I_{Ti} - increase
		K_vLQT1	$I_{K,r}$ - decrease
		$K_{ir}2.1$	$I_{K,s}$ - decrease
			$I_{K,1}$ - decrease
Prolongation of the AP leading to Ca^{2+} oscillation and triggered activity with DADs	4	NCX1	I_{Ti} -increase
		RYR2	SR Ca^{2+} increase
		$K_{ir}2.1$	$I_{K,1}$ - decrease
Resting membrane potential hyperpolarisation and increased automaticity	4	$K_{ir}2.1$	$I_{K,1}$ - increase

Table 3: A summary of the major mechanisms of arrhythmia generation by phase of the AP and channel/current

1.4. The action potential: ion channels and heart failure

Effective organisation of the action potential and its transmural variation is important for co-ordinated electro-mechanical activation and therefore good contractile pump function and relaxation from apex to base and from endocardium to epicardium. The key step in the excitation-contraction coupling (ECC) pathway, is during phase 2 (plateau phase), where the intracellular flow of Ca^{2+} (down a high gradient) leads to Ca^{2+} induced Ca^{2+} release from the sarcoplasmic reticulum. Free Ca^{2+} released from the sarcoplasmic reticulum via RYR2 binds to troponin C which then changes then shape of the entire troponin complex removing troponin I from the myosin head binding site on actin filaments. The exposed myosin head can then in ATP dependent be used to pull the actin filament in a linear fashion, shortening the sarcomere shortening. This procedure is repeated across multiple filaments all shortening leading to cardiac contraction. As the phase 2 of the AP ends and Ca^{2+} influx drops, SERCA2A pumps Ca^{2+} back into the sarcoplasmic reticulum and there is an overall reduction in cytosolic Ca^{2+} which leads to Ca^{2+} being removed from troponin C and the inactivated state is gradually returned to with the myosin binding site being covered by troponin I. The excitation-contraction coupling pathway is summarised in Figure 7 below:

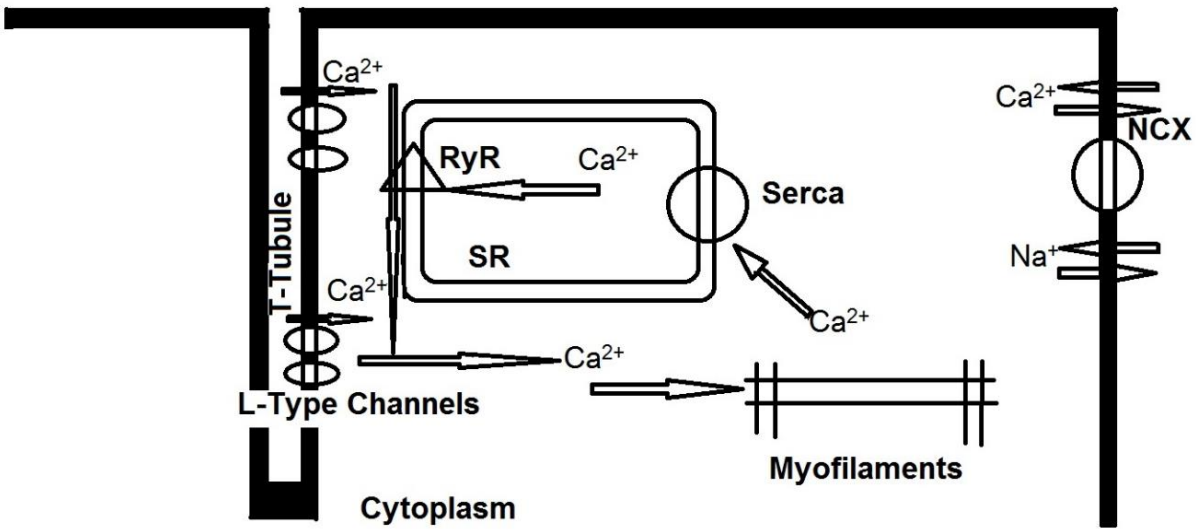

Figure 7: Ca^{2+} handling and contraction in the cardiomyocyte drawn from Andersson and Marks[34]

There are three key changes in the action potential shape in heart failure linked to reduced excitation-contractile performance and they are:

1. Increased phase 0, fast upstroke, amplitude
2. Reduced or absent phase 1, notch, early repolarization
3. Prolongation of the action potential[35]

The first two problems appear to be mainly due to a reduction in outward rectifying K^+ channels, I_{to}[36] while prolongation of the action potential mainly seems to involve reduced inward rectifying channel density and altered function, such as a reduction in $I_{K,1}$[37].

In terms of direct contractile performance, the main problem seems to stem from impairment of the Ca^{2+} induced Ca^{2+} release and hence, impairment of troponin binding and contraction. In the early stages of myopathic or hypertrophic processes it seems that prolongation of the action potential maybe an early adaptive response with reduced I_{to} function enhancing Ca^{2+} entry and reducing Ca^{2+} extrusion[38]. While this may result in a positively inotropic phenotype early on, this does lead to a change in gene expression before there is a maladaptive response and eventually reduced expression of Ca^{2+} entry handling proteins and enzymes[39].

Once the compensatory phase is passed, heart failure and reduced excitation-contraction coupling mediated by Ca^{2+} release occurs through 4 main actions: reduced sarcoplasmic Ca^{2+} release[40], functional defects in the L type Ca^{2+} channel[41], increased space between the L type channel and RYR2[42] and abnormalities of RYR2[43]

In almost all models, human and animal, there is reduced function of SERCA2A and often reduced mRNA expression leading to a reduction in the amount of Ca^{2+} taken up into the sarcoplasmic reticulum and thus available for Ca^{2+} induced Ca^{2+} release[43]. This is in part due to alterations in phospholamban which regulates SERCA2A and may alter the real time dynamics of the enzyme to make it less sensitive to Ca^{2+} and therefore unable to pump it in to the sarcoplasmic reticulum[44]. In a previous study reduced contractile function assessed using the force-frequency method was associated with reduced SERCA2A and the observed contractile impairment is thought to be due to reduced accumulation of Ca^{2+} in the sarcoplasmic reticulum [45].

Functional defects in the L-type Ca^{2+} channel have long been suggested to potentially contribute to reduced contractile function because there is a loss of response of the channel to stimulation in heart failure[41]. L--type channels are important for Ca^{2+} influx and generation of a Ca^{2+} spike that is sufficient to trigger secondary release from the ryanodine receptor and thus when the distance between the L-type channel and RYR2 is increased there is less effective activation of RYR2[42].

RYR2 is affected in several ways in heart failure; firstly, there may be a reduction in receptor numbers leading to reduced calcium release. There is also phosphorylation of the receptor which leads to removal of calstabin (which stabilises the receptor by promoting it in its closed state) leading to a constant leak of Ca^{2+} with reduced peak Ca^{2+} release and reduced contractility[34]. Damage to the receptor also seems to leave some RYR2 proteins spatially disconnected and thus there may be dyssynchronous activation of RYR2 and thus ineffective ECC[46].

After contraction, relaxation of the ventricle is very important as this has been shown to form a vortex twist which encourages optimal ventricular filling for effective cardiac output after contraction. High diastolic levels of calcium due to up-regulation of NCX1 and enhanced Ca^{2+} influx through its reverse mode lead to an inability of ventricular relaxation, high passive tension requiring more energy for the next contractile beat and poor relaxation and impaired filling[47].

These changes seen above provide a general link from cardiac structure, to the action potential and to the development of arrhythmias/heart failure in general and now we can look at how diabetes and obesity may specifically cause a cardiomyopathy.

1.5. Cardiac pathological changes in diabetes

As has been seen in many other organs affected by diabetes, changes occur to the heart in a wide variety of structures and in many different ways. As part of the background to this study, it is important to look at the major areas that have been studied.

1.5.1. Cardiac energy usage and consumption

The heart is one of the most energy demanding organs in the body and uses between two-thirds to one-third ratio of free fatty acids (FFAs) to pyruvate (from glucose and lactate) for energy metabolism. This delicate balance is altered in people with diabetes and leads to a reduction in the heart's ability to meet its energy requirements and thus leads to heart failure[48]. Glucose utilisation is vital in maintaining efficient energy production and also in protecting against periods of ischaemia[49] and in diabetes glucose utilisation is impaired.

Glucose transporter-4 (GLUT-4) is the major membrane glucose transporter in the heart and allows transport of glucose into the cardiac myocyte for metabolism and ATP production. In many patients with heart failure there is a reduction in the expression of the GLUT-4 transporter, which causes reduced energy production. Down regulation of GLUT-4 expression in diabetes occurs through a reduction in the expression of myocyte enhancer factor 2C (MEF2C), which is a regulatory factor for GLUT-4[50]. In diabetes glucose metabolism seems to be reduced due a reduction in the translocation of GLUT-4 from the cytoplasm to the cell membrane, which seems to be the main difference between people with diabetes and heart failure and those without[49]. If the myocyte cannot make significant use of glucose, energy metabolism is shifted to the less efficient and more toxic fatty acid pathway.

Oxidation of FAs is less efficient than glucose metabolism for the production of ATP as it requires more oxygen and as micro and macrovascular ischaemia is common in patients with diabetes this means that there is less energy reserve during periods of ischaemia[51]. These processes lead to a build-up of glucose 6 phosphate within the myocyte which then in turn inhibits hexokinase which prevents utilisation of any further glucose by the myocyte[52]. In animal models, the response to this excess of fats has been to increase CD36 and fatty acid transport protein (FATP) expression and their relocation to increase FA uptake and oxidation[53].

Peripherally in diabetes, adipocytes that generate the excess of offending free fatty acids become resistant to negative signalling and help down regulate insulin mediated glucose uptake in other cells, worsening the situation in the heart[54].

Impaired glucose metabolism secondary to up-regulation of FFA metabolism means the heart's energy demands are not met. FAs have affects other than just on glucose usage;

they are toxic in themselves. In patients with diabetes and diabetic animal models, an excess of FAs and triglycerides leads to the creation of toxic substrates which have a wide range of negative effects[53, 55]. Excess FA metabolism and accumulation leads to the formation of ceramide which up-regulates caspases causing cell apoptosis[56] and in a structure like the heart with very low levels of cell replication this loss of myocytes is not replaced by new myocytes.

Furthermore, the pathological changes that lead to impaired glucose utilisation and excess lipotoxic fatty acid production in diabetes activate the peroxisome proliferator activated receptor-alpha system (PPARα). PPARα is a nuclear transcription factor present commonly in areas of high metabolic activity such as the liver and skeletal muscle and its key role being is the in the regulation of genes that control FA utilisation.

PPARα up regulation leads to inhibitory effects on cardiac metabolism through increased pyruvate dehyrdrogenase kinase 4 levels which inhibits glucose oxidation in the mitochondria[57]. Up regulation of PPARα which controls gene expression changes via the peroxisome proliferator response element leads to an increased fatty acid uptake and oxidation via reduced malonyl CO-A expression[58]. Carnitine palmitoyltransferase I, is an enzyme which controls entry across of the mitochondrial membrane of FAs and in turn binds to and is inhibited by malonyl CO-A. In normal people CPT-I levels and activity are strictly controlled but with PPARα activation in type 2 diabetes, it is up-regulated allowing the excess fatty acid oxidation to continue unhindered [59]. PPARα activation is seen as a common process in other cardiomyopathies in patients without diabetes and this would be suggestive that increased PPARα activity has a negative effect on cardiac function [60].

The long term effect of these changes is to impair contractile function, isovolumetric relaxation and diastolic filing through insufficient energy supply and subsequently a reduction in the diabetic heart's ability to cope with metabolic stress/ischaemia[53].

1.5.2. Reactive oxygen species

One of the major factors in diabetic cardiomyopathy, as opposed to other cardiomyopathies, is the constant production of damaging oxygen free radicals and their effects on the heart.

In times of free radical generation, the body responds in various ways, including free radical absorption (via NADPH [Nicotinamide Adenine Dinucleotide Phosphate] and glutathione), repair to damaged structures and through planned apoptosis. This is a carefully balanced and well-adapted mechanism that helps the body in situations of infection, inflammation and damage from sunlight. It is becoming clear that the diabetic state results in a continuous stream of free radicals that overwhelm natural free radical absorption systems in the body leading to cardiac damage.

The three main pathological mechanisms by which reactive oxygen species (ROS) are created in diabetes are via hyperglycaemia, increased fatty acids and fatty acid oxidation (outlined earlier) and mitochondrial uncoupling[61].

The hypothesised first step in the hyperglycaemia pathway is excess sugar forced into the polyol pathway which oxidises NADPH to NADP removing glutathione, a very important anti-oxidant from the system. Loss of glutathione impairs free radical absorption making it difficult for the body to deal with normal levels of free radical not just the increased free radical levels seen in diabetes[62]. In addition to this, as a by-product there is excess generation of the superoxide free radical which is damaging in its own right and now has less glutathione to correct it[63]. In addition hyperglycaemia also leads to increased expression of inducible nitric oxide synthetase (iNOS) which leads to increased superoxide and peroxynitrite free radical levels[63]. These free radicals are directly damaging to DNA and DNA repair mechanisms, which leads to cardiac myocyte apoptosis[57].

Hyperglycaemia also up regulates the activity of protein kinase C (PKC), which while having a plethora of deleterious effects on vessels, up-regulates the pro-inflammatory NF-κB pathway and causes an increase in ROS generation via NADPH oxidase (Nox-1)[64]. Excess glucose can also be forced into the hexosamine pathway, which increases production of two inflammatory cytokines, TGFβ and plasminogen activator inhibitor type one[65].

Hyperglycaemia thus forces excess glucose into pathways producing harmful effects on the heart and a self-propelling cycle of hyperglycaemia induced ROS, forcing more glucose into these pathological pathways[62, 66, 67].

A review of the metabolic pathways linked to hyperglycaemia is shown below in Figure 8:

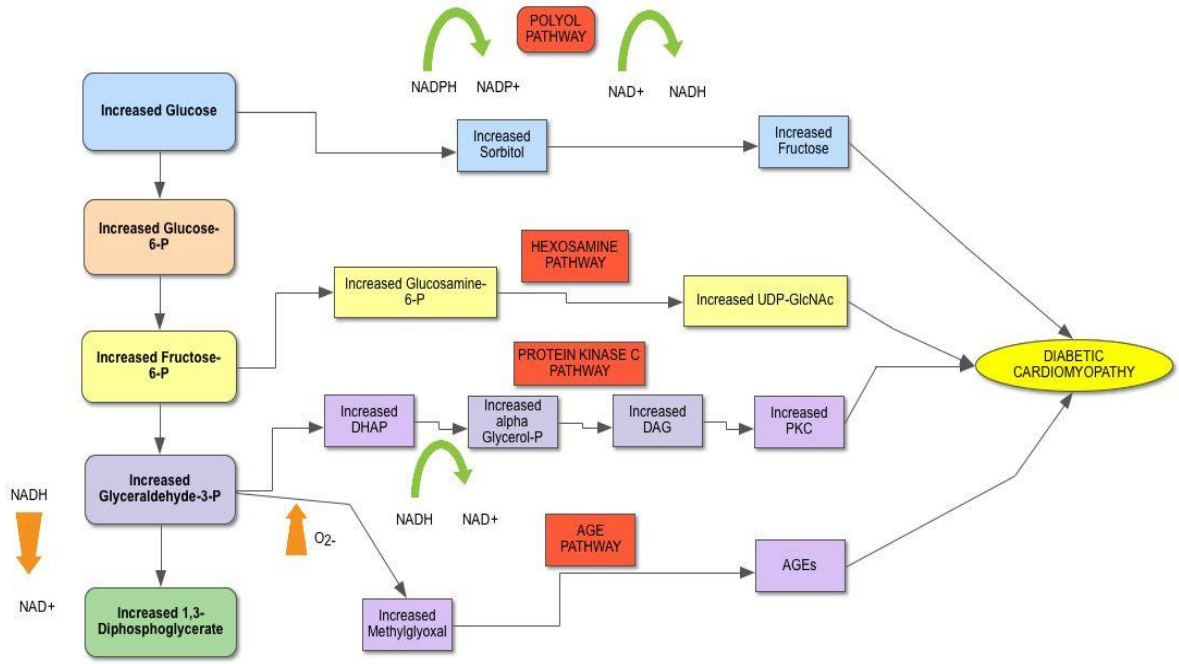

Figure 8: An overview of the metabolic pathways linked to increased glucose and their relationship to diabetic cardiomyopathy

Mitochondria as the key energy creator are vitally important in all areas of human physiology and especially to areas of high-energy usage such as the heart. In diabetic mouse models, increased ROS generation resulted in an increase in mitochondrial uncoupling[68] and impairment of cardiac mitochondrial function, through changes in the genetic expression of proteins involved with mitochondrial respiration[69, 70]. Abnormal function of mitochondrial respiration due to ROS also in turn leads to further ROS generation.

Mitochondria in diabetes, due to the effects of long-term reactive oxygen damage express less ATP synthase, which means that energy production is markedly reduced[57].

This means that the diabetic heart simply cannot generate enough energy to perform as needed in normal conditions and under stress.

Using the free radical damage model outlined above, we can begin to view cardiomyopathy in diabetes as a problem with cellular defence, repair and renewal. In knockout diabetic mouse models where the P66 (a pro-apoptotic gene) gene had been deleted there was an improvement in telomere length and in cardiac progenitor cell numbers and therefore the number of myocytes[71]. P66 is predominantly activated by excess untreated ROS in diabetes and again lends credence to ROS generation being important to the pathogenesis of diabetic cardiomyopathy. P66 has been shown to be increased in other animal models of heart failure and may be one of the missing links in terms of explaining why a cardiomyopathy related to diabetes carries such a poor prognosis[72]. The activation of P66 by ROS is also dependent on angiotensin two binding and this may explain some of the benefits in heart failure of angiotensin converting enzyme inhibitors (ACEi) particularly in people with diabetes above and beyond the haemodynamic benefits[73].

1.5.3. Ca^{2+} signalling and the ryanodine receptor

Ca^{2+} is the principal signalling molecule that activates the contractile machinery of the ventricular myocyte.

RYR2 as an important component of the contractile machinery is impaired by diabetes in a variety of ways.

In age matched rats with diabetes there are higher basal cardiac levels of Ca^{2+} and this may be due to altered function of the NCX1[74]. Surprisingly higher basal rates of Ca^{2+}, does not lead to better contractile function. Damage to SERCA2A, a key sarcoplasmic ATPase, leads to reduced calcium uptake and the rate of rise to peak Ca^{2+} levels[75]. This may then be insufficient to generate a spark causing Ca^{2+} induced Ca^{2+} release (via RYR) or slower/fewer contractile activations.

So while receptor numbers maybe reduced as with other cardiomyopathies, receptor function is also reduced thought principally to be due to ROS induced damage to the receptor and also through a change in the receptor structure because of advanced glycation that renders the receptor less sensitive to its ligands[76].

Chronic damage in diabetes to the receptor means that there is often dyssynchronous release and a persistent diastolic leak (evidenced by a high basal level of Ca^{2+}) impacting on contractility and increasing arrhythmia rates[77].

1.5.4. Cardiac autonomic neuropathy

Long before the pathological mechanisms could be understood clinicians had noticed that diabetic patients had reduced cardiac autonomic function initially described by investigators as a reduction heart rate variability[78]. Eventually heart rate variability was largely realised to be a factor of heart rate[79] and not really a reflection of autonomic function. However autonomic dysfunction in diabetes remained an area of interest for many researchers and current major findings are discussed below.

Eventually it was realised that diabetes affected neuronal function in the heart and this can be through many of the already discussed metabolic problems such as ROS derived damage and AGEs. These processes at the cellular level cause direct damage to cardiac nerves and to the blood supply to these nerves resulting in reduced cardiac neuronal function[80]. Confirmation of a direct loss of nerve function within the heart of patients with diabetes was confirmed using MIBG (a radioactive tracer similar to noradrenaline) with reduced uptake even in patients with normal autonomic function tests[81, 82].

In addition to direct damage, indirectly a depletion of ATP, leads to activation of polyADP ribosylation, which leads to cell necrosis and release of neuronal toxic factors[83]. Long term diabetes leads both peripherally and centrally, to a reduction in neuronal growth factor (NGF) which results in reduced nerve function and potentially a loss in replacement of damaged and dead fibres [84].

Patients with cardiac autonomic neuropathy (CAN) during normal conditions exhibit normal coronary artery flow[85] but under stress there is a reduction in coronary blood flow reserve; leading to regular periods of small but significant ischaemia causing cardiac injury[86]. This is seen elegantly in the heart in labelled perfusion imaging with noradrenaline analogues and in patients with CAN, there is exaggerated proximal retention with proximal vessel constriction and distal hypoinnervation leading to reduced blood flow reserve under sympathetic stress[86].

As the autonomic neuropathy progresses there is over production of catecholamines and increased beta-adrenergic receptor production in the heart. These two factors combine to cause an increase in calcium related myocyte apoptosis via endonucleases,[87] which progressively leads to heart failure. High sympathetic activity and reduced parasympathetic function is a key common pathway in many types of heart failure and important because increasing vagal derived parasympathetic activity leads to reduced inflammatory cytokine production, reduced heart rate, reduced iNOS, anti-inflammatory cytokine production and improved baroreflexes[88].

While CAN has many effects on vessels and myocytes, the neuronal damage also leads to the loss of calcitonin gene related peptide function, which is released directly from nerves. In diabetes this peptide's receptor is down regulated and the peptide itself is not released from the nerve in normal quantities and this is important as this peptide causes vessel relaxation and increases cardiac contractility[89].

Many of the processes discussed above potentially overlap with heart failure caused by other syndromes or are seen as heart failure develops but CAN seems to be very specific to diabetes, especially in the early stages, with close correlation to glycaemic control and some regression with tight glycaemic control[90].

1.5.5. Cardiac Structure

Diabetes and the prolonged effect of hyperglycaemia have metabolic effects on the heart and some of these as described previously lead to changes in cellular function but they also produce changes in the structure of the diabetic heart. Endomyocardial biopsies from diabetic patients show thickening of the capillary basement membrane, myocellular atrophy and hypertrophy with interstitial and myocardial fibrosis and collagen deposition, all of which reduce myocardial function[91].

The most common structural problems seen with diabetes are cardiac fibrosis and left ventricular hypertrophy (LVH) which we will now look at in turn.

In diabetes, up-regulation of the protein kinase C (PKC) system produces increased TGFβ and connective tissue growth factor (CTGF) expression leading to fibrosis and consequently poorly relaxing and poorly contractile hearts[92]. This increased fibrosis may

also be secondary to a variety of elevated circulating proteins such as angiotensin and endothelin caused by inflammatory metabolic and cellular changes[93].

One of the central pathological mechanisms in diabetes is the formation of advanced glycation end products (AGEs). AGEs are a heterogeneous group of molecules formed non-enzymatically, when reducing sugars react with the free amino groups of proteins[94]. These products cause cross-linking between myocardial collagen fibres leading to a decrease in compliance and heart failure[95]. AGEs up-regulate the genetic expression of NF-κβ, endothelin and fibronectin which have been linked with myocardial fibrosis, inflammatory change and increased apoptosis[93].

This occurs because receptors of advanced glycosylation end products (RAGEs) on the cell surface are activated by the high levels of AGEs and they cause downstream intracellular activation of various transcription factors, such as NF-κβ[96]. AGEs are also now thought to cause immune complex formation, in a similar fashion to a variety of other autoimmune diseases, these complexes then activate the complement system and complement mediated cellular inflammation[97].

Patients with diabetes commonly have left ventricular hypertrophy (LVH) and two causal mechanisms have been investigated widely. Primarily, hyperinsulinaemia acts as a local growth factor causing increased left ventricular mass via insulin receptor substrate-1 (IRS1) and activation of IRS1-associated phosphatidylinositol-3 kinase (PI3K)[98]. The other postulated mechanism is that obese patients with type 2 diabetes have high interleukin six levels[99] and high leptin levels[100] which, stimulate growth factors increasing left ventricular mass.

1.6. Pathological changes in obesity cardiomyopathy

Obesity is a major risk factor for the development of type 2 diabetes and it is clear from previous studies, that there is an overlap in some of the downstream effects of both conditions e.g. LVH[101] and although key aspects of the pathology have already been discussed, the obesity specific changes are reviewed below.

1.6.1. Unique changes

In obesity without the development of diabetes there is an infiltrative deposition of triglycerides within the myocardium as the body aims to store the excess caloric intake[102]. This mechanism leads to LVH and to a myocardium that is not lean muscle but stiffer with high levels of fat deposition and is similar in mechanism to the observed obesity related non-alcoholic steatohepatitis. This myocardial fat deposition is not a benign process and has been shown in animal models to cause myocyte apoptosis[103].

One of the key hypertrophic mechanisms in obesity, is via leptin, a satiety and appetite regulatory hormone which is found in high circulating levels in obesity but with increasing levels produces increasing receptor resistance. It has been shown that while the predominant action and role of leptin is in the central nervous system it is also produced within the heart[104].

Leptin is directly hypertrophic via 3 main mechanisms, which begin with activation of the Janus kinase 2 (JAK2) tyrosine kinase and then a series of downstream activations[105]. Firstly, leptin activates JAK2, which stimulates the release of signal transducer and activator of transcription (STAT3) from the cell membrane and relocation of the cell nucleus where it can dock with its transcription targets and cause hypertrophy, predominantly by myocyte elongation[106]. Secondly, high levels of leptin increase rhoA/ROCK pathway activity which causes an increase in the F-actin to G-actin ratio and an enlargement in the cardiac myocyte[107].The final method is via JAK2 activated up-regulation of the PI3K/AKT transcription pathway which is known to cause cell growth and hypertrophy and also actin rearrangement causing hypertrophy[105, 108]. Also indirectly hyperleptinaemia has been shown to enhance endothelin and angiotensin 2 mediated cardiac myocyte hypertrophy in an autocrine manner[109].

Adiponectin, is a key cytokine that is down regulated in obesity probably by adiposity related excess TNFα release and adiponectin has been shown to prevent α-adrenergic mediated LVH[110]. LVH is not a benign adaptive process and represents an early subclinical phase with reduced energy kinetics before overt LV impairment visible on echocardiography. In LVH there is a reduction in the PCr/ATP ratio compared to normal

controls and also reduced creatine kinase which helps maintain high ADP levels in the mitochondria for metabolism to ATP[111].

Obesity is thought to represent a chronic inflammatory condition with whole-body effects some which are thought to be driven by pathological white adipose tissue function. White adipose tissue gene expression has been shown to generate increased inflammatory cytokines and in a mouse model this led to LV fibrosis and hypertrophy[112].

1.6.2. Overlap with type 2 diabetes

In obesity there is activation of the sympathetic nervous system with similar effects to diabetic autonomic neuropathy leading to up-regulation of the renin-angiotensin system (RAAS) which stimulates cardiac fibrosis, hypertrophy and myocyte apoptosis[113].

Obesity and type 2 diabetes both represent a hyperinsulinaemic state with insulin resistance and this phenotype results in augmented white adipose tissue function, overproduction of angiotensin 2[114] and increased hepatic renin production[115].

A major area of overlap between types 2 diabetes and obesity is the switch from predominantly cardiac glucose metabolism to fatty acid metabolism with down regulation of GLUT-4, increased fatty acid uptake and oxidation[116, 117].

As mentioned earlier the excess myocardial deposition of fatty acids and their metabolism leads to deposition of toxic lipid metabolites which cause myocardial apoptosis and seems to be a key overlap mechanism between type 2 diabetes and obesity[118].

In addition to the observations above, free radical damage is an important component of the ongoing pathological process in diabetes and similarly in obesity there is an excess of free radical generation which causes myocardial injury and helps promote the myopathic process[119].

1.7. Arrhythmogenesis in diabetes and obesity

Apart from changes that lead to a reduction in contractile performance, the other important aspect of the cardiomyopathy linked to diabetes and obesity is the change to an arrhythmogenic phenotype, with obese patients having higher rates of atrial[120] and

ventricular arrhythmias[15] and type 2 diabetes also linked to an increased incidence of many arrhythmias[13, 121].

In patients with type 2 diabetes, episodes of hypoglycaemia (defined as a blood glucose of 3 mmol/l or less) were associated with a large increase in the number of ventricular couplets and episodes of ventricular tachycardia compared to a control population[122]. The exact mechanism by which hypoglycaemia contributes to arrhythmias is uncertain but seems to be independent of changes in the QT interval.[122] Hypoglycaemia is thought to be arrhythmogenic by two mechanisms; a large sympathetic adrenergic surge in the context of a high prevalence of autonomic neuropathy plus an abnormal responses to catecholamines[123] and through inhibition of the human ether related a go-go channel (ERG), a key K^+ repolarising channel. In type 2 diabetes episodes of hypoglycaemia are often caused by medications such as sulphonylureas and insulin which can affect electrophysiological channels with sulphonylureas in particular thought to affect cardiac K^+ channels[124].

Autonomic neuropathy is a complication that can occur in patients with diabetes and this can extend to CAN confirmed in patients with type 2 diabetes[125]. CAN is associated with higher resting heart rates which are associated with worse cardiovascular outcomes and higher rates of cardiac arrhythmias. CAN, specifically in patients with diabetes, is related to an increase in the corrected QT interval and higher rates of sudden cardiac death[126].

Another purported mechanism of arrhythmogenesis in patients with type 2 diabetes is a reduction in the number of ryanodine receptors in the sarcoplasmic reticulum of the myocyte, which is very important for Ca^{2+} release[127] and excitation-contraction coupling. Chronic damage, or a reduction in RYR2 numbers, in diabetes often leads to a situation where there is not organised synchronous Ca^{2+} release and a persistent diastolic leak which may cause delayed after-depolarizations (DADs) increasing the incidence of arrhythmias[77]. Other novel mechanisms have been identified by which arrhythmias may be induced through RYR2 receptor induced Ca^{2+} sparks and abnormal waveform generation leading to re-entrant arrhythmias[128].

In diabetes studies have shown that an increase in dispersal of the action-potential has the propensity to form re-entrant circuits leading to sustained arrhythmias[129]. Diabetes has also been shown in a variety of animal models to affect the abundance of rectifying

potassium channels that are important in myocyte repolarization and reduction of these channels can lead to prolongation of the action potential and arrhythmias[130].

Although the mechanisms of arrhythmogenesis in obesity are not fully understood some putative theories have been published. In several studies an increase in the corrected QT interval in obese individuals has been observed and it was suggested this may be due to high levels of circulating fatty acids interfering with myocyte repolarization[131]. An excess of fatty acids also, as discussed in the section on contractile function, affects cardiac energy production in a negative manner and this can impair active ion exchangers by reducing the amount of ATP production. An excess of fatty acids leads to increased oxidative stress within the myocardium and this in turn increases the reverse mode function of NCX1, leading to a delay in inactivation of the late sodium current, prolonging phase 2 of the AP and leading to triggered and ectopic activity[132].

In obese individuals with sudden cardiac death, it was noted that were was an increase in ventricular ectopy, which in many cardiac disease states is linked to prolonged ventricular arrhythmias and death[133]. Obesity is linked to an increase in resting heart rate through increased sympathetic tone and reduced parasympathetic control[134] and increased circulating levels of norepinephrine[135].

In obesity apart an increase in myocardial adipocyte density may alter electro-mechanical coupling leading to reduction in conduction propagation/conduction block and an increase in the incidence of arrhythmias[136].

In obese individuals, as discussed above, there is an increase in leptin expression and increased leptin resistance at the receptor level. This may be important as obesity progresses, as the following potential anti-arrhythmogenic actions of leptin may be lost:

1. Leptin reduces NCX1 forward activity which leads to a reduction in the I_{Ti} current in phase 3/4 and less chance of DADs
2. Leptin inhibits the $I_{K,ss}$ ultra-rapid delayed rectifier channel and thus shortens the APD in the 90% phase of repolarization which has been shown to cardiovert atrial fibrillation[137]

1.8. Cardiac fibrosis: downstream effects of diabetes and obesity

Myocardial fibrosis is a common pathological endpoint in diabetes and obesity and is caused by various changes in gene and protein expression. Fibrosis commonly results from transformation of fibroblasts to myofibroblasts with deposition of type 1 collagen and in comparatively smaller volumes of type 3 collagen, induced by inflammatory cytokines, most importantly by TGFβ. This results in disruption of the extracellular matrix and transformation of a smooth muscle with normal cell to cell connections to a fibrotic muscle with poor cell to cell connections.

Fibrosis has been shown to be pro-arrhythmogenic via several mechanisms including: slowed conduction and re-entrant arrhythmias, increased automaticity, reduced ability to prevent early after depolarizations transferring from one myocyte to another and a reduction in the number of myocytes required to promote an ectopic beat[138]

Fibrosis as a common endpoint of obesity and diabetes is very important in arrhythmogenesis and this has been confirmed in many other cardiac disease processes such as post myocardial infarction and in hypertrophic cardiomyopathy. There is experimental evidence that correction of fibrosis without any treatment of ion channels or electrophysiological proteins directly attenuates the arrhythmogenic phenotype[139].

1.9. Summary

The left ventricle is organised topographically with fibre orientation gradually changing from epicardium to endocardium with corresponding differences in the action potential and potassium repolarising channels.

Optimal organisation of the action potential is required for optimal excitation-contraction coupling and thus cardiac output. When there is abnormal AP activity this acts as a substrate for arrhythmias either as triggered activity or a re-entrant circuit. The contractile performance of the heart is predominantly activated by Ca^{2+} release and binding with troponin/tropomyosin complex. In heart failure changes in L type channels, ryanodine receptor, SERCA2A activity and NCX1 lead to abnormal Ca^{2+} handling and poor excitation-contraction and poor myocardial performance. Abnormal Ca^{2+} handling also impairs ventricular relaxation and may contribute to poor ventricular filling and cardiac output.

Diabetes causes several specific cardiomyopathic processes including left ventricular hypertrophy, fibrosis, reduced glucose metabolism and a switch to increased fatty acid metabolism with apoptotic myocardial steatosis. Diabetes, while causing a peripheral autonomic neuropathy, also leads to a cardiac autonomic neuropathy with up-regulated sympathetic action. Diabetes is a disease characterised by inflammatory ROS generation which is cardiotoxic and may lead to myocyte apoptosis. Diabetes also reduces RYR2 levels, impairs RYR2 function and SERC2a function which all lead to higher rates of arrhythmias and heart failure. Diabetes can also, through the formation of AGEs, directly impair cardiac structure or the RYR2 and both impairments may contribute to the overall cardiomyopathic process.

Obesity shares many of the same processes with diabetes in terms of impairing cardiac function such as higher rates of fatty acid metabolism, LVH, lipotoxicity and high sympathetic activity. A major difference between diabetes and obesity, appears to centre on leptin, which as a transcription factor causes myocyte hypertrophy via several mechanisms. Obesity causes a release of inflammatory cytokines from adipose tissue which may cause cardiac fibrosis, LVH and down regulation of adiponectin which might be protective against LVH.

These changes in both diabetes and obesity result in a phenotype that is pro-arrhythmogenic and results in contractile dysfunction and heart failure with experimental evidence that suggests these effects are independent of traditional cardiovascular risk factors.

It is the working hypothesis of this study that there are common gene expression changes between type 1 diabetes, type 2 diabetes and obesity that may explain the cardiomyopathy seen in these conditions and that the most important area of investigation will be around key electrophysiology genes.

2. Aims and objectives

Given the rapid increase in patients suffering with obesity and diabetes and the cardiac complications caused by the two conditions, a better understanding of the changes in gene expression in the ventricles may help guide the development of future treatments.

qPCR is a well-established technique for understanding the genetic expressional changes in a wide variety of species and disease states and has been used to great effect to understand many aspects of obesity and diabetes. Using qPCR, our aim was to analyse the left ventricular gene expression of a series of key cardiac genes to gain a better understanding of the pathophysiology of diabetes and obesity related cardiomyopathy. These gene changes have then been combined with mathematical modelling software to produce modelled action potential curves. This information has been combined with echocardiographic and ECG/signal averaged ECG results in the human study to look for confirmation of a clinical phenotype and to see if the genetic changes are associated with specific phenotypic changes.

Key aims of the project are:

- To characterise the changes in left ventricular gene expression in type 1 diabetes, type 2 diabetes and obesity
- To look for areas of commonality between the three disease states
- To model the effects of these gene changes on the ventricular action potential
- To look for clinical correlation in a human type 2 diabetes group using echocardiography and the ECG

3. Methods

3.1. Animal tissue preparation and isolation- experiment 1: streptozocin (STZ) rats

This part of the study was primarily undertaken as a reference point for the other two qPCR studies and for practice and refinement of experimental pathology given the fact that Pandit et al.[140] have previously published on this topic using AP modelling.

Animal preparation and experiments were licensed under the UK Animals (Scientific Procedures) Act 1986 and undertaken at the University of Manchester.

Diabetes was induced in 8 Adult male Wistar rats (Charles River, Margate, UK) via intraperitoneal injection of freshly dissolved streptozocin (55mg/kg in sterile saline). This was performed after an overnight fast and confirmation of diabetes induction was made with tail vein blood monitoring. A minimum of blood glucose level of greater than 15mmol at day 4 post injection was considered diagnostic of the induction of diabetes. The STZ model is a well validated model of diabetes typically behaving more like the autoimmune human type 1 disease than what is thought of the more lifestyle related, type 2 disease[141]. Issues with the STZ rat model as a specific type 1 diabetes model have previously been raised including the fact that STZ is eliminated within 48 hours and that the effects of STZ can be reversed partially with insulin[142]. Acknowledging these facts, the STZ model has years of historical data and experimental familiarity and was felt to be an initial useful starting point for this study.

All animals were fed a standard chow diet to and water ad libitum. All animals were kept on a standard 12 hour on/off light cycle. 8 age, weight and sex matched rats were used as controls and kept in identical conditions. After 8 weeks, all rats were terminally anaesthetised with isoflurane (2% in oxygen) and killed by cervical dislocation. The whole rat heart was dissected and removed and placed in freshly made Tyrode solution[143] on ice.

The rat ventricles were then pinned and a full thickness piece of the left ventricular free wall was cut out measuring approximately 5mm long. This piece was then embedded in OCT mounting matrix (VWR, Lutterworth, UK) with the endocardium facing up. The same area was used in all rats and distance from anatomical markers such as the apex, left atrium

and atrial appendage and aorta were used to maintain accuracy. The tissue was then snap frozen in liquid nitrogen at –80^{0}C and stored at –80^{0}C for future use.

The topographically orientated piece was then placed in a cryostat machine at –26^{0}C and 15 x 10μm slices taken of the endocardial layer. After this 20 x 10μm slices were taken and discarded before the procedure was repeated for the mid myocardial and epicardial layers. Visual confirmation was used to confirm that the appropriate layers were being sectioned and approximately a third of the tissue was removed for each section. Each group of 15 slices were placed in a separate labelled cryotube for future use.

Our group have previously used this method locally and it has been used by other groups to look at differential topographical mRNA expression with good reproducibility and has been published in peer-reviewed journals and considered to be experimentally acceptable[144].

3.2. Animal tissue preparation and isolation- experiment 2: high fat diet (HFD) rats

Animal preparation and experiments were licensed under the UK Animals (Scientific Procedures) Act 1986. Animal husbandry and tissue sample collection was undertaken at the University of Liverpool and experiment analysis at the University of Manchester.

16 age matched male Wistar rats (Charles River, Margate, UK) with approximate starting weights of 250 g were split into two groups and one subgroup was fed a diet enriched with saturated fats (lard) for 8 weeks (Research Diets, Inc., New Brunswick, USA). The control group were fed a standard chow diet with 10% calories as fat and the experimental group were fed 40% calories as fat with equal concentrations of the antioxidant tBHQ and protein. All rats had free access to the food sources and water ad libitum. All animals were kept on a standard 12 hour on/off light cycle. This model was used as previous work has shown confirmed induction of obesity in the HFD group with hyperinsulinaemia and islet dysfunction which are both important in insulin resistance and in type 2 diabetes[145].

A breakdown of the percentage diet compositions is shown below in Table 4:

Group	Protein	Carbohydrate	Fat	Kcal per gram
Control	20	70	10	3.85
High Fat	20	40	40	4.58

Table 4: Percentage composition breakdown of the two experimental diets in the obesity rat experiment

Weekly weights were measured, with total weight gain and terminal weight gain recorded. At eight weeks, all animals were terminated with rising carbon dioxide concentration and cervical dislocation. The animals then had a single epididymal fat pad dissected and weighed before dividing this by the final weight as a measure of adiposity as used previously[146].

The rat hearts were in an identical manner to experiment one, dissected out and a section from the left ventricular free wall removed and mounted in OCT with the endocardial layer facing up and the tissue was then snap frozen in liquid nitrogen at –80^{0}C and stored at –80^{0}C for future use.

The topographically orientated piece was then placed in a cryostat machine identically to experiment 1 and 15 x 10μm slices were taken of the endocardial layer and discarded. After this 20 x 10μm slices were taken and discarded before once at the mid myocardial layer a single 10μm section was taken and mounted on labelled poly L-lysine coated microscope slides (Sigma-Aldrich, Poole, UK). Slides were then frozen at -80^{0}C for future use. Then as in experiment one, 15 x 10μm slices were taken from the mid-myocardium and stored in a labelled cryotube at -80^{0}C for future use.

3.3. RT-PCR for gene expression-rat experiments

3.3.1. RNA Isolation

RNA was isolated from the tissue using proprietary RNeasy™ mini spin column kit (Qiagen, Manchester, UK). This kit uses tissue lysis to bind RNA to a guanidine salt section on the

column before sequential washing, drying and elution steps to purify and remove RNA from the tissue.

Briefly, buffer RLT and β-mercaptoethanol warmed with carrier RNA was added to the sectioned tissue to inhibit RNase and stabilise the tissue and this tissue mixture was homogenised for 2 minutes using a polytron rotor homogeniser. At the end of 2 minutes RNase free water and proteinase K were added and mixed which digested any remaining protein. The sample was heated at 55°C for 10 minutes until the sample was completely clear and centrifuged for 5 minutes at 13,000 rpm at room temperature. 455μl of the supernatant was placed in a 1.5ml Eppendorf tube and mixed by pipetting with 227.5μl of 100% ethanol and transferred to an RNeasy mini spin column and collecting tube and centrifuged for 15 seconds at 10,000 rpm. The flow through was discarded and 350μl of buffer RW1 added to the column and centrifuged again for 15 seconds at 10,000 rpm with the flow through discarded. 80μl of an RDD/DNase I mixture was added to the silica gel area in the centre of the column to allow digestion of genomic DNA on the gel before a repeat of the wash step with the RW1 solution. Next, 500μl of buffer RPE was added to each column and centrifuged for 15 seconds at 10,000 rpm and the flow through discarded.

To dry the RNA on the columns 80% ethanol was added to each tube before centrifuging for 2 minutes at 10,000 rpm and discarding the flow through before opening the column lid and centrifuging again for 5 minutes at 13,000 rpm.

Finally, the column was placed into a final collection tube and RNA free water was added and the tube is centrifuged to remove all the purified RNA, this step being repeated twice to ensure maximal yield.

3.3.2. RNA quantification and quality assurance

RNA quality was measured using the NanoDrop™ (Thermo-Fisher, West Sussex, UK) spectrophotometry system as previously described[147]. In summary, after blanking the machine with 1.2μl of RNase free water, 1.2μl of the RNA solution was added and a machine derived curve is obtained with an absolute total RNA detected value in ng/nl, a

260nm/280nm spectrophotometry and a 260nm/230nm spectrophotometry absorbance ratio value.

Good quality RNA occupies the spectrum between 260nm: 280nm with a ratio of around 2 (less than 1.9 suggestive is of contamination and over 2.1 suggestive of RNA degradation) consistent with local protocols and data from other centres[148]. An example curve and values from a good quality sample is shown below with 260nm: 280nm ratio of 2.07 in Figure 9:

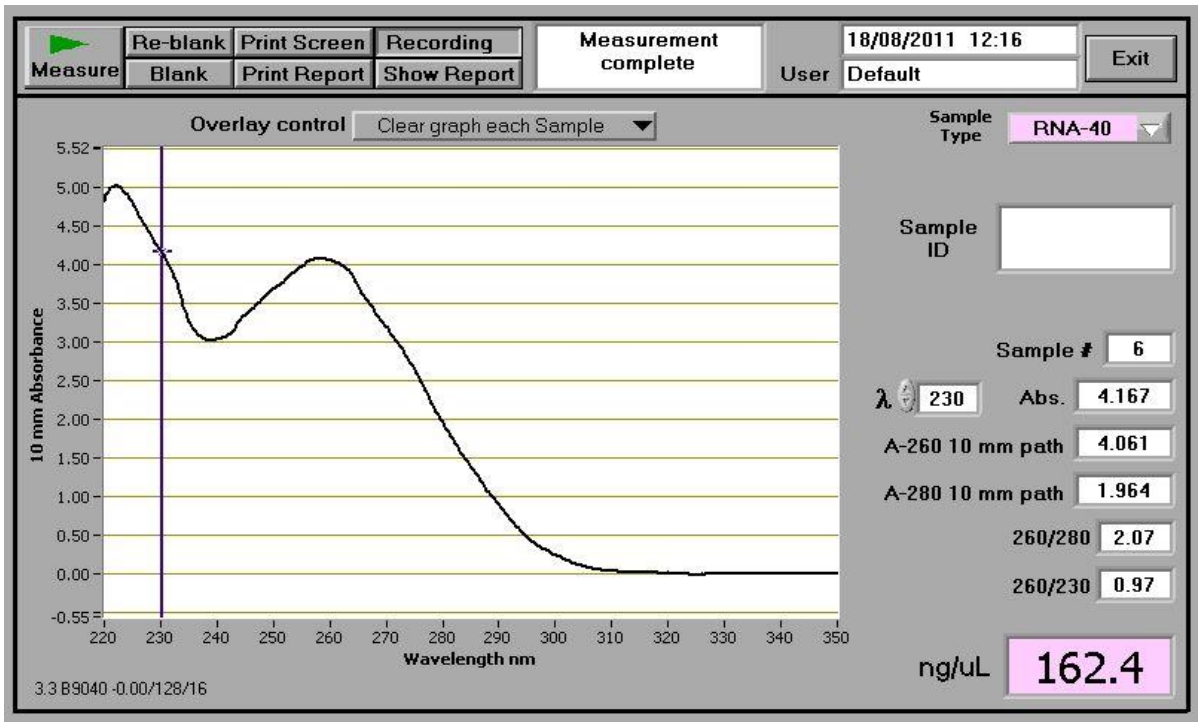

Figure 9: Example of a NanoDrop curve and reading for a good quality RNA sample

3.3.3. Reverse transcription

RNA was then reverse transcribed to cDNA using high capacity RNA to cDNA master mix and a 9800 Fast Thermal Cycler with 96-well aluminium sample block module (both Applied Biosystems, Paisley, UK).

This system uses purified reverse transcriptase from *e.coli* with the *pol* gene from the Moloney Murine Leukaemia Virus which encodes reverse transcriptase. Using this system, a variety of primers bind to the Poly A tail 3 end of the mRNA and after this reverse transcriptase was added which uses the primer end to form a complementary strand of DNA. This system is widely used in RT-PCR and gene expression studies[149].

Briefly, to allow for accurate quantification comparing more than 1 sample, to make a total sample volume of 20µl, 4µl of the high capacity master mix was added to a mix of nuclease free water and a volume of the diluted RNA sample, to make a total of 16 µl. The volume of RNA solution added was altered depending on the amount of RNA per µl to ensure that the amount of RNA per sample for RT-PCR in each tube was identical. This was done to prove that quantitative expression changes were not a result of differing amounts of RNA extracted in each sample. The experimental mixture was then centrifuged for 10 seconds at 10,000rpm before being put in the thermocycler at 25^{0}C for 5 minutes, 42^{0}C for 30 minutes and then 85^{0}C for 5 minutes before the mixture was held at 4^{0}C for 15 minutes. Finally, the sample was diluted with nuclease free water to a total volume of 100 µl. The mixture was then stored at -20^{0}C.

3.3.4. Quantitative PCR

Quantitative PCR was then performed using a custom loaded Taqman™ low density array card and a 7900 HT PCR machine (Applied Biosystems, Paisley, UK). This technology uses 5' nuclease chemistry with VIC dye and minor groove binding probe with a non-fluorescent quencher on the 3' end, to allow for specific gene expression measurement and no primer-dimer amplification as seen with SYBR green technology. Using specific sequence probes, there is specific binding to cDNA only.

In this technique, the DNA mixture is denatured at high temperature and the quencher binds to the 5' end Taqman gene specific probe. After this, the reaction is cooled and the Taqman gene specific probe can bind to its target and then DNA polymerase and primers loaded in the reaction mix allow formation of a complimentary DNA strand and in the process cleave the dye at the 5' end giving off measurable fluorescence. With each PCR cycle, more dye can be released depending on the amount of DNA available.

Results are reported in terms of threshold cycles (C_t), which is the machine calculated number of PCR cycles for the amount of fluorescence to reach greater than 10 times the standard deviation of the baseline fluorescence. If after 40 cycles of amplification, the target has not amplified it is considered that it is not present in the tissue.

To summarise after thawing on ice 30µl of the cDNA solution was added to 20 µl of water and then 50µl of TAQMAN™ universal PCR mastermix (Applied Biosystems, Paisley, UK) to make a reaction volume of 100µl. The contents were vortexed and then centrifuged. Next, custom 384 well TAQMAN™ probe loaded microfluidic cards (Applied Biosystems, Paisley, UK) with 48 gene targets in replicates of 8 were removed from the fridge and allowed to reach room temperature. The reaction mix was loaded into the respective loading port of the card and when all ports were filled, the card was centrifuged for 1 minute twice at 1200 rpm.

3.3.5. Gene targets

The target genes for this study were chosen on the basis of the department's previously published work on the cardiac action potential[150-152], key energy production genes and some neuronal proteins, hypothesised to be involved in cardiac dysfunction.

The gene symbol, full gene name, the context sequence for the RNA and the chromosomal location of the gene for both rat experiments are shown below in Table 5 using the national centre for biotechnology information (NCBI) gene database as a reference source[153]:

Gene	Gene Name	Context Sequence	Chromosome
18-S	Eukaryotic 18-S	CCATTGGAGGGCAAGTCTGGTGCCA	14
ATP1A1	Na^+/K^+ ATPase 1a1	AGTGAACCAGGTGAACCCCAGAGAT	2q34
ATP1A2	Na^+/K^+ ATPase 1a2	AGCAGGGCATGAAGAACAAGATCCT	13q24-q26
ATP1A3	Na^+/K^+ ATPase 1a3	GGTGACAATCTGTACCTGGGCATAG	1q21
ATP2A2	Cardiac Sarcoplasmic Reticulum Ca^{2+}Activated- ATPase 2a	GGAAATTGCTGTTGGTGACAAAGTT	12q16
CACNA1C	L-type Voltage-Gated Ca^{2+} Channel Alpha Subunit 1c	GCCCGGCTTGCCCACCGGATCTCCA	4q42
CLCN2	Cl^- Channel 2	TTCTTTGCACAAGACCCACACCATC	11q23
CLCN3	Cl^- Channel 3	GAGACCTGACAATTGCAATAGAAAG	16p12
GAPDH	Glyceraldehyde-3-phosphate dehydrogenase	AGGAGTCCCCATCCCAACTCAGCCC	4
GJA1	Gap Junction Alpha 1	GTGAAAGAGAGGTGCCCAGACATGG	20q11
HCN1	Hyperpolarisation Activated Gated K^+ Channel 1	AAATGAAATGGTTAATGATTCATGG	2q15
HCN2	Hyperpolarisation Activated Gated K^+ Channel 2	AACATGGTGAACCACTCGTGGAGCG	7q11
HCN4	Hyperpolarisation Activated Gated K^+ Channel 4	ATGGCTCCTATTTTGGAGAGATCTG	8q24
KCNA4	K^+ voltage-gated channel, shaker-related subfamily, 4	AACAGCACACGATTCCTGCTTTAAA	3q33
KCNA5	K^+ voltage-gated channel, shaker-related subfamily, 5	GGGGGCAAGATCGTGGGTTCACTGT	4q42
KCND2	K^+ voltage-gated channel, Shal-related subfamily, 2	GGAGAAAACCACGAACCATGAGTTT	4q22
KCND3	K^+ voltage-gated channel, Shal-related subfamily, 3	GCTGACCGGCACCCCAGAAGAGGAG	2q34
KCNH2	Human Ether Related a Go-Go channel	TACTGACAAGGACACAGAGCAGCCA	4q11
KCNIP2	K_v channel-interacting protein 2	TGTCAACAGGACGAGAACATCATGA	1q54
KCNJ2	K^+ inwardly-rectifying channel, subfamily J, 2	ATCTCCACAACCAGGCGAGCGTGCC	10q32.1
KCNJ3	K^+ inwardly-rectifying channel, subfamily J, 3	GCTGCTCAAATCTCGGCAGACACCT	3q31-q35
KCNJ5	K^+ inwardly-rectifying channel, subfamily J, 5	TCTACGACTATGGCCGGTGATTCTA	8q21
KCNQ1	K^+ voltage-gated channel, KQT-like subfamily 1	TGTGTCACAGCTGCGGGATCACCAT	1q41
MT-ATP6	Mitochondrially Encoded ATP Synthetase 6	CCCCCACAATAATAGGTCTACCAAT	N/A
MT-ATP8	Mitochondrially Encoded ATP Synthetase 8	AATCATCTCCTCAATAGCCACACTA	N/A
NGF	Nerve Growth Factor	TGGCCACTCTGAGGTGCATAGCGTA	2q34
RYR2	Ryanodine Receptor 2	ACAAGAAAAGTTTCAGGAGCAGAAG	17
SlC2A4	Glucose Transporter 4	TCTGCTGCTGCTGGAGCGGGTTCCA	8q32
SLC8A1	Na^+/Ca^{2+} Exchanger	AAAGATGTATGGCCAACCTGTCTTC	10q24
SCN5A	Na^+ Channel, Voltage-Gated Type Vα	TTTGAGGGCATGCGGGTGGTGGTCA	6q12
TAC1	Tachykinin 1	CAAATCAAGGAGGCAATGCCGGAGC	4q21
TACR1	Tachykinin Receptor 1	TATGAGAAAGCGTACCACATCTGCG	4q34
TH	Tyrosine Hydroxylase	CAAGGACAAGCTCAGGAACTATGCC	1q41
TTYH1	Tweety Homolog 1	TGCCGCAGTCTGCACAAGGACTATG	11
TTYH3	Tweety Homolog 3	GTCCCCACCGCCCTCATACACCTCC	12
UCHL1	Ubiquitin Carboxyl-Terminal Esterase L1	GGCCCAGCATGAAAACTTCAGGAAA	14p11

Table 5: Gene targets in both rat experiments

3.3.6. Gene expression

In an experiment such as this with multiple runs of different tissue samples for multiple gene targets a method is required to reference results obtained from different samples/runs and make them comparable. In this study we used the relative quantification method where an abundant gene known to be highly expressed is used as a housekeeper gene to reference the expression of other genes to. This allows the expression of a target gene to be compared from one tissue sample to another even where the total amount of RNA may have been vastly different. In this method, the abundance of a transcript was measured against the housekeeper gene abundance value to establish a ΔC_t value. The cards were then sealed and placed in the PCR machine and the PCR run was begun.

Based on the local laboratory experience, poor tissue quality and unreliable experimental results have been found when a sample recorded an absolute threshold cycle value of greater than 20 for 18-s (the commonly used housekeeper gene in the laboratory and a very abundant target). Any sample recording threshold cycle values beyond 20 for 18-s were therefore excluded. Inappropriate amplification was then confirmed by analysis of the PCR curves to prove that there had been inefficient amplification likely due to human error at some point in the experiment.

An example PCR plot, with nuclease free water used as a control sample plotted against the endogenous housekeeper 18-s with normal amplification is shown below in Figure 10:

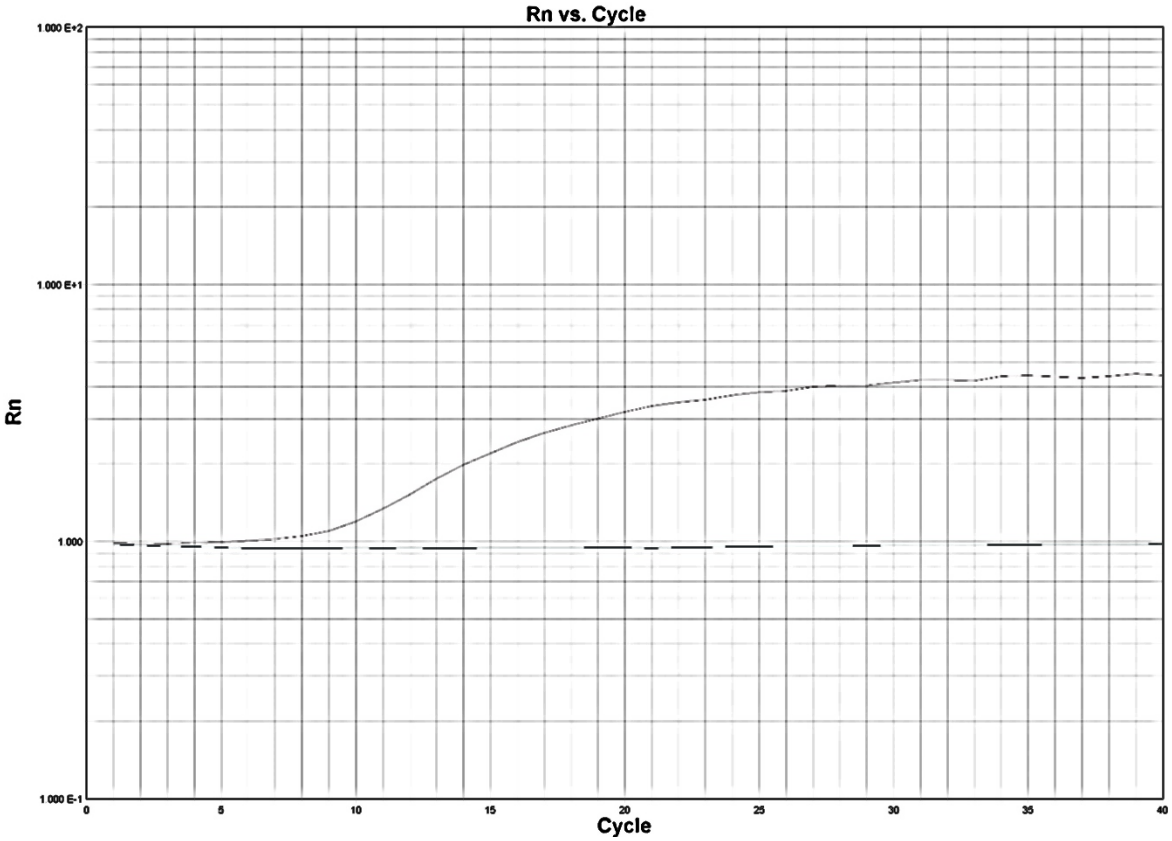

Figure 10: PCR curves for 18-S from nuclease free water (bottom) and 18-s from a control tissue sample (top)

3.3.7. Choosing the endogenous control

Currently there is no definitive housekeeper used in gene expression studies and the choice of housekeeper is normally chosen depending on local experience and the tissue type analysed. Commonly used endogenous controls are 18-S, 28-S and GAPDH and in this experiment 18-S, GAPDH and Cx43 were provisionally identified as housekeepers that could be used in final expression calculations.

Using automated geNORM™ (Statminer, Intergromics, Granada, Spain) analysis software, we were able to compare the raw C_t values for a variety of potential housekeeper genes with each other and use the standard deviations of logarithmically transformed expression ratios, to give an M value - or stability measure. The lowest M value suggests the most stable housekeeper[154]. This method was then checked by looking grossly at the distribution and standard error bars of the raw C_t values for each potential housekeeper seen (Figure 11):

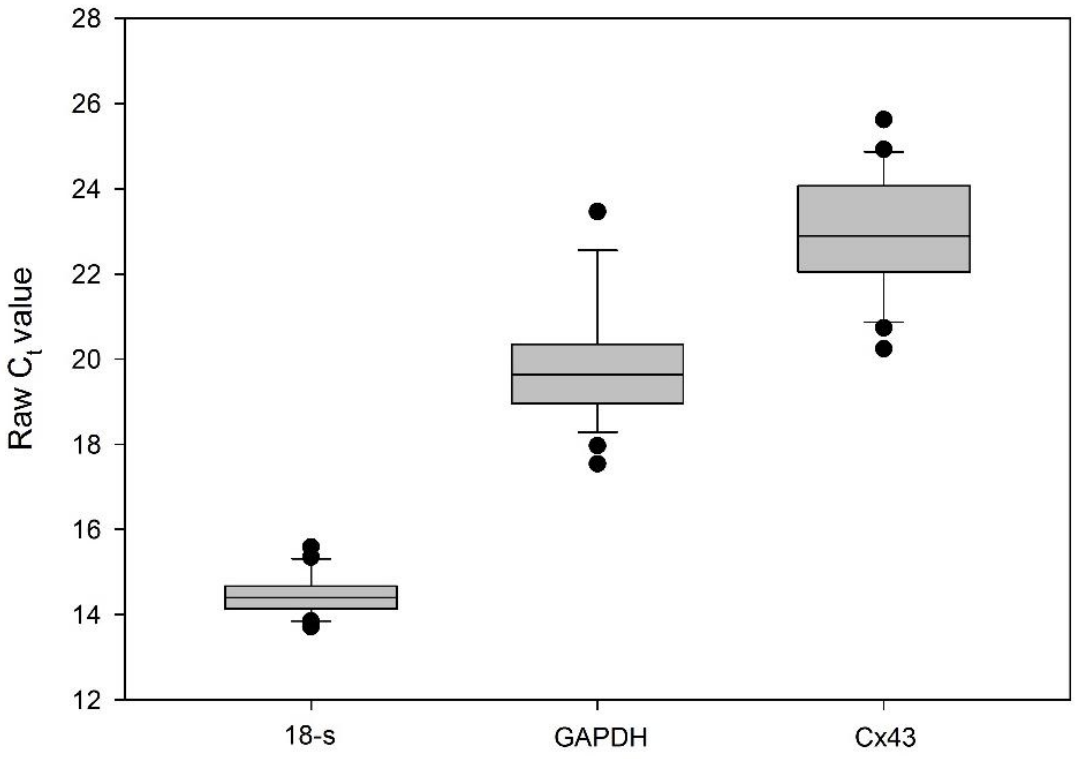

Figure 11: Raw C_t distribution with bars for the 3 genes selected as potential housekeeper genes with the median, 10th, 25th, 75th and 90th percentiles with error bars

Here we can see that the smallest distribution of values is for 18-S, this gene codes for part of the ribosome and has been widely used in cardiac genetic expression experiments and has not previously been demonstrated to be differentially expressed in diabetes or obesity[155, 156]. A selection of the gene expression results were then repeated with GAPDH and Cx43 to make sure that any changes seen with 18-s were along similar lines with the other housekeepers to give confidence to the existing results obtained using 18-S as our housekeeper. Whilst different values were obtained, there were no significantly different trends.

3.3.8. Conversion to relative abundance

As each single decrease in the number of cycles required for replication, equates to a doubling of the amount of mRNA, all values were logarithmically transformed to reflect the fact that a small change in ΔC_t value translates into a large change in mRNA expression.

Increasing ΔC_t values suggest a smaller amount of mRNA present as more replication cycles are required to amplify up to a detectable level. For the entirety of the study the results are presented in arbitrary units based on target gene expression referenced to 18-s.

3.4. Immunofluorescence (IF)

This technique is based on the use of specific antibodies to target proteins and then secondary multiple secondary antibody binding to the primary antibody with labelled fluorophores which can then be detected with microscopy.

The 10μm cryosection microscope slides were fixed in buffered 10% formalin. Sections were then washed in 1x phosphate buffered saline (PBS) before permeabilisation with 0.1% Triton-X 100 and non-specific blocking with bovine serum albumin (bSA) diluted in PBS (all, Sigma-Aldrich, Poole, UK).

Sections were then incubated overnight at 4°C in the dark with 1:100 primary antibody (rabbit anti-HCN4, Alomone, Jerusalem, Israel) in 1% bSA in PBS before washing with PBS and incubation in the dark at room temperature with 1: 500 secondary antibody diluted (donkey anti rabbit IgG, rhodamine, Millipore, Watford, UK) in 1% bSA in PBS for 2 hours. A negative control was undertaken using a section from a control animal incubated with secondary but no primary antibody based on previously reported specificity from this group and others [157, 158].

Sections were then washed with PBS before mounting with vectashield and analysis with confocal microscopy and quantitative signal intensity measurements in arbitrary manufacturer units.

3.5. Mathematical modelling of the action potential

Mathematical modelling has been used for some years in electrophysiological studies and is based on data recorded in myocytes with reconstruction of the currents and action potential using equations developed by Hodgkin and Huxley[159]. In this study we have used the model developed by Pandit et al.[160] and which can be used to look at the following ion currents and then to generate action potential curves for the epicardium and endocardium, thus reflecting a depolarization gradient:

- $I_{Ca\text{-}L}$-Long lasting Ca^{2+} Current
- I_F-Funny Current
- $I_{K,1}$-Inward K^+ Rectifying Current
- $I_{K,ss}$-Slowly Activating K^+ Rectifying Current
- I_{Na}- Na^+ Current
- $I_{Na/Ca}$-Na^+- Ca^{2+} Exchanger Current
- I_{to}-Transient Outward Current
- $I_{Na\text{-}K}$-Na^+- K^+ ATPase Current
- SR Ca^{2+} Release

This model while not exhaustive has been very widely used and validated [140, 161] and does provide useful modelling data based on mRNA expression as seen previously [162].

Before specific modelling of the funny current (I_f), the original model in Pandit et al.[160] was modified to incorporate experimental data models from Cerbai et al.[163] more specifically. The activation curve from Cerbai et al.[163], was fitted using the Boltzmann distribution (V_H = -87.74mV, k = -10.12):

$$y_\infty = \frac{1.0}{1.0 + e^{(V+87.74)/10.12}}$$

Where y_∞, is the steady-state value of the activation variable, y and v is the membrane potential. The time constant of I_f activation was reformulated based on data from Cerbai et al.[163]:

$$\tau_y = \frac{1.0}{0.1177 * e^{(V+86.78)/29.5}} + 0.8141 * e^{-(V+86.78)/14.75}$$

Where τ_Y. The rate of change in the activation variable, y, was calculated from:

$$\frac{dy}{dt} = \frac{y_\infty - y}{\tau_y}$$

Finally, I_f was calculated assuming that it is carried by a mixture of Na^+ and K^+:

$$I_f = g_f y[f_{Na}(V - E_{Na}) + f_K(V - E_K)]$$

Where g_f is the conductance f_{Na} and f_K are the fractions of I_f carried by Na^+ and K^+, E_{Na} and E_K are the equilibrium potentials of Na^+ and K^+ and $f_{Na} = 0.2$ and $f_K = 1 - f_{Na}$.

The maximum conductance, g_f (0.0043μS), was obtained by matching simulated current traces of I_f to experimental data.

As the original Pandit et al.[160] model for I_f, was altered to incorporate more closely experimental data from Cerbai[163] we have shown below our modelled values compared to the original data from Cerbai[163], with the activation curve shown in Figure 12a, voltage-dependence of the time constant of I_f activation in Figure 12b and finally the modelled I_f current density in Figure 12c.

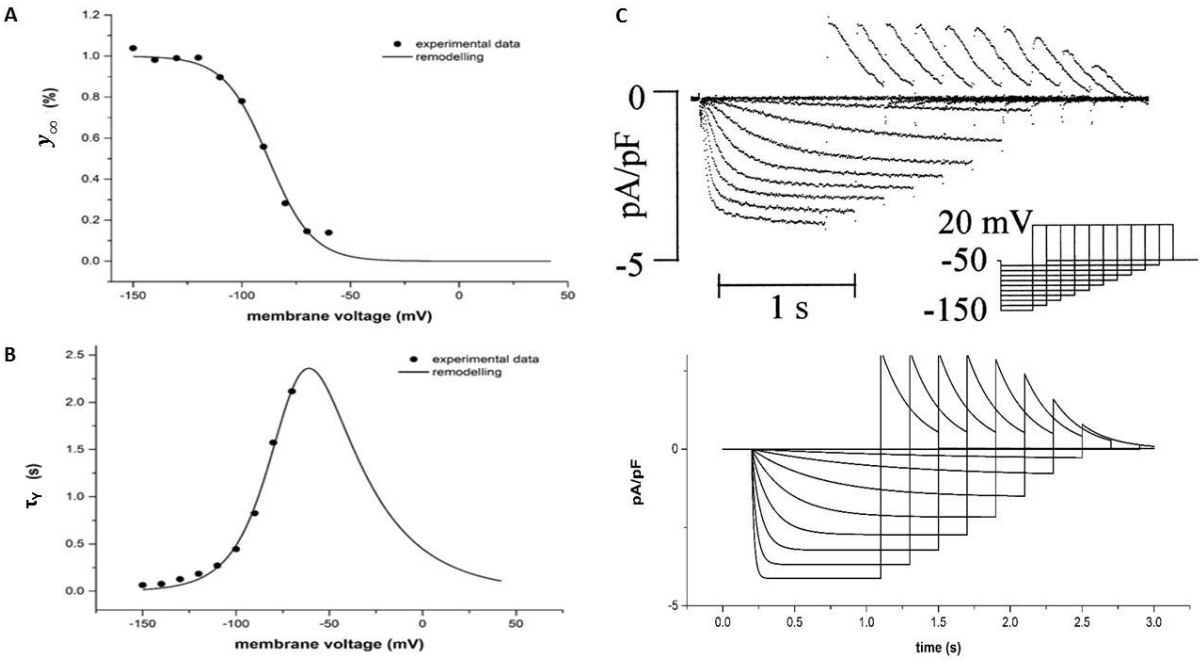

Figure 12: (A), I_f activation curve with experimental modelling and original data points from Cerbai et al.[163], (B), voltage-dependence of time constant of I_f activation with experimental modelling and original data points from Cerbai et al.[163] and (C), Experimental recordings from Cerbai et al.[163](top) and simulation (bottom) of I_f during the protocol.

For the rest of the ion channels, the Pandit et al.[160] model was used unchanged. In normal and obesity conditions, the models were run for a 5s period to obtain a stable state condition before a sequence of external stimulus pulses (with an amplitude of 0.8 nA, duration of 6 ms and frequency of 1 Hz) were applied to evoke an action potential. Ion

current density was scaled from the normal model based on a percentage change in mRNA expression compared in the obese model. In order to evaluate the relative role of each of the remodelled ionic currents, simulations were also performed by considering changes to each individual ionic current alone.

3.6. Human study

3.6.1. Patient recruitment

Written informed consent was obtained from all patients taking part in the study and the study was ethically approved by the Liverpool East Ethics Committee with subsequent NHS site approval at University Hospital Aintree and Liverpool Heart and Chest Hospital prior to the initiation of recruitment.

Subjects were male and females all aged 18 years and above diagnosed with types 2 diabetes and a control group without type 2 diabetes who were able to give informed consent. Criteria for inclusion were patients referred for aortic valve replacement for aortic stenosis with a normal left ventricular function being defined according to the definition of a preserved ejection fraction of greater than 50% as stated by the European Society of Cardiology [164].

Exclusion criteria for the study comprised of atrial fibrillation due to the effect on LV function, the presence of other conditions which may affect LV function (non-ischaemic causes of heart failure, untreated thyroid disease, anaemia with a Haemoglobin (Hb) of less than 10, history of alcohol abuse, presence of AV fistula, significant regurgitant valvular heart disease or hypertensive heart disease (clinical history of uncontrolled hypertension with echocardiographic criteria of left ventricular hypertrophy). Other exclusion criteria were chronic renal failure with an eGFR less than 30 mls/min/1.73m^2, requirement for additional surgery to CABG/AVR, the use of insulin in the treatment of their diabetes and patients with type 1 diabetes

3.6.2. Rationale for patient selection

The main factor for the choice of our patient population was the safety and surgical availability to obtain samples. The surgical team at our local centre perform a large amount of coronary bypass surgery off cardiopulmonary bypass i.e. with the heart moving so a safe biopsy would not be able to be taken. The surgeons at our centre perform aortic valve replacements on cardiopulmonary bypass and thus the heart is relatively static and a safe biopsy which is paramount can be taken. By minimising any confounding factors which may cause electrical remodelling or heart failure such as eliminating patients with atrial fibrillation we tried to find a group where any experimental change could be as closely linked to diabetes as possible.

Key pathological effects of type 2 diabetes and obesity in the myocardium, are the induction of LV hypertrophy[165] and myocardial fibrosis[166] both of which are associated with higher rates of arrhythmias[138, 167]. There are many potential mechanisms of arrhythmogenesis related to hypertrophy and fibrosis including slowed conduction, early after-depolarizations and enhanced automaticity[138] as mentioned previously. Cardiac hypertrophy and fibrosis in the absence of other causes such as high blood pressure or ischaemic heart disease can be seen in other cardiac diseases such as valvular aortic stenosis[168] again with increased rates of arrhythmias[169]. It is unclear how much of the arrhythmic potential seen in diabetes/obesity relates to hypertrophy and fibrosis and how much is due to specific genetic changes related to diabetes or obesity. In preparation for this study we have reviewed many studies which while researching changes in diabetes and obesity have tended to use normal animals/patients as the control while not addressing the potential concern that much of the arrhythmogenic potential is related to hypertrophy and fibrosis. We chose to compare our group with diabetes with a control group of patients with aortic stenosis, which causes pressure overload and results in LV hypertrophy and fibrosis and so hopefully will help prove that any changes are related to a diabetic process specifically and not just due to hypertrophy/fibrosis. We have also taken into account the fact that type diabetes is closely associated with the metabolic syndrome and obesity and again have tried to match our control group closely in terms of average BMI and central adiposity so that the control group would be similar to the diabetes group so that again this

would give us the best chance of showing that the changes seen are related specifically to diabetes and not obesity.

In our study we have chosen not to include patients on insulin treatment as insulin has been shown to have a wide range of effects within the myocardium including positive inotropy, reduced oxidative stress, improved metabolism and reduced apoptosis[170]. It was felt that these effects may suppress the pathological process and ameliorate any changes seen in our group with diabetes. As a large part of the clinical burden of cardiomyopathies is arrhythmogenic, we felt that when looking at the gene expression changes underlying this including patients with insulin would not be appropriate. This is due to the fact that insulin has been shown to activate a voltage-dependent, nonselective cation channel with prolongation of the action potential[171]. Insulin has also been shown to alter cardiac calcium levels and action of NCX1[172]. Previous studies have shown that experimental differences seen in animal models of diabetes, specifically in cardiac potassium channel gene expression can be reversed with the administration of insulin[173], and for this reason and the other reasons mentioned above, we did not include any patient who was receiving insulin treatment.

By selecting a control group that unlike many other studies is subject to similar hypertrophic/fibrotic changes and by omitting insulin usage in our group with diabetes, we feel that our results should reflect changes related to diabetes as specifically as possible.

3.6.3. Patient characteristics

Patients then had their height, weight and waist circumference measured, BMI calculated and patients with diabetes had their most recent glycated haemoglobin recorded. All patients had the use of statin drugs, beta blockers, ACE inhibitors/angiotensin receptor II blockers (ARBs) and patients with diabetes had their diabetes treatments recorded. We also recorded if any of the patients with diabetes were known to have any complications of diabetes such as retinopathy, neuropathy or nephropathy.

3.6.4. ECG protocol

All patients had their resting standard 12 lead ECG reviewed for their corrected QT interval (QTc) as measured by automated computer software installed with each ECG machine.

Standard electrocardiography is limited to frequencies up to 150Hz and many of the highest amplitude signals of the heart are above this. Therefore, standard electrocardiography may miss some of the higher frequency signals whereas signal averaged electrocardiography allows for a much broader bandwidth and therefore the ability of these higher frequency cardiac electrical signals. The signal averaged ECG also allows for processing over a prolonged period with noise reduction filtering to remove skeletal muscle noise and allow for a more accurate averaged measure of the QRS.

The signal averaged ECG has been shown to be superior to the standard ECG for the detection of a variety of cardiac electrocardiographic abnormalities compared to a standard electrocardiogram including for the detection of coronary ischaemia[174].

All patients underwent signal averaged ECG monitoring following a period of rest for 10 minutes in the supine position for 10 minutes using a MAC 500 machine (GE healthcare, Amersham, UK) prior to cardiac surgery.

Electrodes were placed in the standard position for the procedure as described previously[175].

Digital filtering was performed with a 40-250HZ band pass bidirectional filter and averages were taken over 250 beats with maximum acceptable noise of 0.5μV.
All ECGs were analysed for late potentials using previously reported values consisting of two of the following three criteria: filtered QRS greater than 114ms, voltage of the root mean square of the terminal 40 msec of the vector QRS less than 20ms and/or low amplitude signals greater than 38ms[176]

3.6.5. Echocardiography

Echocardiography is a well-known and well-validated method of assessing cardiac structure and performance in a non-invasive way, quickly and reproducibly. Echocardiography is based on the use of transducer generated sound waves reflected through the body and processed through a computer to generate images of the heart.

3.6.5.1. Strain analysis

Using the Doppler principle, echocardiography can be used to measure myocardial deformation and therefore strain by tracking areas of the heart muscle and measure their movement over a distance and thus strain using the formula, as an example for longitudinal strain.

$$\frac{L_{strain}\%= L_{start}-L_{end}}{L_{end}}$$

This will give a negative percentage for contraction and positive for elongation, except when measuring radial contraction, where the value will be positive. This method allows for a degree of measurement of the actual myocardium and thus an inference about the contractile performance.

Using a suppression software to ignore the higher velocity signals from blood flow, the machinery can pick up the lower velocity signal from the myocardium and track the process of the muscle either by tracking of the unique speckle pattern (speckle tracking imaging-STI) or by placing a region of interest (ROI) cursor over a specific muscle area (tissue velocity imaging-TVI).

An example of speckle tracking is shown below in Figure 13:

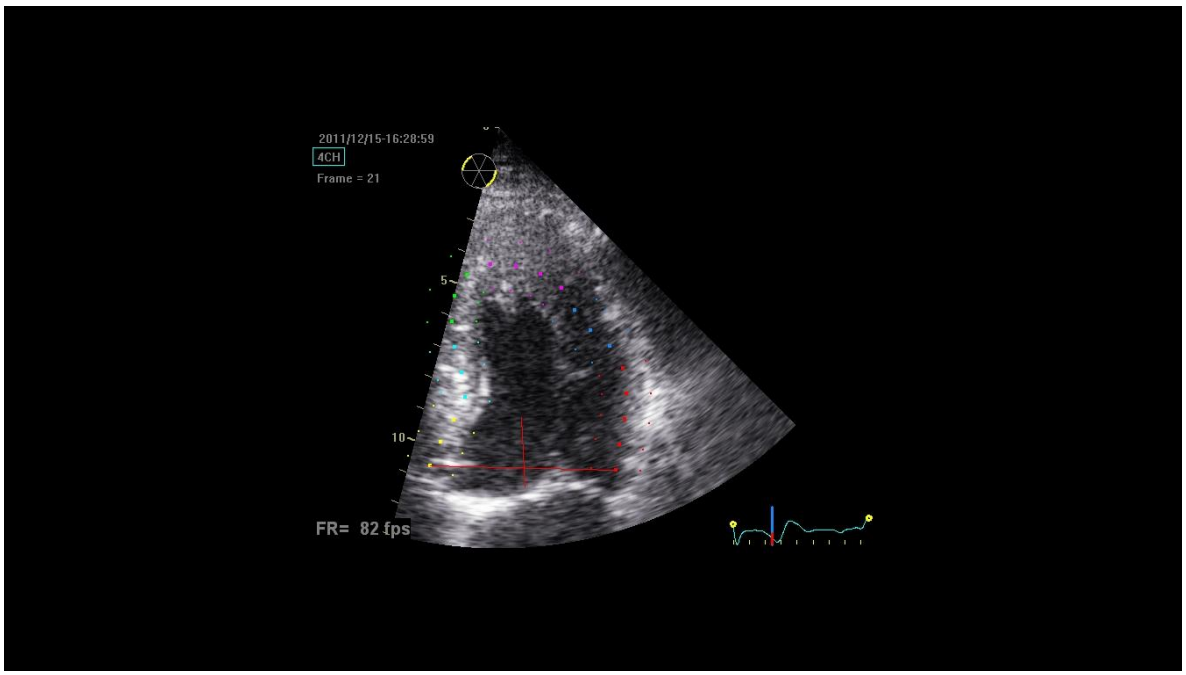

Figure 13: Echocardiographic speckle tracking of the myocardium in the apical 4 chamber view

This then allows for production of strain curves and strain values in a variety of different directions including longitudinal, radial and circumferential covering the different fibre orientations and contractile directions of the heart.

An example of strain curves is shown below for circumferential strain using speckle tracking in Figure 14:

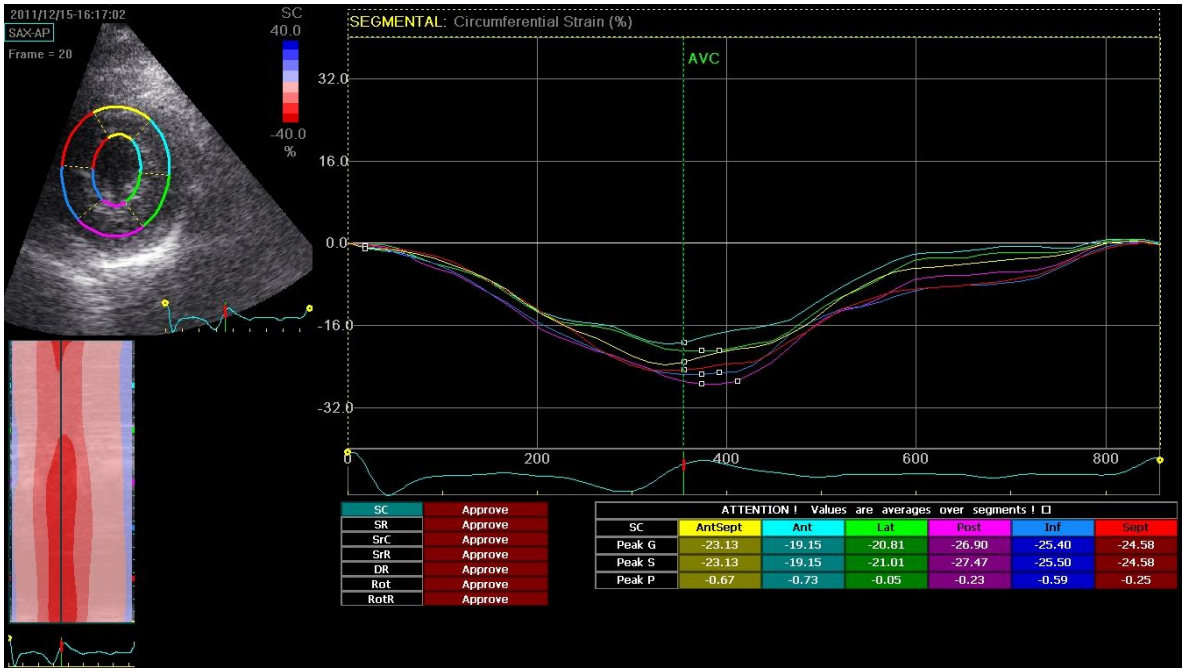

Figure 14: Strain curves and values using speckle tracking in the parasternal short axis for circumferential strain

3.6.5.2. Speckle vs. tissue velocity imaging

Both methods can be used to measure myocardial strain and accurately assess the contractile performance of the left ventricle and share some common methodologies and some important differences which are reviewed below.

TVI, measures myocardial deformation by measuring in a region of interest between two frames, the instantaneous velocity of a point and the acquisition time of one frame to

another, which then can be used to infer the displacement of that point between frames. This region of interest is placed by the operator and normally is placed in the mid-myocardium but may capture epi- or endocardium depending on image quality. TVI uses high frequency pulse wave repetition to enable capture at high heart rates and frame rates. STI, tracks the unique myocardial speckle pattern and by measuring the time between two frames, myocardial speckle velocity can be calculated and this is then averaged across the epi-to endocardium.

Because the myocardium accelerates and decelerates and is not at a constant velocity with a sudden stop, the two methods are not interchangeable [177] but comparable for general trends. Also due to the complexity of the methodology, STI cannot be used at very high frame rates or heart rates as tracking of the speckles, is not possible which is not an issue using TVI. TVI can be performed online while acquiring images which is useful in time limited clinical situations and STI can only be performed offline. STI, by comparison because it is not dependent on the angle of a pulse wave signal does not become less accurate if the insonation beam is not in line with the deforming myocardium [178]. STI therefore can be used to assess radial strain in a way that TVI cannot reliably be used due to issues with the angle of insonation. STI, has one important area of superiority in diseased states compared to TDI in that it is not subject to the tethering effect whereas TVI is [179]. The tethering effect is caused when non-moving fibrous/scar tissue is pulled by the adjacent moving myocardium. In this situation TVI derived strain assumes the pulled area of myocardium to have contracted appropriately and assigns strain to it despite the fact it does contract itself. As STI measures speckles directly, it sees the non-moving speckle and accordingly assigns it to a zero strain value, signifying a diseased piece of myocardium. In this study we have predominantly used speckle tracking as measurements are being made offline and for superior reliability we believe based on the information above and because of the variability in curve analysis and region of interest placement.

3.6.5.3. Correlation with myocardial fibrosis

Myocardial fibrosis can be assessed commonly by two methods, cardiac MRI or histological examination but there have been studies in hypertrophic cardiomyopathy [180], Fabry's

disease[181], aortic stenosis[168] and diabetes[182] looking at the correlation of 2d speckle tracking strain rate using echocardiography with fibrosis.

In many studies a global contrast-enhanced myocardial T_1 mapping time on MRI of less than 500ms has been shown to correlate clearly with fibrosis[183] and a T1 mapping time of less than 500ms has been correlated with a global longitudinal strain of less than -18% using 2D speckle tracking echocardiography[182]. In this study as we unfortunately did not have access to cardiac MRI imaging or potentially enough human tissue for full histological analysis, the use of strain analysis has been used to infer fibrosis within the ventricle in both our human groups. By showing that both groups have probable evidence of fibrosis, we hope to show that whatever changes we see in terms of gene expression are not a consequence of fibrosis and not a common final pathway but changes specific to diabetes.

In this study to show that there was subclinical dysfunction that could not be seen using standard method such as an ejection fraction, we compared our global longitudinal strain values to published normal reference values[184] to try and show clear evidence of a myopathic phenotype.

3.6.5.4. Echocardiography protocol

All patients underwent 2-dimensional echocardiography prior to cardiac surgery using commercially available vivid Q, vivid 7 (GE healthcare, Amersham, UK) and IE 9 (Phillips, Guilford, Surrey) systems and a 3.5 MHz transducer.

Patients were studied in the left lateral decubitus position following a 15-minute rest period. Conventional imaging allowing M-mode and two-dimensional assessment of left ventricular dimension and function was performed according to published guidelines and using the 16 segment model [185]. All images were acquired over three successive cycles and all measurements averaged over the three cycles. Images were taken with a narrowed sector width and with a frame rate of 50-100 fps and then at 100 fps and above.

Images were taken in the following positions for the following measurements summarised in Table 6:

Echo window	Measurement
Parasternal long axis view	Measurement of LV septal width, end systolic and diastolic diameters,
Parasternal short axis view-mitral level	WMSI
Parasternal short axis view-basal level	WMSI and speckle track strain
Apical 4 chamber	WMSI and speckle track strain
	M mode of the lateral mitral annulus systolic excursion, Simpson's
	biplane ejection fraction, WMSI, speckle track strain, TVI strain, left
Apical 2 chamber	atrial size and left atrial volumes
	Simpson's biplane ejection fraction, WMSI, TVI strain, left atrial size,
Apical 3 chamber	left atrial expansion index, speckle track strain and left atrial volumes
	Simpson's biplane ejection fraction, WMSI, speckle track strain and TVI
	strain

Table 6: Standard echocardiographic measurements used in this study

Wall motion scoring index (WMSI) was calculated as 1 for a normal segment, 2 for a hypokinetic segment, 3 for an akinetic segment, 4 for a dyskinetic segment and 5 for an aneurysmal segment with 16 being a normal score as previously published[186].

Filling and diastolic function was assessed using pulsed-wave Doppler imaging of mitral inflow at the mitral valve leaflet tips at a frame rate of 80-100 fps for calculation of a maximal E velocity, A velocity and E: A ratio. Tissue velocity imaging was then performed of the lateral mitral valve annuluses for E/E' ratios as a measurement of LV filling pressures and diastolic function.

Measurements of LV end diastolic, systolic and septal width diameter were all made using a cursor placed across the LV septum with a straight line just in front of the tips of the mitral valve leaflets in accordance with published guidelines[187].

M mode of the lateral mitral valve systolic annulus excursion (MAPSE) was measured with the standard M mode cursor at angle of less than 15^0 of insonation and measured from the top of the baseline to the peak of the curve.

Measurement of left atrial pathology was made in several ways with calculation of left atrial (LA) area made by free hand outlining of the left atrial area in the apical four chamber position just before the opening of the mitral valve. The left atrial volume was calculated using the area/length method in the apical 2 and 4 chamber views[185].

Active atrial function was measured in three ways using the respective formulae:

Left atrial expansion index (LAEI)= left atrial maximal volume —left atrial minimal volume/ left atrial minimal volume x 100. This measures the ability of the left atrium to acts as a reservoir for blood.

Left atrial passive emptying fraction (LAPEF)=maximal left atrial volume -- left atrial volume on the ECG P wave/maximum left atrial x100. This represents the left atrial conduit function.

Left atrial active emptying fraction (LAAEF)= left atrial volume on the ECG P wave – left atrial minimal volume/ left atrial volume on the ECG P wave x 100. This assess the pure pump function of the left atrium[188].

Offline measurement of strain (ECHOPAC™, GE healthcare, Amersham, UK) was made predominantly using speckle tracking software but with a comparison of measurements using TVI strain. All speckle measurements were made over a single cycle using the commercially available automated software.

Offline images were analysed using automated border tracking software and systolic yo-yo tool for confirmation visually of appropriate speckle tracking. When the operator was satisfied with image / tracking quality, the automated tracking software, would then attempt to measure speckle movement for each region and if successful would visually represent this with a green tick. If the tracking quality was poor the segment would be rejected and the operator could manually readjust the border tracking to attempt to improve the speckle tracking, depicted below in Figure 15.

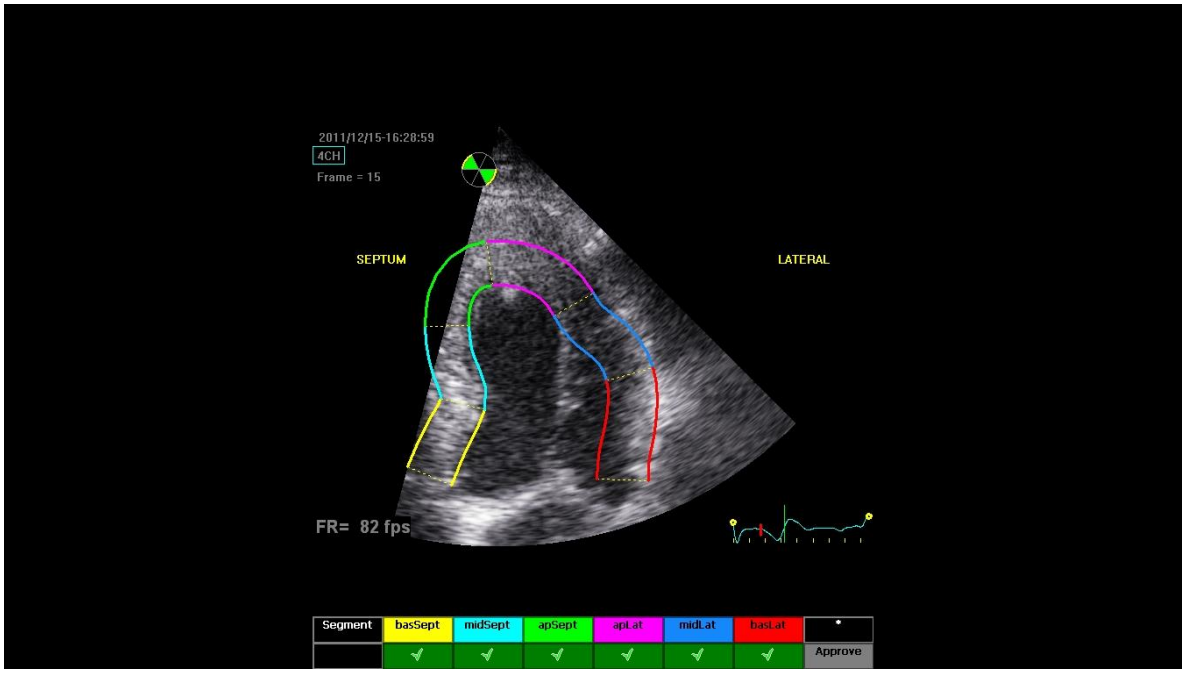

Figure 15: Automated confirmation of appropriate speckle tracking

Once complete, the automated software would then generate an automatic set of peak systolic strain timed to aortic valve opening as seen in Figure 15 as the peak S value.

Measurements were made in apical 2, 3 and 4 chamber for global longitudinal strain with values from each segment being averaged from 6 segments for a mean score. Circumferential and radial strain was measured using a mean score from 6 segments in the parasternal short axis at the mid wall level as previously described[189].

Tissue Velocity measurements were made in apical 2, 3 and 4 chamber and in the parasternal short axis at the mitral valve leaflet level for longitudinal strain and circumferential strain respectively. Measurement of strain was made offline with the pre-recorded 3 cycle TVI loops at which point a ROI cursor was placed over the respective region to be interrogated using the 16 segment model. A strain curve was obtained and the peak systolic value recorded and this repeated over the three cycles for an average value.
An example curve is shown below in Figure 16:

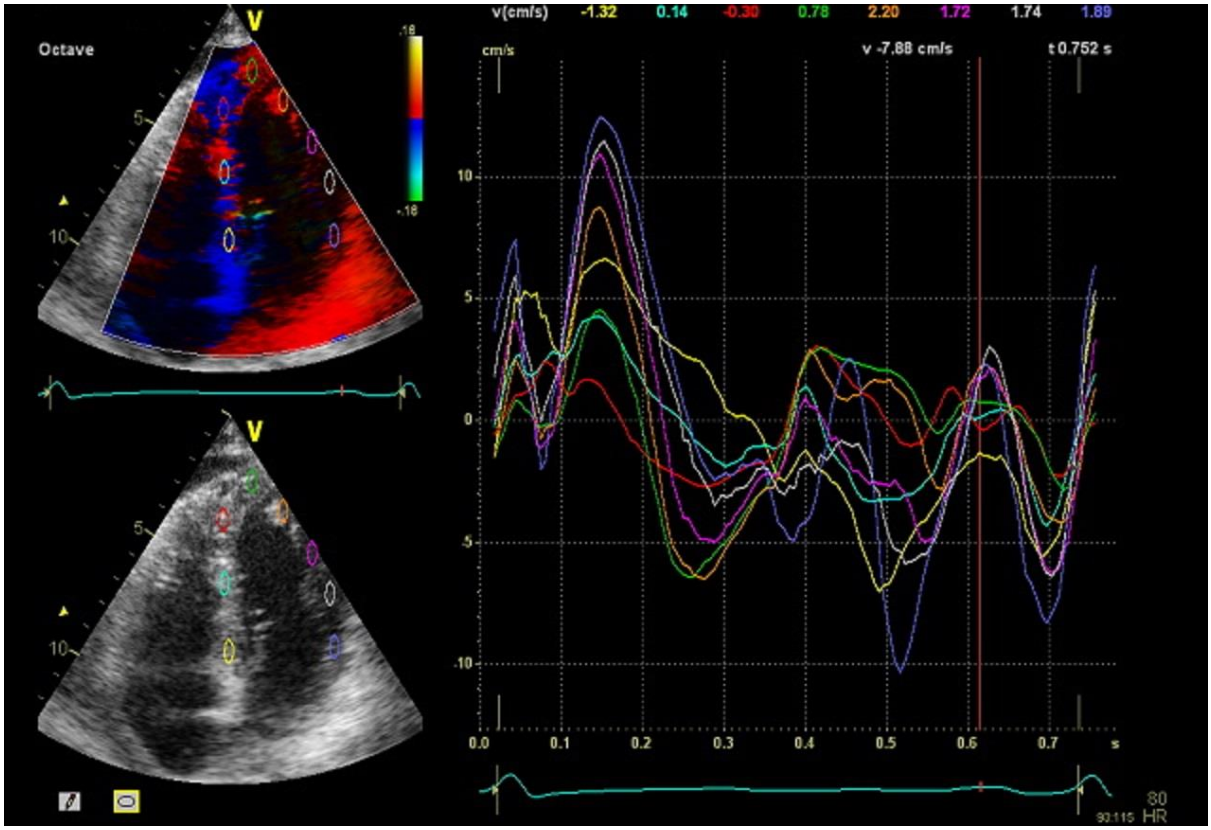

Figure 16: An example of TVI strain curves

For evaluation of the methods used, 5 selected patients (with the clearest image quality) had a selection of the echocardiographic measurements re-measured for intra-observer variability, inter-observer variability by a second blinded British Society of Echocardiography accredited echocardiographer and for a comparison of TVI vs. speckle tracked strain. The repeated standard measurements investigated at for variability were ejection fraction, septal width and lateral MAPSE

For analysis of methodology, a visual Bland-Altman plot was used based on its widespread as the predominant measurement of observer variability in echocardiography studies[190, 191] and due to the fact that there is no recommendation from the expert consensus groups in echocardiography. All measurements were also compared using a t-test.

3.6.6. Left ventricular biopsy

All patients had their biopsy sample taken by an experienced consultant cardiothoracic surgeon at the LV apex in the anatomical position normally used for puncture of the LV in

transapical aortic valve implantation. The biopsy was performed using a single TRUCUT™ biopsy needle (Cardinal Health, Dublin, Eire) just prior to the insertion of cardioplegia solution. The sample was then taken and immediately placed in physiological Hartman's solution (Baxter, Newbury, UK) before immediate transfer to the lab for processing. Initially, the experimental plan was to take all the samples and process them topographically as in the streptozocin rat experiment but unfortunately due to the variable quality and size of samples, it could not always be confirmed a full thickness sample encompassing all layers was taken. All samples were placed in OCT before flash freezing liquid nitrogen.

3.6.7. RT-PCR for human samples

3.6.7.1. Left ventricle RNA isolation

The left ventricle tissue was processed in a similar manner to the rat tissue for RNA isolation but with the proprietary mirVana™ RNA isolation kit (Invitrogen, Paisley, UK) which uses a slightly different filter method to enable capture of very small amounts of RNA.

The left ventricular tissue was taken from the freezer and added to 300µl of lysis buffer to the sample and homogenised for 2 minutes using a polytron rotor homogeniser. To this 30µl of miRNA homogenate additive was added and mixed by vortexing before 300µl of acid-phenol: chloroform was added and mixed by vortexing for 1 minute. The solution was centrifuged at 10,000 rpm for 5 minutes and the supernatant removed to a fresh tube and 375µl of 100% ethanol added and mixed by pipetting. This mixture was then transferred to a filter cartridge in a collection tube and centrifuged at 10,000rom for 15 seconds and the flow through discarded before 700µl of wash solution 1 was added to the cartridge and centrifuged for 15 seconds and the flow though discarded again. The mixture was washed twice with 500µl of wash solution 2/3 and centrifuged at 10,000 rpm for 30 seconds with the flow through discarded.

The cartridge was placed in a new collection tube and 100µl of heated elution solution (95^{0}C) added and centrifuged at 10,000rpm for 30 seconds. The resulting RNA was then frozen at -80^{0}C.

3.6.7.2. RNA processing and qPCR

The obtained RNA samples were processed for qPCR using similar laboratory techniques as the two rat experiments and identical laboratory supplies. The qPCR probe information is shown below in Table 7 again using the NCBI gene database as a reference[153].

Gene	Gene Name	Context Sequence	Chromosome
18-S	Eukaryotic 18-S	CCATTGGAGGGCAAGTCTGGTGCCA	22p12
ANO1	Anoctamin 1	GTTCTTCAAAGGCCGGTTTGTTGGA	11q13.3
ATP1A1	Na^+/K^+ ATPase 1a1	GTATCCCCTCAAACCTACCTGGTGG	1p21
ATP1A2	Na^+/K^+ ATPase 1a2	GACCTGTCCAAGGGCCTCACCAACC	1q23.2
ATP1A3	Na^+/K^+ ATPase 1a3	GTTAACCCCCGGGATGCCAAGGCCT	19q13.31
ATP2A2	Cardiac Sarcoplasmic Reticulum Ca^{2+} Activated- ATPase 2a	AGATGTCTGTCTGCAAGATGTTTAT	12q24.11
BEST1	Bestrophin 1	GGAAAACAGGGATGAAGCACATTCC	11q13
BEST2	Bestrophin 2	CTTCGTGCTTGGCTTTTATGTGACG	19p13.2
BEST3	Bestrophin 3	ACCACGTGGTTGAAGCAGGTTTTAT	12q14.2-q15
CACNA1C	L-type Voltage-Gated Ca^{2+} Channel Alpha Subunit 1c	ACCAATTCCAACCTGGAACGAGTGG	12p13.3
CACNA1D	L-type Voltage-Gated Ca^{2+} Channel Alpha Subunit 1d	GAATGGAAACCATTTGACATATTTA	3p14.3
CLCN2	Cl^- Channel 2	AGACCCTGATGTATGGCCGGTACAC	3q27.1
CLCN3	Cl^- Channel 3	GTGACACTGCAGTTGGAACTCATTA	4q33
GAPDH	Glyceraldehyde-3-phosphate dehydrogenase	GACCAGTGGTGCGCTGAGCCCTGCC	12p13
GJA1	Gap Junction Alpha 1	GAGGAGGAAAAGAAGCAGAAGTTTT	6q22.31
GJA5	Gap Junction Alpha 5	CTTACAGTGATTTCAGGTTTTACTG	1q21.1
HCN1	Hyperpolarisation Activated Gated K^+ Channel 1	ATCAGTGGGAGGAGATCTTCCACAT	5p12
HCN2	Hyperpolarisation Activated Gated K^+ Channel 2	CCCTACAGTGACTTCAGATTTTACT	19p13.3
HCN4	Hyperpolarisation Activated Gated K^+ Channel 4	ATGATGGCTTATTACAGTGGCAATG	15q24.1
KCNA4	K^+ voltage-gated channel, shaker-related subfamily, 4	ATGGGAGGCTTGCTGAACATGGATA	11p14
KCNA5	K^+ voltage-gated channel, shaker-related subfamily, 5	TCTAACAGCCGATCCAGTTTAAATG	12p13
KCND2	K^+ voltage-gated channel, Shal-related subfamily, 2	CACAACCAGTCGCTCCAGCCTTAAT	7q31
KCND3	K^+ voltage-gated channel, Shal-related subfamily, 3	CTCTGGCTCTGAGGAGCTGATCGGG	1p13.3
KCNH2	Human Ether Related a Go-Go	CAGTTCTTTCCTCAAGGAGACTCCA	7q36.1
KCNIP2	K_v channel-interacting protein 2	CCTGCGCCAGCAACAGGACATGTTC	10q24
KCNJ2	K^+ inwardly-rectifying channel, subfamily J, 2	AAGCTGCTCAAATCTCGGCAGACAC	17q24.3
KCNJ3	K^+ inwardly-rectifying channel, subfamily J, 3	GTGGAAGCCACAGGCATGACCTGCC	2q24.1
KCNJ5	K^+ inwardly-rectifying channel, subfamily J, 5	CACCCACATCTCACAGCTGCGGGAA	11q24
KCNQ1	K^+ voltage-gated channel, KQT-like subfamily, 1	CATTACTGCAGGCCACCTACTCATG	11p15.5
MT-ATP6	Mitochondrially Encoded ATP Synthetase 6	GGCCCACCATAATTACCCCCATACT	N/A
MT-ATP8	Mitochondrially Encoded ATP Synthetase 8	CTCAAAGCAGCAGGAGCAGATCCCC	N/A
NGF	Nerve Growth Factor	CTCTCTATTTGTGGACAACTGAGAC	1p13.1
RYR2	Ryanodine Receptor 2	CCCGCCAGACACGACCACGCCATCG	1q43
SLC2A4	Glucose Transporter 4	ACAGATAGGCTCCGAAGATGGGGAA	17p13
SLC8A1	Na^+-Ca^{2+} Exchanger	TCACTGTCAGTGCTGGGGAAGATGA	2p22.1
SCN5A	Na^+ Channel, Voltage-Gated Type Vα	TGAGAAAGTGTACCACATCTGTGTG	3p21
TACR1	Tachykinin Receptor 1	GATTCGGCGGGACGGGCTGCTCCTG	2p12
TH	Tyrosine Hydroxylase	TGGCCCAGGCAGTCAGATCATCTTC	11p15.5
TTYH-1	Tweety Homolog 1	CTCCCCTCCGCCTACGTACTCTCCC	19q13.4
TTYH-2	Tweety Homolog 2	TCCCCGCCGCCCTCATACACCTCCA	17q25.1
TTYH-3	Tweety Homolog 3	ACAGGAAGGCCAATGTCGGGTAGAT	7p22
Uchl1	Ubiquitin Carboxyl-Terminal Esterase L1	CCATTGGAGGGCAAGTCTGGTGCCA	4p14

Table 7: Gene targets in the human study

Between the human and rat experiments some gene targets were changed, this was on the basis of poor results with some targets and positive results with other which suggested expansion of a particular gene group of interest (e.g. extra Cl^- channels in the human experiment).

3.6.8. Mathematical modelling of the action potential

In the human experiment, we again used mathematical modelling to look at the putative effects of our qPCR results on the AP and to try and infer how these changes may prove arrhythmogenic. Similar to our obesity experiment, we used a previously published system the O'Hara-Rudy dynamic model which uses experimental data based from non-diseased human ventricular cells and then mathematical analysis to generate a mathematical model of the human AP[192]. Mathematical modelling is very important in electrophysiological study of human subjects as the obtainment of multiple tissue samples to perform multiple patch clamp experiments can be very difficult to justify from a safety point of view.

The O'Hara-Rudy dynamic model is able to model 14 currents and incorporate 41 different equations to model effects on the human AP but we have chosen to use it because it illustrates the effect of I_{Kr} blockage more effectively than other AP models. Using this model, channel conductance was scaled according to the measured average ratio of mRNA between the control and the diabetes groups. In the control and the diabetes groups, the models were run for a 5 s period to obtain a stable state condition before a sequence of external stimulus pulses (with an amplitude of 0.8 nA, duration of 5 ms and frequency of 1 Hz) were applied to evoke an action potential and record the change globally. In a similar manner to our rat experiment, we used scaled mRNA expression changes in our diabetes group compared to control in order to scale changes in current expression. In order to evaluate the relative role of each of the remodelled ion channels, simulations were also performed by looking at the change to each individual ion channel alone.

3.7. Statistical analysis

Prior to the study beginning, a decision was made to set up this project as an exploratory project which may then identify areas of interest for further work with larger sample sizes.

We then reviewed the published research output of department in terms of gene expression studies and the number of subjects previously used in these experiments which suggested groups of a minimum of six were required for useful data to be obtained and compared [193]. As we were dealing with small groups in an exploratory fashion, a power calculation was not undertaken with the knowledge that any findings in this project would not be definitive and would need larger samples for confirmation.

All experimental work was analysed using SigmaPlot™ version 12.5 (Systat, San Jose, USA). Significant results were taken as being with a p value of <0.05. All statistical methodology was chosen after consultation with a statistician at the University of Liverpool. Grouped mean data are reported as mean ± standard error of the mean (SEM).

The STZ rat experiment was analysed using a two-way ANOVA to look for significant differences across the LV wall by region and then between the overall mean in the STZ group and control group. To identify where specifically the differences were located by region, a Tukey's honestly significant difference (HSD) post hoc multiple pairwise comparison test was applied. All single variable experimental work was analysed for significance using an unpaired student's t-test again if the data passed a Shapiro-Wilk test of normality and if not then a rank sum test was applied. Analysis of categorical variables for significant differences between the two groups was undertaken using a Fischer exact test. Results were taken as being significant with a p value of <0.05.

Methodological comparison was undertaken using the well-established Bland-Altman (BA) method which is often used as the gold standard in medical methodological comparison in cardiac imaging studies [194]. The BA method allows for the sample visual representation of how well two methods agree without the difficulties encountered using the correlation coefficient or regression analyses. Methods are considered to agree if when plotted, the difference between the methods and their mean fall with 1.96 standard deviations (representing the 95% confidence interval (CI)). If there is poor agreement between the two methods, multiple scatter dots will be seen outside the 95% CI bars.

4. STZ rat: Type 1 diabetes model

4.1. Animal characteristics

Baseline and terminal weights with weight gain are shown below for control and STZ animals with significantly poorer weight gain in the STZ group and lower final weight (p<0.01). Results are shown in Table 8:

Group	Base Weight (G)	Final Weight (G)	Gain (G)	Glucose (mmol)
STZ	362.78(5.51)	383.44(16.71)	20.66(12.66)	Unrecordable (above 25mmol/l)
Control	358.38(7.01)	579.75(13.65)**	221.37(8.32)**	5.33 (0.28)

Table 8: Baseline and final rat characteristics showing means ± SEM shown (n=8/group). **Significantly different from the control group (p<0.01).

4.2. STZ rat RT-PCR results

4.2.1. Major ion channels active during the action potential

Expression of the major ion channel genes in the left ventricle were measured in all three myocardial layers for the STZ rat (n=8) and for the control group (n=8). Primary analysis was made looking at a difference of the mean for STZ group vs. the control with a post-hoc analysis to look for a specific regional difference.

Expression of SCN5A responsible for the primary cardiac Na^+ current (I_{Na}) was significantly lower in its expression in the STZ group with this reduction located in the mid-myocardial layer (p<0.01 Figure 17). Expression of the L-type Ca^{2+} channel, $Ca_v1.2$ (CACNA1c), responsible for the L-type Ca^{2+} current ($I_{Ca\text{-}L}$) was not significantly different between the two groups (p=0.175). Expression of $K_v1.4$ (KCNA4) which is responsible for the slow transient outward K^+ current ($I_{to\text{-}s}$) was significantly increased in the STZ group in all three layers of the LV (P<0.01) but $K_v1.5$ (KCNA5), the ultra-rapid delayed rectifier K^+ current ($I_{K,ss}$) was not statistically altered in its expression between groups (p=0.357). Expression of $K_v4.2$ (KCND2) and $K_v4.3$ (KCND3) which are responsible for the fast transient outward K^+ current, were not significantly different in the two groups but the auxiliary subunit KChIP2 (KCNIP2) was significantly reduced in the STZ, predominantly in the mid and epicardial layers (P<0.01 and

0.026 respectively). In the STZ group, there was significantly reduced (P<0.01) expression of ERG responsible for the rapid delayed rectifier K^+ current ($I_{K,r}$) with this change located in the mid-myocardial layer, as was expression of K_vLQT1 (KCNQ1) responsible for the slow delayed rectifier K^+ current ($I_{K,s}$) (p<0.01).

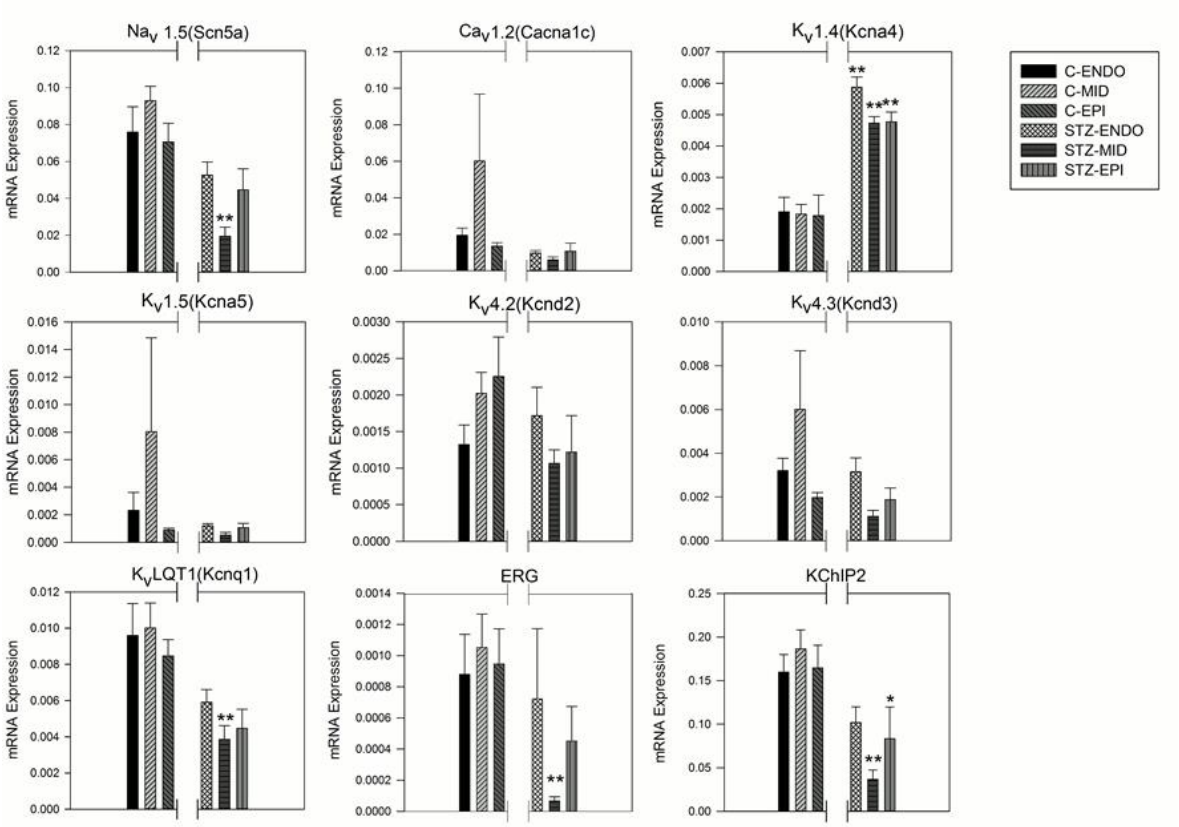

Figure 17: Expression of mRNA for major ion channels active during the action potential in the left ventricle of the control and STZ groups for each section of the myocardium displayed in arbitrary units referenced to expression of 18-s (housekeeper gene). C=control STZ=streptozocin, Endo=endocardium, Mid=mid-myocardium and Epi=epicardium. Means ± SEM shown (n=8/group). *Significantly different from the control group (p<0.05). **Significantly different from the control group (p<0.01).

4.2.2. Major ion channels active during diastole

Three channel isoforms, HCN1, HCN2 and HCN4, are responsible in varying amounts for the funny current (I_F), an important pacemaker current, both cardiologically and neurologically. Expression of all three isoforms tended to be lower in the STZ group, but only the decrease in HCN2 (predominantly expressed in the nervous system [195]) was significant with the

reduction primarily in the endocardium and mid-myocardium with a smaller reduction in the epicardium (p<0.01, p<0.01 and p=0.021 respectively; Figure 18). There was no significant change in expression (p=0.413) of K_{ir}2.1 (KCNJ2) responsible for the background inward rectifier K^+ current ($I_{K,1}$). Expression of K_{ir}3.1 (KCNJ3), primarily an atrial channel responsible for the ACh-activated K^+ current ($I_{K,ACh}$) (in conjunction with and K_{ir}3.4 (KCNJ5) as a tetrameric channel) was significantly reduced in the STZ group compared to control with the difference focussed in the mid-myocardial layer (p<0.01). We did not observe any significant difference in K_{ir}3.4 (KCNJ5) expression between groups which composed the other half of the channel (p=0.081) but expression tended to be similarly lower in the mid-level.

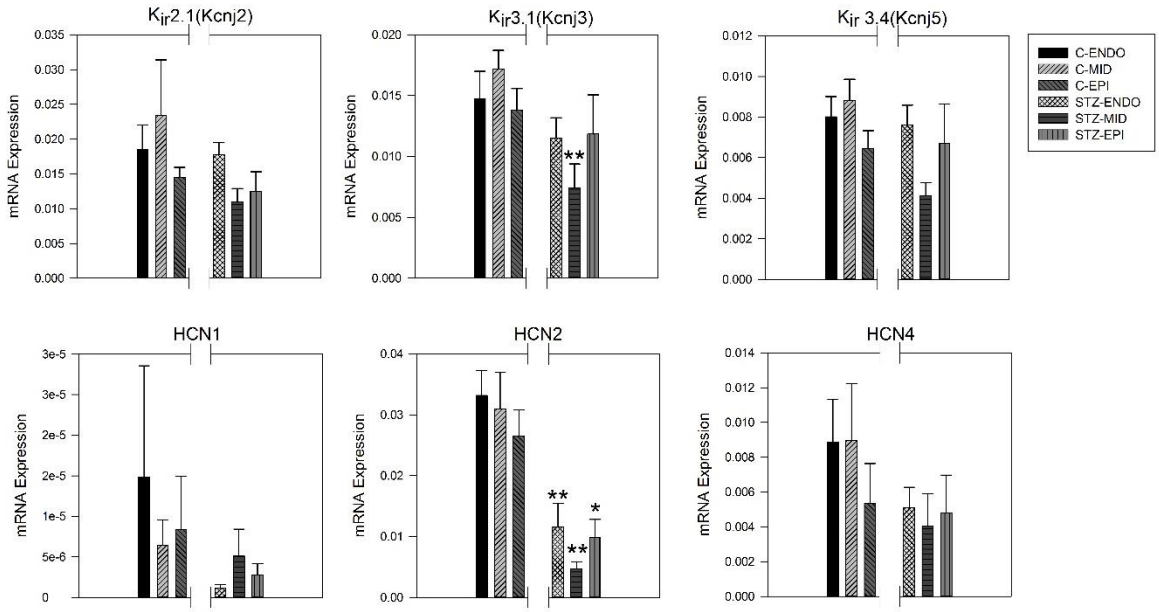

Figure 18: Expression of mRNA for major ion channels active largely during diastole in the left ventricle of the control and STZ groups for each section of the myocardium displayed in arbitrary units referenced to expression of 18-s (housekeeper gene). C=control STZ=streptozocin, Endo=endocardium, Mid=mid-myocardium and Epi=epicardium. Means ± SEM shown (n=8/group). Means ± SEM shown (n=8/group). *Significantly different from the control group (p<0.05). **Significantly different from the control group (p<0.01).

4.2.3. Intracellular Ca^{2+} handling transcripts

Intracellular Ca^{2+} plays an important role in arrhythmogenesis and contractility and three important intracellular Ca^{2+}-handling genes were investigated in this study: NCX1 (the Na^{+}-Ca^{2+} exchanger), SERCA2A (ATP2a2, the sarcoplasmic reticulum's Ca^{2+} pump) and RYR2 (the ryanodine receptor, the SR's Ca^{2+} release channel).

No significant variation between the STZ animals and control group was observed for NCX1 or RYR2 but a significant decrease in SERCA2A gene expression was noted in the STZ group, with this mainly in the mid-myocardium (p<0.01) and to a lesser degree in the endocardium (p=0.018; Figure 19).

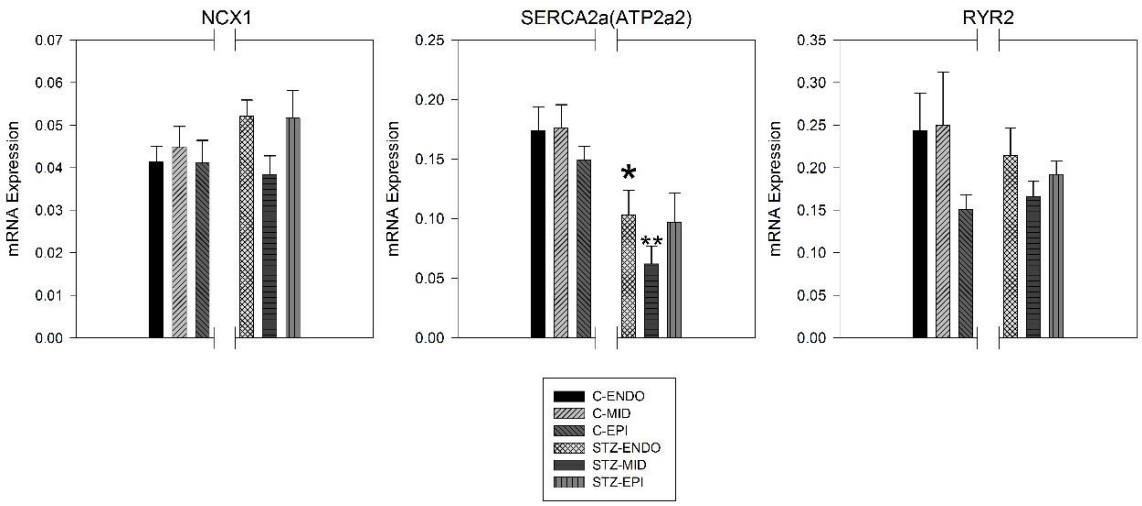

Figure 19: Expression of mRNA for intracellular Ca^{2+} handling proteins in the left ventricle of the control and STZ groups for each section of the myocardium. C=control STZ=streptozocin, Endo=endocardium, Mid=mid-myocardium and Epi=epicardium displayed in arbitrary units referenced to expression of 18-s (housekeeper gene). Means ± SEM shown (n=8/group). *Significantly different from the control group (p<0.05). **Significantly different from the control group (p<0.01).

4.2.4. Other electrophysiological channels and associated proteins/enzymes

Of all the ions so far discussed and investigated Cl^- channels are the least investigated and poorest understood from a cardiac AP perspective and so to investigate from a preliminary perspective if they are affected by diabetes, 4 Cl^- channels were chosen: CLCN-2, CLCN-3, TTYH-1 and TTYH-3. CLCN-2 is a hyperpolarization-activated inward-rectifier Cl^- channel, which is sensitive to changes in cell volume and extracellular pH[196] and it generates a current ($I_{Cl,ir}$) which is similar to I_f and CLCN-2 has also been shown to be involved in pacemaking [196, 197] but the exact role of this is not fully understood. CLCN-3 is thought to be responsible for the $I_{Cl,vol}$ [196] current which is a volume sensitive current and is thought to have some pacemaking activity as well. TTYH-1 potentially encodes a Ca^{2+}-independent volume-sensitive Cl^- channel and TTYH-3 may encode a Ca^{2+}-activated Maxi-Cl^- channel[198].

Of all four Cl^- channels only CLCN-2 was significantly different with a reduction in expression, focussed in the mid-level (p=0.031; Figure 20). There was no clear pattern that emerged in terms of expression for the other Cl^- channels (p=ns for all).

The three isoforms of the Na^+-K^+ pump: α1 (ATP1a1), α2 (ATP1a2) and α3 (ATP1a3) had significantly reduced expression levels in the STZ group vs. control group with each isoform reduced in expression in the mid-layer but α2 and α3 also had reduced expression in the endocardial layer (Figure 20).

Connexin43 (Cx43; GJA1) is the major connexin/gap junction isoform in the heart and is responsible for electrical coupling between myocytes. Expression of Cx43 was significantly reduced in the STZ group with this change primarily in the mid-myocardial layer (p<0.01; Figure 20)

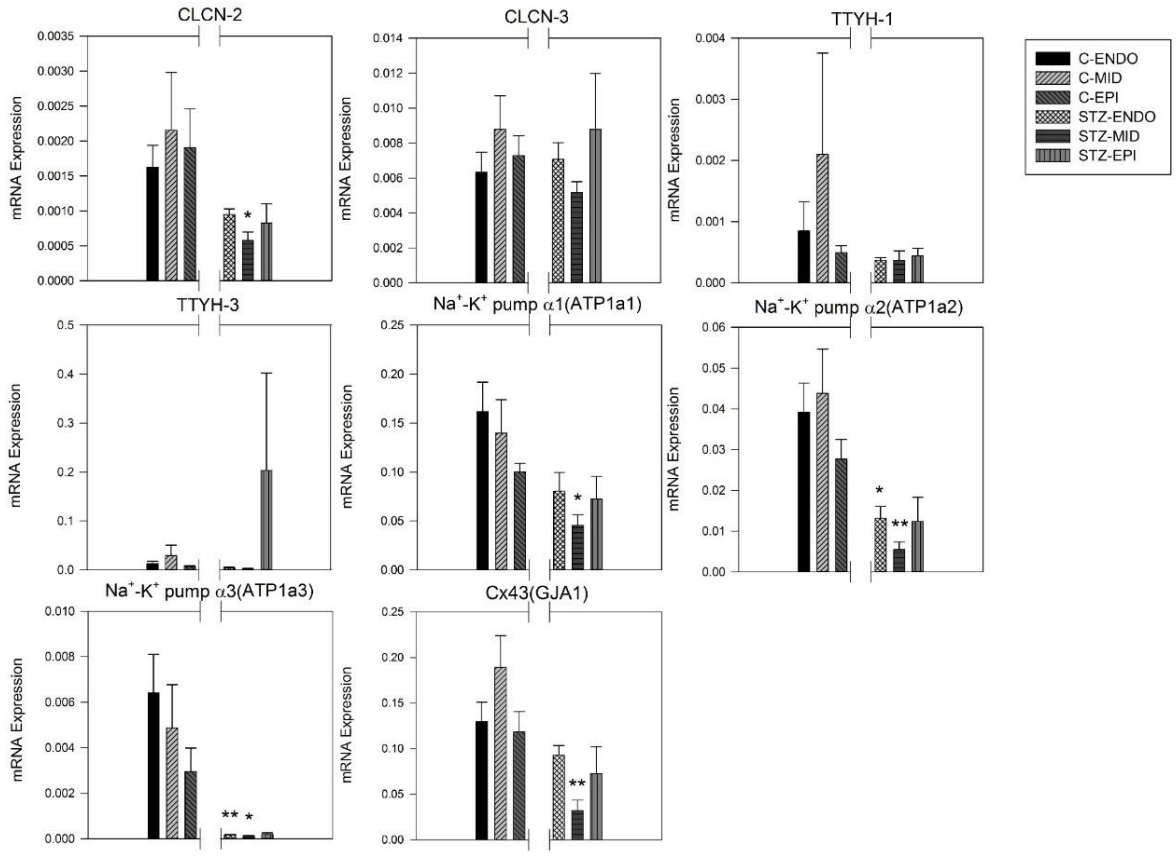

Figure 20: Expression of mRNA for Cl^- channels, Na^+-K^+ ATPases and Cx43 in the left ventricle of the control and STZ groups for each section of the myocardium. C=control STZ=streptozocin, Endo=endocardium, Mid=mid-myocardium and Epi=epicardium displayed in arbitrary units referenced to expression of 18-s (housekeeper gene). Means ± SEM shown (n=8/group). *Significantly different from the control group (p<0.05). **Significantly different from the control group (p<0.01).

4.2.5. Cardiac energy production

As the heart is a major area of energy consumption and diabetes significantly alters energy production, GLUT-4, the major cardiac glucose transporter and two major mitochondrial ATPases, 6 and 8 were selected for analysis. Expression of the primary cardiac glucose transporter GLUT-4 was significantly reduced in the STZ group across all 3 layers of the myocardium but maximally in the endo- and mid-myocardium (p<0.01; Figure 21). No

significant difference in expression or pattern change was noted for the mitochondrial encoded ATPases 6 and 8.

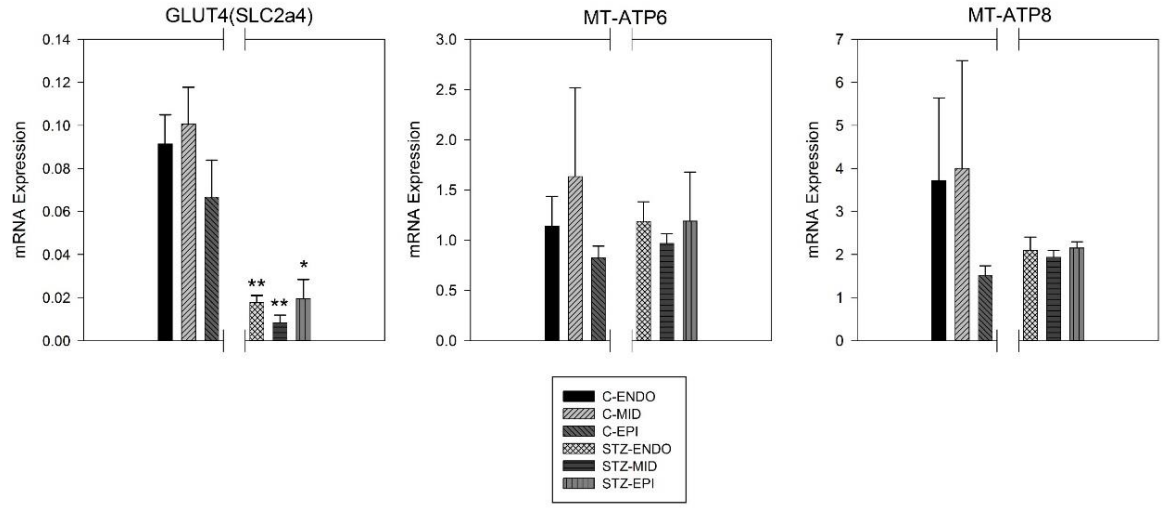

Figure 21: Cardiac energy production gene expression in the left ventricle of the control and STZ groups for each section of the myocardium. C=control STZ=streptozocin, Endo=endocardium, Mid=mid-myocardium and Epi=epicardium displayed in arbitrary units referenced to expression of 18-s (housekeeper gene). Means ± SEM shown (n=8/group). *Significantly different from the control group (p<0.05). **Significantly different from the control group (p<0.01).

4.2.6. Neuronal genes

The final area of analysis in this study was expression of genes that relate to neuronal function given the evidence we have seen of a diabetes related cardiac autonomic neuropathy and analysis was undertaken of nerve growth factor (NGF1), the pain receptor (TACR1), tyrosine hydroxylase (TH), key in production of neurotransmitters and UCHL1 which is important in the prevention of neurodegeneration[199].

For unclear reasons, we were unable to measure TH expression in both groups and the most likely explanation for this is probably related to experimental error at some point, given that the same cards were used successfully in identical animals/settings in our HFD vs. control group. Expression of NGF1, TACR1 and UCHL1 were not significantly different between

groups but there did appear to be a trend towards higher UCHL1 in the STZ group (Figure 22).

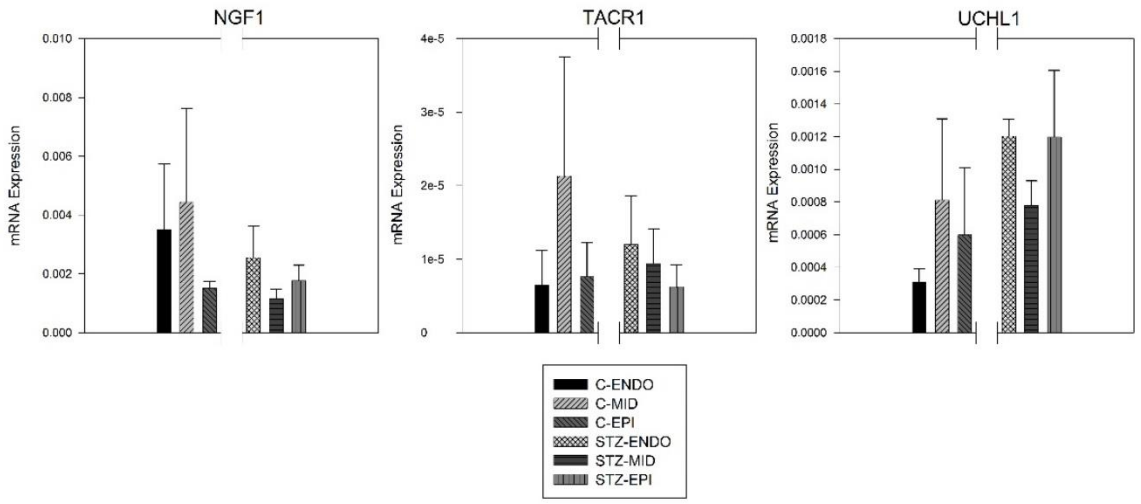

Figure 22: Cardiac neuronal gene expression in the left ventricle of the control and STZ groups for each section of the myocardium. C=control STZ=streptozocin, Endo=endocardium, Mid=mid-myocardium and Epi=epicardium displayed in arbitrary units referenced to expression of 18-s (housekeeper gene). Means ± SEM shown (n=8/group).

4.3. Discussion

4.3.1. STZ Rat: Whole animal data

Similar to many other STZ experiments on rats, we observed severe hyperglycaemia in our experimental group and failure to thrive compared to the control, with significantly reduced weight gain at 8 weeks[200]. Ideally in this study we would have had a weight matched control for the STZ rat in addition to our other control, as there is the possibility that the low weight and failure to thrive have affected mRNA expression. Whilst this is an issue, lower weight is a trend commonly seen in human studies, where children with type 1 diabetes have been observed to have a lower BMI at diagnosis on average compared to matched controls at diagnosis[201].

Whilst the STZ model has been extensively used in research on diabetes and the heart, there are important limitations to its use, firstly STZ as used in our experimental protocol induces diabetes at a rate that is not similar to the long process observed in human and so global changes over and above pancreatic β cell destruction may not be initially observed. STZ, is very effective at destroying pancreatic β cells leading to hypoinsulinaemia and hyperglycaemia but it does this without the global autoimmune effects of type 1 diabetes in the human[202]. This does mean that there is the possibility that we may not have seen all the changes possible from type 1 diabetes in this study as a result of this lack of autoimmunity.

4.3.2. STZ: Arrhythmogenesis

Before analysis of the changes we observed in our STZ model, it is useful to look at the modelled ventricular AP in the original STZ paper by Pandit et al.[140] to then explain how the changes we saw may be pro-arrhythmic or affect contractility.

In this study the team modelled an elongation of phase 2 and 3 of the AP. This had also been experimentally confirmed in previous work[203]. As already discussed this can lead to re-entrant circuits and arrhythmias.

4.3.2.1. $Na_v1.5$ down-regulation in type 1 diabetes

In our experiment we were able to see a marked reduction in $Na_v1.5$ in the STZ group with the change being localised to the mid-myocardial wall layer of our STZ rats and has previously been reported in the diabetic ventricle in animal models[204]. SCN5A, encodes the main alpha subunit of the cardiac sodium channel protein $Na_v1.5$ which forms the I_{Na} current which is the predominant cardiac sodium channel in humans. These channels (99% of them) open briefly for less than 1ms in phase 0 of the action potential resulting in rapid depolarization[19] and have rapid deactivation and inactivation kinetics. The I_{Na} current and the $Na_v1.5$ protein that creates the channel producing the current is voltage inactivated.

While predominantly open during phase 0, a tiny number of channels may reopen during the plateau phase creating a later transient inward current, I_{Ti}.

Lots of work has previously been done on the effect of a reduction in $Na_v1.5/I_{Na}$ in the heart and its effect of arrhythmogenesis and a short list of conditions where $Na_v1.5/I_{Na}$ is reduced include Brugada syndrome linked to ventricular fibrillation and sudden death, conduction disorders such as AV block[205], sick sinus syndrome with bradycardia[206] and atrial standstill[207]

Similarly to what has been shown in the Pandit experiment[140], a reduction in I_{Na} can experimentally be induced using class 1c anti-arrhythmic agents such as sotalol and flecainide with marked prolongation of the ventricular myocyte AP[208].

From a purely ventricular perspective reduced I_{Na} leads to reduced conduction velocities across the ventricle[204] and alterations in the transmural electrical gradient affecting repolarization. Firstly, as slowed conduction, a wave front leaving one zone of slowed conduction and travelling faster through normal areas of the heart may have enough time to reach back to the area of slowed conduction that gave rise to the original wave front and if it is not fully refractory, re-excite this area forming a stable circuit. This method of ventricular arrhythmia generation has previously been confirmed in $SCN5A^{-/-}$ mice[209].

Further evidence for reduced SCN5A/$Na_v1.5$ and abnormal repolarization comes from the Brugada syndrome which is one of the most widely studied SCN5A/$Na_v1.5$ disorders. In the Brugada syndrome, there is loss of the 'dome' encompassing phase 2 of the AP, due to $Na_v1.5$ down-regulation/loss of function with accentuation of I_{to} which creates a

transmural gradient in repolarization and increased dispersion in the epicardium which can then allow phase re-entry and with the right trigger VT/VF[210].

Both mechanisms described above due to reduced I_{Na} are powerfully pro-arrhythmic and potentially could explain the higher incidence of ventricular arrhythmias in patients with type 1 diabetes. Further support for a role of $Na_v1.5$ in arrhythmogenesis in diabetes comes indirectly as cardiac PI3k is reduced in diabetes[211] and reduction of PI3k signalling reduces I_{Na} and this causes AP and QT prolongation[212].

4.3.2.2. $K_v1.4$ up-regulation in type 1 diabetes

$K_v1.4$ is thought to be responsible for the I_{to-s} current within the human endocardial layer and to represent the slower I_{to-s} current, which is active during phase 1 of the AP and creates a transient outward K^+ current activated by rapid depolarization in phase 0 creating a flow of K^+ out, reducing the membrane potential and determining the level of the plateau phase. This channel also affects the activity of I_{Ca-L} and $I_{K,r}$ which is important in the regulation of the overall APD[213].

$K_v1.4$ and the slower I_{to-s} current are preferentially expressed in the mid and epicardial layers of the ventricle and help to regulate the duration of the AP to allow for the correct duration of transmural depolarization and repolarization, with differing AP duration as discussed in the introduction. In our experiment we saw an increase in all three layers of the ventricle wall of $K_v1.4$, a factor which is common in left ventricular hypertrophy and leads to prolongation of the AP, a consistently pathological change in many ventricular arrhythmias[214]. Also, as discussed when we reviewed down regulation of I_{Na}, there is a compensatory increase in I_{to} increasing transmural dispersion and allowing for re-entrant circuits and arrhythmia formation. In part this may be due to the fact that in diabetes, there is a switch from I_{to-F} to I_{to-S}, encoded by $K_v1.4$ with a prolongation of the AP due to the slower inactivation recovery of $K_v1.4$[215].

Our results are supported by other experimental work confirming an increase in $K_v1.4$ expression in diabetes animal models, both type 1 and type 2[173, 216].

4.3.2.3. KChiP2 down-regulation in type 1 diabetes

KChIP2 is an important regulatory subunit helping predominantly to stabilise and regulate expression of K_v4.2, the $I_{to\text{-}F}$ current[217] without particularly having any effect on the AP on its own[218]. While we did not observe a significant reduction in the $I_{to\text{-}F}$ genes in our STZ animals we did see a large increase in the expression of in K_v1.4 which encodes for the $I_{to\text{-}S}$ current and this has been previously reported in response to reduced KChIP2[217]. The switch in I_{to} phenotype is arrhythmogenic as discussed above although conversely in a heart failure knockout mice model without KChiP2, arrhythmia susceptibility was markedly reduced[219]. Overall, a reduction in KChip2 would be consistent with the increase observed in K_v1.4, though a specific role in arrhythmia prevention or generation is difficult to prove definitively with the available data.

4.3.2.4. ERG down-regulation in type 1 diabetes

In our diabetes group we saw a reduction in the expression of ERG, which encodes for the $I_{K,r}$ current which in the rat has very little effect on the AP but in humans is the key outward delayed rectifying potassium current and vital in prevention of ventricular arrhythmias. Reduced ERG function and prolongation of the AP and thus the QT on the surface electrocardiogram has been seen previously and can be caused by ROS damage, insulin deficiency and hypoglycaemia[130, 220]. The risk of sudden arrhythmogenic death in patients with type 1 diabetes is thought primarily to centre on dysfunction of the ERG and the $I_{K,r}$ current from lots of potential mechanisms, three of which are mentioned above. We know that the mid-myocardial layer of three ventricular wall layers has the longest AP duration and that a specific reduction here in $I_{K,r}$ will lead to an increase in transmural dispersion of repolarization (TDR)[221] through an increase in the gradient between the endocardium and mid-myocardium. When the TDR is increased previous experimental work has shown that this leads to EADs in late phase 2 and re-entry mediated polymorphic VT[222].

Whilst, not potentially clinically important in the rat model, the data derived from this are strongly suggestive of an arrhythmogenic phenotype in diabetes and particularly based on the location of change in the mid-layer.

4.3.2.5. K_vLQT1 down-regulation in type 1 diabetes

K_vLQT1 is the channel responsible for the $I_{K,s}$ delayed rectifying K^+ current in the ventricle of humans and is not modelled in the Pandit et al. system[160]. This current is a voltage gated slowly inactivating and deactivating current that seems to only be expressed in very small amounts in the mid-myocardium helping to prolong the AP at this level[223] but at the expense of an increase in TDR. The other important physiological element specific to this current is that compared to other rectifying currents, it is the only one that is up-regulated by increased sympathetic activity[224] and increased at higher heart rates. The combination of $I_{K,s}$ $I_{K,r}$ and $I_{K,1}$ form the majority of the repolarization reserve in the human ventricle and act in a synergistic manner.

Clinically and electrophysiologically, $I_{K,s}$ when reduced or dysfunctional is associated with long QT syndrome, 1 which is associated with ventricular arrhythmias and sudden death, commonly on exercise or with emotional stress. Previous experimental work has shown that current activity is increased at higher heart rates or with sympathetic drive[225] which would be in keeping with the clinical features described above. In animal studies $I_{K,s}$ seems to have a role as a compensatory mechanism when ERG/ $I_{K,r}$ is reduced to prevent ventricular arrhythmias[225]. The reduction we have observed of both $I_{K,s}$/ $I_{K,r}$ in combination would based on animal work and clinical Long QT syndromes to be proarrhythmic.

The specific reduction we have seen in the mid-myocardium, an area where expression is already low, may be of extra significance due to the increase in AP duration it will cause and the increase in TDR, which has been shown to lead to EADs and re-entry[226].

4.3.2.6. K_{ir}3.1 down-regulation in type 1 diabetes

K_{ir}3.1 and the respective current $I_{K,ACh}$ is an acetylcholine activated rectifying atrial channel predominantly[227] with very little described ventricular expression. What has been shown before in the human is that activation of this channel in the ventricle shortens the APD[228] though whether this is clinically significant given the small levels of ventricular expression is unclear.

4.3.2.7. HCN2 down-regulation in type 1 diabetes

HCN2 is one the isoforms that contributes to the generation of the I_f current which forms a pacemaking current in the heart and brain. HCN2 in cardiac tissue predominantly is found in the contractile tissue and not in the conduction tissue surprisingly, where the major HCN isoform is HCN4. Previous experimental studies have suggested that while HCN4 is primarily responsible for the pacemaker current in the human, HCN2 may form part of a heteromeric channel with HCN4 that is important for normal functioning of the sinus node and conduction through the contractile tissue[229]. Despite this primarily sinus node activity and evidence of a more predominant neuronal function, a reduction in ventricular HCN2 in rat models was associated with a prolongation of the QT and reduced heart rate variability[230].

4.3.2.8. SERCA2A down-regulation in type 1 diabetes

SERCA2A is the predominant Ca^{2+} transporter from the cytosol to the lumen of the SR, after ECC thus replenishing the luminal stores for RYR2 to release and allow the next round of ECC. Previous studies have shown a clear reduction in SERC2A expression in the STZ rat model[231] and in many other animal models of the diabetic cardiomyopathy[232] and we have found similar expressional change. While the major importance of SERCA2A will be assessed in the section on contractile function, reductions in SERCA2A are well reported in heart failure[233] and this appears to lead to an increase in cytosolic leakage of Ca^{2+}[234]. This excess leakage of Ca^{2+} leads to increased exchange via NCX1 which creates a late inward current, I_{TI}, and can allow reactivation of the late Na^+ current and this in turn leads to delayed Ca^{2+} sparks, and DADs[235]. These changes also lead to AP prolongation.

While there is primary physiological data on the role of SERCA2A and arrhythmogenesis, interesting information on the role of SERCA2A and arrhythmias comes from gene transfer studies, where transfer of SERCA2A in a post infarct model has reduced Ca^{2+} leak and the incidence of ventricular arrhythmias[236]. Two other anti-arrhythmic functions have been shown to be related to replacement of SERCA2A, firstly, a reduction in Ca^{2+} level flux, which causes electrical alternans and is markedly pro-arrhythmic and secondly, by abbreviating the APD, through inactivation of $I_{Ca\text{-}L}$[235].

The reduction we have seen in SERCA2A expression, would appear to be arrhythmogenic based on other work and in the Pandit et al. STZ experiment[140], modelled SR Ca^{2+} loss led to AP prolongation.

4.3.2.9. Cx43 down-regulation in type 1 diabetes

Cx43, is the primary gap junction isoform present in the ventricle of humans and rats and so was analysed based on the fact the other gap junction isoforms are mainly atrially expressed or present in conduction tissue. The cardiac gap junction is located at the intercalated disk region of myocytes and is formed by two channels, made of hexamers of connexins connecting the cytoplasm of two myocytes to each other[237]. The role of gap junctions is important as signal conduction through the myocardium, depends of electrical coupling of cells mediated by gap junctions.

In studies with a similar level of Cx43 reduction to that which we have observed, close to 20% of control levels in the mid-myocardial layer, conduction velocity is 50% of normal, suggesting a large reserve in the heart with a significant reduction in Cx43 levels being required to affect conduction velocities[238]. This level of Cx43 reduction has been shown to cause anisotropic reduction in conduction velocities and the creation of stable re-entrant ventricular arrhythmias[238]. The heterogenic reduction in Cx43, may also be significant as conduction heterogeneity is a significant risk for arrhythmia generation and anything that exacerbates this is likely to prove pro-arrhythmic.

The second postulated mechanism by which a reduction in Cx43 may prove arrhythmogenic is that in areas of reduced Cx43 there seems to be reduced expression of $Na_v1.5$ which is what we observed in the mid-myocardial layer of our STZ rats[239]. As shown above reductions in $Na_v1.5$ are significantly arrhythmogenic on their own but the combination leads to marked conduction slowing, a reduced I_{Na} current and increased activation dispersal and an increase in VT[239].

4.3.2.10. CLCN2 down-regulation in type 1 diabetes

As mentioned earlier, CLCN2, generates a current ($I_{Cl,ir}$) similar to I_f and CLCN-2 has been shown to be contribute to cardiac pacemaking[196, 197]. Very little is currently known about the

role from an electrophysiological point of view about CLCN2 in the ventricle and no background literature was available to reference the reduction in ventricular CLCN2 observed here. What is reported in the literature is that it may contribute to pacemaker activity as it becomes activated by hyperpolarisation and acts potentially as an inwardly rectifying current[240, 241]. What is expected from the basic physiology of the channel is that as it is mainly activated at more negative membrane potentials, the prolongation of the AP we would expect especially at phase 2/3 should lead to reduced Cl^- efflux[241] but this requires further confirmatory work. There has been no previous work reporting reduced CLCN2 in diabetes.

4.3.2.11. Na^+-K^+ ATPase down-regulation in type 1 diabetes

In this experiment, a reduction in Na^+-K^+ ATPase isoforms, α1-3 was observed in the STZ group predominantly in the mid-myocardium but also for the α2 and α3 isoforms in the endocardium and reductions in Na^+-K^+ ATPase isoforms has previously been experimentally reported in diabetes[242].

The function of the Na^+-K^+ ATPases, is to actively transport Na^+ out in exchange for K^+ and help repolarise the cell to resting membrane potential and allow restitution of the electrochemical gradients, for the next depolarization. From an arrhythmia perspective, there are two observed actions to review, firstly reduced Na^+-K^+ ATPase activity leads to increased intra-cellular Na^+ activity which leads to reduced forward NCX1 exchange of Ca^{2+} and increased SR levels of Ca^{2+}. This is the mechanism by which cardiac glycosides are positively inotropic[243] but is also the mechanism by which digoxin toxicity leads to polymorphic VT. In contrast, contrary to earlier work, inhibition of Na^+-K^+ ATPase isoforms appeared to shorten the AP in a biphasic approach by favouring reverse mode NCX1 activity and Ca^{2+} inflow and generation of an outward current- 3 Na^+ for 1 Ca^{2+}[244, 245].
Overall, the exact arrhythmogenic balance struck by reduced Na^+-K^+ ATPase is difficult to be certain of and is largely going to depend on the model used or clinical situation and how this may interact with our observed changes in SERCA2A and $Na_v1.5$.

4.3.3. Contractility in type 1 diabetes

As discussed in detail in the introduction, diabetes leads to significant impairment of contractile function of the ventricle and in animal STZ models this can be apparent after only two weeks[246].

Based on the gene expression changes we have seen, there are several potential explanations and these are reviewed now.

Firstly, a reduction in $Na_v1.5$ and the I_{Na} current, slows conduction through the ventricle and this results in an increase in QRS width on the ECG and an increase in markers of dyssynchrony with an accompanied reduction in contractile function[247]. Secondly, the I_{Na} current whilst not directly linked to ECC, does have important effects on Ca^{2+} entry in the myocyte which are enough to induce contractile dysfunction. With reduced I_{Na} current amplitude, there is a knock on effect with reduced opening of the L-type Ca^{2+} channel and reduced plateau phase Ca^{2+} release [248]. The other effect is via reduced reverse mode NCX1, which has an important role in priming the dyadic cleft with Ca^{2+} to produce Ca^{2+} induced Ca^{2+} release and ECC[249, 250]. Clinically this syndrome is reproducible with flecainide which inhibits $Na_v1.5$ and the I_{Na} current and produces a negative inotropic effect[251].

CX43 down regulation has predominantly been thought of as an issue primarily of conduction and arrhythmogenic significance but it is possible that through local variation in gap junction expression wavefront speed and homogeneity may be altered leading to dyssynchrony and reduced contractile function[252]. There has been some corroborative evidence for this theory using pacing induced heart failure, where the dyssynchronous pacing arm had much lower levels of Cx43 compared to the non-dyssynchronous arm with heart failure.

The second major gene change which is likely to impact on cardiac contractility is the observed reduction SERCA2A which has been reported in many models of heart failure [235].

Reduced SERCA2A leads to accumulation of Ca^{2+} in the cytosol with prolonged relaxation times and reduced SR-Ca^{2+} levels and release for Ca^{2+} induced Ca^{2+} release which all lead to reduced contractile function.

In the STZ experiment here, similar to many other heart failure and contractility experiments there was an observed reduction in Na^+-K^+ ATPases. As discussed in the arrhythmia section, this would be expected to result in potentially increased contractility via increased SR levels of Ca^{2+}. As modelled by Pandit[140] and as we would expect based on our gene expression changes, there is prolongation of the AP and other work has shown that this is inotropic through increased Ca^{2+} accumulation[253].

From a clinical perspective, the last two changes described may be adaptive changes to increase contractile force in the setting of a diabetic cardiomyopathy. The majority of clinical data suggests that the predominant phenotype is reduced contractility[254] and certainly we have observed several changes which would contribute to this.

4.3.4. Cardiac energy production

In this study we observed a significant reduction in the expression of GLUT-4, the major cardiac glucose transporter. GLUT-4 in its inactive state is found mainly in intracellular compartments and is translocated via Insulin mediated pathways and in response to contraction to the sarcolemma and to the T-tubules where glucose diffuses across a gradient[255].

Previously, in STZ models, expression of cardiac GLUT-4 has been shown to be reduced[256] as it has been in type 2 diabetes models[165] and in the human ventricle[257]. From the introduction section we know that glucose is a much more efficient energy source than fatty acids and any reduction in glucose transport to the sarcolemma is likely to impact energy production and in due course reduce cardiac contractile efficiency. GLUT-4 is known to be up-regulated in response to ischaemia in non-diabetics to increase glycolysis and in diabetes which is associated with a higher rate of coronary artery disease the observed reduction in GLUT-4 we and others have seen may lead to increased damage during ischaemia[258].

4.3.5. Neuronal function

While a peripheral and autonomic neuropathy is extensively reported in the STZ rat model[259] and a cardiac neuropathy less so[260], no significant differences in the neuronal genes tested was observed in this study. On review of the literature only one study directly measured

cardiac mRNA expression of a neuronal gene in diabetes, in this case calcitonin gene related peptide and general neuronal protein gene product 9.5 , with only one of these altered in their study[261]. One study did report a reduction in NGF1 expression in the ventricle of mice with cancer[262] and while not significant, there appeared to be a trend towards reduced NGF1 in our STZ animals.

The expected reduction in neuronal gene expression that was not observed may be down to methodological flaws within the study potentially including: incorrect experimental technique, wrong rat model[261], insufficiently long study duration and weight loss affecting neuronal gene expression

Overall, this would certainly seem an area that requires further investigation based on the significant peripheral and central neuronal dysfunction seen in type 1 diabetes.

4.3.6. Overall genotype

Overall, our experiment similar to others suggest a genotypic change that would most likely result in a prolongation of the action potential and reduced contractility, primarily as a result of reductions in SERCA2A, $Na_v1.5$, $K_v1.4$, CX43, GLUT-4 and K_vLQT1 expression. A possible compensatory reduction in Na^+-K^+ ATPase expression which may have some positive effect of contractility and arrhythmogenesis.

5. HFD rat: obesity model

5.1. Animal characteristics

Through the study HFD-fed rats consumed more energy ($28.1\pm1.0x10^3$ vs $23.7\pm0.9x10^3$ kJ; +18%, $p<0.01$ vs controls) and increased their weight more than the control animals (+32%; $p<0.01$). This led to an increase in levels of adipose tissue in HFD rats. (+40%; $p<0.01$). Due to the high energy content of the HFD, a smaller intake was required to cause weight gain in this group compared to controls (-10%; $p=0.0165$). These results are similar to previously reported experimental work on the induction of obesity using a high fat diet in rats[263]. Mean energy consumption with final weight gain and percentage adiposity are shown below for control and HFD animals as mean ±SEM in Table 9:

Diet	Energy Consumed (kJ/g)	Body Weight Gain (g)	Adiposity (%)
Control	102.8±2.9	232.9±12.4	1.032±0.081
HFD	92.2±2.6*	308.6±18.5**	1.449±0.010**

Table 9: Baseline and final rat characteristics showing means ± SEM shown (n=8/group). **Significantly different from the control group ($p<0.05$). **Significantly different from the control group ($p<0.01$).

5.2. HFD rat RT-PCR results

In an identical manner to the STZ experiment, we analysed a wide range of genes we thought may be implicated in obesity cardiomyopathy for many of the same reasons as outlined in the STZ section.

5.2.1. Major ion channels active during the action potential

Expression of ion channels in the left ventricle of the HFD rats (n=8) was measured at the mRNA level using quantitative PCR and compared to that in the control lean rats (n=8). Expression of the principle Na^+ channel, $Na_v1.5$ (SCN5A), tended to be greater in the HFD group (but not significantly so; $p=0.127$; Figure 23). However, expression of the principle L-

type Ca^{2+} channel, $Ca_v1.2$ (CACNA1C) was significantly increased in the HFD group ($p<0.01$). Expression of $K_v1.4$ (KCNA4) and $K_v1.5$ (KCNA5) tended to be greater in the HFD group but not significantly and similarly expression of $K_v4.2$ (KCND2) and $K_v4.3$ (KCND3) and the auxiliary subunit KChIP2 (KCNIP2) were not significantly different in the two dietary groups (but expression of $K_v4.2$ and $K_v4.3$ tended to be greater in the HFD group). In the HFD group, there was significantly reduced (p=0.029) expression of ERG but expression of K_vLQT1 (KCNQ1) tended to be greater (but not significantly so; p=0.128).

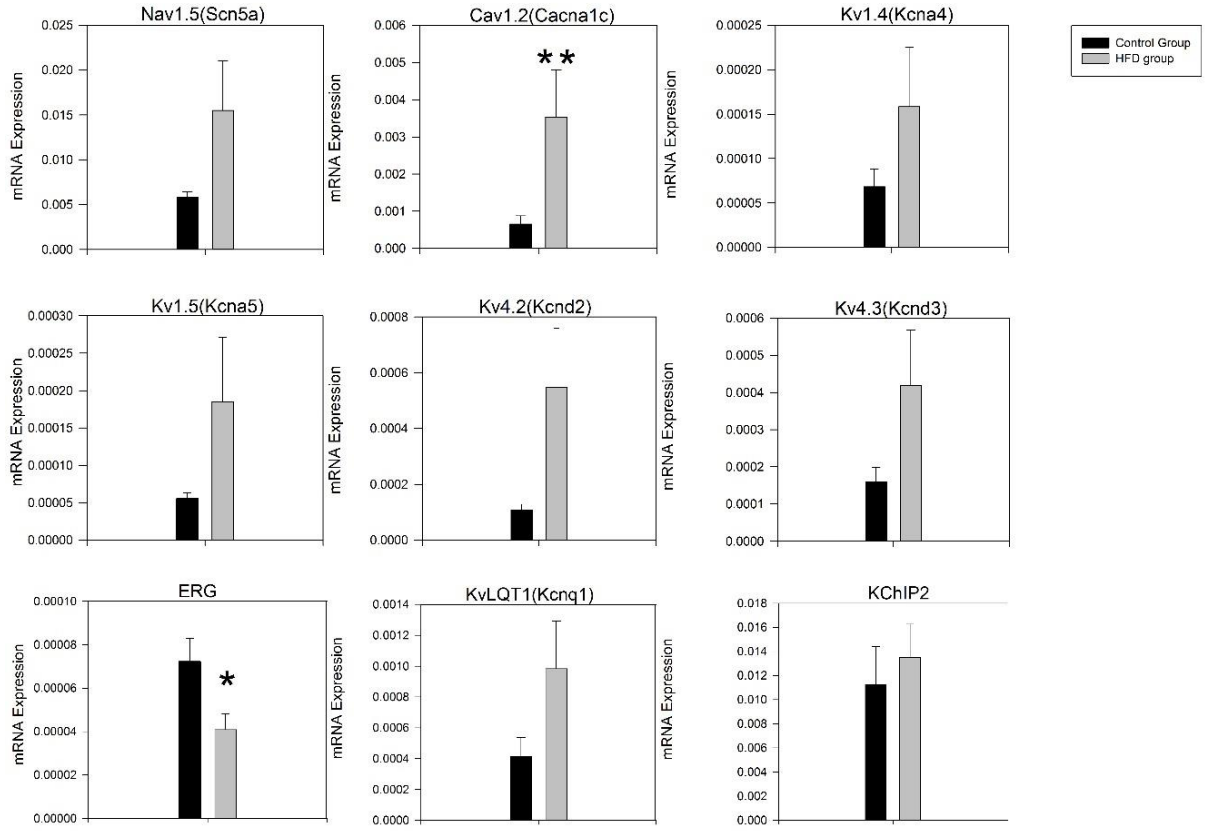

Figure 23: Expression of mRNA for major ion channels active during the action potential in the left ventricle of the control and HFD groups displayed in arbitrary units referenced to expression of 18-s (housekeeper gene). Means ± SEM shown (n=8/group). *Significantly different from the control group ($p<0.05$). **Significantly different from the control group ($p<0.01$).

5.2.2. Major ion channels active during diastole

Expression of the three major pacemaker channel isoforms, HCN1, HCN2 and HCN4 tended to be greater in the HFD group, but only the increase in HCN4 was significant (HCN1, p=0.18; HCN2, p=0.089; HCN4, p=0.03; Figure 24). In the HFD group, there was significantly increased expression of K_{ir}2.1 (KCNJ2) (p=0.032). Expression of K_{ir}3.1 (KCNJ3) and K_{ir}3.4 (KCNJ5) tended to be greater in the HFD group (but not significantly so; p=0.77 and 0.20 respectively).

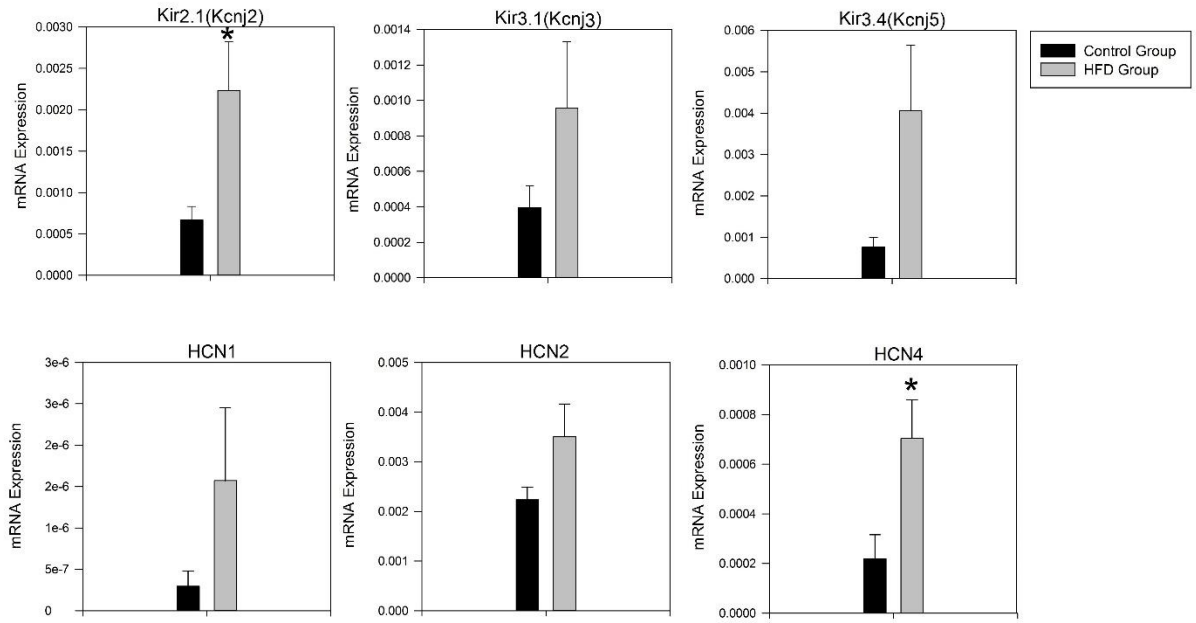

Figure 24: Expression of mRNA for major ion channels active largely during diastole in the left ventricle of the control and HFD groups displayed in arbitrary units referenced to expression of 18-s (housekeeper gene). Means ± SEM shown (n=8/group). *Significantly different from the control group (p<0.05).

5.2.3. Intracellular Ca2+-handling transcripts

As stated earlier, given the key role intracellular Ca2+ plays, NCX1, SERCA2A and RYR2 were analysed in the HFD experiment. Expression of all three was significantly increased in the HFD group (p<0.01, <0.01 and 0.04, respectively; Figure 25).

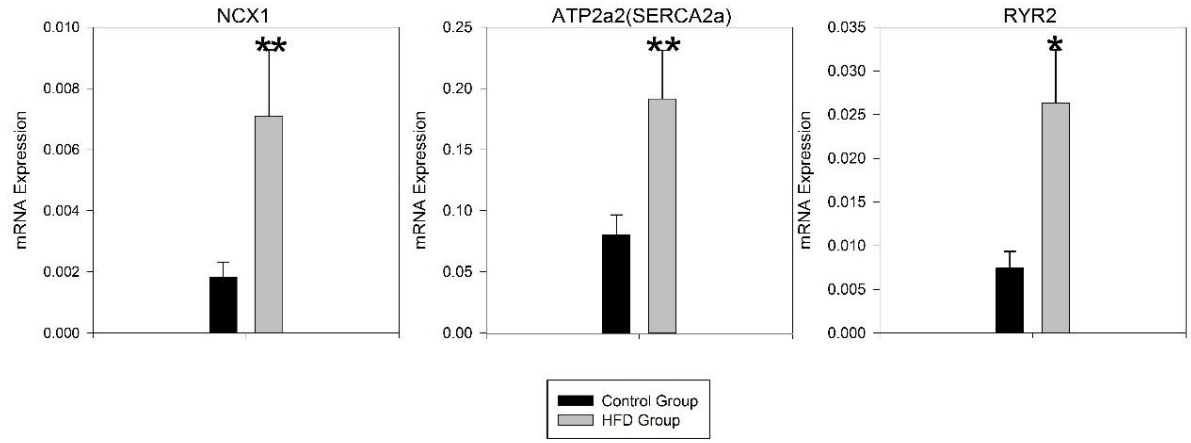

Figure 25: Expression of mRNA for major Ca^{2+}-handling molecules in the left ventricle of the control and HFD groups displayed in arbitrary units referenced to expression of 18-s (housekeeper gene). Means ± SEM shown (n=8/group). *Significantly different from the control group (p<0.05). **Significantly different from the control group (p<0.01).

5.2.4. Other electrophysiological channels and associated proteins/enzymes

Expression of all four Cl- channels tended to be greater in the HFD group, but only CLCN-3 had a significantly increased up-regulation (CLCN-2, p=0.238; CLCN-3, p=0.029; TTYH-1, p=0.155; TTYH-3, p=0.056; Figure 26). There was a significant difference in expression between dietary feeding groups in ATPase mRNA levels, for the α1 and α2 isoforms tended in the HFD group but not the α3 isoform (Na+-K+ pump α1, p<0.01; Na+-K+ pump α2, p<0.01; Na+-K+ pump α3, p=0.758). Expression of Cx43 tended to be greater in the HFD group (but not significantly so; p=0.121).

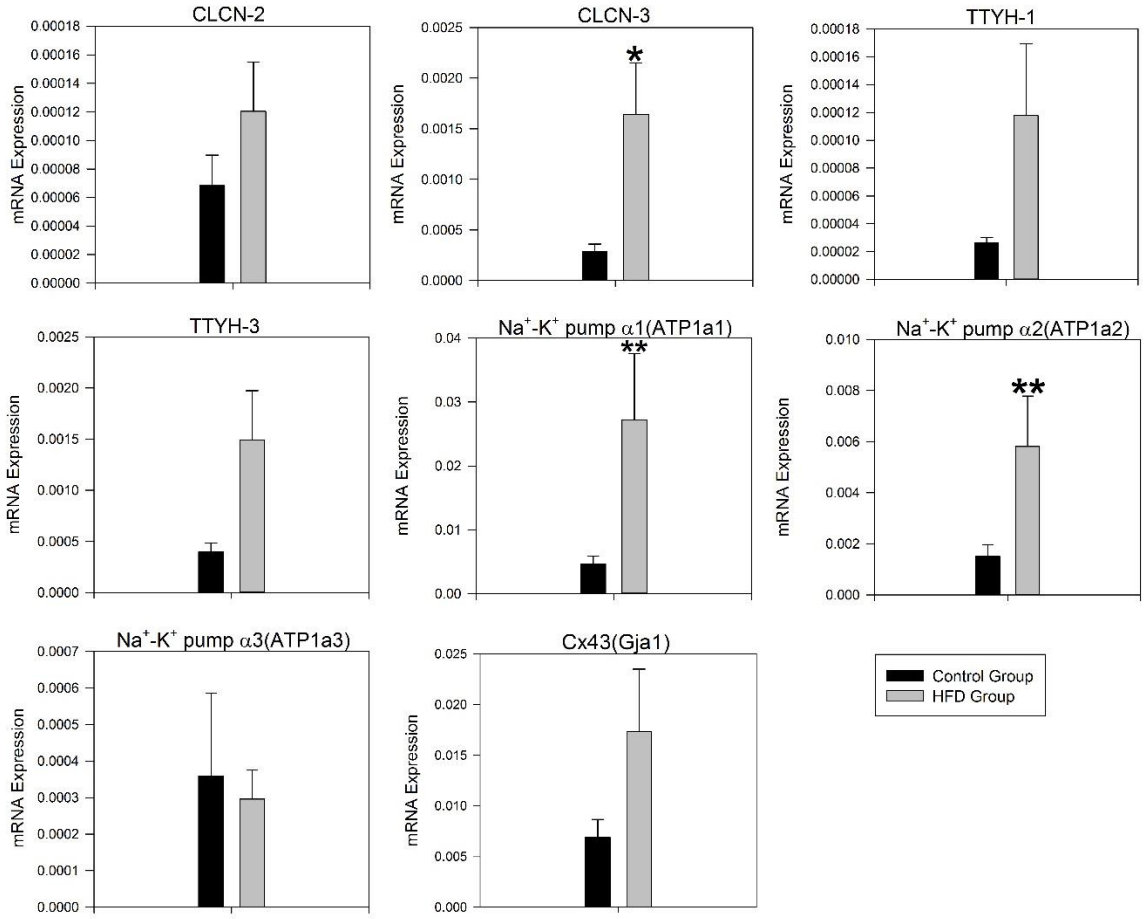

Figure 26: Expression of mRNA for Cl^- channels, α subunits of the Na^+-K^+ pump and the gap junction Cx43 in the left ventricle of the control and HFD groups displayed in arbitrary units referenced to expression of 18-s (housekeeper gene). Means ± SEM shown (n=8/group). *Significantly different from the control group (p<0.05). **Significantly different from the control group (p<0.01).

5.2.5. Cardiac energy production

The heart is one of the most energy intense organs in the body consuming requiring a significant amount of energy production to meet the requirements, given the effects of obesity on metabolism, once again GLUT-4, MT-ATP6 and MT-ATP 8 expression were analysed. We can see that there was no significant change in expression in GLUT-4, but significantly increased levels of mRNA in the ventricle of MT-ATP 6 and 8 (p<0.01; Figure 27)

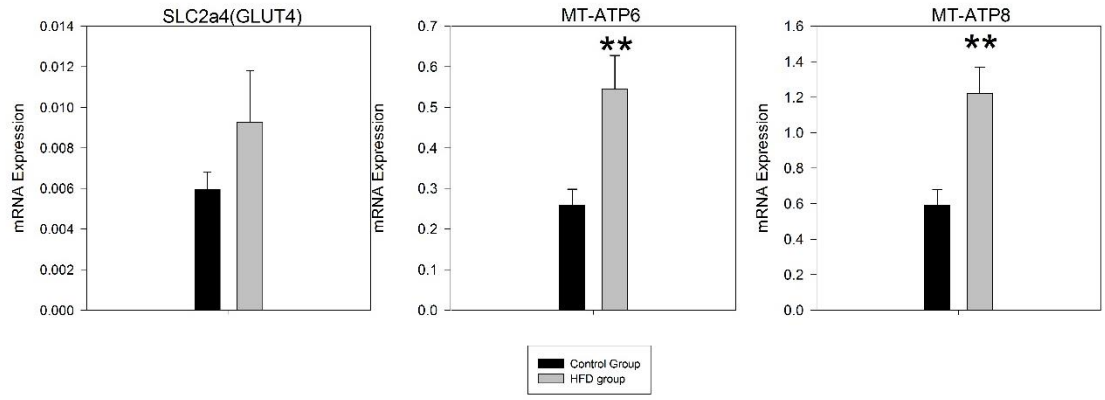

Figure 27: Expression of mRNA for important cardiac energy production genes in the left ventricle of the control and HFD groups displayed in arbitrary units referenced to expression of 18-s (housekeeper gene). Means ± SEM shown (n=8/group). **Significantly different from the control group (p<0.01).

5.2.6. Neuronal genes

In the final section for analysis, genes related to neuronal function, an analysis was made of the same 4 genes as in the STZ experiment. In the HFD group, an up-regulation of TH, which codes for tyrosine hydroxylase was observed (p=0.023; Figure 28) but no significant change was noted for the other gene transcripts, UCHL1, NGF1, TACR1 between groups.

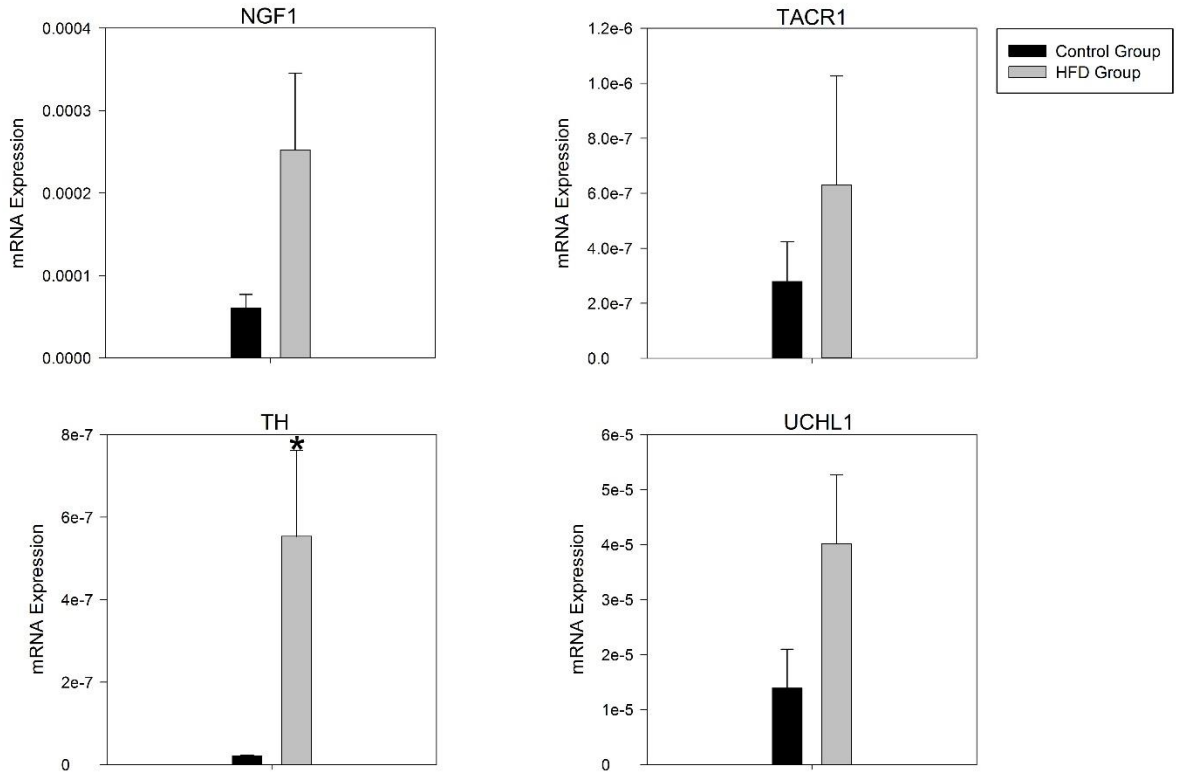

Figure 28: Expression of mRNA for cardiac neuronal genes in the left ventricle of the control and HFD groups displayed in arbitrary units referenced to expression of 18-s (housekeeper gene). Means ± SEM shown (n=8/group). *Significantly different from the control group (p<0.05).

5.3. Immunofluorescence

Primarily this study has been mRNA based study and the use of this methodology is based on the experience of the department with the TAQMAN™ system and the reliability and translatability of mRNA results in terms of function/protein correlation[151, 152, 264].

As a result, we decided to look at comparative protein analysis try and assess the reliability of our mRNA results as a predominantly quality assessment tool of the experimental mRNA techniques. As already there exists other confirmatory work available for several gene transcripts using the TAQMAN™ system[265], a decision was made to look at one of the less expected results from the RT-PCR study. HCN4 being primarily an atrial based pacemaker gene, was not expected to be significantly altered at the ventricular level between groups and we could not find any previous work looking at the correlation between RT-PCR and

immunofluorescence. To show that the RT-PCR expression change of HCN4 should lead to a change in protein expression of HCN4 at the ventricular level, quantitative IF was undertaken of HCN4.

Quantitative immunofluorescent labelling of HCN4 in the rat tissue samples showed a more than 2-fold increase in HCN4 labelling (p<0.01; Figure 29) in the HFD group.

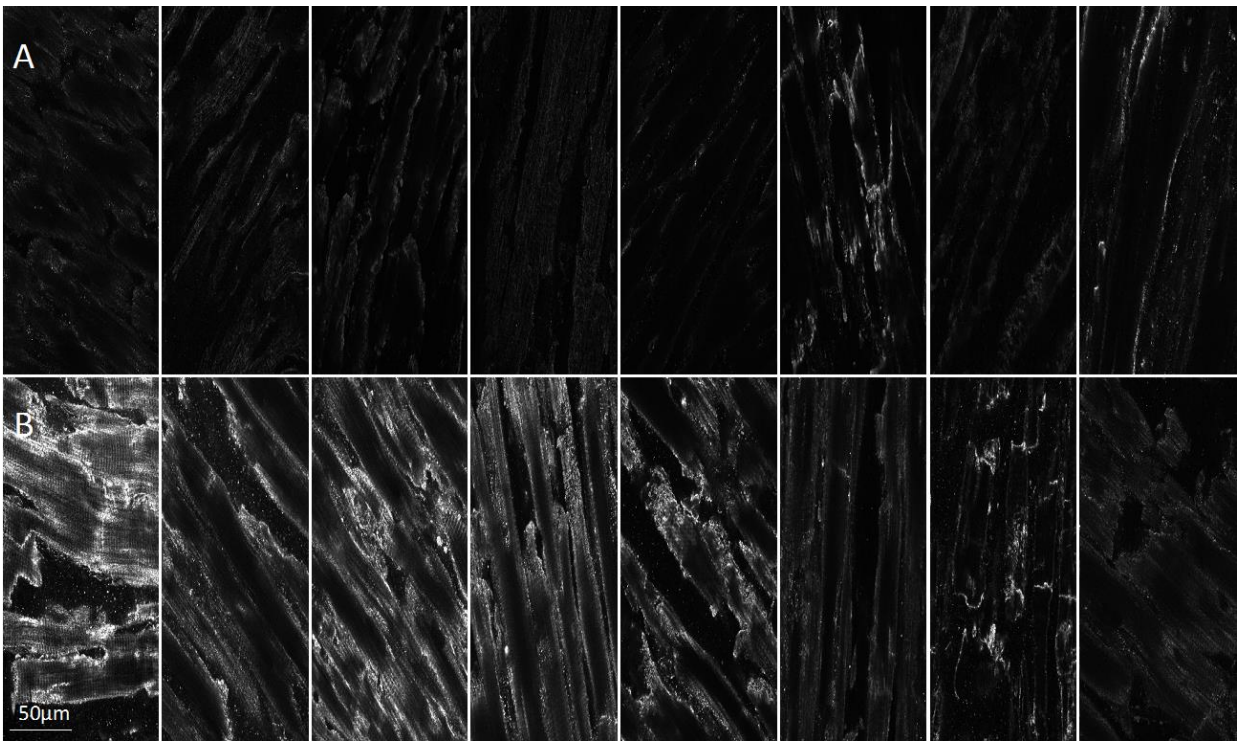

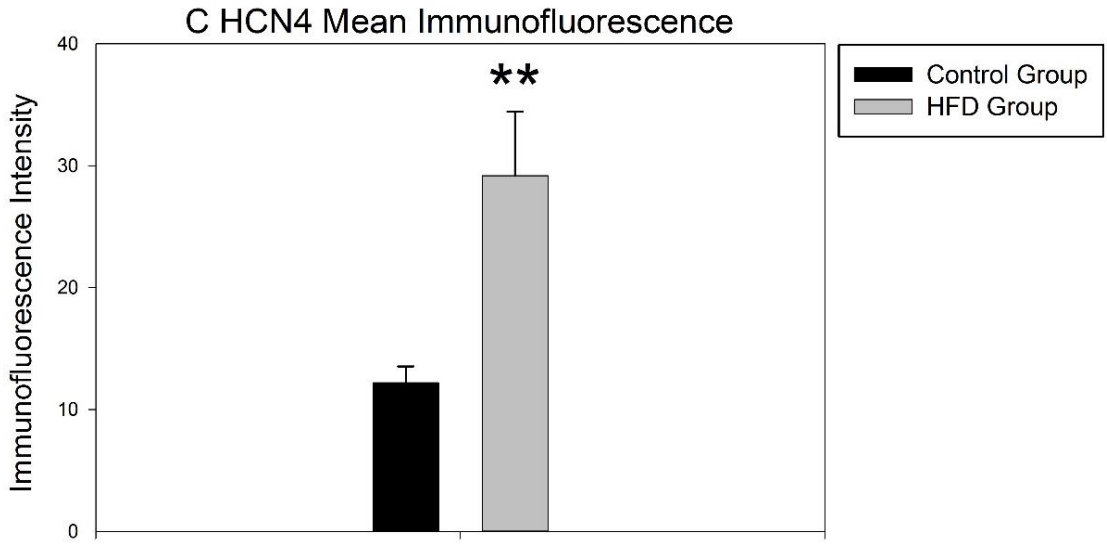

Figure 29: Expression of HCN4 protein in the left ventricle of the control and HFD groups. A and B, representative images of HCN4 immunolabelling (white signal) in the left ventricle of eight control (A) and eight HFD (B) animals. C, mean (+SEM) intensity of HCN4 immunolabelling in the left ventricle of the control and HFD groups (n=8/group). **significantly different from the control group (p<0.01).

5.4. AP Modelling

To simulate the effects of obesity, the channel conductance for each of the presumed remodelled ionic currents in the Pandit et al.[160] models was scaled according to the measured average percentage change of the corresponding mRNA between the control and the obesity groups (Table 10):

Channel	Current	HFD group change
$Na_v1.5$	I_{Na}	+163.60%
$Ca_v1.2$	$I_{Ca,L}$	+441.28%
$K_v1.4$, $K_v4.2$ and $K_v4.3$	I_{to}	+240.45%
$K_v1.5$	$I_{K,ss}$	+232.73%
HCN4	I_f	+222%
$K_{ir}2.1$	$I_{K,1}$	+233.83%
NCX1	I_{NaCa}	+290.10%
SERCA2A	SR Ca^{2+} uptake	+139%
RYR2	SR Ca^{2+} Release	+253.97%
ATP1α1-3	I_{NaK}	251%

Table 10: Simulated changes in current density based on the mRNA expression differences.

Figure 30 shows simulated action potentials (top row) of rat endocardial (Figure 30A) and epicardial (Figure 30B) ventricular cells in control and obesity conditions, accompanied by underlying ionic currents and the intracellular Ca^{2+} concentration. In both cell models, remodelled ion channels in the obesity condition produced increased amplitude of the

action potential, elevation in the plateau phase and an increase in the action potential duration (APD; Figure 30 A and B). Notably, there was a pronounced slow tail of repolarization following the action potential; slow tails of repolarization following the rat ventricular action potential have been reported in experiments[266]. The changes in the action potential are attributable to the integral actions of increased I_{Na} (reflecting the increase of $Na_v1.5$), I_{to} (reflecting the increase of $K_v1.4$, 4.2 and 4.3), $I_{Ca,L}$ (reflecting the increase of $Ca_v1.2$), sustained outward K^+ current $I_{K,ss}$ (reflecting the increase of $K_v1.5$), $I_{K,1}$ (reflecting the increase of $K_{ir}2.1$), Na^+-Ca^{2+} exchange current (I_{NaCa}; reflecting the increase of NCX1), Na^+-K^+ pump current (I_{NaK}; reflecting the increase of the $\alpha 1$, $\alpha 2$ and $\alpha 3$ subunits of the Na^+-K^+ pump) and I_f (reflecting the increase of HCN4). In the HFD condition, simulation results also showed that the amplitude of the intracellular Ca^{2+} concentration was increased (Figure 30 A and B).

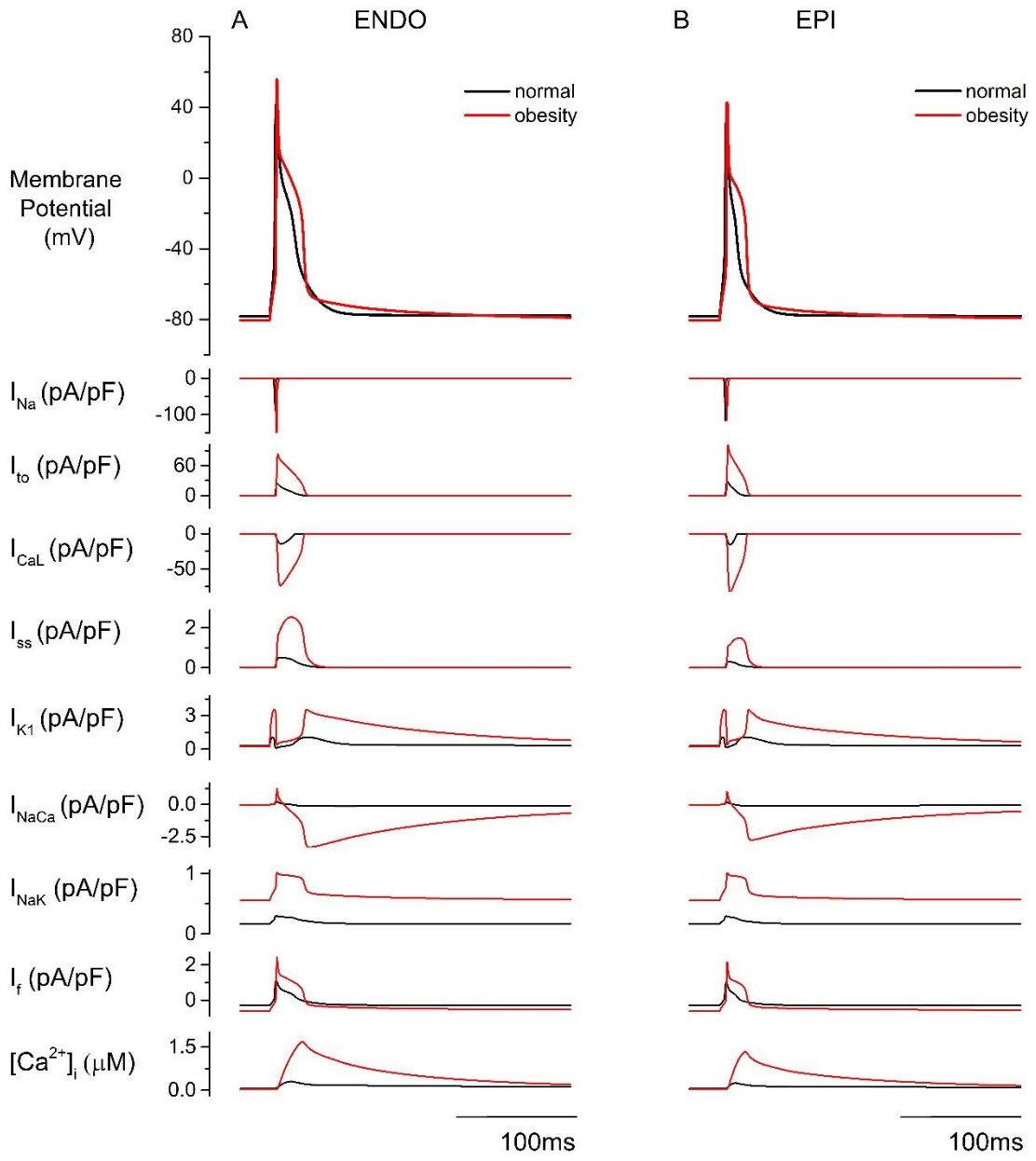

Figure 30: Simulated rat ventricular endocardial (A; ENDO) and epicardial (B; EPI) action potentials and underlying ionic currents and intracellular Ca^{2+} concentration in control and HFD conditions.

Potential effects of each of the remodelled ion channels on the ventricular action potential were investigated. Results are shown in Figure 31. The potential increase in I_{Na} alone had negligible effects on APD, but increased the amplitude of the action potential (Figure 31A). The potential increase in $I_{Ca,L}$ alone produced a dramatic increase in the duration of the plateau phase, leading to a failure of repolarization; consequentially, the models failed to

produce a full action potential (Figure 31B). The potential increase in I_{to} alone abbreviated APD and reduced the AP amplitude (Figure 31C). Modelled up-regulation of the I_{NaK} current led to marked abbreviation of the action potential. The potential increase in $I_{K,ss}$ (Figure 31E), $I_{K,1}$ (Figure 31F) isolated on their own resulted in small APD abbreviations. Up-regulation of in I_{NaCa} (Figure 31G) resulted in a small delay in phase 3 repolarization more obviously at the endocardial level. Changes in I_f (Figure 31H), Ca^{2+} release via RYR2 (Figure 31I) or Ca^{2+} uptake via SERCA2A (Figure 31I) alone produced negligible effects on the action potential. Therefore, the simulations suggest that the obesity-induced changes in ion channels could result in a prolongation of action potential primarily as a result of an increase in $I_{Ca,L}$ the effects of which are offset to a degree by increased in $I_{K,ss,}$ I_{NaK} and $I_{K,1}$.

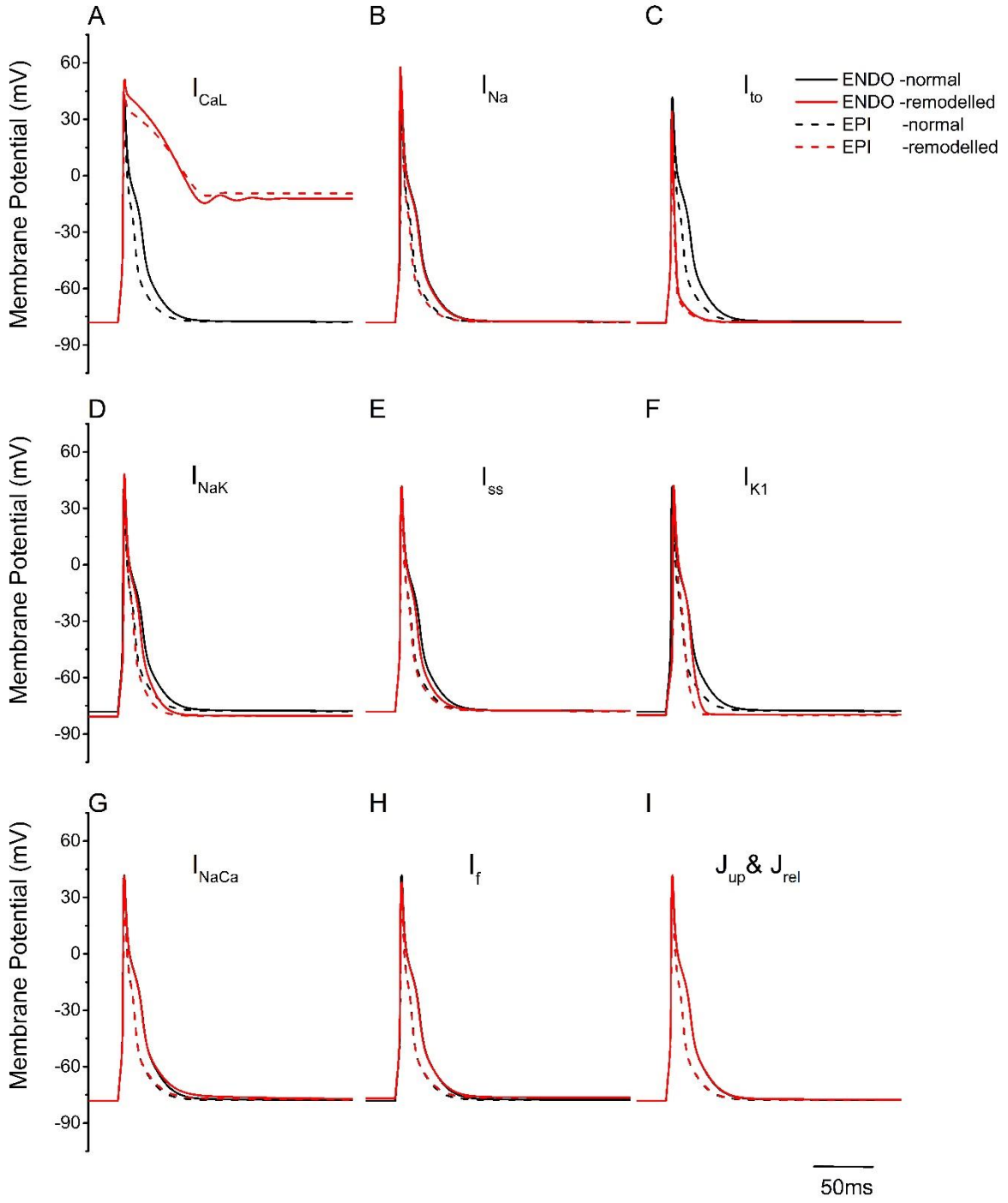

Figure 31: Simulated rat ventricular endocardial and epicardial action potentials in control and HFD conditions when each of the remodelled ion channels/ionic currents was modified one at a time. A, only $I_{Ca,L}$ considered. B, only I_{Na} considered. C, only I_{to} considered. D, only I_{NaK} considered. E, only I_{ss} considered. F, only $I_{K,1}$ considered. G, only I_{NaCa} considered. H, only I_f considered. I, only SR Ca^{2+} uptake and release considered (J-Up and J-Rel. respectively).

5.5. Discussion

5.5.1. HFD rat: Whole animal data

In our HFD group we were able to show clear weight gain and increased adiposity compared to the control group and using a simple dietary feeding method to induce obesity. Similarly, to our other animal experiment with the STZ rat, this type of homogenous feeding model is unable to fully reflect the heterogeneous methods by which humans become obese such as excessive fat and carbohydrate intake and reduced physical activity and as a result our data has to be interpreted with a degree of caution if attempting to translate directly to humans. Despite this experimental limitation, we did achieve our desired experimental model i.e. obese rats and we can say that our results reflect changes secondary to high fat intake induced obesity.

5.5.2. Arrhythmogenesis

As with our STZ experiment, reviewed below are the major mRNA changes and the AP modelling results and a discussion of how these relate to an arrhythmogenic phenotype in the obese rat.

5.5.2.1. $Ca_v1.2$ up-regulation in obesity

The first major area of discussion from our results, was the increase in gene expression of the key Ca^{2+} channel, $Ca_v1.2$ with a large modelled increase in current density with the effect of prolonging the AP through increased Ca^{2+} entry. This experimental finding is of importance as previously, clinical work has found a strong link between obesity and QT duration[267].

$I_{Ca\text{-}L}$ normally begins to activate at voltages more positive than -40mV and peaking in terms of activation at 0-10mV with an increase in activation speed at more positive voltages and is both voltage and Ca^{2+} inactivated[268]. An increase in the $I_{Ca\text{-}L}$ current leads to a prolongation of the APD mainly by extension of the plateau phase of the AP and this can create a window where there is a reduction in voltage inactivation and Ca^{2+} inactivation of $I_{Ca\text{-}L}$. Reduction of $I_{Ca\text{-}L}$ inactivation allows some inactivated $Ca_v1.2$ channels to re-open, which

can then generate a further inward Ca^{2+} current and upstroke in the AP creating EADs which can generate ectopic beats and arrhythmias[269]. As might be expected given an increase in $Ca_v1.2$ channels and as we have seen from our modelling, this results in a much larger and prolonged Ca^{2+} current in our HFD group. Previous experimental work suggests a link to direct and indirect promotion of EADs and DADs, which can generate ectopic beats and arrhythmias[269, 270] via increases in the Ca^{2+} current. Supporting evidence for the role of increased $I_{Ca\text{-}L}$ in arrhythmogenesis comes from the rare Timothy syndrome where a mutation in CACNA1C leads to gain of function in the $Ca_v1.2$ channel, then subsequently to increased and prolonged calcium entry, a prolonged QT and a high incidence of ventricular arrhythmias[271]. As well as Timothy syndrome, patients with myotonic dystrophy where there is, similar to obesity, often signs of LVH, have been found to have an up-regulation in $Ca_v1.2$ again with an increase in arrhythmias[272].

Rat experimental work on $I_{Ca\text{-}L}$ current by other groups has revealed a reduction in $I_{Ca\text{-}L}$ inactivation and that this leads to QT prolongation though in their study this was not related to an increase in $I_{Ca\text{-}L}$ expression[273], though while the prolongation of the QT in obesity between research groups seems ubiquitous not all have demonstrated changes in the $I_{Ca\text{-}L}$ current[274], though it is possible some of this relates to variation in feeding models/animals used.

5.5.2.2. NCX1 up-regulation in obesity

In our HFD group, we observed an increase in NCX1 gene expression, which when modelled, suggests a large increase in the $I_{Na/Ca}$ current density leading to a small delay in late repolarization, generating a late transient inward current (I_{TI}) in phase 3 of the AP.
In normal conditions, at -30mV and below NCX1 works in its forward mode (1 Ca^{2+} ion exchanged for every 3 Na^+ ions) and above this in the reverse mode (small amounts of Ca^{2+} in). In situations of increased Ca^{2+}, such as the increase in $Ca_v1.2$ and Ca^{2+} transient we have seen, NCX1's forward mode activity can be increased by up to 67% with generation of an inward current that prolongs the AP[275] and may add to a small degree the AP prolongation we have seen in conjunction with $I_{Ca\text{-}L}$. The other main current generated by NCX1 is the late I_{TI} current which despite the fall in Ca^{2+} levels during phase 3 of the AP, occurs when the

change in membrane potential outstrips the sodium-calcium exchange reverse potential forcing NCX 1 back into a forward mode[276]. The I_{Ti} current generated is bigger when the rate of membrane change is larger[276] and in our modelled APs we can see a particularly sharp membrane potential drop followed by a later repolarization in the HFD group and when large enough this inward current can generate a delayed after depolarization (DAD) and can also cause Ca^{2+} mediated DAD via SR Ca^{2+} release in the Ca^{2+} overloaded state[277]. NCX1 when up-regulated has been shown to lead to an increase in Ca^{2+} transient amplitude (as we have seen in our modelling) and an increase in SR Ca^{2+} levels all of which are likely to cause an overload of SR Ca^{2+} with oscillatory levels of Ca^{2+} and abnormal Ca^{2+} release generating DADs[278]. An arrhythmogenic role for NCX1 in obesity would be supported from work in other pathological states such as hypertrophy and heart failure which both demonstrate increased NCX1 levels[279, 280].

5.5.2.3. SERCA2A/RYR2 up-regulation in obesity and SR Ca^{2+} release

Similar to other groups looking at obesity[281], we have seen an increase in SERCA2A and RYR2 mRNA and increased SERCA2A expression has previously been explained as a response to oxidative damage in the SR caused by excess free radical generation in obesity[282]. Several studies have suggested that increased SERCA2A activity leading to Ca^{2+} overload in the SR, can generate abnormal Ca^{2+} release and DADs leading to arrhythmias[283, 284], although other work has shown increased SERCA2A to be anti-arrhythmogenic[285]. Despite the increase in mRNA content, an assumption that this leads to increased functional SERCA2A as other work has shown that in obesity SERCA2A activity was reduced through oxidative injury[119], but this study revealed a prolonged Ca^{2+} transient within the rat ventricle as our modelling data suggests. In addition to the increase in SERCA2A mRNA in our HFD group, we saw an increase in RYR2 expression and as the main channel, for SR Ca^{2+} release this would help explain the large modelled increase in SR calcium release we propose in conjunction with $I_{Ca\text{-}L}$. Excess Ca^{2+} leak from RYR2 when the receptor is defective is a well described mechanism of I_{Ti} generation and then DADS, classically seen in catecholamingeric polymorphic ventricular tachycardia[286]. From other studies[287], it is known that excess SR Ca^{2+} leads to an

increase in SR Ca^{2+} release via RYR2 and this again may contribute to the generation of the I_{TI}.

While the mRNA changes we have seen and the modelled AP is more arrhythmogenic, how much of the increase in NCX1/SERCA2A/RYR2 expression is pathological is still uncertain in obesity. Certainly NCX1 up-regulation is a normal response at higher heart rates in normal physiology[288], a common finding in obese individuals. Also in the early stages of LV hypertrophy, SERCA2A has previously been shown to be up-regulated[289] and NCX1 similarly[290], and so before the development of overt heart failure these may represent adaptive changes to maintain contractile function though at the cost of an arrhythmogenic phenotype and this is discussed in more detail in the section on contractility.

5.5.2.4. K_{ir} 2.1 up-regulation in obesity

We have seen increased gene expression of KCNJ2 (K_{ir}2.1), which as stated before is responsible for part of the $I_{K,1}$ current, which repolarises the myocyte late in the action potential and helps maintains the resting membrane potential, allowing Na^+ channel recovery. Up-regulation of this would seem desirable for an arrhythmogenic perspective, as experimentally, over-expression of the $I_{K,1}$ current results in acceleration of the final phase of repolarization and a shorter APD[291]. Despite, the theoretical advantage of increased $I_{K,1}$, the physiological effect has been associated with familial short QT syndrome[292], familial atrial fibrillation[293] and stabilisation and maintenance of re-entry arrhythmias leading to ventricular tachycardia[294]. Another mechanism by which up-regulated KCNJ2 has been seen in other studies to be arrhythmogenic is where an increase in the $I_{K,1}$ current causes an increase in transmural dispersion of repolarization[295] and this allows the formation of re-entry arrhythmias[296].

Whilst many effects of increased $I_{K,1}$ may be pro-arrhythmic two mechanisms may be compensatory, firstly, the AP prolongation caused by increased calcium transit may be opposed by increased $I_{K,1}$ which will act to increase the K^+ outward current accelerating phase 3 repolarization and attempting to abbreviate the AP prolongation. Secondly, as $I_{K,1}$ sets the membrane resting potential through the K^+ outward current, it directly opposes any

pacemaker diastolic currents[297] and in this case directly opposes the I_f increase we have seen to try and prevent ventricular ectopic activity.

Experimentally, the simulated AP change we observed, appears relatively small despite the large increase in KCNJ2 and this is something previously observed by the group and by other groups with very large increases in $I_{K,1}$ required to generate AP changes in simulation studies[298]. This may mean that some of the restorative effect of increased $I_{K,1}$ on the modelled AP is lost and that *in vivo* the effect may be greater.

5.5.2.5. ERG down-regulation in obesity

In our HFD group, we observed a significant reduction in ERG gene expression, which is a rapid delayed potassium-rectifying channel that helps repolarise cells to their resting state and helps prevent prolongation of the APD, through the $I_{K,r}$ current. As $I_{K,r}$ does not play an important role in repolarization in the ventricle of the rat, its effect is difficult to discuss in this section, however it is a key channel in humans. Reduced expression or drug blockade of ERG is a well-known cause of human APD/QT prolongation and ventricular arrhythmias[299].

The arrhythmogenic risk of ERG blockade or reduction has shown to be reduced if there is a reduction of the inward calcium current[300] and so the combination of reduced ERG and increased inward calcium may prove synergistically arrhythmogenic.

5.5.2.6. Na^+-K^+ ATPase 1 and 2 up-regulation in obesity

Na^+-K^+ ATPases function to maintain a low intracellular Na^+ and a high K^+ and this is done in an ATP dependent manner, with 3 Na^+ ions out for 2 K^+ ions into the cell, this primarily helps to create a Na^+ gradient for Ca^{2+} exchange by NCX1. This movement of current helps to generate a largely negative current and tends to hyperpolarise the cell[301].

There have been many studies showing that a reduction in cardiac Na^+-K^+ ATPase is pathological and is found in other cardiomyopathies[302]. From an arrhythmogenic perspective, what we have modelled is an abbreviation of the action potential and in other studies, increased Na^+-K^+ ATPase activity has limited Na^+/Ca^{2+} overload reducing the rate of arrhythmias[303].

It is important to note that this particular result in this study has not been reproduced in other work and Na^+-K^+ ATPase was down-regulated in obesity[304].

5.5.2.7. Pacemaker currents up-regulation in obesity

In our study, we found a significant up-regulation of HCN4 at the mRNA level and protein level in the ventricle of the obese rat. HCN4, forms the largest part of the I_f channel which is the major cardiac pacemaker current in the sinus node and knockout animals have been seen to suffer from severe bradycardias[305]. To our knowledge this is the first time this has been demonstrated and represents a potential substrate for arrhythmias and ectopic activity in obesity. This would fit in with previously published results from rats with hypertrophy from pressure overload[306] and left ventricular hypertrophy; common problems in obese individuals[307]. In non-pathological states, there is low expression of HCN4 in the ventricle but after myocardial infarction ventricular up-regulation of HCN4 causes a high volume of ventricular ectopic beats and potentially prolonged ventricular arrhythmias[22].

Overexpression of HCN4, may represent a target for increased sympathetic drive within the heart[308] and thus explain why there are higher resting heart rates and levels of ventricular ectopy seen in obese individuals. HCN4 protein levels have also been shown to be increased in the SAN in obese animal models and the total area of HCN4 tissue within the SAN increased[264]. The role of HCN4 in the ventricle compared to the SAN is likely to be much more pathological and represent an ectopic focus as opposed to organised pacemaker activity. Experimentally we were never able to show that the increase specifically in I_f on its own (even with the complete removal of $I_{K,1}$) would be enough to generate diastolic depolarization though with all the other current changes combined there was a diastolic potential generated. This does cast doubt on a primary role for I_f in ectopic pacemaker activity though this may simply reflect that at a ventricular level I_f is only relevant in the context of other pathological changes as we have seen and in the other disease states listed above.

We have been able to demonstrate an increase in CLCN3 gene expression in our HFD group and while the chloride channels are a group that is less well studied and also there is a lack of biophysical models to use, some information about the possible role of CLCN3 in

arrhythmias is available. CLCN3, codes for a volume activated large chloride channel, $I_{Cl\text{-}vol}$ which has complex electrophysiological effects which are often different under stress conditions such as hypoxia and reperfusion[309]. There is some evidence that CLCN3 contributes to the potassium independent I_{to} current[310]. In conditions of cell swell such as hypoxia, activation of CLCN3 leads to shortening of the APD and the refractory period causing a reduction in length of conduction needed to sustain a re-entry arrhythmia[309, 311].

Conversely, in heart failure, activation of CLCN3 has been shown to limit APD prolongation and reduce early after-depolarizations which are key methods of calcium overload activated arrhythmias[312]. One other potential area exists where up-regulation of CLCN3 may be pro-arrhythmic and that is in the SAN, where mechanical stretch has been shown to activate a chloride channel with similar characteristics to $I_{Cl\text{-}vol}$ and so this channel may in addition have a role in pacemaker activity[196]. We know also that other similar chloride channels have a potential role in pacemaker activity such as CLCN2 where knockout animals are bradycardic[197].

At this stage further functional studies would be required to look at the role of this channel in human obesity to look at its specific role and interaction with other channels.

5.5.3. Contractility in obesity

There are many studies showing that in obesity there is an increase in myocardial mass and left ventricular hypertrophy both concentric and eccentrically distributed[313] and that there is an increase in stroke volume and cardiac afterload[314]. To maintain output initially at least some compensatory mechanisms are required, such as increased circulating volumes, higher heart rates or increased contractility.

In our discussion on arrhythmogenesis, we have predominantly seen an increase in and prolongation of Ca^{2+} entry with a subsequent prolongation of the action potential and an increase in expression of RYR2, the key channel for SR Ca^{2+} release and excitation-contraction coupling activation.

In previous studies in humans mild to moderate obesity up to a BMI of 35kg/m^2 contractile function was noted to be increased by a variety of parameters[315]. It should be noted however that in animal models this change was not reproduced [316] and others have

shown a worsening of contractile function[317]. Much of this heterogeneity is related to leptin which is thought by many to cause suppression of myocardial contractility, though the exact mechanism is unclear. A key common area, in the wide variety of obesity models seems to be elevated intracellular Ca^{2+}, reduced extrusion and reduced sensitivity of the myocyte to Ca^{2+} [318]. Increased levels of Ca^{2+} are key to the release of more troponin complexes from their resting state and the generation of more actin-myosin cross bridges and thus increased contractile force.

Supportive evidence for the role of increased Ca^{2+} as an early compensatory mechanism comes from studies in hypertensive rats, were an increase in Ca^{2+} transient with APD prolongation has been associated with an increase in contractile function as an early response[319]. Our qPCR and modelling data suggest an increase in Ca^{2+} levels, Ca^{2+} transient with reduced extrusion and this would fit in with these previously reported functional changes. Despite what we think may be an adaptive response, it is worth noting that despite the increase in Ca^{2} induced contractility, this response is smaller in obese animals than in lean animals[318]. In the study alluded to above, an early increase in systolic force has been shown in obesity[315] at the expense of myocardial relaxation which leads to impaired filling times and excess energy consumption in the long run.

Overall it would seem that at the expense of an arrhythmogenic phenotype, the changes in Ca^{2+} transient and APD may afford theoretically some increase in contractility, which may be important in obesity in maintenance of systolic function in the early phase.

5.5.4. Cardiac energy production in obesity

In our obesity experiment, we were able to show increased levels of mRNA for MT-ATP 6 and 8 which, code for 2 of the 13 protein subunits which form complex V, ATP synthase[320]. ATP synthase, uses the electrochemical energy created by the movement of H^{+} ions across mitochondrial membranes into the energy creating central matrix which then allows for oxidative phosphorylation of ADP.

Most of our knowledge of the role of mitochondrial diseases comes from patients studied with infantile cardiomyopathies and mutations that causes loss of mitochondrial function[320] and reduced cardiac energy production[321] and translating these results to a more

general population is difficult. Looking at the impact of our results in our obese rats, we know that the heart is an organ with a high energy requirement and that in particular obese individuals myocardial 0_2 ($mV0_2$) consumption is significantly increased compared to normal controls[322]. While $mV0_2$ consumption is higher in obesity, lots of this energy is wasted through mitochondrial un-coupling, generation of free radicals and just through supporting extra mass[323]. It would seem that up-regulation of MT-ATP 6 and 8 would appear to be appropriate responses in the face of increased myocardial 0_2 demand and potentially one of the sources of increased free radical generation previously described as important in obesity generated cardiac dysfunction[119]. It is worth noting that these mitochondrial genes are not nuclear, so they do not wrap round protective histone proteins and therefore are more susceptible to damage, thereby potentially promoting or reducing their expression.
We do know that as weight is lost there is a reduction in $mV0_2$ and an improvement in LV diastolic function[322], whether this is related to our observed changes in MT-ATP 6 and 8, deserves further study. Functionally it would appear that as weight is lost, energy efficiency improves[324], energy demand drops[325] and thus more energy can be diverted from maintaining systolic function to diastolic function[326] and a longitudinal analysis of MT-ATP 6 and 8 would help clarify this question.

It would seem that the increase in MT-ATP 6 and 8 mRNA we have seen may be an early adaptive response to maintain cardiac energy production in the face of increasing energy demand created by adiposity and also a potent creator of free radicals that could prove pathological overtime.

5.5.5. Neuronal function in obesity

In our qPCR work we observed a trend towards an increase for all the neuronal genes we studied but a definite significant increase in tyrosine hydroxylase, which converts the amino acid L-tyrosine to L-3,4-dihydroxyphenylalanine (L-DOPA), a key step in the production of noradrenaline and adrenaline, important catecholamines in the sympathetic nervous system.

Obesity is a condition in which there is an increase in whole body and cardiac sympathetic activity[327] and this increase in sympathetic activity is replicated in patients with heart failure[328]. Increased sympathetic drive may be pathological by several mechanisms

including development of LVH[329], a common finding as already described, through direct toxicity and altered adrenoceptor activity. Chronic increased sympathetic nervous activity in the heart is directly toxic through stimulation of interstitial fibrosis, increased sarcolemma permeability with calcium overload and via the formation of oxidative metabolites which stimulate the ROS-TNF apoptosis pathway[330].

In the human there are 3 types of α1 adrenoceptor, 3 α2 receptors and 3 β receptors all with varying activities, with the heart predominantly containing β1 and β2 adrenoceptors. These receptors when stimulated increase contractility, relaxation, heart rate and conduction through the atrioventricular node all desirable effects and which are necessary to respond in normal situations such as exercise. As heart failure progresses, there is down regulation of β-adrenoceptor numbers and reduced sensitivity to stimulation[331]. Similarly, to some of the other changes we have seen and their postulated pathological effects, it would seem that an initial increase in tyrosine hydroxylase would be compensatory in obesity before eventually proving pathological via the mechanisms already outlined.

5.6. Overall Genotype and modelled phenotype

The overall genotype observed in this study was one with an up-regulation of the main calcium channel Cav1.2 and other important Ca^{2+} handling proteins such as RYR2, NCX1 and SERCA2A. We also observed an up-regulation in the majority of Na^{+}-K^{+} ATPase genes and K_{ir} 2.1 and the pacemaker gene HCN4, which was also confirmed to have increased at protein level. The modelled phenotype was for a prolonged AP with a much sharper repolarization slope compared to the control animals. We also observed increases in mitochondrial energy genes and an increase in tyrosine hydroxylase mRNA, both of which would appear to fit with the higher energy requirements and higher sympathetic activity observed in obesity.

6. Human type 2 diabetes experiment

6.1. Clinical characteristics

Clinical characteristics for the two patient groups are shown below in Table 11 with 95% confidence intervals and show that both groups are comparable in terms of age, BMI, waist circumference with no significant differences between groups (p=ns for all) in Table 11.

Group	No.	Age (Years)	Male	Waist (Cm)	BMI (Kg/m^2)	HbA1c (mmol/mol)
Control	9	78.8 (72.4-85)	6	35.8 (33.7-39.7)	27.8 (26-29.6)	n/a
Diabetes	7	74.9 (63-86.7)	4	39.7 (31.6-47.9)	31.2 (24.9-37.5)	57.9 (44.4-71.4)

Table 11: Clinical characteristics of the control and diabetes groups

Comparatively, the diabetes group had a tendency to more often be on cardiac medications than the control group but with no statistical significance in treatment differences (Table 12).

Group	ACE/ARB	Beta Blocker	Statin	Sulfonylurea	Metformin
Control	5 (55.5%)	3 (33.3%)	4 (44.4%)	n/a	n/a
Diabetes	5 (71.4%)	3 (42.8%)	6 (85.7%)	2 (28.6%)	4 (57.1%)

Table 12: Medication usage in each experimental group

In our study only one a patient had a complication of diabetes with that patient suffering mild renal impairment as evidenced by an increased albumin-creatinine ratio but an eGFR well above 30 mls/min/1.73m^2 and a normal serum creatinine level as measured by the hospital laboratory.

6.2. ECG analysis

Comparison of the standard 12 lead ECG measured corrected QT interval was made between the two groups with a QTc in the control group of 451ms±6.58ms and 467ms±13.67ms in the group with diabetes which was significantly different (p=0.011: Figure 32). Based on

previous experimental work we expected there to be arrhythmogenic changes in gene expression in the diabetes group and we planned to see if this might result in more positive late potentials but SAECG assessment of our two groups yielded only one patient in each group with a positive SAECG for late potentials with no difference between groups (p=ns). Measurements of the QRS width, HFLA signals, mean voltage in the terminal 40mSec of the QRS and the root mean square voltage in the terminal 40mSec were all not statistically different in the two groups (p=0.292, 0.28, 0.73, 0.814 and 0.63 respectively; Figure 32).

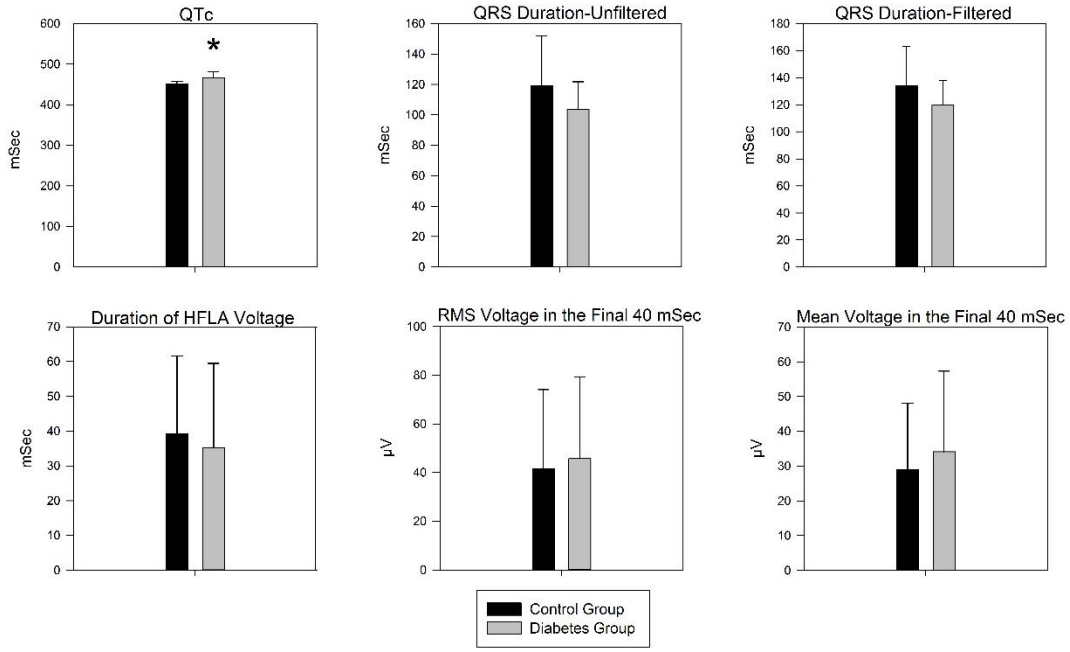

Figure 32: Key measurements from the standard 12 lead ECG and signal averaged ECG for the control (n=9) diabetes (n=7) groups. Means ± SEM shown.

6.3. Echocardiography

6.3.1. Inter- and intra-observer variation

As a measurement of quality control and reliability, inter- and intra-observer variability of some of the standard echocardiographic measurements used in this study were assessed and are shown below as Bland-Altman plots in line with previously published echocardiography studies and best practice (183):

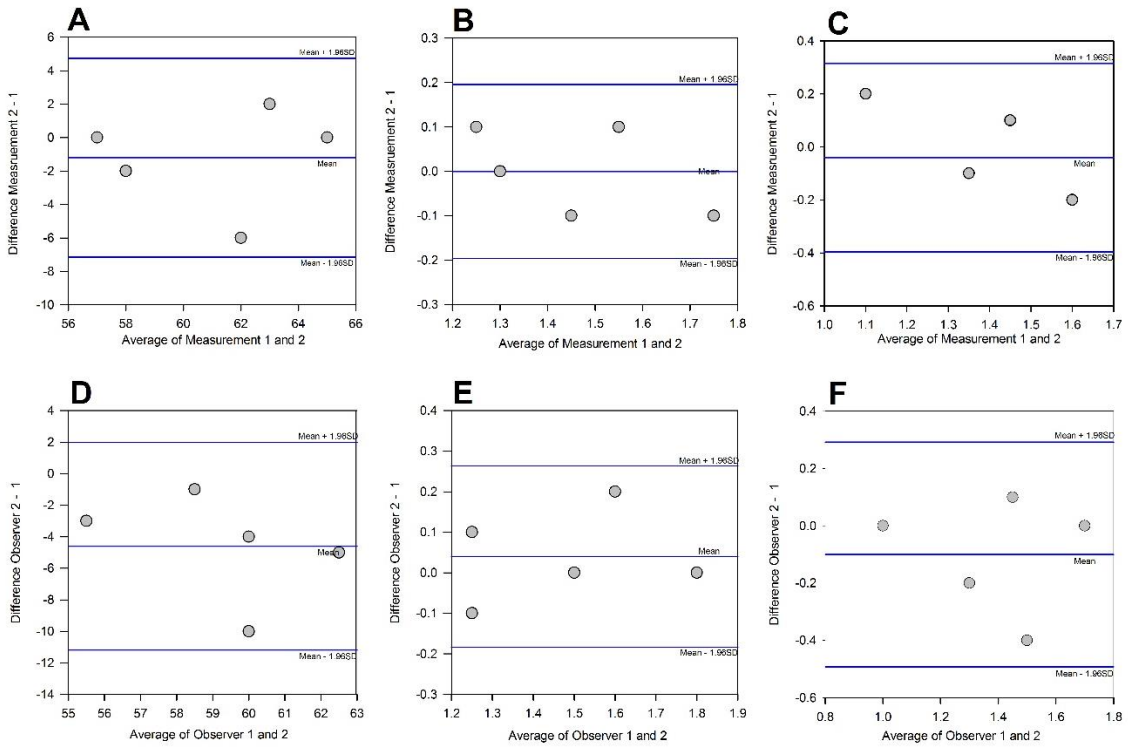

Figure 33: Bland-Altman plots of intra- and inter-observer variability of some of the most important standard echocardiographic measurements with mean and standard deviation lines (n=5 for each assessment).A, Intra-observer variability of EF. B, Intra-observer variability of septal width. C, Intra-observer variability of MAPSE. D, Inter-observer variability of EF. E, Inter-observer variability of septal width. F, Inter-observer variability of MAPSE.

As seen above, there is good agreement visually between observers and by the same observer repeating the analysis with no results outside the 95% lines. This suggests therefore reasonable validity in the measurements made and reliability in the reproducibility of the results obtained in this study. This is in part due to the methodology used in this study which has come in large part from consensus guidelines based on multiple large studies. Also, both observers were trained in the same department which does in all probability help add to agreement between observers. A comparative t-test for each measurement between observers and intra-observer yielded no significant differences.

As with the standard 2D echocardiographic measurements made above methodological analysis of the global average strain rate data was made using Bland-Altman plots shown below:

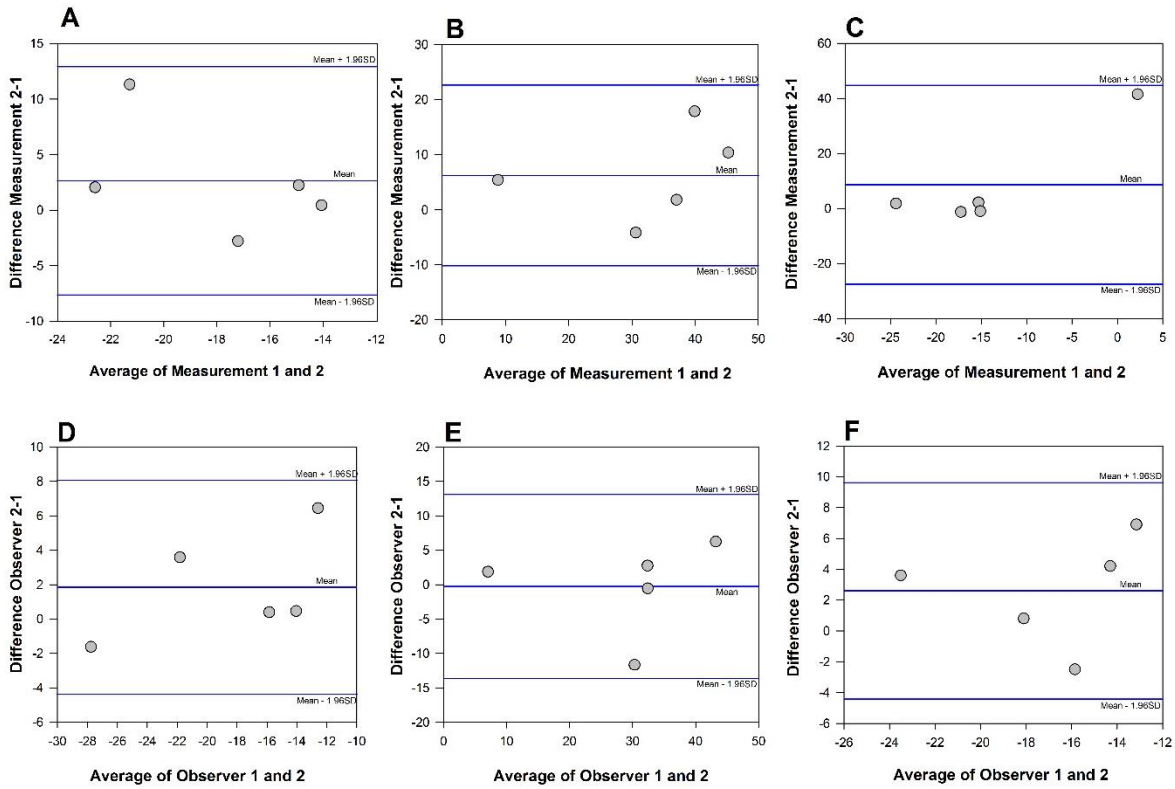

Figure 34: Bland-Altman plots of inter- and intra-observer variability of speckle derived longitudinal and circumferential stain with mean and standard deviation lines (n=5 for each assessment. A, Intra-observer variability of circumferential strain by speckle. B, Intra-observer variability of radial strain by speckle. C, Intra-observer variability of longitudinal strain by speckle. D, Inter-observer variability of circumferential strain by speckle E, Inter-observer variability of radial strain by speckle. F, Inter-observer variability of longitudinal strain by speckle.

As we can see there is acceptable agreement in the strain analysis suggesting reasonable reproducibility of results obtained via strain analysis. Again, a t-test of each measurement between observers and intra-observer yielded no significant differences.

6.3.2. Standard echocardiographic measurements

Prior to more detailed assessment of strain rates between the two groups, standard echocardiographic assessment was made of the patients in each group shown below in Table 13 with means, SEMs and *p* value between the groups:

Echocardiographic Parameter	Control Group	Diabetes Group	*p* Value
Ejection Fraction (%)	63.88 (2.31)	58.21 (1.16)	0.09
LV Septal Width (Cm)	1.56 (0.08)	1.68 (0.02)	0.53
End Systolic Volume (Mls)	31.55 (5.08)	37.80 (2.78)	0.39
End Diastolic Volume (Mls)	76.19 (9.37)	89.60 (6.97)	0.33
Mitral Annular Planar Systolic Excursion (Cm)	1.57 (0.09)	1.12 (0.09)	**<0.01**
Left Atrial Area (Cm^2)	20.42 (0.78)	26.94 (2.47)	**0.01**
E/A ratio	0.88 (0.07)	0.918 (0.10)	0.81
E/e' Lateral	11.16 (1.33)	12.79 (1.53)	0.44

Table 13: Standard echocardiographic measurements in each group

Our results show that both study groups are not statistically different in terms of traditional measurements of left ventricular function (ejection fraction) and left ventricular wall thickness (septal width). Both groups showed significant hypertrophy of the left ventricle septum when compared to reference values[185] as would be expected with significant aortic stenosis. We did see however that longitudinal function was depressed in the group with diabetes and there was an increase in left atrial size which are well recognised features of diabetes, thought to be due to sub-endocardial damage causing reduced longitudinal function and higher LV filling pressures resulting in increased LA size. These results show that we have a control group and an experimental group who would, by traditional assessment, have similar contractile performance and hypertrophic change, which we believe provides a useful comparison of the effect of type 2 diabetes on the human left ventricle over and above LVH.

6.3.3. Atrial function

Following on from the higher LA size and published work on higher LA pressures in patients with diabetes[332], measurement of active left atrial function between groups showed that there was no statistically significant difference in left atrial passive or active emptying (p=ns for both; Figure 35) but that the left atrial expansion index was significantly reduced by nearly 50% in the group with diabetes (p=0.035) and this measures the LA reservoir function.

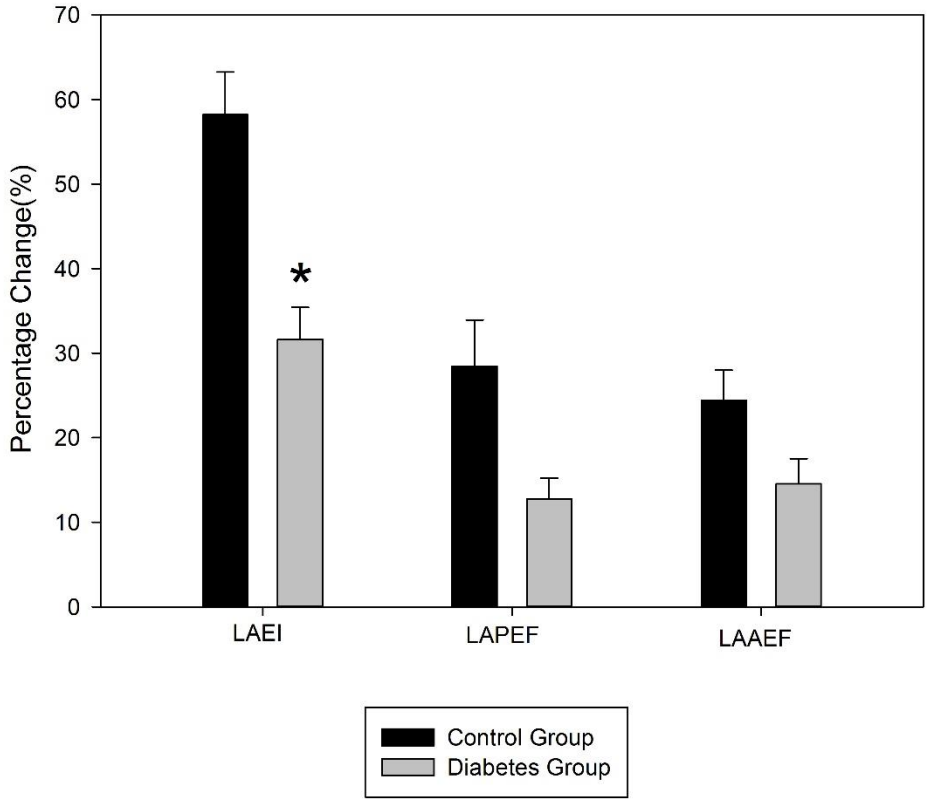

Figure 35: Comparison of the left atrial expansion index (LAEI), left atrial passive emptying fraction (LAPEF) and left atrial active emptying fraction (LAAEF). Means ± SEM shown (Control; n=9/Diabetes; n=7). *significantly different from the control group (P<0.05).

6.3.4. Strain analysis

As discussed in the methodology section we have primarily focussed on the use of speckle tracking in this study because of easier use and superior reliability[333] but to show that the

trends we obtained would be similar using TVI, comparison of longitudinal and circumferential strain was made between the two methods using the Bland-Altman method.

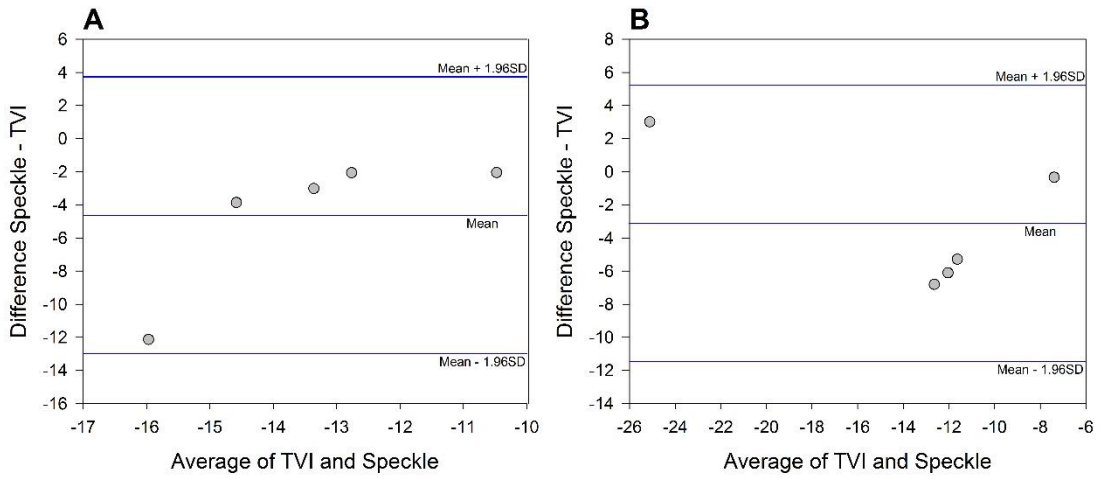

Figure 36: Bland-Altman comparison of longitudinal and circumferential strain using TVI and speckle tracking. (n=5 for each assessment). A, TVI vs. speckle for longitudinal strain. B, TVI vs. speckle circumferential for longitudinal strain

As mentioned earlier, radial strain is not well measured by TVI imaging [179] and so was not included in the methodological comparison but as we can see in the two plots there is good agreement between the two methods and this has previously been reported [334] and helps supports the reliability/reproducibility of our strain rate trends measured in this study (Figure 36). In addition to this there was no significant difference in the measurements when they were analysed using a t-test for both groups.

Both groups had a mean global longitudinal strain rate which is lower than previously published normal values of -21%+/- 2%[184] and longitudinal strain measurements (below -18%) in the range associated with myocardial fibrosis in diabetes [182] and in aortic stenosis alone [168] in previous studies. Both groups had strain values that are much lower than previously reported control values and strain values consistent with results correlating with myocardial fibrosis. These findings would support an indirect suggestion of interstitial fibrosis in both groups, and that the changes in the diabetes group are likely to relate to diabetes and not just interstitial fibrosis.

Comparative strain analysis between the groups to look for subtle left ventricular dysfunction was assessed in the circumferential, radial and longitudinal planes and shows that global circumferential (p=<0.01; Figure 37) and longitudinal strain (p=0.013) were markedly lower (by nearly 50% and 25% respectively) in the group with diabetes suggesting dysfunction specific to patients with diabetes over and above that expected in aortic valve disease (Figure 37).

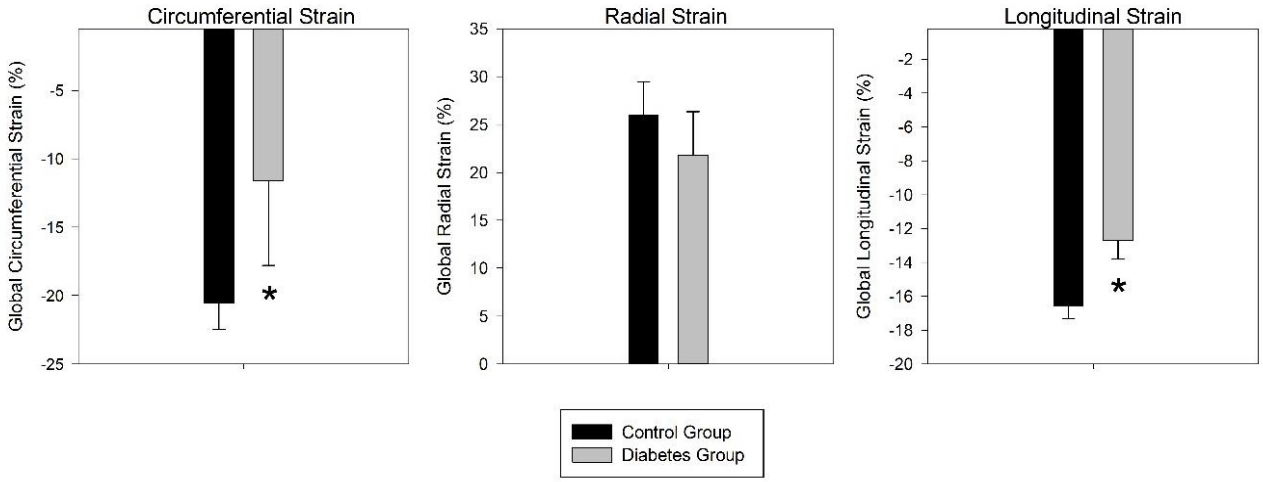

Figure 37: 2D Speckle derived measurements of strain in the longitudinal, circumferential and radial vectors. Means ± SEM shown (Control; n=9/Diabetes; n=7). *significantly different from the control group (p<0.05).

6.4. RT- PCR results

6.4.1. Main ion channels active during the action potential

Expression of left ventricular ion channel genes in the diabetes group (n=7) was measured quantitatively at the mRNA level using PCR and compared to the non-diabetic control group (n=9). Expression of the primary cardiac Na^+ channel, ($Na_v1.5$) was slightly higher in the diabetes group but not significantly (p=0.50). Expression of the L-type voltage gated Ca^{2+} channels ($Ca_v1.2$ and $Ca_v1.3$) responsible for the $I_{Ca\text{-}L}$ current were not significantly altered in the diabetes group (p=0.98 and 0.92 respectively) compared to the control group. Expression

of K_v1.4 and K_v1.5, which are responsible for the slow transient outward K^+ current ($I_{to\text{-}S}$) and the ultra-rapid delayed rectifier K^+ current ($I_{K,ss}$), tended to be greater in the diabetes group (but not significantly so; p=0.77 and 0.73 respectively). Expression of K_v4.2 (KCND2) and K_v4.3 (KCND3) and the auxiliary subunit KChIP2 (Kcnip2), which are responsible for the fast transient outward K^+ current ($I_{to\text{-}F}$), were not significantly different between groups but tended to be higher in the diabetes group. In the diabetes patients, the major finding, was a significant reduction by 65% (p<0.01; Figure 38) in expression of ERG (K_v11.1) responsible for the rapid delayed rectifier K^+ current ($I_{K,r}$). Expression of K_vLQT1 (KCNQ1) was not significantly altered between groups (p=0.83).

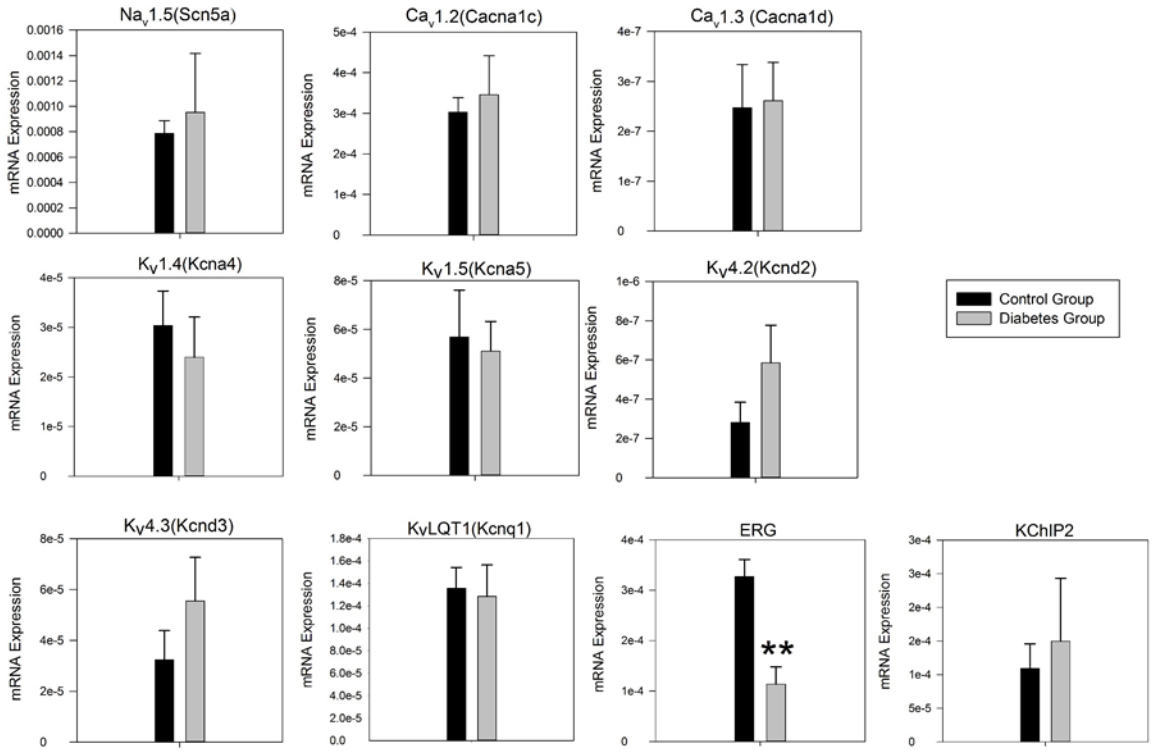

Figure 38: Expression of mRNA for major ion channels active during the action potential in the left ventricle of the control and diabetes groups displayed in arbitrary units referenced to expression of 18-s (housekeeper gene). Means ± SEM shown (Control; n=9/Diabetes; n=7). **significantly different from the control group (p<0.01).

6.4.2. Main ion channels active during diastole

In our assessment of major channels active during diastole, we were able to see expression of KCNJ3 which encodes $K_{ir}3.1$, a G-protein activated subunit of the $I_{k,ACh}$ channel (acetylcholine activated inward rectifying current), was reduced by nearly 50% in the group with diabetes (p=0.039; Figure 39). We also saw that there was an 85% and 68% increase in mRNA levels of KCNJ2 and KCNJ5 respectively (p=<0.01), which encode $K_{ir}2.1$ and $K_{ir}3.4$ respectively, in the group with diabetes. We did not observe any differences in gene expression of the major cardiac gap junction proteins, connexins Cx40 and Cx43 or in the Na^+/K^+ hyperpolarisation activated cyclic nucleotide-gated channels 1, 2 and 4 (HCN1, 2 and 4) which are responsible for the funny current (I_f), an important pacemaker current, which is a current predominantly expressed in the foetal human ventricle or sino-atrial node.

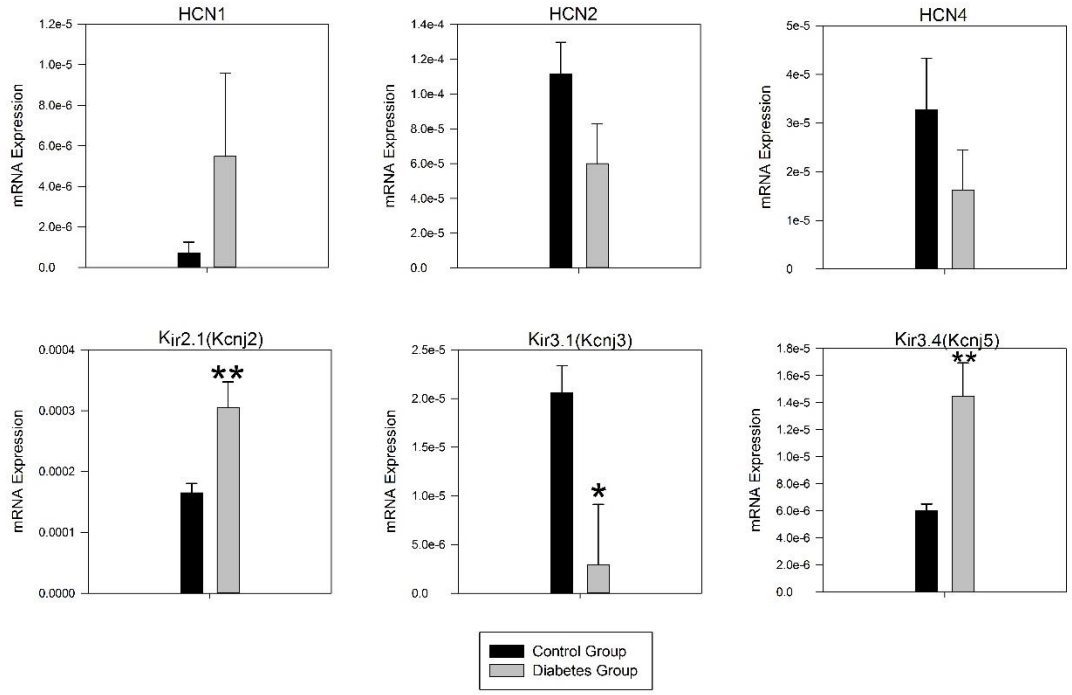

Figure 39: Expression of mRNA for major ion channels active during diastole in the left ventricle of the control and diabetes groups displayed in arbitrary units referenced to expression of 18-s (housekeeper gene). Means ± SEM shown (Control; n=9/Diabetes; n=7). *significantly different from the control group (p<0.05). **significantly different from the control group (p<0.01).

6.4.3. Cardiac Ca^{2+} handling Proteins

In our group with diabetes we observed that ventricular expression of NCX1 (Na^{+}-Ca^{2+} calcium exchanger) was 240% higher compared to the control group (p=0.047; Figure 40) but that expression of RYR2 (the sarcoplasmic reticulum's – SR's – Ca^{2+} channel) and SERCA2A (the sarcoplasmic reticulum's – SR's – Ca^{2+} pump) tended to be lower in the diabetes group but not significantly so (p= 0.78 and 0.75 respectively).

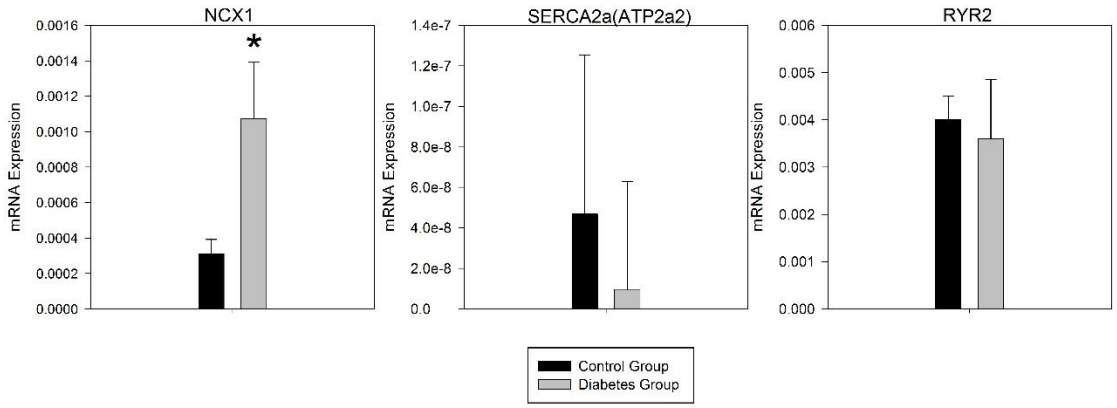

Figure 40: Expression of mRNA for cardiac Ca^{2+} handling proteins in the left ventricle of the control and diabetes groups displayed in arbitrary units referenced to expression of 18-s (housekeeper gene). Means ± SEM shown (Control; n=9/Diabetes; n=7). *significantly different from the control group (p<0.05).

6.4.4. Other channels and proteins

Similarly, to the previous rat studies, a selection of Cl^{-} channels was investigated: CLCN-2, CLCN-3, TTYH-1 TTYH-3 and BEST1 which is thought to encode for the I_{ClCa} current which allows Ca^{2+} mediated Cl^{-} efflux. There was no clear pattern of chloride expression between the two groups with no significant difference between groups in expression (p=ns for all; Figure 41). There was no significant difference in expression between groups of Na^{+}-K^{+} ATPases with very similar values for each isoform. Expression of Cx43 tended to be greater in the diabetes group (but not significantly so; p=0.237) and expression of Cx40, which encoded for gap junction alpha 5, another connexin important in cardiac conduction was slightly lower in the diabetes group but not significantly (p=0.394).

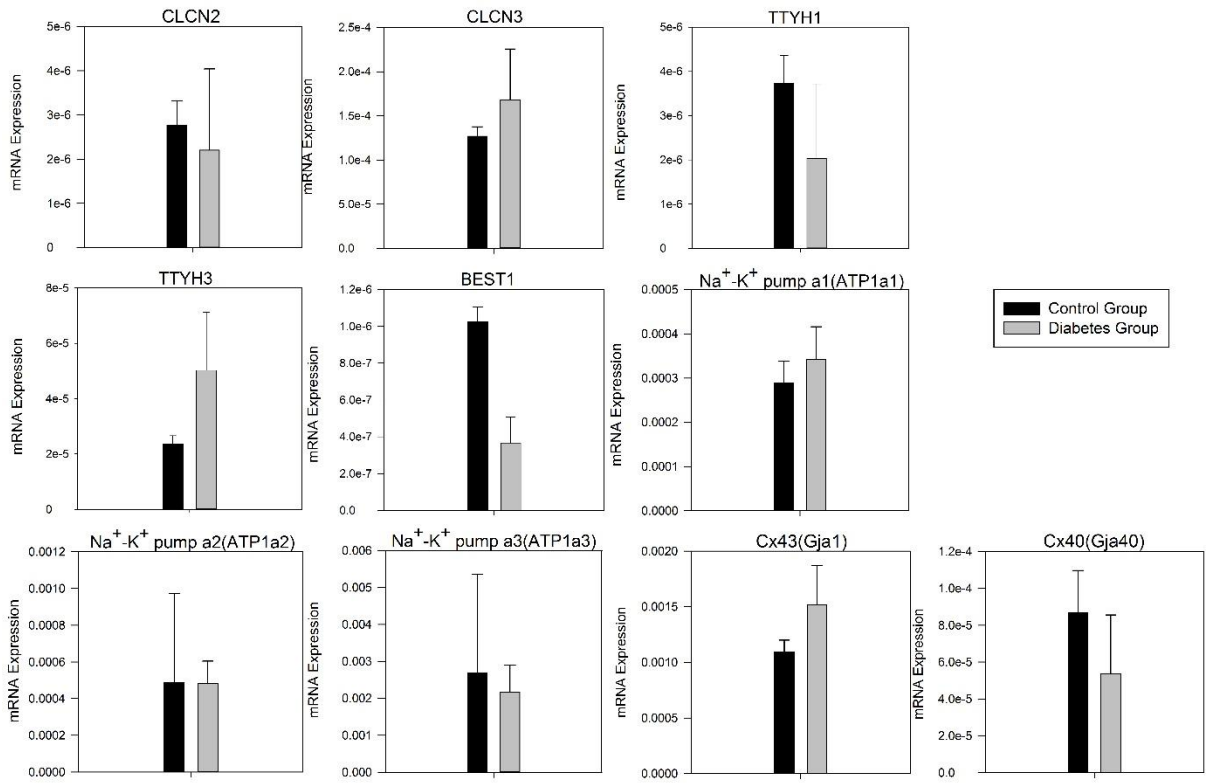

Figure 41: Expression of mRNA for Cl^- channels, α subunits of the Na^+-K^+ pump and the gap junctions Cx43/Cx40 in the left ventricle of the control and diabetes groups displayed in arbitrary units referenced to expression of 18-s (housekeeper gene). Means ± SEM shown (Control; n=9/Diabetes; n=7).

6.4.5. Cardiac energy production

As in the previous experiments, GLUT-4, MT-ATP6 and MT-ATP 8 expression were analysed again to look for an effect of type 2 diabetes on cardiac energy production. No observed significant difference in expression of GLUT-4 or MT-ATP8 was noted but a 17% reduction in MT-ATP 6 was noted (p=0.042; Figure 42) in the diabetes group.

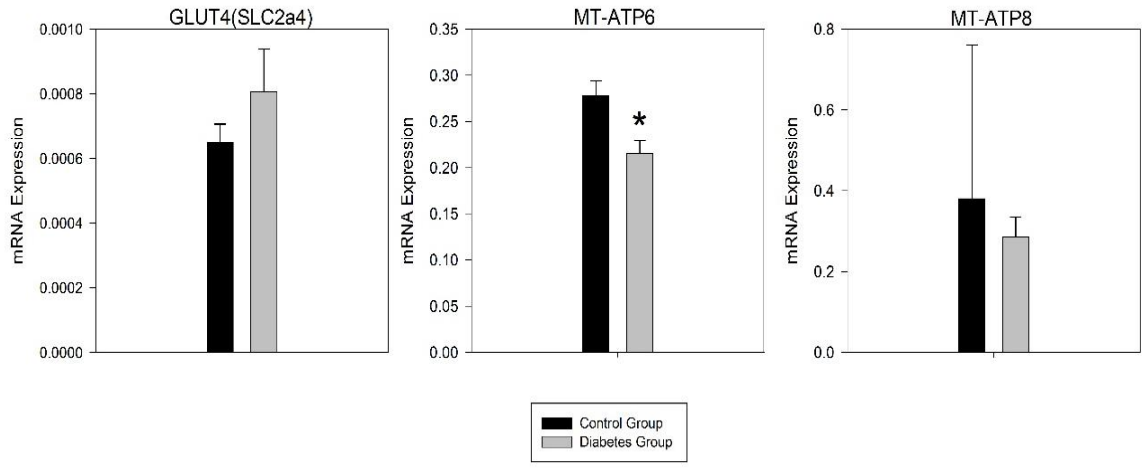

Figure 42: Expression of mRNA for important cardiac energy production genes in the left ventricle of the control and diabetes groups displayed in arbitrary units referenced to expression of 18-s (housekeeper gene). Means ± SEM shown (Control; n=9/Diabetes; n=7). *significantly different from the control group (p<0.05).

6.4.6. Neuronal genes

As the final section for analysis, genes related to neuronal function, TH, UCHL1, NGF1, TACR1 were once again measured for differences in qPCR expression. There was no observable significant difference in expression for any of the 4 genes between the diabetes and control group (Figure 43).

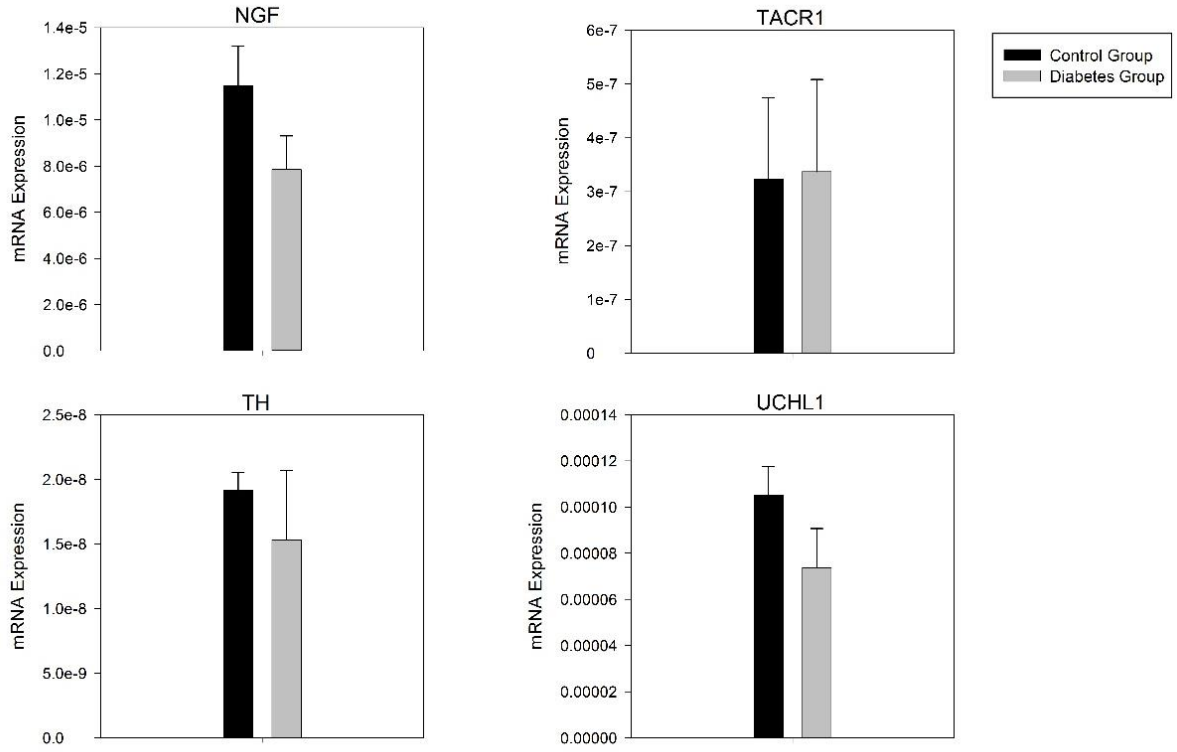

Figure 43: Expression of mRNA for important cardiac neuronal genes in the left ventricle of the control and diabetes groups displayed in arbitrary units referenced to expression of 18-s (housekeeper gene). Means ± SEM shown (Control; n=9/Diabetes; n=7).

6.5. Action Potential Modelling

Using the results from our RT-PCR experiment we were able to use this to model the effect this would have if translated at the protein level to their respective channels that are testable using the O'Hara-Rudy model. Based on the testable currents available from the O'Hara-Rudy model, the quantitative qPCR data for these currents were converted to relative expression changes shown below in Table 14 and then converted to current conductance changes:

Channel	Current	Expression change in diabetes group
$Na_v1.5$	I_{Na}	+21.08%
$Ca_v1.2$ and 1.3	$I_{Ca\text{-}L}$	+14.18%
$K_v1.4$, 4.2 and 4.3	I_{to}	+26.04%
ERG	$I_{K,r}$	-65.24%
K_vLQT1	$I_{K,s}$	-5.38%
$K_{ir}2.1$	$I_{K,1}$	+85.23%
NCX1	I_{NaCa}	+243.83%
RYR2	SR Ca^{2+} release	-10.07%
ATP1a1-3	$I_{Na\text{-}K}$	0%

Table 14: Relative current expression changes based on mRNA change in the diabetes group

Using this data in a similar manner to the HFD experiment, the Figure shows simulated action potentials (top row) from the human endocardial (Figure 44A) and epicardial (Figure 44B) ventricular cell in the control and diabetes groups, accompanied by the cardiac currents and the intracellular Ca^{2+} concentration fluctuation. In both the endocardial and epicardial cell models, remodelled ion channels based on gene expression change in the diabetes group produced an increase in the amplitude of the action potential, elevation of the plateau phase and an increase in the APD. In particular, at the endocardial level, there was generation of an early-after depolarization which was not reproduced in the epicardial cell. APD prolongation is potentially attributable to the increase in many of the currents observed in the diabetes group and to elucidate which of these genes were most responsible, each current was separately tested to identify which were the drivers of the AP changes seen.

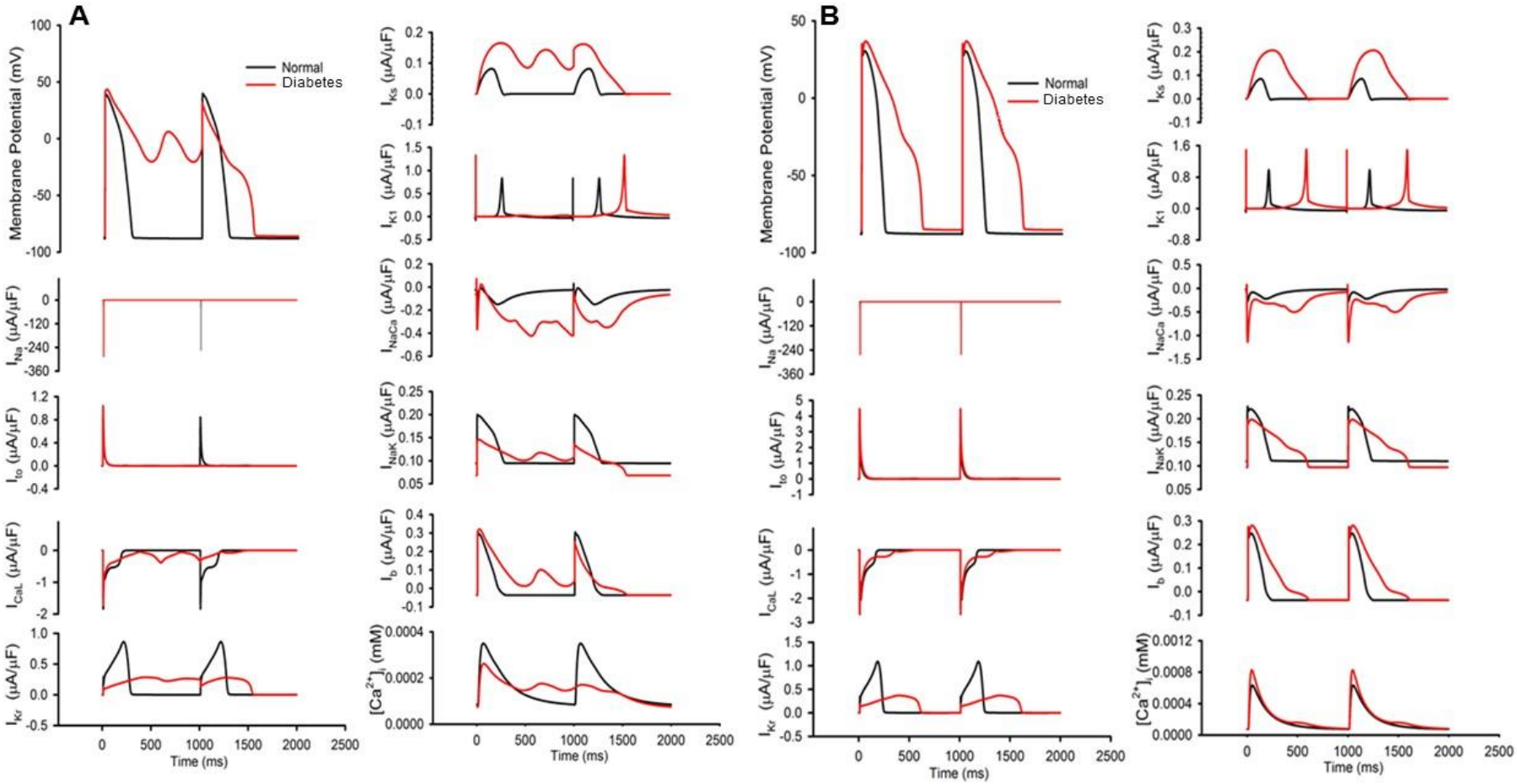
A
B
Normal
Diabetes
Membrane Potential (mV)
I_{Ks} (μA/μF)
I_{K1} (μA/μF)
I_{Na} (μA/μF)
I_{NaCa} (μA/μF)
I_{to} (μA/μF)
I_{NaK} (μA/μF)
I_{CaL} (μA/μF)
I_b (μA/μF)
I_{Kr} (μA/μF)
$[Ca^{2+}]_i$ (mM)
Time (ms)

Figure 44: Simulated human ventricular endocardial (A; ENDO) and epicardial (B; EPI) action potentials and underlying ionic currents and intracellular Ca^{2+} concentration in control and diabetes groups

When each channel was tested singularly, (shown in Figure 45) the modelled increases of $I_{Ca\text{-}L}$, I_{Na} and I_{to} independently had negligible effects on APD and the amplitude of the action potential (Figure 45A-C). Modelling of the small decrease in $I_{K,s}$ had no noticeable effect on the AP as might be expected from the very minor mRNA change (Figure 45D). The modelled reduction of $I_{K,r}$ led to a dramatic prolongation of the AP in both simulated muscle layers and an increase in the maximum membrane potential (Figure 45E). The increase in $I_{K,1}$ (Figure 32F) alone resulted in APD abbreviation especially in phase 3, where $I_{K,1}$ sharpens the rate of descent. The increase in I_{NaCa} led to prolongation of the AP, elevation of the resting membrane potential and failure to fully repolarise (Figure 45G). Ca^{2+} release via RYR2 (Figure 45H) which was modelled to be reduced by a small amount, produced negligible effects on the action potential and very little change in calcium level change. Therefore, the simulations suggest that the diabetes induced changes in ion channels could result in a prolongation of APD primarily as a result of an increase in I_{NaCa} and a reduction in $I_{K,r}$ with generation at the endocardial layer of an EAD.

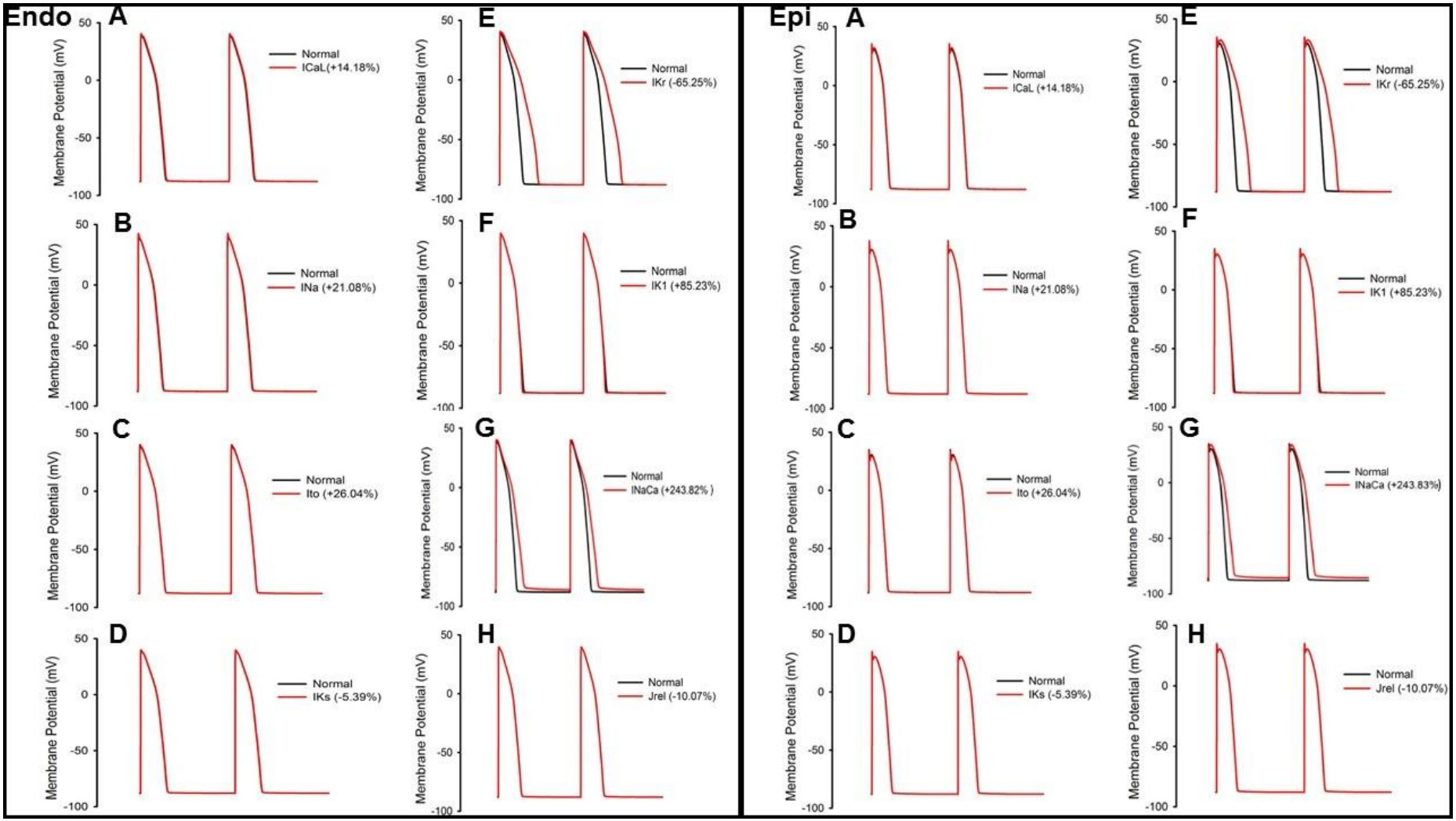
Endo
A
Normal
ICaL(+14.18%)
B
Normal
INa (+21.08%)
C
Normal
Ito (+26.04%)
D
Normal
IKs (-5.39%)
E
Normal
IKr (-65.25%)
F
Normal
IK1 (+85.23%)
G
Normal
INaCa (+243.82%)
H
Normal
Jrel (-10.07%)
Epi
A
Normal
ICaL (+14.18%)
B
Normal
INa (+21.08%)
C
Normal
Ito (+26.04%)
D
Normal
IKs (-5.39%)
E
Normal
IKr (-65.25%)
F
Normal
IK1 (+85.23%)
G
Normal
INaCa (+243.83%)
H
Normal
Jrel (-10.07%)
Membrane Potential (mV)
50
0
-50
-100

Figure 45: Simulated human ventricular endocardial and epicardial action potentials in control and diabetes groups with each of the remodelled ion channels/ionic currents modified singularly. A, only $I_{Ca,L}$ considered. B, only I_{Na} considered. C, only I_{to} considered. D, only $I_{K,s}$ considered. E, only $I_{K,r}$ considered. F, only $I_{K,1}$ considered. G, only I_{NaCa} considered. H, only SR Ca^{2+} release considered (J-Rel. respectively).

6.6. Discussion

6.6.1. Human study-type 2 diabetes: Clinical characteristics

In this study we were fortunate to have two very similarly matched groups in terms of age, BMI, waist circumference and the diabetes group only had 1 person with a reported complication from their diabetes (minor nephropathy-evidenced by a slightly increased albumin-creatinine ratio). Overall, we consider that this, compared to many studies, gives a small but comparable cohort.

6.6.2. Arrhythmogenesis

As with our previous 2 experiments, reviewed below are the major mRNA changes and the AP modelling results and a discussion of how these relate to an arrhythmogenic phenotype in the diabetes patient.

6.6.2.1. Down-regulation of ERG in type 2 diabetes

In our group with diabetes, we have seen a marked reduction in ventricular mRNA expression of ERG which encodes the pore forming subunit of the $I_{K,r}$ channel, the major outward delayed rectifying current with a marked prolongation of the AP.

Functionally $I_{K,r}$ causes K^+ efflux with slow activation and fast recovery from inactivation, creating a positive feedback loop to help keep the AP duration appropriate[335] and prevent AP prolongation, one of the prime steps in arrhythmogenesis. This function of the ERG channel is very important as in the context of an ectopic waveform, quick recovery from inactivation allows a short, high transient outward current to be generated by the ectopic waveform through the ERG channel and prevents the waveform generating a current large enough to promote an ectopic beat[336]. $I_{K,r}$ also has a secondary function which is to remain open during the resting phase of the AP for a period and this helps to maintain cell refractoriness.

Our AP modelling shows that down-regulation of ERG creates early after depolarizations at the endocardial level at the plateau phase of the AP, which is a previously reported phenomena in the context of normal cellular coupling[337]. This is thought to be due

to reactivation of the $I_{Ca\text{-}L}$, created by extension of the plateau phase and occurs in the endocardium predominantly as the sharper electrical gradient between the epicardium and mid-myocardium allows formation of a 'sink' for excess current in the epicardium reducing EADs in the mid- and epicardial layers[337]. As well as the other pro-arrhythmic consequences of reduced ERG we know from previous studies that down-regulation of ERG leads to a reversal of the repolarization gradient from apex to base and increased dispersion and thus the formation of re-entrant circuits and arrhythmias[338].

The role of reduced ERG expression and or ERG blockade clinically in arrhythmogenesis [339] is well reported and particularly so in patients with diabetes[130]. In previous studies it has been shown that both myocardial hypertrophy[340] and myocardial fibrosis[341] leads to reduced ERG and it is not clear that diabetes had a specific effect on ERG expression within the myocardium or whether down-regulation of ERG was a function of hypertrophy/fibrosis. By comparing our group with diabetes to a control population with hypertrophy and likely fibrosis, we have shown that there may be a specific effect of diabetes on ERG expression within the myocardium and that this may go some way to explaining higher arrhythmia rates in patients with diabetes.

6.6.2.2. Up-regulation of $K_{ir}2.1$ in type 2 diabetes

In our group with diabetes, there was an up-regulation of KCNJ2, which is the gene responsible for the main component of $I_{K,1}$ channel, which sets the resting membrane potential at more negative potentials allowing for increasing potassium efflux. Our AP modelling has shown that this probably has only a small effect on the AP (again this maybe a function of AP simulations), most obviously in acceleration in phase 3 of repolarization to give a sharper terminal part of the curve. Other experimental work has suggested that increased or gain function, mutations in KCNJ2, leads to a more negative membrane resting potential, shorter terminal phase 3 and shorter action potential, similar to what we have observed, when testing this current only.

Clinically an association between increased $I_{K,1}$ has been seen with atrial fibrillation[213], ventricular tachycardia[292] and elimination of the slow T wave in the ECG[293].

Experimentally, if over-expression of $I_{K,1}$ is not pro-arrhythmic on its own, studies have shown that it renders the heart more susceptible to arrhythmias[342].

Whilst, lots of evidence points to a pro-arrhythmic action, as discussed above it may be that the up-regulation of KCNJ2 we have seen is compensatory with an increase in $I_{K,1}$ an attempt to balance the increase in APD and try to counter the effect of reduced ERG. This appears to be a consistent finding from our obesity experiment which as noted in the introduction is a major risk factor for type 2 diabetes.

6.6.2.3. Down-regulation of K_{ir}3.1 in type 2 diabetes

We have also seen that there is comparatively reduced expression of KCNJ3 in the group with diabetes, which codes for a tetrameric, acetylcholine responsive rectifying channel that predominantly is expressed in atria. Due to the fact that this is mainly an atrial channel we were not able to incorporate this into our biophysical model and thus look at a potential effect on the AP and so theoretical information on how it may contribute comes from other studies.

In atrial studies inhibition of the $I_{K,ACh}$ channel, resulted in prolongation of the action potential in the atria with a change in the APD repolarization curve[343] with similar findings in the single human ventricular cell[228]. Interestingly this effect with the atria was protective with reduced arrhythmogenesis. Expression of the $I_{K,ACh}$ channel tends to be in an opposite manner to $I_{K,1}$, with mainly ventricular expression of $I_{K,1}$[344]. It has previously been shown that there is a regional variation in the effectiveness of the $I_{K,ACh}$ channel and that in epicardial cells within the left ventricle, activation of this channel is negatively inotropic[345].

Whether these effects would be directly reproduced in the human ventricle would require physiological testing but if the down-regulation did produce the effects noted above such as prolongation of the AP or reduced contractility, this would be consistent with our observed functional findings on the EGG (prolonged QTc) and echocardiogram (reduced strain).

Interestingly we observed the same changes in the STZ experiment in the ventricle of the rat, whether this represents a diabetes specific process linked to nervous system function could be explored further.

6.6.2.4. Up-regulation of $K_{ir}3.4$ in type 2 diabetes

Opposite to KCNJ3, we saw an up-regulation in expression in KCNJ5, which codes for the other two of the four subunits of the $I_{K,ACh}$ channel and has stretch related properties, which provide electro-mechanical feedback and inhibit the channel, in high stretch situations[213]. This up-regulation of the stretch sensitive subunits would suggest, that the higher LV filling pressures (our diabetes group did have larger left atria which often correlated with higher LV end diastolic pressures) commonly seen in diabetes, may present a mechanism for further $I_{K,ACh}$ channel inhibition and QT prolongation. The $I_{K,Ach}$ channel is an important therapeutic target in the treatment of human arrhythmias, ventricular and atrial, with blockade of this channel prolonging the action potential, but any potential role in ventricular arrhythmias in diabetes is unclear, though this channel has been shown to be down-regulated in chronic atrial fibrillation[346]. Again as with $K_{ir}2.1$ further experimental work would be needed to look at the role of $K_{ir}3.4$ in the ventricle and its functionality in the obese individual.

6.6.2.5. **Up-regulation of NCX1 in type 2 diabetes**

We have seen an increase in NCX1 mRNA expression and this finding has been repeated in a wide variety of cardiac disease states such as heart failure and ventricular tachycardia[347] as we have discussed already in the obesity section.

While many of the mechanisms of arrhythmia generation will be the same in the two disease states, obesity and diabetes, several particular areas require specific review. Firstly, hyperglycaemia is known to inhibit the sarcolemma Na^+–K^+ exchanger with resulting higher levels of intracellular Na^+, which results in increased reverse flow of NCX1, leading to Ca^{2+} overload within the cell and sarcoplasmic reticulum. This excess of Ca^{2+}, can cause spark formation leading to generation of DADs and to triggered activity and ventricular arrhythmias. Secondly, NCX1 over expression may tie in with the other changes we have seen, as prolongation of the action potential, leads to stimulation of the NCX1 forward mode and reactivation of $I_{Ca\text{-}L}$ which then can generate DADs, through generation of I_{Ti} in phase 4 of the action potential, which is something we were able to model at the endocardial level. Finally, in identical fashion to our animal obesity model we have been able to show

down regulation of $I_{K,1}$ with as expected a sharper membrane potential drop in the terminal phase of repolarization which synergistically may potentially lead to creation of the arrhythmogenic I_{Ti} current.

NCX1 expression has been seen to be increased in LV hypertrophy[348] and by comparing our group with diabetes who traditionally have been seen to have increased LV mass, with a control with LV hypertrophy, we can see that diabetes on its own does seem to stimulate NCX1 overexpression. There seem to be many mechanisms as discussed here whereby an increase in NCX1, is arrhythmogenic and whilst this study cannot prove the validity of each postulated mechanism, there is enough evidence elsewhere to suggest an important role for NCX1.

6.6.2.6. ECG-correlation with qPCR

Similarly, to many other studies[349, 350] we were able to observe a prolongation of the QTc in our group with diabetes compared to the control subjects. This is supportive of the arrhythmogenic changes we have seen at the mRNA level and with our AP modelling. By looking at two comparable groups, it would appear that this change is primarily a function of their diabetes.

In our study we have seen that in 2 similar groups of patients that the presence of type 2 diabetes did not cause any significant differences in the QRS width, late voltages or positive signal averaged ECG assessment. On review of the literature we did find reports of increased prevalence of positive SAECGs in patients of all ages with diabetes[351], though the level of diabetic complications[352] was not always stated and this has made comparing our data difficult. We know from previous work that there is an increased incidence of positive SAECGs in patients with aortic stenosis[353] and it may be that a potential difference here has been removed because our control group unlike other studies also had a disease process causing LVH and potentially myocardial fibrosis.

6.6.3. Contractility

The qPCR data obtained predominantly reflects a genotype that leads to a modelled increase in AP duration and this normally would lead to an increase in duration of the calcium

transient and thus the SR Ca^{2+} load which is then linked to Ca^{2+} induced ECC. Looking at our AP modelling this would certainly seem to be the case and by allowing for increased time, an increase in Ca^{2+} entry may compensate in the early stages for deficient contractile function or larger LV mass[354]. Whether as the disease progresses the altered Ca^{2+} load leads to abnormal handling and impairment of the Ca^{2+} linked ECC has not been fully proven. The only gene change which may prove directly negatively inotropic was our observed increase in the $I_{K,ACh}$ channel gene which in turn are stimulated by vagally released acetylcholine. Previous work has shown that there may be a directly negatively inotropic action of $I_{K,ACh}$ but also that this may oppose sympathetic mediated β-adrenoceptor positive inotropic activity[355, 356]. We do know that the majority of the $I_{K,Ach}$ current is expressed in the atria, so any reduction in function is likely to be primarily in the atria compared to the ventricle, interestingly we did observe a significant reduction in one active atrial function parameter, LAEI and a trend for all others to be reduced. The left atrium exists under similar conditions to the left ventricle and the Frank-Starling's law applies similarly to the LAEI's reservoir function and this phase of atrial function is characterised by passive enlargement allowing filling from the pulmonary veins in ventricular systole. This function is characterised firstly by atrial relaxation, then compliance and a stretchable left atrium but as we might expect with increasing left atrial size and in a condition marked by fibrosis, hypertrophy and vascular stiffness (diabetes) as compliance falls, so does the LAEI. This result would be consistent with previously published worked on age related reductions in the LAEI with complimentary increases in LA area[357].

Previous studies suggest that much of the impaired ventricular contractile function relates to changes in the structure of the diabetic heart with changes in collagen deposition and marked fibrotic change within the ventricle.

As expected, we did see that both groups had significant levels of left ventricular hypertrophy and that despite a normal ejection fraction value, both groups had strain values below the normal reported range and consistent with myocardial fibrosis. As outlined above reduced contractile function in diabetes is thought in large part to be due to structural abnormalities such as myocardial fibrosis with increasing fibrosis linked to poorer function and lower strain rates to higher rates of fibrosis[358].

Our group with diabetes comparatively had larger atrial areas and lower longitudinal function and this is a commonly reported [359] phenomena potentially due to increased collagen deposition and fibrosis leading to subclinical dysfunction and lower compliance for LV filling.

Further work would be needed to longitudinally track the prolonged AP gene changes we observed and the relationship to ventricular function to see whether this truly represents an early adaptive phase prior to clinical symptoms.

6.6.4. Energy production in type 2 diabetes

Despite the wide ranging metabolic effects of diabetes, the only observable change seen in gene expression was a down regulation in MT-ATP6.

MT-ATP6 dysfunction is commonly seen as Leigh's syndrome, a severe multi-system disorder with severe neurological features as well as energetic disorders. What we do know from some animal studies is that a lack of MT-ATP6 leads to a loss of complex V function which is important in the normal oxidative phosphorylation process leading to an increase in atypical energy pathway use [360] which is less effective. Previous studies have shown clear energy production abnormalities in type 2 diabetes within the heart relating to mitochondrial dysfunction [361].

Interestingly MT-ATP6 polymorphisms have been linked to the development of type 2 diabetes [362] and to inherited cardiomyopathies [363] increasing the likelihood of there being a common pathological themes.

6.6.5. Neuronal function in type 2 diabetes

In this study, whilst neuropathy of varying degrees is a well reported consequence of diabetes there was no significant change in any of the gene targets tested between groups. This is somewhat surprising given the background information summarised in the introduction but given the heterogeneity of the human population compared to animal controls may be simply a result of our patient group. Overall, by trying to find a cohort with diabetes without confounding complications such as renal failure our population had little in the way of complications which may mean a phenotype not severe enough yet to cause

autonomic or neuronal dysfunction. It also has to be borne in mind that while we did not observe changes in classical neuronal genes, we did not measure clinically or biochemically for signs of neuronal dysfunction and therefore a lack of gene changes does not mean no neuronal dysfunction in our diabetes group. In a future study, clinical and biochemical testing for neuronal dysfunction coupled with a larger cohort for gene expression testing would certainly be worthwhile.

Given, the lack of positive results it is difficult to comment further, though whether the increased $I_{K,ACh}$ is a response to the commonly found increased sympathetic drive observed in patients with diabetes maybe an area for exploration[364].

6.6.6. Overall genotype/phenotype

In this study, we observed a marked downregulation in the diabetes group of ERG mRNA production along with increases in K_{ir} 2.1, 3.1, 3.4 and NCX1. These changes overall were modelled to lead to a significant increase in the AP duration with the formation of EADs at the endocardial layer, which has previously shown to be a pro-arrhythmogenic phenotype. Phenotypically, we observed an increase in the QT time in our diabetes group which would be supportive of the gene changes we observed. Also, in our diabetes group we observed an increase in left atrial area and reduced left atrial expansion index with reduced longitudinal ventricular function. We also observed a reduction in the diabetes group of circumferential and longitudinal strain compared to the control arm.

Overall, these findings would suggest a diabetic cardiomyopathy with arrhythmogenic genotypic and phenotypic changes along with reduced ventricular/atrial function and that these changes were not apparent in a control group with similar LV hypertrophy or possible fibrosis.

7. Limitations

As with all experiments there are limitations to this study which have to be reflected upon when reviewing the results presented and the major limitations of this study are discussed below.

As a small exploratory study, we did not perform a preliminary power calculation prior to beginning the work and relied on the experimental experience of the groups in Liverpool and Manchester; hence there is the possibility that some variations in the data or lack of difference may relate to a lack of power in the study. It was the intention that this study may be used to identify areas of interest for a further larger targeted study and the results here are not presented as definitive final findings but areas of interest that do merit further work.

One major limitation to all our sub-studies, is that we only have mRNA data and not quantitative protein measurements to corroborate the mRNA findings except in the case of HCN4 in our obesity study. As stated above, this study was conceived as an initial exploratory study and so we wished to identify areas in a further study for quantitative analysis of protein. Allowing for this, results using the TAQMAN™ system have proved reliable in terms of translation from mRNA to protein[150, 152] and we did observe that when HCN4 mRNA was increased so was the protein expression. In a similar fashion, in this study it is impossible to claim mRNA changes lead to altered functional protein expression and even in the case of HCN4 protein up-regulation, it is not claimed with certainty that this protein is functional protein.

Initially, this study was conceived without the aid of action potential modelling and as such we would have to interpret the data based on other experiments. While the modelling is illustrative of how mRNA changes if translated would play out, modelling is not the same as direct electrophysiological measurements such as patch clamp testing or intracardiac electrograms. It is not the claim of this study that the modelling data should be considered directly equivalent and directly translatable to intracardiac electrophysiology measurements. In the part of our study where there was corroborative electrophysiology, in the shape of 12 lead ECGs, the AP modelling, which suggested a prolonged QT was borne

out in the shape of the 12 lead ECG, where the diabetes group did have a longer QT compared to control.

Overall, while there are several limitations in this study, we do believe that this study does highlight areas of interest for further investigation based on methods that have been shown to be reproducible by several other groups.

8. Common themes

A summary of the significant gene expression changes in the experimental groups compared to the control groups from the three experiments in this study are shown below in Table 15:

Gene	Current	STZ	HFD	Type 2 diabetes
SCN5A	I_{Na}	**Reduced: mid myocardium**	No change	No change
CACNA1c	$I_{Ca\text{-}L}$	No change	Increased	No change
KCNA4	$I_{to\text{-}s}$	**Increased: all wall layers**	No change	No change
KChIP2	I_{to}	**Increased: mid and epicardial layers**	No change	No change
ERG	$I_{K,r}$	**Reduced: mid myocardium**	**Reduced**	**Reduced**
KCNQ1	$I_{K,s}$	**Reduced: mid myocardium**	No change	No change
KCNJ2	$I_{K,1}$	No change	**Increased**	**Increased**
KCNJ3	$I_{K,ACh}$	**Reduced: mid myocardium**	No change	**Reduced**
KCNJ5	$I_{K,ACh}$	No change	**Increased**	**Increased**
HCN2		**Increased: all wall layers**	No change	No change
HCN4	I_{F}	No change	**Increased**	No change
NCX1	I_{NaCa}	No change	**Increased**	**Increased**
SERCA2a	*SR-Ca^{2+} uptake*	**Reduced: endo and mid myocardium**	**Increased**	No change
RYR2	*SR-Ca^{2+} release*	No change	**Increased**	No change
CLCN-2	$I_{Cl,ir}$	**Reduced: mid myocardium**	No change	No change
CLCN-3	$I_{Cl,vol}$	No change	**Increased**	No change
ATP1a1	$I_{Na\text{-}K}$	**Reduced: mid myocardium**	**Increased**	No change
ATP1a2	$I_{Na\text{-}K}$	**Reduced: endo and mid myocardium**	**Increased**	No change
ATP1a3	$I_{Na\text{-}K}$	**Reduced: endo and mid myocardium**	No change	No change
Cx43		**Reduced: mid myocardium**	No change	No change
GLUT-4		**Reduced: all wall layers**	No change	No change
MT-ATP6		No change	**Increased**	**Reduced**
MT-ATP8		No change	**Increased**	No change

TH	Not recorded	**Increased**	No change

Table 15: Summary gene changes from the three experiments in this study

Across all three experiments there was only consistent finding in the qPCR data, which was a reduction in expression of ERG and subsequently in AP modelling prolongation of the APD. Changes in ERG expression and the APD, are important in two major areas, electrophysiologically and contractile function and below, common themes are discussed. Firstly, as discussed previously, a reduction in ERG leads to prolongation of the AP and a failure of repolarization with a concomitant increase in rates of ventricular arrhythmias in many disease states. Other pro-arrhythmic consequences of reduced ERG include: an increase in transmural dispersion of repolarization, reduced ability to prevent ectopic beat generation-following an ectopic waveform, maintenance of cell refractoriness and reversal of the repolarization gradient

All of these effects would potentially be sufficient to explain the higher rates of ventricular arrhythmias observed clinically in diabetes and obesity and may suggest a common pathological process, though whether it is a final downstream effect of diabetes/obesity or primarily part of both conditions is difficult to elucidate based on this study.

Secondly, all three experimental subject groups have been shown to have impaired contractile function, as reported in other studies and seen in this study in our echocardiographic analysis. When ERG is reduced and the AP is prolonged there is reported to be a compensatory small increase in Ca^{2+} transient and an attempt to maintain excitation-contraction coupling via this mechanism, though with a long term cost of maladaptive gene change[365, 366]. Whilst this compensatory change is likely to have a small beneficial effect on systolic function, prolongation of the AP, leads to a shorter diastolic filling time and eventually a reduction in output due to inadequate filling[367, 368]. The significant increase in LA size we observed and the reduction in the LAEI in our diabetes group could potentially be related to this to some degree.

Whilst, we only observed a common change in ERG across all three experiments, we did see some similar themes as one might expect between the obesity experiment and the human type 2 group, with both groups having an increase in NCX1 and increased $K_{ir}2.1$. Increased NCX1 activity as outlined before, is likely to lead to an increase in SR-Ca^{2+} levels and probably along with the reduced ERG we have seen a prolonged AP which similar to ERG leads to a small compensatory potential increase in systolic function at the cost of increased arrhythmias and reduced diastolic time. Increased $K_{ir}2.1$, looking at many of the other gene changes is probably a small compensatory mechanism to try and abbreviate the AP prolongation caused by many of the other changes such as reduced ERG/increased NCX1.

Overall, it would appear that all three conditions are characterised by gene expression changes that prolong the AP possibly as a compensatory mechanism for structural changes that affect systolic function at the cost of an increased rate of arrhythmias and reduced diastole. Further work would be required to look at the role of AP prolongation/ERG reduction in diabetes and obesity as to the role of this as a primary function of the conditions as a consequence of the conditions.

9. Future directions

This study has described several interesting changes in mRNA expression in the STZ rat model, the HFD rat model and a human group with type 2 diabetes, which may have implications for arrhythmogenesis and contractile function and we discuss now some aspects which may merit future study.

One of the first areas for future work would be to perform detailed protein quantification of the key altered genes in this study firstly in the rat models and then in a similar human study. The lack of confirmatory protein expression has been a major limitation of this study and when performed would need to be accompanied by direct electrophysiological assessment of the channel/current function, which may then prove the importance of the measured mRNA changes we have seen.

Moving forward from the models and results presented here, several interesting future avenues of investigation present themselves from an obesity perspective including whether

obesity from carbohydrates induces the same cardiac changes as obesity related to the high fat diet we used here. Following this, adding an exercise component to see whether high fat or high calorific diets lead to pathological cardiac changes if an animal does not develop obesity would be of great interest.

In human research, a complimentary study using obese patients with aortic stenosis compared to lean controls would potentially provide further insight and be very interesting to look at overlap/differences with the type 2 diabetes population we have investigated here. The heterogeneity of the human population in terms of exercise/diet offers many opportunities for further work on the effect of obesity and diabetes on the cardiac system.

10. References

[1] American Heart Association: *Obesity, insulin resistance, diabetes, and cardiovascular risk in children: an American Heart Association scientific statement from the Atherosclerosis, Hypertension, and Obesity in the Young Committee (Council on Cardiovascular Disease in the Young) and the Diabetes Committee (Council on Nutrition, Physical Activity, and Metabolism)*. Circulation, 2003, pp. 1448-1453.

[2] Morgan CL, Peters JR, Currie CJ: The changing prevalence of diagnosed diabetes and its associated vascular complications in a large region of the UK. Diabetic medicine : a journal of the British Diabetic Association 2010; 27:673-678.

[3] British Heart Foundation: *Coronary Heart Disease Statistics* London, 2012, pp.

[4] Rubler S, Dlugash J, Yuceoglu YZ, Kumral T, Branwood AW, Grishman A: New type of cardiomyopathy associated with diabetic glomerulosclerosis. The American journal of cardiology 1972; 30:595-602.

[5] Miki T, Yuda S, Kouzu H, Miura T: Diabetic cardiomyopathy: pathophysiology and clinical features. Heart Fail Rev 2013; 18:149-166.

[6] Horowitz JD, Kennedy JA: Time to address the cardiac metabolic "triple whammy" ischemic heart failure in diabetic patients. Journal of the American College of Cardiology 2006; 48:2232-2234.

[7] Bauters C, Lamblin N, Mc Fadden EP, Van Belle E, Millaire A, de Groote P: Influence of diabetes mellitus on heart failure risk and outcome. Cardiovascular diabetology 2003; 2:1.

[8] Kenchaiah S, Evans JC, Levy D, Wilson PW, Benjamin EJ, Larson MG, Kannel WB, Vasan RS: Obesity and the risk of heart failure. The New England journal of medicine 2002; 347:305-313.

[9] Schiller NB, Shah PM, Crawford M, DeMaria A, Devereux R, Feigenbaum H, Gutgesell H, Reichek N, Sahn D, Schnittger I, et al.: Recommendations for quantitation of the left ventricle by two-dimensional echocardiography. American Society of Echocardiography Committee on Standards, Subcommittee on Quantitation of Two-Dimensional Echocardiograms. Journal of the American Society of Echocardiography : official publication of the American Society of Echocardiography 1989; 2:358-367.

[10] Salem M, El Behery S, Adly A, Khalil D, El Hadidi E: Early predictors of myocardial disease in children and adolescents with type 1 diabetes mellitus. Pediatric diabetes 2009; 10:513-521.

[11] Kosmala W, Wong C, Kuliczkowska J, Leano R, Przewlocka-Kosmala M, Marwick TH: Use of body weight and insulin resistance to select obese patients for echocardiographic assessment of subclinical left ventricular dysfunction. The American journal of cardiology 2008; 101:1334-1340.

[12] Varadarajan P, Pai RG: Prognosis of congestive heart failure in patients with normal versus reduced ejection fractions: results from a cohort of 2,258 hospitalized patients. Journal of cardiac failure 2003; 9:107-112.

[13] Panova EI, Korneva KG: [The peculiarities of cardial arrhythmias in patients with type 2 diabetes]. Klinicheskaia meditsina 2006; 84:21-24.

[14] Suarez GA, Clark VM, Norell JE, Kottke TE, Callahan MJ, O'Brien PC, Low PA, Dyck PJ: Sudden cardiac death in diabetes mellitus: risk factors in the Rochester diabetic neuropathy study. Journal of neurology, neurosurgery, and psychiatry 2005; 76:240-245.

[15] Pietrasik G, Goldenberg I, McNitt S, Moss AJ, Zareba W: Obesity as a risk factor for sustained ventricular tachyarrhythmias in MADIT II patients. Journal of cardiovascular electrophysiology 2007; 18:181-184.

[16] de Simone G, Devereux RB: Rationale of echocardiographic assessment of left ventricular wall stress and midwall mechanics in hypertensive heart disease. European journal of echocardiography : the journal of the Working Group on Echocardiography of the European Society of Cardiology 2002; 3:192-198.

[17] Trew ML, Caldwell BJ, Sands GB, Hooks DA, Tai DC, Austin TM, LeGrice IJ, Pullan AJ, Smaill BH: Cardiac electrophysiology and tissue structure: bridging the scale gap with a joint measurement and modelling paradigm. Experimental physiology 2006; 91:355-370.

[18] Amin AS, Tan HL, Wilde AA: Cardiac ion channels in health and disease. Heart rhythm : the official journal of the Heart Rhythm Society 2010; 7:117-126.

[19] Grant AO: Cardiac ion channels. Circulation Arrhythmia and electrophysiology 2009; 2:185-194.

[20] Sridhar A, da Cunha DN, Lacombe VA, Zhou Q, Fox JJ, Hamlin RL, Carnes CA: The plateau outward current in canine ventricle, sensitive to 4-aminopyridine, is a constitutive contributor to ventricular repolarization. British journal of pharmacology 2007; 152:870-879.

[21] Cerbai E, Pino R, Sartiani L, Mugelli A: Influence of postnatal-development on I(f) occurrence and properties in neonatal rat ventricular myocytes. Cardiovascular research 1999; 42:416-423.

[22] Song T, Yang J, Yao Y, Li H, Chen Y, Zhang J, Huang C: Spironolactone diminishes spontaneous ventricular premature beats by reducing HCN4 protein expression in rats with myocardial infarction. Molecular medicine reports 2011; 4:569-573.

[23] Martin CA, Matthews GD, Huang CL: Sudden cardiac death and inherited channelopathy: the basic electrophysiology of the myocyte and myocardium in ion channel disease. Heart 2012; 98:536-543.

[24] Colli Franzone P, Pavarino LF, Scacchi S, Taccardi B: Modeling ventricular repolarization: effects of transmural and apex-to-base heterogeneities in action potential durations. Mathematical biosciences 2008; 214:140-152.

[25] Rosenthal JE, Ferrier GR: Contribution of variable entrance and exit block in protected foci to arrhythmogenesis in isolated ventricular tissues. Circulation 1983; 67:1-8.

[26] Gaztanaga L, Marchlinski FE, Betensky BP: Mechanisms of cardiac arrhythmias. Revista espanola de cardiologia 2012; 65:174-185.

[27] Weiss JN, Garfinkel A, Karagueuzian HS, Chen PS, Qu Z: Early afterdepolarizations and cardiac arrhythmias. Heart rhythm : the official journal of the Heart Rhythm Society 2010; 7:1891-1899.

[28] Fink M, Noble PJ, Noble D: Ca(2)(+)-induced delayed afterdepolarizations are triggered by dyadic subspace Ca2(2)(+) affirming that increasing SERCA reduces aftercontractions. American journal of physiology Heart and circulatory physiology 2011; 301:H921-935.

[29] Hessen SE, Michelson EL: Mechanisms of Ventricular arrhythmias: from laboratory to bedside.. American College of Cardiology Current Journal Review 1994; 4:11-16.

[30] Morita H, Zipes DP, Wu J: Brugada syndrome: insights of ST elevation, arrhythmogenicity, and risk stratification from experimental observations. Heart rhythm : the official journal of the Heart Rhythm Society 2009; 6:S34-43.

[31] Chauhan VS, Downar E, Nanthakumar K, Parker JD, Ross HJ, Chan W, Picton P: Increased ventricular repolarization heterogeneity in patients with ventricular arrhythmia vulnerability and cardiomyopathy: a human in vivo study. American journal of physiology Heart and circulatory physiology 2006; 290:H79-86.

[32] Matthews GD, Martin CA, Grace AA, Zhang Y, Huang CL: Regional variations in action potential alternans in isolated murine Scn5a (+/-) hearts during dynamic pacing. Acta physiologica 2010; 200:129-146.

[33] Anumonwo JM, Pandit SV: Ionic mechanisms of arrhythmogenesis. Trends in cardiovascular medicine 2015; 25:487-496.

[34] Andersson DC, Marks AR: Fixing ryanodine receptor Ca leak - a novel therapeutic strategy for contractile failure in heart and skeletal muscle. Drug Discovery Today Disease Mechanisms 2010; 7:e151-e157.

[35] Cooper PJ, Soeller C, Cannell MB: Excitation-contraction coupling in human heart failure examined by action potential clamp in rat cardiac myocytes. Journal of molecular and cellular cardiology 2010; 49:911-917.

[36] Beuckelmann DJ, Nabauer M, Erdmann E: Alterations of K+ currents in isolated human ventricular myocytes from patients with terminal heart failure. Circulation research 1993; 73:379-385.

[37] Koumi S, Backer CL, Arentzen CE: Characterization of inwardly rectifying K+ channel in human cardiac myocytes. Alterations in channel behavior in myocytes isolated from patients with idiopathic dilated cardiomyopathy. Circulation 1995; 92:164-174.

[38] Bouchard RA, Clark RB, Giles WR: Effects of action potential duration on excitation-contraction coupling in rat ventricular myocytes. Action potential voltage-clamp measurements. Circulation research 1995; 76:790-801.

[39] Feldman AM, Weinberg EO, Ray PE, Lorell BH: Selective changes in cardiac gene expression during compensated hypertrophy and the transition to cardiac decompensation in rats with chronic aortic banding. Circulation research 1993; 73:184-192.

[40] Hobai IA, O'Rourke B: Decreased sarcoplasmic reticulum calcium content is responsible for defective excitation-contraction coupling in canine heart failure. Circulation 2001; 103:1577-1584.

[41] Piot C, Lemaire S, Albat B, Seguin J, Nargeot J, Richard S: High frequency-induced upregulation of human cardiac calcium currents. Circulation 1996; 93:120-128.

[42] Gomez AM, Valdivia HH, Cheng H, Lederer MR, Santana LF, Cannell MB, McCune SA, Altschuld RA, Lederer WJ: Defective excitation-contraction coupling in experimental cardiac hypertrophy and heart failure. Science 1997; 276:800-806.

[43] Yano M: Ryanodine receptor as a new therapeutic target of heart failure and lethal arrhythmia. Circulation journal : official journal of the Japanese Circulation Society 2008; 72:509-514.

[44] Voss J, Jones LR, Thomas DD: The physical mechanism of calcium pump regulation in the heart. Biophysical journal 1994; 67:190-196.

[45] Hasenfuss G, Reinecke H, Studer R, Meyer M, Pieske B, Holtz J, Holubarsch C, Posival H, Just H, Drexler H: Relation between myocardial function and expression of sarcoplasmic reticulum Ca(2+)-ATPase in failing and nonfailing human myocardium. Circulation research 1994; 75:434-442.

[46] Litwin SE, Zhang D, Bridge JH: Dyssynchronous Ca(2+) sparks in myocytes from infarcted hearts. Circulation research 2000; 87:1040-1047.

[47] Yano M, Ikeda Y, Matsuzaki M: Altered intracellular Ca2+ handling in heart failure. The Journal of clinical investigation 2005; 115:556-564.

[48] Sharma V, McNeill JH: Diabetic cardiomyopathy: where are we 40 years later? The Canadian journal of cardiology 2006; 22:305-308.

[49] Dutka DP, Pitt M, Pagano D, Mongillo M, Gathercole D, Bonser RS, Camici PG: Myocardial glucose transport and utilization in patients with type 2 diabetes mellitus, left ventricular dysfunction, and coronary artery disease. Journal of the American College of Cardiology 2006; 48:2225-2231.

[50] Boudina S, Abel ED: Diabetic cardiomyopathy, causes and effects. Reviews in endocrine & metabolic disorders 2010; 11:31-39.

[51] Burkhoff D, Weiss RG, Schulman SP, Kalil-Filho R, Wannenburg T, Gerstenblith G: Influence of metabolic substrate on rat heart function and metabolism at different coronary flows. The American journal of physiology 1991; 261:H741-750.

[52] Fox JJ, Strauss HW: One step closer to imaging vulnerable plaque in the coronary arteries. Journal of nuclear medicine : official publication, Society of Nuclear Medicine 2009; 50:497-500.

[53] An D, Rodrigues B: Role of changes in cardiac metabolism in development of diabetic cardiomyopathy. American journal of physiology Heart and circulatory physiology 2006; 291:H1489-1506.

[54] Rijzewijk LJ, van der Meer RW, Lamb HJ, de Jong HW, Lubberink M, Romijn JA, Bax JJ, de Roos A, Twisk JW, Heine RJ, Lammertsma AA, Smit JW, Diamant M: Altered myocardial substrate metabolism and decreased diastolic function in nonischemic human diabetic cardiomyopathy: studies with cardiac positron emission tomography and magnetic resonance imaging. Journal of the American College of Cardiology 2009; 54:1524-1532.

[55] Kusminski CM, Shetty S, Orci L, Unger RH, Scherer PE: Diabetes and apoptosis: lipotoxicity. Apoptosis 2009; 14:1484-1495.

[56] Hickson-Bick DL, Buja LM, McMillin JB: Palmitate-mediated alterations in the fatty acid metabolism of rat neonatal cardiac myocytes. Journal of molecular and cellular cardiology 2000; 32:511-519.

[57] Boudina S, Abel ED: Diabetic cardiomyopathy revisited. Circulation 2007; 115:3213-3223.

[58] Campbell FM, Kozak R, Wagner A, Altarejos JY, Dyck JR, Belke DD, Severson DL, Kelly DP, Lopaschuk GD: A role for peroxisome proliferator-activated receptor alpha (PPARalpha) in the control of cardiac malonyl-CoA levels: reduced fatty acid oxidation rates and increased glucose oxidation rates in the hearts of mice lacking PPARalpha are associated with higher concentrations of malonyl-CoA and reduced expression of malonyl-CoA decarboxylase. The Journal of biological chemistry 2002; 277:4098-4103.

[59] Finck BN: The role of the peroxisome proliferator-activated receptor alpha pathway in pathological remodeling of the diabetic heart. Current opinion in clinical nutrition and metabolic care 2004; 7:391-396.

[60] Schupp M, Kintscher U, Fielitz J, Thomas J, Pregla R, Hetzer R, Unger T, Regitz-Zagrosek V: Cardiac PPARalpha expression in patients with dilated cardiomyopathy. European journal of heart failure 2006; 8:290-294.

[61] Khullar M, Al-Shudiefat AA, Ludke A, Binepal G, Singal PK: Oxidative stress: a key contributor to diabetic cardiomyopathy. Can J Physiol Pharmacol; 88:233-240.

[62] Brownlee M: Biochemistry and molecular cell biology of diabetic complications. Nature 2001; 414:813-820.

[63] Di Filippo C, Cuzzocrea S, Rossi F, Marfella R, D'Amico M: Oxidative stress as the leading cause of acute myocardial infarction in diabetics. Cardiovascular drug reviews 2006; 24:77-87.

[64] Rolo AP, Palmeira CM: Diabetes and mitochondrial function: role of hyperglycemia and oxidative stress. Toxicology and applied pharmacology 2006; 212:167-178.

[65] Gabriely I, Yang XM, Cases JA, Ma XH, Rossetti L, Barzilai N: Hyperglycemia induces PAI-1 gene expression in adipose tissue by activation of the hexosamine biosynthetic pathway. Atherosclerosis 2002; 160:115-122.

[66] Du XL, Edelstein D, Rossetti L, Fantus IG, Goldberg H, Ziyadeh F, Wu J, Brownlee M: Hyperglycemia-induced mitochondrial superoxide overproduction activates the hexosamine pathway and induces plasminogen activator inhibitor-1 expression by increasing Sp1 glycosylation. Proceedings of the National Academy of Sciences of the United States of America 2000; 97:12222-12226.

[67] Nishikawa T, Edelstein D, Du XL, Yamagishi S, Matsumura T, Kaneda Y, Yorek MA, Beebe D, Oates PJ, Hammes HP, Giardino I, Brownlee M: Normalizing mitochondrial superoxide production blocks three pathways of hyperglycaemic damage. Nature 2000; 404:787-790.

[68] Boudina S, Sena S, Theobald H, Sheng X, Wright JJ, Hu XX, Aziz S, Johnson JI, Bugger H, Zaha VG, Abel ED: Mitochondrial energetics in the heart in obesity-related diabetes: direct evidence for increased uncoupled respiration and activation of uncoupling proteins. Diabetes 2007; 56:2457-2466.

[69] Bugger H, Chen D, Riehle C, Soto J, Theobald HA, Hu XX, Ganesan B, Weimer BC, Abel ED: Tissue-specific remodeling of the mitochondrial proteome in type 1 diabetic akita mice. Diabetes 2009; 58:1986-1997.

[70] Bugger H, Boudina S, Hu XX, Tuinei J, Zaha VG, Theobald HA, Yun UJ, McQueen AP, Wayment B, Litwin SE, Abel ED: Type 1 diabetic akita mouse hearts are insulin sensitive but manifest structurally abnormal mitochondria that remain coupled despite increased uncoupling protein 3. Diabetes 2008; 57:2924-2932.

[71] Rota M, LeCapitaine N, Hosoda T, Boni A, De Angelis A, Padin-Iruegas ME, Esposito G, Vitale S, Urbanek K, Casarsa C, Giorgio M, Luscher TF, Pelicci PG, Anversa P, Leri A, Kajstura J: Diabetes promotes cardiac stem cell aging and heart failure, which are prevented by deletion of the p66shc gene. Circulation research 2006; 99:42-52.

[72] Cesselli D, Jakoniuk I, Barlucchi L, Beltrami AP, Hintze TH, Nadal-Ginard B, Kajstura J, Leri A, Anversa P: Oxidative stress-mediated cardiac cell death is a major determinant of ventricular dysfunction and failure in dog dilated cardiomyopathy. Circulation research 2001; 89:279-286.

[73] Messina E, Giacomello A: Diabetic cardiomyopathy: a "cardiac stem cell disease" involving p66Shc, an attractive novel molecular target for heart failure therapy. Circulation research 2006; 99:1-2.

[74] Schaffer SW, Ballard-Croft C, Boerth S, Allo SN: Mechanisms underlying depressed Na+/Ca2+ exchanger activity in the diabetic heart. Cardiovascular research 1997; 34:129-136.

[75] Choi KM, Zhong Y, Hoit BD, Grupp IL, Hahn H, Dilly KW, Guatimosim S, Lederer WJ, Matlib MA: Defective intracellular Ca(2+) signaling contributes to cardiomyopathy in Type 1 diabetic rats. American journal of physiology Heart and circulatory physiology 2002; 283:H1398-1408.

[76] Bidasee KR, Nallani K, Yu Y, Cocklin RR, Zhang Y, Wang M, Dincer UD, Besch HR, Jr.: Chronic diabetes increases advanced glycation end products on cardiac ryanodine receptors/calcium-release channels. Diabetes 2003; 52:1825-1836.

[77] Shao CH, Rozanski GJ, Patel KP, Bidasee KR: Dyssynchronous (non-uniform) Ca2+ release in myocytes from streptozotocin-induced diabetic rats. Journal of molecular and cellular cardiology 2007; 42:234-246.

[78] Pfeifer MA, Weinberg CR, Cook DL, Reenan A, Halter JB, Ensinck JW, Porte D, Jr.: Autonomic neural dysfunction in recently diagnosed diabetic subjects. Diabetes care 1984; 7:447-453.

[79] Monfredi O, Lyashkov AE, Johnsen AB, Inada S, Schneider H, Wang R, Nirmalan M, Wisloff U, Maltsev VA, Lakatta EG, Zhang H, Boyett MR: Biophysical characterization of the underappreciated and important relationship between heart rate variability and heart rate. Hypertension 2014; 64:1334-1343.

[80] Vinik AI, Maser RE, Mitchell BD, Freeman R: Diabetic autonomic neuropathy. Diabetes care 2003; 26:1553-1579.

[81] Kahn JK, Zola B, Juni JE, Vinik AI: Radionuclide assessment of left ventricular diastolic filling in diabetes mellitus with and without cardiac autonomic neuropathy. Journal of the American College of Cardiology 1986; 7:1303-1309.

[82] Langen KJ, Ziegler D, Weise F, Piolot R, Boy C, Hubinger A, Gries FA, Muller-Gartner HW: Evaluation of QT interval length, QT dispersion and myocardial m-iodobenzylguanidine uptake in insulin-dependent diabetic patients with and without autonomic neuropathy. Clinical science 1997; 93:325-333.

[83] Pacher P, Obrosova IG, Mabley JG, Szabo C: Role of nitrosative stress and peroxynitrite in the pathogenesis of diabetic complications. Emerging new therapeutical strategies. Current medicinal chemistry 2005; 12:267-275.

[84] Ieda M, Kanazawa H, Ieda Y, Kimura K, Matsumura K, Tomita Y, Yagi T, Onizuka T, Shimoji K, Ogawa S, Makino S, Sano M, Fukuda K: Nerve growth factor is critical for cardiac sensory innervation and rescues neuropathy in diabetic hearts. Circulation 2006; 114:2351-2363.

[85] Di Carli MF, Bianco-Batlles D, Landa ME, Kazmers A, Groehn H, Muzik O, Grunberger G: Effects of autonomic neuropathy on coronary blood flow in patients with diabetes mellitus. Circulation 1999; 100:813-819.

[86] Stevens MJ, Dayanikli F, Raffel DM, Allman KC, Sandford T, Feldman EL, Wieland DM, Corbett J, Schwaiger M: Scintigraphic assessment of regionalized defects in myocardial sympathetic innervation and blood flow regulation in diabetic patients with autonomic neuropathy. Journal of the American College of Cardiology 1998; 31:1575-1584.

[87] Stewart BW: Mechanisms of apoptosis: integration of genetic, biochemical, and cellular indicators. Journal of the National Cancer Institute 1994; 86:1286-1296.

[88] Olshansky B, Sabbah HN, Hauptman PJ, Colucci WS: Parasympathetic nervous system and heart failure: pathophysiology and potential implications for therapy. Circulation 2008; 118:863-871.

[89] Chottova Dvorakova M, Kuncova J, Pfeil U, McGregor GP, Sviglerova J, Slavikova J, Kummer W: Cardiomyopathy in streptozotocin-induced diabetes involves intra-axonal accumulation of calcitonin gene-related peptide and altered expression of its receptor in rats. Neuroscience 2005; 134:51-58.

[90] Stevens MJ, Raffel DM, Allman KC, Schwaiger M, Wieland DM: Regression and progression of cardiac sympathetic dysinnervation complicating diabetes: an assessment by C-11 hydroxyephedrine and positron emission tomography. Metabolism: clinical and experimental 1999; 48:92-101.

[91] Das AK, Das JP, Chandrasekar S: Specific heart muscle disease in diabetes mellitus--a functional structural correlation. International journal of cardiology 1987; 17:299-302.

[92] Way KJ, Isshiki K, Suzuma K, Yokota T, Zvagelsky D, Schoen FJ, Sandusky GE, Pechous PA, Vlahos CJ, Wakasaki H, King GL: Expression of connective tissue growth factor is increased in injured myocardium associated with protein kinase C beta2 activation and diabetes. Diabetes 2002; 51:2709-2718.

[93] Chen S, Evans T, Mukherjee K, Karmazyn M, Chakrabarti S: Diabetes-induced myocardial structural changes: role of endothelin-1 and its receptors. Journal of molecular and cellular cardiology 2000; 32:1621-1629.

[94] Vlassara H: Advanced glycation end-products and atherosclerosis. Annals of medicine 1996; 28:419-426.

[95] Candido R, Forbes JM, Thomas MC, Thallas V, Dean RG, Burns WC, Tikellis C, Ritchie RH, Twigg SM, Cooper ME, Burrell LM: A breaker of advanced glycation end products

attenuates diabetes-induced myocardial structural changes. Circulation research 2003; 92:785-792.

[96] Cheng M, Gao HQ, Xu L, Li BY, Zhang H, Li XH: Cardioprotective effects of grape seed proanthocyanidins extracts in streptozocin induced diabetic rats. Journal of cardiovascular pharmacology 2007; 50:503-509.

[97] Ruan BH, Li X, Winkler AR, Cunningham KM, Kuai J, Greco RM, Nocka KH, Fitz LJ, Wright JF, Pittman DD, Tan XY, Paulsen JE, Lin LL, Winkler DG: Complement C3a, CpG oligos, and DNA/C3a complex stimulate IFN-alpha production in a receptor for advanced glycation end product-dependent manner. J Immunol; 185:4213-4222.

[98] Cook SA, Varela-Carver A, Mongillo M, Kleinert C, Khan MT, Leccisotti L, Strickland N, Matsui T, Das S, Rosenzweig A, Punjabi P, Camici PG: Abnormal myocardial insulin signalling in type 2 diabetes and left-ventricular dysfunction. Eur Heart J; 31:100-111.

[99] Bahrami H, Bluemke DA, Kronmal R, Bertoni AG, Lloyd-Jones DM, Shahar E, Szklo M, Lima JA: Novel metabolic risk factors for incident heart failure and their relationship with obesity: the MESA (Multi-Ethnic Study of Atherosclerosis) study. Journal of the American College of Cardiology 2008; 51:1775-1783.

[100] Xu FP, Chen MS, Wang YZ, Yi Q, Lin SB, Chen AF, Luo JD: Leptin induces hypertrophy via endothelin-1-reactive oxygen species pathway in cultured neonatal rat cardiomyocytes. Circulation 2004; 110:1269-1275.

[101] Kasper EK, Hruban RH, Baughman KL: Cardiomyopathy of obesity: a clinicopathologic evaluation of 43 obese patients with heart failure. The American journal of cardiology 1992; 70:921-924.

[102] Szczepaniak LS, Victor RG, Orci L, Unger RH: Forgotten but not gone: the rediscovery of fatty heart, the most common unrecognized disease in America. Circulation research 2007; 101:759-767.

[103] Zhou YT, Grayburn P, Karim A, Shimabukuro M, Higa M, Baetens D, Orci L, Unger RH: Lipotoxic heart disease in obese rats: implications for human obesity. Proceedings of the National Academy of Sciences of the United States of America 2000; 97:1784-1789.

[104] Purdham DM, Zou MX, Rajapurohitam V, Karmazyn M: Rat heart is a site of leptin production and action. American journal of physiology Heart and circulatory physiology 2004; 287:H2877-2884.

[105] Karmazyn M, Purdham DM, Rajapurohitam V, Zeidan A: Leptin as a cardiac hypertrophic factor: a potential target for therapeutics. Trends in cardiovascular medicine 2007; 17:206-211.

[106] Abe Y, Ono K, Kawamura T, Wada H, Kita T, Shimatsu A, Hasegawa K: Leptin induces elongation of cardiac myocytes and causes eccentric left ventricular dilatation with compensation. American journal of physiology Heart and circulatory physiology 2007; 292:H2387-2396.

[107] Zeidan A, Paylor B, Steinhoff KJ, Javadov S, Rajapurohitam V, Chakrabarti S, Karmazyn M: Actin cytoskeleton dynamics promotes leptin-induced vascular smooth muscle hypertrophy via RhoA/ROCK- and phosphatidylinositol 3-kinase/protein kinase B-dependent pathways. The Journal of pharmacology and experimental therapeutics 2007; 322:1110-1116.

[108] Oda A, Taniguchi T, Yokoyama M: Leptin stimulates rat aortic smooth muscle cell proliferation and migration. The Kobe journal of medical sciences 2001; 47:141-150.

[109] Rajapurohitam V, Javadov S, Purdham DM, Kirshenbaum LA, Karmazyn M: An autocrine role for leptin in mediating the cardiomyocyte hypertrophic effects of angiotensin II and endothelin-1. Journal of molecular and cellular cardiology 2006; 41:265-274.

[110] Shibata R, Ouchi N, Ito M, Kihara S, Shiojima I, Pimentel DR, Kumada M, Sato K, Schiekofer S, Ohashi K, Funahashi T, Colucci WS, Walsh K: Adiponectin-mediated modulation of hypertrophic signals in the heart. Nature medicine 2004; 10:1384-1389.

[111] Jameel MN, Zhang J: Myocardial energetics in left ventricular hypertrophy. Current cardiology reviews 2009; 5:243-250.

[112] Cittadini A, Mantzoros CS, Hampton TG, Travers KE, Katz SE, Morgan JP, Flier JS, Douglas PS: Cardiovascular abnormalities in transgenic mice with reduced brown fat: an animal model of human obesity. Circulation 1999; 100:2177-2183.

[113] Wong C, Marwick TH: Alterations in myocardial characteristics associated with obesity: detection, mechanisms, and implications. Trends in cardiovascular medicine 2007; 17:1-5.

[114] Giacchetti G, Faloia E, Mariniello B, Sardu C, Gatti C, Camilloni MA, Guerrieri M, Mantero F: Overexpression of the renin-angiotensin system in human visceral adipose tissue in normal and overweight subjects. American journal of hypertension 2002; 15:381-388.

[115] Goodfriend TL, Kelley DE, Goodpaster BH, Winters SJ: Visceral obesity and insulin resistance are associated with plasma aldosterone levels in women. Obesity research 1999; 7:355-362.

[116] Peterson LR, Herrero P, Schechtman KB, Racette SB, Waggoner AD, Kisrieva-Ware Z, Dence C, Klein S, Marsala J, Meyer T, Gropler RJ: Effect of obesity and insulin resistance on myocardial substrate metabolism and efficiency in young women. Circulation 2004; 109:2191-2196.

[117] Wong C, Marwick TH: Obesity cardiomyopathy: pathogenesis and pathophysiology. Nature clinical practice Cardiovascular medicine 2007; 4:436-443.

[118] Chiu HC, Kovacs A, Ford DA, Hsu FF, Garcia R, Herrero P, Saffitz JE, Schaffer JE: A novel mouse model of lipotoxic cardiomyopathy. The Journal of clinical investigation 2001; 107:813-822.

[119] Balderas-Villalobos J, Molina-Munoz T, Mailloux-Salinas P, Bravo G, Carvajal K, Gomez-Viquez NL: Oxidative stress in cardiomyocytes contributes to decreased SERCA2a activity in rats with metabolic syndrome. American journal of physiology Heart and circulatory physiology 2013; 305:H1344-1353.

[120] Lin YK, Chen YC, Chen JH, Chen SA, Chen YJ: Adipocytes modulate the electrophysiology of atrial myocytes: implications in obesity-induced atrial fibrillation. Basic Res Cardiol 2012; 107:293.

[121] Movahed M-R, Hashemzadeh M, Jamal M: Increased prevalence of ventricular fibrillation in patients with type 2 diabetes mellitus. Heart Vessels 2007; 22:251-253.

[122] Stahn A, Pistrosch F, Ganz X, Teige M, Koehler C, Bornstein S, Hanefeld M: Relationship between hypoglycemic episodes and ventricular arrhythmias in patients with type 2 diabetes and cardiovascular diseases. Diabetes care 2013.

[123] Frier BM, Schernthaner G, Heller SR: Hypoglycemia and cardiovascular risks. Diabetes care 2011; 34 Suppl 2:S132-137.

[124] Brady PA, Terzic A: The sulfonylurea controversy: more questions from the heart. Journal of the American College of Cardiology 1998; 31:950-956.

[125] Nagamachi S, Fujita S, Nishii R, Futami S, Tamura S, Mizuta M, Nakazato M, Kurose T, Wakamatsu H: Prognostic value of cardiac I-123 metaiodobenzylguanidine imaging in patients with non-insulin-dependent diabetes mellitus. Journal of nuclear cardiology : official publication of the American Society of Nuclear Cardiology 2006; 13:34-42.

[126] Ewing DJ, Boland O, Neilson JM, Cho CG, Clarke BF: Autonomic neuropathy, QT interval lengthening, and unexpected deaths in male diabetic patients. Diabetologia 1991; 34:182-185.

[127] Pereira L, Matthes J, Schuster I, Valdivia HH, Herzig S, Richard S, Gomez AM: Mechanisms of [Ca2+]i transient decrease in cardiomyopathy of db/db type 2 diabetic mice. Diabetes 2006; 55:608-615.

[128] Erickson JR, Pereira L, Wang L, Han G, Ferguson A, Dao K, Copeland RJ, Despa F, Hart GW, Ripplinger CM, Bers DM: Diabetic hyperglycaemia activates CaMKII and arrhythmias by O-linked glycosylation. Nature 2013; 502:372-376.

[129] Xu Z, Patel KP, Lou MF, Rozanski GJ: Up-regulation of K(+) channels in diabetic rat ventricular myocytes by insulin and glutathione. Cardiovascular research 2002; 53:80-88.

[130] Zhang Y, Xiao J, Wang H, Luo X, Wang J, Villeneuve LR, Zhang H, Bai Y, Yang B, Wang Z: Restoring depressed HERG K+ channel function as a mechanism for insulin treatment of abnormal QT prolongation and associated arrhythmias in diabetic rabbits. American journal of physiology Heart and circulatory physiology 2006; 291:H1446-1455.

[131] Mathew B, Francis L, Kayalar A, Cone J: Obesity: effects on cardiovascular disease and its diagnosis. Journal of the American Board of Family Medicine 2008; 21:562-568.

[132] Rennison JH, Van Wagoner DR: Impact of dietary fatty acids on cardiac arrhythmogenesis. Circulation Arrhythmia and electrophysiology 2009; 2:460-469.

[133] Messerli FH, Nunez BD, Ventura HO, Snyder DW: Overweight and sudden death. Increased ventricular ectopy in cardiopathy of obesity. Archives of internal medicine 1987; 147:1725-1728.

[134] Masi CM, Hawkley LC, Rickett EM, Cacioppo JT: Respiratory sinus arrhythmia and diseases of aging: obesity, diabetes mellitus, and hypertension. Biological psychology 2007; 74:212-223.

[135] Prior LJ, Eikelis N, Armitage JA, Davern PJ, Burke SL, Montani JP, Barzel B, Head GA: Exposure to a high-fat diet alters leptin sensitivity and elevates renal sympathetic nerve activity and arterial pressure in rabbits. Hypertension 2010; 55:862-868.

[136] Lin YK, Chen YJ, Chen SA: Potential atrial arrhythmogenicity of adipocytes: implications for the genesis of atrial fibrillation. Medical hypotheses 2010; 74:1026-1029.

[137] Lin YK, Chen YC, Huang JH, Lin YJ, Huang SS, Chen SA, Chen YJ: Leptin modulates electrophysiological characteristics and isoproterenol-induced arrhythmogenesis in atrial myocytes. Journal of biomedical science 2013; 20:94.

[138] Karagueuzian HS: Targeting cardiac fibrosis: a new frontier in antiarrhythmic therapy? American journal of cardiovascular disease 2011; 1:101-109.

[139] Massare J, Berry JM, Luo X, Rob F, Johnstone JL, Shelton JM, Bassel-Duby R, Hill JA, Naseem RH: Diminished cardiac fibrosis in heart failure is associated with altered ventricular arrhythmia phenotype. Journal of cardiovascular electrophysiology 2010; 21:1031-1037.

[140] Pandit SV, Giles WR, Demir SS: A mathematical model of the electrophysiological alterations in rat ventricular myocytes in type-I diabetes. Biophysical journal 2003; 84:832-841.

[141] Mansor LS, Gonzalez ER, Cole MA, Tyler DJ, Beeson JH, Clarke K, Carr CA, Heather LC: Cardiac metabolism in a new rat model of type 2 diabetes using high-fat diet with low dose streptozotocin. Cardiovascular diabetology 2013; 12:136.

[142] Grossman EJ, Lee DD, Tao J, Wilson RA, Park SY, Bell GI, Chong AS: Glycemic control promotes pancreatic beta-cell regeneration in streptozotocin-induced diabetic mice. PloS one 2010; 5:e8749.

[143] Tyrode's solution. Cold Spring Harbor Protocols 2006; 2006:pdb.rec10479.

[144] Stones R, Calaghan SC, Billeter R, Harrison SM, White E: Transmural variations in gene expression of stretch-modulated proteins in the rat left ventricle. Pflugers Archiv : European journal of physiology 2007; 454:545-549.

[145] Winzell MS, Ahren B: The high-fat diet-fed mouse: a model for studying mechanisms and treatment of impaired glucose tolerance and type 2 diabetes. Diabetes 2004; 53 Suppl 3:S215-219.

[146] Fatani S, Pickavance LC, Sadler CJ, Harrold JA, Cassidy R, Wilding JP, Naderali EK: Differential vascular dysfunction in response to diets of differing macronutrient composition: a phenomenonological study. Nutrition & metabolism 2007; 4:15.

[147] Imbeaud S, Graudens E, Boulanger V, Barlet X, Zaborski P, Eveno E, Mueller O, Schroeder A, Auffray C: Towards standardization of RNA quality assessment using user-independent classifiers of microcapillary electrophoresis traces. Nucleic acids research 2005; 33:e56.

[148] Fleige S, Pfaffl MW: RNA integrity and the effect on the real-time qRT-PCR performance. Molecular aspects of medicine 2006; 27:126-139.

[149] Zanon-Moreno V, Asensio-Marquez EM, Ciancotti-Oliver L, Garcia-Medina JJ, Sanz P, Ortega-Azorin C, Pinazo-Duran MD, Ordovas JM, Corella D: Effects of polymorphisms in vitamin E-, vitamin C-, and glutathione peroxidase-related genes on serum biomarkers and associations with glaucoma. Molecular vision 2013; 19:231-242.

[150] Allah EA, Tellez JO, Yanni J, Nelson T, Monfredi O, Boyett MR, Dobrzynski H: Changes in the expression of ion channels, connexins and Ca2+-handling proteins in the sino-atrial node during postnatal development. Experimental physiology 2011; 96:426-438.

[151] Yanni J, Tellez JO, Maczewski M, Mackiewicz U, Beresewicz A, Billeter R, Dobrzynski H, Boyett MR: Changes in ion channel gene expression underlying heart failure-induced sinoatrial node dysfunction. Circulation Heart failure 2011; 4:496-508.

[152] Abd Allah ES, Aslanidi OV, Tellez JO, Yanni J, Billeter R, Zhang H, Dobrzynski H, Boyett MR: Postnatal development of transmural gradients in expression of ion channels and Ca(2)(+)-handling proteins in the ventricle. Journal of molecular and cellular cardiology 2012; 53:145-155.

[153] Information NCfB: *Gene*. 2013, pp.

[154] Vandesompele J, De Preter K, Pattyn F, Poppe B, Van Roy N, De Paepe A, Speleman F: Accurate normalization of real-time quantitative RT-PCR data by geometric averaging of multiple internal control genes. Genome biology 2002; 3:RESEARCH0034.

[155] Karakikes I, Chaanine AH, Kang S, Mukete BN, Jeong D, Zhang S, Hajjar RJ, Lebeche D: Therapeutic cardiac-targeted delivery of miR-1 reverses pressure overload-induced cardiac hypertrophy and attenuates pathological remodeling. Journal of the American Heart Association 2013; 2:e000078.

[156] Chen S, Puthanveetil P, Feng B, Matkovich SJ, Dorn GW, 2nd, Chakrabarti S: Cardiac miR-133a overexpression prevents early cardiac fibrosis in diabetes. Journal of cellular and molecular medicine 2014; 18:415-421.

[157] Altomare C, Terragni B, Brioschi C, Milanesi R, Pagliuca C, Viscomi C, Moroni A, Baruscotti M, DiFrancesco D: Heteromeric HCN1-HCN4 channels: a comparison with native pacemaker channels from the rabbit sinoatrial node. Journal of physiology 2003; 549:347-359.

[158] Yamamoto M, Dobrzynski H, Tellez J, Niwa R, Billeter R, Honjo H, Kodama I, Boyett MR: Extended atrial conduction system characterised by the expression of the HCN4 channel and connexin45. Cardiovasc Research 2006; 72:271-281.

[159] Hodgkin AL, Huxley AF: A quantitative description of membrane current and its application to conduction and excitation in nerve. The Journal of physiology 1952; 117:500-544.

[160] Pandit SV, Clark RB, Giles WR, Demir SS: A mathematical model of action potential heterogeneity in adult rat left ventricular myocytes. Biophys Journal 2001; 81:3029-3051.

[161] Stones R, Billeter R, Zhang H, Harrison S, White E: The role of transient outward K+ current in electrical remodelling induced by voluntary exercise in female rat hearts. Basic research in cardiology 2009; 104:643-652.

[162] Benoist D, Stones R, Drinkhill M, Bernus O, White E: Arrhythmogenic substrate in hearts of rats with monocrotaline-induced pulmonary hypertension and right ventricular hypertrophy. American journal of physiology Heart and circulatory physiology 2011; 300:H2230-2237.

[163] Cerbai E, Barbieri M, Mugelli A: Occurrence and properties of the hyperpolarization-activated current If in ventricular myocytes from normotensive and hypertensive rats during aging. Circulation 1996; 94:1674-1681.

[164] Nagueh SF, Appleton CP, Gillebert TC, Marino PN, Oh JK, Smiseth OA, Waggoner AD, Flachskampf FA, Pellikka PA, Evangelisa A: Recommendations for the evaluation of left ventricular diastolic function by echocardiography. European journal of echocardiography : the journal of the Working Group on Echocardiography of the European Society of Cardiology 2009; 10:165-193.

[165] Cook SA, Varela-Carver A, Mongillo M, Kleinert C, Khan MT, Leccisotti L, Strickland N, Matsui T, Das S, Rosenzweig A, Punjabi P, Camici PG: Abnormal myocardial insulin signalling in type 2 diabetes and left-ventricular dysfunction. European heart journal 2010; 31:100-111.

[166] Pitt B, Zannad F: The detection of myocardial fibrosis: an opportunity to reduce cardiovascular risk in patients with diabetes mellitus? Circulation Cardiovascular imaging 2012; 5:9-11.

[167] Aronow WS, Epstein S, Koenigsberg M, Schwartz KS: Usefulness of echocardiographic left ventricular hypertrophy, ventricular tachycardia and complex ventricular arrhythmias in predicting ventricular fibrillation or sudden cardiac death in elderly patients. The American journal of cardiology 1988; 62:1124-1125.

[168] Weidemann F, Herrmann S, Stork S, Niemann M, Frantz S, Lange V, Beer M, Gattenlohner S, Voelker W, Ertl G, Strotmann JM: Impact of myocardial fibrosis in patients with symptomatic severe aortic stenosis. Circulation 2009; 120:577-584.

[169] Sorgato A, Faggiano P, Aurigemma GP, Rusconi C, Gaasch WH: Ventricular arrhythmias in adult aortic stenosis: prevalence, mechanisms, and clinical relevance. Chest 1998; 113:482-491.

[170] Ng KW, Allen ML, Desai A, Macrae D, Pathan N: Cardioprotective effects of insulin: how intensive insulin therapy may benefit cardiac surgery patients. Circulation 2012; 125:721-728.

[171] Zhang YH, Hancox JC: A novel, voltage-dependent nonselective cation current activated by insulin in guinea pig isolated ventricular myocytes. Circulation research 2003; 92:765-768.

[172] Hiraoka M: A novel action of insulin on cardiac membrane. Circulation research 2003; 92:707-709.

[173] Lengyel C, Virag L, Biro T, Jost N, Magyar J, Biliczki P, Kocsis E, Skoumal R, Nanasi PP, Toth M, Kecskemeti V, Papp JG, Varro A: Diabetes mellitus attenuates the repolarization reserve in mammalian heart. Cardiovascular research 2007; 73:512-520.

[174] Abboud S, Belhassen B, Miller HI, Sadeh D, Laniado S: High frequency electrocardiography using an advanced method of signal averaging for non-invasive detection of coronary artery disease in patients with normal conventional electrocardiogram. Journal of electrocardiology 1986; 19:371-380.

[175] Majeed I, Khan MA, Hussain MM: High Resolution Electrocardiography. Pakistan Journal of Physiology 2005; 1:1-2.

[176] Okin PM, Stein KM, Lippman N, Lerman BB, Kligfield P: Performance of the signal-averaged electrocardiogram: relation to baseline QRS duration. American heart journal 1995; 129:932-940.

[177] Ferferieva V, Van den Bergh A, Claus P, Jasaityte R, La Gerche A, Rademakers F, Herijgers P, D'Hooge J: Assessment of strain and strain rate by two-dimensional speckle tracking in mice: comparison with tissue Doppler echocardiography and conductance catheter measurements. European heart journal cardiovascular Imaging 2012.

[178] Blessberger H, Binder T: Two dimensional speckle tracking echocardiography: clinical applications. Heart 2010; 96:2032-2040.

[179] Marwick TH: Measurement of strain and strain rate by echocardiography: ready for prime time? Journal of the American College of Cardiology 2006; 47:1313-1327.

[180] Popovic ZB, Kwon DH, Mishra M, Buakhamsri A, Greenberg NL, Thamilarasan M, Flamm SD, Thomas JD, Lever HM, Desai MY: Association between regional ventricular function and myocardial fibrosis in hypertrophic cardiomyopathy assessed by speckle tracking echocardiography and delayed hyperenhancement magnetic resonance imaging. Journal of the American Society of Echocardiography : official publication of the American Society of Echocardiography 2008; 21:1299-1305.

[181] Kramer J, Niemann M, Liu D, Hu K, Machann W, Beer M, Wanner C, Ertl G, Weidemann F: Two-dimensional speckle tracking as a non-invasive tool for identification of myocardial fibrosis in Fabry disease. European heart journal 2013; 34:1587-1596.

[182] Ng AC, Auger D, Delgado V, van Elderen SG, Bertini M, Siebelink HM, van der Geest RJ, Bonetti C, van der Velde ET, de Roos A, Smit JW, Leung DY, Bax JJ, Lamb HJ: Association between diffuse myocardial fibrosis by cardiac magnetic resonance contrast-enhanced T(1) mapping and subclinical myocardial dysfunction in diabetic patients: a pilot study. Circulation Cardiovascular imaging 2012; 5:51-59.

[183] Iles L, Pfluger H, Phrommintikul A, Cherayath J, Aksit P, Gupta SN, Kaye DM, Taylor AJ: Evaluation of diffuse myocardial fibrosis in heart failure with cardiac magnetic resonance contrast-enhanced T1 mapping. Journal of the American College of Cardiology 2008; 52:1574-1580.

[184] Kearney LG, Lu K, Ord M, Patel SK, Profitis K, Matalanis G, Burrell LM, Srivastava PM: Global longitudinal strain is a strong independent predictor of all-cause mortality in patients with aortic stenosis. European heart journal cardiovascular Imaging 2012; 13:827-833.

[185] Lang RM, Bierig M, Devereux RB, Flachskampf FA, Foster E, Pellikka PA, Picard MH, Roman MJ, Seward J, Shanewise JS, Solomon SD, Spencer KT, Sutton MS, Stewart WJ, Chamber Quantification Writing G, American Society of Echocardiography's G, Standards C, European Association of E: Recommendations for chamber quantification: a report from the American Society of Echocardiography's Guidelines and Standards Committee and the Chamber Quantification Writing Group, developed in conjunction with the European Association of Echocardiography, a branch of the European Society of Cardiology. Journal of the American Society of Echocardiography : official publication of the American Society of Echocardiography 2005; 18:1440-1463.

[186] Lee YS, Kim KS: Relationship between post-systolic motion during dobutamine stress echocardiography and functional recovery of myocardium after successful percutaneous coronary intervention. Korean circulation journal 2009; 39:477-481.

[187] British Soceity of Echocardiography: Echocardiography: Guidelines for Chamber Quantification. http://wwwbhforguk/plugins/PublicationsSearchResults/DownloadFileaspx?docid=74cb72a2-ea7f-41b2-92e7-f9ca1dfb9712&version=-1&title=Echocardiography+guidelines+for+chamber+quantification&resource=G407 2012.

[188] Nikitin NP, Witte KK, Thackray SD, Goodge LJ, Clark AL, Cleland JG: Effect of age and sex on left atrial morphology and function. European journal of echocardiography : the journal of the Working Group on Echocardiography of the European Society of Cardiology 2003; 4:36-42.

[189] Hung CL, Verma A, Uno H, Shin SH, Bourgoun M, Hassanein AH, McMurray JJ, Velazquez EJ, Kober L, Pfeffer MA, Solomon SD, investigators V: Longitudinal and circumferential strain rate, left ventricular remodeling, and prognosis after myocardial infarction. Journal of the American College of Cardiology 2010; 56:1812-1822.

[190] Manovel A, Dawson D, Smith B, Nihoyannopoulos P: Assessment of left ventricular function by different speckle-tracking software. European journal of echocardiography : the journal of the Working Group on Echocardiography of the European Society of Cardiology 2010; 11:417-421.

[191] Abbas AE, Franey LM, Marwick T, Maeder MT, Kaye DM, Vlahos AP, Serra W, Al-Azizi K, Schiller NB, Lester SJ: Noninvasive assessment of pulmonary vascular resistance by Doppler echocardiography. Journal of the American Society of Echocardiography : official publication of the American Society of Echocardiography 2013; 26:1170-1177.

[192] O'Hara T, Virag L, Varro A, Rudy Y: Simulation of the undiseased human cardiac ventricular action potential: model formulation and experimental validation. PLoS computational biology 2011; 7:e1002061.

[193] Chandler NJ, Greener ID, Tellez JO, Inada S, Musa H, Molenaar P, Difrancesco D, Baruscotti M, Longhi R, Anderson RH, Billeter R, Sharma V, Sigg DC, Boyett MR, Dobrzynski H: Molecular architecture of the human sinus node: insights into the function of the cardiac pacemaker. Circulation 2009; 119:1562-1575.

[194] Bland JM, Altman DG: Statistical methods for assessing agreement between two methods of clinical measurement. Lancet 1986; 1:307-310.

[195] Emery EC, Young GT, Berrocoso EM, Chen L, McNaughton PA: HCN2 ion channels play a central role in inflammatory and neuropathic pain. Science 2011; 333:1462-1466.

[196] Duan DD, Huang ZM: *The Functional Role of Chloride Channels in Cardiac Pacemaker Activity*. Modern Pacemakers-Present and Future.

http://www.intechopen.com/books/modern-pacemakers-present-and-future/the-functional-role-of-chloride-channels-in-cardiac-pacemaker-activity: In Tech, 2011, pp.

[197] Huang ZM, Prasad C, Britton FC, Ye LL, Hatton WJ, Duan D: Functional role of CLC-2 chloride inward rectifier channels in cardiac sinoatrial nodal pacemaker cells. Journal of molecular and cellular cardiology 2009; 47:121-132.

[198] Suzuki M, Mizuno A: A novel human Cl^- channel family related to Drosophila flightless locus. Journal of Biological Chemistry 2004; 279:22461-22468.

[199] Bilguvar K, Tyagi NK, Ozkara C, Tuysuz B, Bakircioglu M, Choi M, Delil S, Caglayan AO, Baranoski JF, Erturk O, Yalcinkaya C, Karacorlu M, Dincer A, Johnson MH, Mane S, Chandra SS, Louvi A, Boggon TJ, Lifton RP, Horwich AL, Gunel M: Recessive loss of function of the neuronal ubiquitin hydrolase UCHL1 leads to early-onset progressive neurodegeneration. Proceedings of the National Academy of Sciences of the United States of America 2013; 110:3489-3494.

[200] Fujisawa G, Okada K, Muto S, Fujita N, Itabashi N, Kusano E, Ishibashi S: Spironolactone prevents early renal injury in streptozotocin-induced diabetic rats. Kidney international 2004; 66:1493-1502.

[201] Kaminski BM, Klingensmith GJ, Beck RW, Tamborlane WV, Lee J, Hassan K, Schatz D, Kollman C, Redondo MJ: Body Mass Index at the Time of Diagnosis of Autoimmune Type 1 Diabetes in Children. The Journal of Pediatrics; 162:736-740.e731.

[202] Chatzigeorgiou A, Halapas A, Kalafatakis K, Kamper E: The Use of Animal Models in the Study of Diabetes Mellitus. In Vivo 2009; 23:245-258.

[203] Shimoni Y, Firek L, Severson D, Giles W: Short-term diabetes alters K+ currents in rat ventricular myocytes. Circulation research 1994; 74:620-628.

[204] Stables CL, Musa H, Mitra A, Bhushal S, Deo M, Guerrero-Serna G, Mironov S, Zarzoso M, Vikstrom KL, Cawthorn W, Pandit SV: Reduced Na(+) current density underlies impaired propagation in the diabetic rabbit ventricle. Journal of molecular and cellular cardiology 2014; 69:24-31.

[205] Wang DW, Viswanathan PC, Balser JR, George AL, Jr., Benson DW: Clinical, genetic, and biophysical characterization of SCN5A mutations associated with atrioventricular conduction block. Circulation 2002; 105:341-346.

[206] Benson DW, Wang DW, Dyment M, Knilans TK, Fish FA, Strieper MJ, Rhodes TH, George AL, Jr.: Congenital sick sinus syndrome caused by recessive mutations in the cardiac sodium channel gene (SCN5A). The Journal of clinical investigation 2003; 112:1019-1028.

[207] Groenewegen WA, Firouzi M, Bezzina CR, Vliex S, van Langen IM, Sandkuijl L, Smits JP, Hulsbeek M, Rook MB, Jongsma HJ, Wilde AA: A cardiac sodium channel mutation cosegregates with a rare connexin40 genotype in familial atrial standstill. Circulation research 2003; 92:14-22.

[208] Echt DS, Berte LE, Clusin WT, Samuelsson RG, Harrison DC, Mason JW: Prolongation of the human cardiac monophasic action potential by sotalol. The American journal of cardiology 1982; 50:1082-1086.

[209] Papadatos GA, Wallerstein PM, Head CE, Ratcliff R, Brady PA, Benndorf K, Saumarez RC, Trezise AE, Huang CL, Vandenberg JI, Colledge WH, Grace AA: Slowed conduction and ventricular tachycardia after targeted disruption of the cardiac sodium channel gene Scn5a. Proceedings of the National Academy of Sciences of the United States of America 2002; 99:6210-6215.

[210] Yan GX, Antzelevitch C: Cellular basis for the Brugada syndrome and other mechanisms of arrhythmogenesis associated with ST-segment elevation. Circulation 1999; 100:1660-1666.

[211] Lu Z, Jiang Y-P, Wu C-YC, Ballou LM, Liu S, Carpenter ES, Rosen MR, Cohen IS, Lin RZ: Increased Persistent Sodium Current Due to Decreased PI3K Signaling Contributes to QT Prolongation in the Diabetic Heart. Diabetes 2013; 62:4257-4265.

[212] Lu Z, Wu CY, Jiang YP, Ballou LM, Clausen C, Cohen IS, Lin RZ: Suppression of phosphoinositide 3-kinase signaling and alteration of multiple ion currents in drug-induced long QT syndrome. Science translational medicine 2012; 4:131ra150.

[213] Tamargo J, Caballero R, Gomez R, Valenzuela C, Delpon E: Pharmacology of cardiac potassium channels. Cardiovascular research 2004; 62:9-33.

[214] Matsubara H, Suzuki J, Inada M: Shaker-related potassium channel, Kv1.4, mRNA regulation in cultured rat heart myocytes and differential expression of Kv1.4 and Kv1.5 genes in myocardial development and hypertrophy. The Journal of clinical investigation 1993; 92:1659-1666.

[215] Nishiyama A, Ishii DN, Backx PH, Pulford BE, Birks BR, Tamkun MM: Altered K(+) channel gene expression in diabetic rat ventricle: isoform switching between Kv4.2 and Kv1.4. American journal of physiology Heart and circulatory physiology 2001; 281:H1800-1807.

[216] Shimoni Y: Inhibition of the formation or action of angiotensin II reverses attenuated K+ currents in type 1 and type 2 diabetes. The Journal of physiology 2001; 537:83-92.

[217] Foeger NC, Wang W, Mellor RL, Nerbonne JM: Stabilization of Kv4 protein by the accessory K(+) channel interacting protein 2 (KChIP2) subunit is required for the generation of native myocardial fast transient outward K(+) currents. The Journal of physiology 2013; 591:4149-4166.

[218] Guo W, Jung WE, Marionneau C, Aimond F, Xu H, Yamada KA, Schwarz TL, Demolombe S, Nerbonne JM: Targeted deletion of Kv4.2 eliminates I(to,f) and results in electrical and molecular remodeling, with no evidence of ventricular hypertrophy or myocardial dysfunction. Circulation research 2005; 97:1342-1350.

[219] Speerschneider T, Grubb S, Metoska A, Olesen SP, Calloe K, Thomsen MB: Development of heart failure is independent of K+ channel-interacting protein 2 expression. The Journal of physiology 2013; 591:5923-5937.

[220] Zhang Y, Han H, Wang J, Wang H, Yang B, Wang Z: Impairment of human ether-a-go-go-related gene (HERG) K+ channel function by hypoglycemia and hyperglycemia. Similar phenotypes but different mechanisms. The Journal of biological chemistry 2003; 278:10417-10426.

[221] Sicouri S, Antzelevitch D, Heilmann C, Antzelevitch C: Effects of sodium channel block with mexiletine to reverse action potential prolongation in in vitro models of the long term QT syndrome. Journal of cardiovascular electrophysiology 1997; 8:1280-1290.

[222] Haraguchi R, Ashihara T, Namba T, Tsumoto K, Murakami S, Kurachi Y, Ikeda T, Nakazawa K: Transmural dispersion of repolarization determines scroll wave behavior during ventricular tachyarrhythmias. Circulation journal : official journal of the Japanese Circulation Society 2011; 75:80-88.

[223] Di Diego JM, Belardinelli L, Antzelevitch C: Cisapride-induced transmural dispersion of repolarization and torsade de pointes in the canine left ventricular wedge preparation during epicardial stimulation. Circulation 2003; 108:1027-1033.

[224] Terrenoire C, Clancy CE, Cormier JW, Sampson KJ, Kass RS: Autonomic control of cardiac action potentials: role of potassium channel kinetics in response to sympathetic stimulation. Circulation research 2005; 96:e25-34.

[225] Overholser BR, Zheng X, Tisdale JE: Paroxysmal beta-adrenergic receptor-mediated alterations in ventricular repolarization at rapid heart rates during inhibition of delayed rectifier currents. J Cardiovasc Pharmacol 2009; 54:253-262.

[226] Yan GX, Wu Y, Liu T, Wang J, Marinchak RA, Kowey PR: Phase 2 early afterdepolarization as a trigger of polymorphic ventricular tachycardia in acquired long-QT syndrome : direct evidence from intracellular recordings in the intact left ventricular wall. Circulation 2001; 103:2851-2856.

[227] Schram G, Pourrier M, Melnyk P, Nattel S: Differential distribution of cardiac ion channel expression as a basis for regional specialization in electrical function. Circulation research 2002; 90:939-950.

[228] Koumi S, Sato R, Nagasawa K, Hayakawa H: Activation of inwardly rectifying potassium channels by muscarinic receptor-linked G protein in isolated human ventricular myocytes. The Journal of membrane biology 1997; 157:71-81.

[229] Baruscotti M, Bottelli G, Milanesi R, DiFrancesco JC, DiFrancesco D: HCN-related channelopathies. Pflugers Archiv : European journal of physiology 2010; 460:405-415.

[230] Powell KL, Jones NC, Kennard JT, Ng C, Urmaliya V, Lau S, Tran A, Zheng T, Ozturk E, Dezsi G, Megatia I, Delbridge LM, Pinault D, Reid CA, White PJ, O'Brien TJ: HCN channelopathy and cardiac electrophysiologic dysfunction in genetic and acquired rat epilepsy models. Epilepsia 2014; 55:609-620.

[231] Cheng YS, Dai DZ, Ji H, Zhang Q, Dai Y: Sildenafil and FDP-Sr attenuate diabetic cardiomyopathy by suppressing abnormal expression of myocardial CASQ2, FKBP12.6, and SERCA2a in rats. Acta pharmacologica Sinica 2011; 32:441-448.

[232] Sulaiman M, Matta MJ, Sunderesan NR, Gupta MP, Periasamy M, Gupta M: Resveratrol, an activator of SIRT1, upregulates sarcoplasmic calcium ATPase and improves cardiac

function in diabetic cardiomyopathy. American journal of physiology Heart and circulatory physiology 2010; 298:H833-843.

[233] Hasenfuss G: Alterations of calcium-regulatory proteins in heart failure. Cardiovascular research 1998; 37:279-289.

[234] Kass RS, Lindegger N, Hagen B, Lederer WJ: Another calcium paradox in heart failure. Journal of molecular and cellular cardiology 2008; 45:28-31.

[235] Sikkel MB, Hayward C, MacLeod KT, Harding SE, Lyon AR: SERCA2a gene therapy in heart failure: an anti-arrhythmic positive inotrope. British journal of pharmacology 2014; 171:38-54.

[236] Lyon AR, Bannister ML, Collins T, Pearce E, Sepehripour AH, Dubb SS, Garcia E, O'Gara P, Liang L, Kohlbrenner E, Hajjar RJ, Peters NS, Poole-Wilson PA, Macleod KT, Harding SE: SERCA2a gene transfer decreases sarcoplasmic reticulum calcium leak and reduces ventricular arrhythmias in a model of chronic heart failure. Circulation Arrhythmia and electrophysiology 2011; 4:362-372.

[237] Jansen JA, van Veen TA, de Bakker JM, van Rijen HV: Cardiac connexins and impulse propagation. Journal of molecular and cellular cardiology 2010; 48:76-82.

[238] Gutstein DE, Morley GE, Tamaddon H, Vaidya D, Schneider MD, Chen J, Chien KR, Stuhlmann H, Fishman GI: Conduction slowing and sudden arrhythmic death in mice with cardiac-restricted inactivation of connexin43. Circulation research 2001; 88:333-339.

[239] Jansen JA, Noorman M, Musa H, Stein M, de Jong S, van der Nagel R, Hund TJ, Mohler PJ, Vos MA, van Veen TA, de Bakker JM, Delmar M, van Rijen HV: Reduced heterogeneous expression of Cx43 results in decreased Nav1.5 expression and reduced sodium current that accounts for arrhythmia vulnerability in conditional Cx43 knockout mice. Heart rhythm : the official journal of the Heart Rhythm Society 2012; 9:600-607.

[240] Adkins GB, Curtis MJ: Potential role of cardiac chloride channels and transporters as novel therapeutic targets. Pharmacology & therapeutics 2014.

[241] Clark S, Jordt SE, Jentsch TJ, Mathie A: Characterization of the hyperpolarization-activated chloride current in dissociated rat sympathetic neurons. The Journal of physiology 1998; 506 (Pt 3):665-678.

[242] Kato K, Chapman DC, Rupp H, Lukas A, Dhalla NS: Alterations of heart function and Na+-K+-ATPase activity by etomoxir in diabetic rats. Journal of applied physiology 1999; 86:812-818.

[243] Schwinger RH, Bundgaard H, Muller-Ehmsen J, Kjeldsen K: The Na, K-ATPase in the failing human heart. Cardiovascular research 2003; 57:913-920.

[244] Bueno-Orovio A, Sanchez C, Pueyo E, Rodriguez B: Na/K pump regulation of cardiac repolarization: insights from a systems biology approach. Pflugers Archiv : European journal of physiology 2014; 466:183-193.

[245] Armoundas AA, Hobai IA, Tomaselli GF, Winslow RL, O'Rourke B: Role of sodium-calcium exchanger in modulating the action potential of ventricular myocytes from normal and failing hearts. Circulation research 2003; 93:46-53.

[246] Zeng S, Jiang T, Zhou QC, Yuan L, Zhou JW, Cao DM: Time-course changes in left ventricular myocardial deformation in STZ-induced rabbits on velocity vector imaging. Cardiovascular ultrasound 2014; 12:17.

[247] van Middendorp LB, Strik M, Houthuizen P, Kuiper M, Maessen JG, Auricchio A, Prinzen FW: Electrophysiological and haemodynamic effects of vernakalant and flecainide in dyssynchronous canine hearts. Europace : European pacing, arrhythmias, and cardiac electrophysiology : journal of the working groups on cardiac pacing, arrhythmias, and cardiac cellular electrophysiology of the European Society of Cardiology 2014; 16:1249-1256.

[248] Dong M, Niklewski PJ, Wang HS: Ionic mechanisms of cellular electrical and mechanical abnormalities in Brugada syndrome. American journal of physiology Heart and circulatory physiology 2011; 300:H279-287.

[249] Goldhaber JI, Philipson KD: Cardiac sodium-calcium exchange and efficient excitation-contraction coupling: implications for heart disease. Advances in experimental medicine and biology 2013; 961:355-364.

[250] Larbig R, Torres N, Bridge JH, Goldhaber JI, Philipson KD: Activation of reverse Na+-Ca2+ exchange by the Na+ current augments the cardiac Ca2+ transient: evidence from NCX knockout mice. The Journal of physiology 2010; 588:3267-3276.

[251] Aliot E, Capucci A, Crijns HJ, Goette A, Tamargo J: Twenty-five years in the making: flecainide is safe and effective for the management of atrial fibrillation. Europace : European pacing, arrhythmias, and cardiac electrophysiology : journal of the working groups on cardiac pacing, arrhythmias, and cardiac cellular electrophysiology of the European Society of Cardiology 2011; 13:161-173.

[252] Kaprielian RR, Gunning M, Dupont E, Sheppard MN, Rothery SM, Underwood R, Pennell DJ, Fox K, Pepper J, Poole-Wilson PA, Severs NJ: Downregulation of immunodetectable connexin43 and decreased gap junction size in the pathogenesis of chronic hibernation in the human left ventricle. Circulation 1998; 97:651-660.

[253] Sun H, Oudit GY, Ramirez RJ, Costantini D, Backx PH: The phosphoinositide 3-kinase inhibitor LY294002 enhances cardiac myocyte contractility via a direct inhibition of Ik,slow currents. Cardiovascular research 2004; 62:509-520.

[254] Abdel-Salam Z, Khalifa M, Ayoub A, Hamdy A, Nammas W: Early changes in longitudinal deformation indices in young asymptomatic patients with type 1 diabetes mellitus: assessment by speckle-tracking echocardiography. Minerva cardioangiologica 2014.

[255] Fazakerley DJ, Lawrence SP, Lizunov VA, Cushman SW, Holman GD: A common trafficking route for GLUT4 in cardiomyocytes in response to insulin, contraction and energy-status signalling. Journal of cell science 2009; 122:727-734.

[256] Guo Z, Xia Z, Yuen VG, McNeill JH: Cardiac expression of adiponectin and its receptors in streptozotocin-induced diabetic rats. Metabolism: clinical and experimental 2007; 56:1363-1371.

[257] Armoni M, Harel C, Bar-Yoseph F, Milo S, Karnieli E: Free fatty acids repress the GLUT4 gene expression in cardiac muscle via novel response elements. The Journal of biological chemistry 2005; 280:34786-34795.

[258] Tian R, Abel ED: Responses of GLUT4-deficient hearts to ischemia underscore the importance of glycolysis. Circulation 2001; 103:2961-2966.

[259] Lo Giudice P, Careddu A, Magni G, Quagliata T, Pacifici L, Carminati P: Autonomic neuropathy in streptozotocin diabetic rats: effect of acetyl-L-carnitine. Diabetes research and clinical practice 2002; 56:173-180.

[260] Kurata C, Okayama K, Wakabayashi Y, Shouda S, Mikami T, Tawarahara K, Sugiyama T: Cardiac sympathetic neuropathy and effects of aldose reductase inhibitor in streptozotocin-induced diabetic rats. Journal of nuclear medicine : official publication, Society of Nuclear Medicine 1997; 38:1677-1680.

[261] Marangoni MN, Brady ST, Chowdhury SA, Piano MR: The co-occurrence of myocardial dysfunction and peripheral insensate neuropathy in a streptozotocin-induced rat model of diabetes. Cardiovascular diabetology 2014; 13:11.

[262] Muhlfeld C, Das SK, Heinzel FR, Schmidt A, Post H, Schauer S, Papadakis T, Kummer W, Hoefler G: Cancer induces cardiomyocyte remodeling and hypoinnervation in the left ventricle of the mouse heart. PloS one 2011; 6:e20424.

[263] van den Brom CE, Bulte CS, Kloeze BM, Loer SA, Boer C, Bouwman RA: High fat diet-induced glucose intolerance impairs myocardial function, but not myocardial perfusion during hyperaemia: a pilot study. Cardiovascular diabetology 2012; 11:74.

[264] Yanni J, Tellez JO, Sutyagin PV, Boyett MR, Dobrzynski H: Structural remodelling of the sinoatrial node in obese old rats. Journal of molecular and cellular cardiology 2010; 48:653-662.

[265] Harris IS, Treskov I, Rowley MW, Heximer S, Kaltenbronn K, Finck BN, Gross RW, Kelly DP, Blumer KJ, Muslin AJ: G-Protein Signaling Participates in the Development of Diabetic Cardiomyopathy. Diabetes 2004; 53:3082-3090.

[266] duBell WH, Boyett MR, Spurgeon HA, Talo A, Stern MD, Lakatta EG: The cytosolic Ca^{2+} transient modulates the action potential of rat ventricular myocytes. Journal of physiology 1991; 436:347-369.

[267] Carella MJ, Mantz SL, Rovner DR, Willis PW, 3rd, Gossain VV, Bouknight RR, Ferenchick GS: Obesity, adiposity, and lengthening of the QT interval: improvement after weight loss. International journal of obesity and related metabolic disorders : journal of the International Association for the Study of Obesity 1996; 20:938-942.

[268] Benitah JP, Alvarez JL, Gomez AM: L-type Ca(2+) current in ventricular cardiomyocytes. Journal of molecular and cellular cardiology 2010; 48:26-36.

[269] Yamada M, Ohta K, Niwa A, Tsujino N, Nakada T, Hirose M: Contribution of L-type $Ca2^{+}$ channels to early afterdepolarizations induced by $I_{K,r}$ and $I_{K,s}$ channel suppression in guinea pig ventricular myocytes. The Journal of membrane biology 2008; 222:151-166.

[270] Berlin JR, Cannell MB, Lederer WJ: Cellular origins of the transient inward current in cardiac myocytes. Role of fluctuations and waves of elevated intracellular Ca^{2+}. Circulation research 1989; 65:115-126.

[271] Yarotskyy V, Gao G, Peterson BZ, Elmslie KS: The Timothy syndrome mutation of cardiac $Ca_v1.2$ (L-type) channels: multiple altered gating mechanisms and pharmacological restoration of inactivation. The Journal of physiology 2009; 587:551-565.

[272] Rau F, Freyermuth F, Fugier C, Villemin JP, Fischer MC, Jost B, Dembele D, Gourdon G, Nicole A, Duboc D, Wahbi K, Day JW, Fujimura H, Takahashi MP, Auboeuf D, Dreumont N, Furling D, Charlet-Berguerand N: Misregulation of miR-1 processing is associated with heart defects in myotonic dystrophy. Nature structural & molecular biology 2011; 18:840-845.

[273] Lin YC, Huang J, Kan H, Castranova V, Frisbee JC, Yu HG: Defective calcium inactivation causes long QT in obese insulin-resistant rat. American journal of physiology Heart and circulatory physiology 2012; 302:H1013-1022.

[274] Huang H, Amin V, Gurin M, Wan E, Thorp E, Homma S, Morrow JP: Diet-induced obesity causes long QT and reduces transcription of voltage-gated potassium channels. Journal of molecular and cellular cardiology 2013; 59:151-158.

[275] Ter Keurs HE, Boyden PA: Calcium and arrhythmogenesis. Physiological reviews 2007; 87:457-506.

[276] Janvier NC, Boyett MR: The role of Na-Ca exchange current in the cardiac action potential. Cardiovascular research 1996; 32:69-84.

[277] Meszaros J, Khananshvili D, Hart G: Mechanisms underlying delayed afterdepolarizations in hypertrophied left ventricular myocytes of rats. American journal of physiology Heart and circulatory physiology 2001; 281:H903-914.

[278] Chorvatova A, Hart G, Hussain M: Na+/Ca2+ exchange current (I(Na/Ca)) and sarcoplasmic reticulum Ca2+ release in catecholamine-induced cardiac hypertrophy. Cardiovascular research 2004; 61:278-287.

[279] Iwamoto T: Na^{2+}-Ca^{2+} exchange inhibitors: therapeutic potential in cardiovascular diseases. Future cardiology 2005; 1:519-529.

[280] Wagner S, Seidler T, Picht E, Maier LS, Kazanski V, Teucher N, Schillinger W, Pieske B, Isenberg G, Hasenfuss G, Kogler H: Na^{+} - Ca^{+} exchanger overexpression predisposes to reactive oxygen species-induced injury. Cardiovascular research 2003; 60:404-412.

[281] Lima-Leopoldo AP, Sugizaki MM, Leopoldo AS, Carvalho RF, Nogueira CR, Nascimento AF, Martinez PF, Luvizotto RA, Padovani CR, Cicogna AC: Obesity induces upregulation of genes involved in myocardial $Ca2^{+}$ handling. Brazilian journal of medical and biological research 2008; 41:615-620.

[282] Yang R, Barouch LA: Leptin signaling and obesity: cardiovascular consequences. Circulation research 2007; 101:545-559.

[283] Sedej S, Heinzel FR, Walther S, Dybkova N, Wakula P, Groborz J, Gronau P, Maier LS, Vos MA, Lai FA, Napolitano C, Priori SG, Kockskamper J, Pieske B: Na^{+} dependent SR Ca^{2+} overload induces arrhythmogenic events in mouse cardiomyocytes with a human CPVT mutation. Cardiovascular research 2010; 87:50-59.

[284] Chen Y, Escoubet B, Prunier F, Amour J, Simonides WS, Vivien B, Lenoir C, Heimburger M, Choqueux C, Gellen B, Riou B, Michel JB, Franz WM, Mercadier JJ: Constitutive cardiac overexpression of sarcoplasmic/endoplasmic reticulum Ca^{2+}-ATPase delays myocardial failure after myocardial infarction in rats at a cost of increased acute arrhythmias. Circulation 2004; 109:1898-1903.

[285] Erkasap N: SERCA in genesis of arrhythmias: what we already know and what is new? The Anatolian journal of cardiology 2007; 7 Suppl 1:43-46.

[286] Thireau J, Pasquie JL, Martel E, Le Guennec JY, Richard S: New drugs vs. old concepts: a fresh look at antiarrhythmics. Pharmacology & therapeutics 2011; 132:125-145.

[287] Donoso P, Prieto H, Hidalgo C: Luminal calcium regulates calcium release in triads isolated from frog and rabbit skeletal muscle. Biophysical journal 1995; 68:507-515.

[288] Herrmann S, Lipp P, Wiesen K, Stieber J, Nguyen H, Kaiser E, Ludwig A: The cardiac sodium-calcium exchanger NCX1 is a key player in the initiation and maintenance of a stable heart rhythm. Cardiovascular research 2013; 99:780-788.

[289] Feldman AM, Weinberg EO, Ray PE, Lorell BH: Selective changes in cardiac gene expression during compensated hypertrophy and the transition to cardiac decompensation in rats with chronic aortic banding. Circulation research 1993; 73:184-192.

[290] Terracciano CM, Philipson KD, MacLeod KT: Overexpression of the Na^+ - Ca^{2+} exchanger and inhibition of the sarcoplasmic reticulum Ca^{2+} -ATPase in ventricular myocytes from transgenic mice. Cardiovascular research 2001; 49:38-47.

[291] Sekar RB, Kizana E, Smith RR, Barth AS, Zhang Y, Marban E, Tung L: Lentiviral vector-mediated expression of GFP or Kir2.1 alters the electrophysiology of neonatal rat ventricular myocytes without inducing cytotoxicity. American Journal of Physiology and Heart Circulatory Physiology 2007; 293:H2757-2770.

[292] Priori SG, Pandit SV, Rivolta I, Berenfeld O, Ronchetti E, Dhamoon A, Napolitano C, Anumonwo J, di Barletta MR, Gudapakkam S, Bosi G, Stramba-Badiale M, Jalife J: A novel form of short QT syndrome (SQT3) is caused by a mutation in the KCNJ2 gene. Circulation research 2005; 96:800-807.

[293] Li J, McLerie M, Lopatin AN: Transgenic upregulation of $I_{K,1}$ in the mouse heart leads to multiple abnormalities of cardiac excitability. American journal of physiology Heart and circulatory physiology 2004; 287:H2790-2802.

[294] Noujaim SF, Pandit SV, Berenfeld O, Vikstrom K, Cerrone M, Mironov S, Zugermayr M, Lopatin AN, Jalife J: Up-regulation of the inward rectifier K+ current (I K1) in the mouse heart accelerates and stabilizes rotors. J Physiol 2007; 578:315-326.

[295] Antzelevitch C, Oliva A: Amplification of spatial dispersion of repolarization underlies sudden cardiac death associated with catecholaminergic polymorphic VT, long QT, short QT and Brugada syndromes. Journal of internal medicine 2006; 259:48-58.

[296] Extramiana F, Antzelevitch C: Amplified transmural dispersion of repolarization as the basis for arrhythmogenesis in a canine ventricular-wedge model of short-QT syndrome. Circulation 2004; 110:3661-3666.

[297] Chan YC, Siu CW, Lau YM, Lau CP, Li RA, Tse HF: Synergistic effects of inward rectifier (I) and pacemaker (I) currents on the induction of bioengineered cardiac automaticity. Journal of cardiovascular electrophysiology 2009; 20:1048-1054.

[298] Seemann G, Sachse FB, Weiss DL, Ptacek LJ, Tristani-Firouzi M: Modeling of IK1 mutations in human left ventricular myocytes and tissue. American journal of physiology Heart and circulatory physiology 2007; 292:H549-559.

[299] Recanatini M, Poluzzi E, Masetti M, Cavalli A, De Ponti F: QT prolongation through hERG K^+ channel blockade: current knowledge and strategies for the early prediction during drug development. Medical Research Reviews 2005; 25:133-166.

[300] Bril A, Gout B, Bonhomme M, Landais L, Faivre JF, Linee P, Poyser RH, Ruffolo RR, Jr.: Combined potassium and calcium channel blocking activities as a basis for antiarrhythmic efficacy with low proarrhythmic risk: experimental profile of BRL-32872. The Journal of pharmacology and experimental therapeutics 1996; 276:637-646.

[301] Levi AJ, Dalton GR, Hancox JC, Mitcheson JS, Issberner JON, Bates JA, Evans SJ, Howarth FC, Hobai IA, Jones JV: Role of Intracellular Sodium Overload in the Genesis of Cardiac Arrhythmias. Journal of cardiovascular electrophysiology 1997; 8:700-721.

[302] Norgaard A, Bagger JP, Bjerregaard P, Baandrup U, Kjeldsen K, Thomsen PE: Relation of left ventricular function and Na,K-pump concentration in suspected idiopathic dilated cardiomyopathy. The American journal of cardiology 1988; 61:1312-1315.

[303] Pavlovic D, Hall AR, Kennington EJ, Aughton K, Boguslavskyi A, Fuller W, Despa S, Bers DM, Shattock MJ: Nitric oxide regulates cardiac intracellular Na(+) and Ca(2)(+) by modulating Na/K ATPase via PKCepsilon and phospholemman-dependent mechanism. Journal of molecular and cellular cardiology 2013; 61:164-171.

[304] Obradovic M, Zafirovic S, Jovanovic A, Milovanovic ES, Mousa SA, Labudovic-Borovic M, Isenovic ER: Effects of 17β-estradiol on cardiac Na+/K+-ATPase in high fat diet fed rats. Molecular and Cellular Endocrinology 2015; 416:46-56.

[305] Baruscotti M, Bucchi A, Viscomi C, Mandelli G, Consalez G, Gnecchi-Rusconi T, Montano N, Casali KR, Micheloni S, Barbuti A, DiFrancesco D: Deep bradycardia and heart block caused by inducible cardiac-specific knockout of the pacemaker channel gene HCN4. Proceedings of the National Academy of Sciences of the United States of America 2011; 108:1705-1710.

[306] Fernandez-Velasco M, Goren N, Benito G, Blanco-Rivero J, Bosca L, Delgado C: Regional distribution of hyperpolarization-activated current (If) and hyperpolarization-

activated cyclic nucleotide-gated channel mRNA expression in ventricular cells from control and hypertrophied rat hearts. Journal of physiology 2003; 553:395-405.

[307] de Simone G, Devereux RB, Roman MJ, Alderman MH, Laragh JH: Relation of obesity and gender to left ventricular hypertrophy in normotensive and hypertensive adults. Hypertension 1994; 23:600-606.

[308] Nof E, Antzelevitch C, Glikson M: The Contribution of HCN4 to normal sinus node function in humans and animal models. Pacing and clinical electrophysiology : PACE 2010; 33:100-106.

[309] Duan DD: The ClC-3 chloride channels in cardiovascular disease. Acta pharmacologica Sinica 2011; 32:675-684.

[310] Zygmunt AC, Gibbons WR: Calcium-activated chloride current in rabbit ventricular myocytes. Circulation research 1991; 68:424-437.

[311] Ren Z, Raucci FJ, Jr., Browe DM, Baumgarten CM: Regulation of swelling-activated Cl(-) current by angiotensin II signalling and NADPH oxidase in rabbit ventricle. Cardiovascular research 2008; 77:73-80.

[312] Baumgarten CM, Clemo HF: Swelling-activated chloride channels in cardiac physiology and pathophysiology. Progress in biophysics and molecular biology 2003; 82:25-42.

[313] Cuspidi C, Rescaldani M, Sala C, Grassi G: Left-ventricular hypertrophy and obesity: a systematic review and meta-analysis of echocardiographic studies. Journal of hypertension 2014; 32:16-25.

[314] Vasan RS: Cardiac function and obesity. Heart 2003; 89:1127-1129.

[315] Pascual M, Pascual DA, Soria F, Vicente T, Hernandez AM, Tebar FJ, Valdes M: Effects of isolated obesity on systolic and diastolic left ventricular function. Heart 2003; 89:1152-1156.

[316] Dong F, Zhang X, Yang X, Esberg LB, Yang H, Zhang Z, Culver B, Ren J: Impaired cardiac contractile function in ventricular myocytes from leptin-deficient ob/ob obese mice. The Journal of endocrinology 2006; 188:25-36.

[317] Hintz KK, Aberle NS, Ren J: Insulin resistance induces hyperleptinemia, cardiac contractile dysfunction but not cardiac leptin resistance in ventricular myocytes.

International journal of obesity and related metabolic disorders : journal of the International Association for the Study of Obesity 2003; 27:1196-1203.

[318] Li SY, Yang X, Ceylan-Isik AF, Du M, Sreejayan N, Ren J: Cardiac contractile dysfunction in Lep/Lep obesity is accompanied by NADPH oxidase activation, oxidative modification of sarco(endo)plasmic reticulum Ca2+-ATPase and myosin heavy chain isozyme switch. Diabetologia 2006; 49:1434-1446.

[319] McCrossan ZA, Billeter R, White E: Transmural changes in size, contractile and electrical properties of SHR left ventricular myocytes during compensated hypertrophy. Cardiovascular research 2004; 63:283-292.

[320] Ware SM, El-Hassan N, Kahler SG, Zhang Q, Ma YW, Miller E, Wong B, Spicer RL, Craigen WJ, Kozel BA, Grange DK, Wong LJ: Infantile cardiomyopathy caused by a mutation in the overlapping region of mitochondrial ATPase 6 and 8 genes. Journal of medical genetics 2009; 46:308-314.

[321] Diodato D, Invernizzi F, Lamantea E, Fagiolari G, Parini R, Menni F, Parenti G, Bollani L, Pasquini E, Donati MA, Cassandrini D, Santorelli FM, Haack TB, Prokisch H, Ghezzi D, Lamperti C, Zeviani M: Common and Novel TMEM70 Mutations in a Cohort of Italian Patients with Mitochondrial Encephalocardiomyopathy. Journal of inherited metabolic disorders reports 2014.

[322] Lin CH, Kurup S, Herrero P, Schechtman KB, Eagon JC, Klein S, Davila-Roman VG, Stein RI, Dorn GW, 2nd, Gropler RJ, Waggoner AD, Peterson LR: Myocardial oxygen consumption change predicts left ventricular relaxation improvement in obese humans after weight loss. Obesity 2011; 19:1804-1812.

[323] Sawyer DB, Colucci WS: Mitochondrial oxidative stress in heart failure: "oxygen wastage" revisited. Circulation research 2000; 86:119-120.

[324] Labbe SM, Noll C, Grenier-Larouche T, Kunach M, Bouffard L, Phoenix S, Guerin B, Baillargeon JP, Langlois MF, Turcotte EE, Carpentier AC: Improved cardiac function and dietary fatty acid metabolism after modest weight loss in subjects with impaired glucose tolerance. American journal of physiology Endocrinology and metabolism 2014; 306:E1388-1396.

[325] Carey DG, Pliego GJ, Raymond RL: Body composition and metabolic changes following bariatric surgery: effects on fat mass, lean mass and basal metabolic rate: six months to one-year follow-up. Obesity surgery 2006; 16:1602-1608.

[326] Willens HJ, Chakko SC, Byers P, Chirinos JA, Labrador E, Castrillon JC, Lowery MH: Effects of weight loss after gastric bypass on right and left ventricular function assessed by tissue Doppler imaging. The American journal of cardiology 2005; 95:1521-1524.

[327] Davy KP, Hall JE: Obesity and hypertension: two epidemics or one? American journal of physiology Regulatory, integrative and comparative physiology 2004; 286:R803-813.

[328] Leimbach WN, Jr., Wallin BG, Victor RG, Aylward PE, Sundlof G, Mark AL: Direct evidence from intraneural recordings for increased central sympathetic outflow in patients with heart failure. Circulation 1986; 73:913-919.

[329] Greenwood JP, Scott EM, Stoker JB, Mary DA: Hypertensive left ventricular hypertrophy: relation to peripheral sympathetic drive. Journal of the American College of Cardiology 2001; 38:1711-1717.

[330] Triposkiadis F, Karayannis G, Giamouzis G, Skoularigis J, Louridas G, Butler J: The sympathetic nervous system in heart failure physiology, pathophysiology, and clinical implications. Journal of the American College of Cardiology 2009; 54:1747-1762.

[331] Lohse MJ, Engelhardt S, Eschenhagen T: What is the role of beta-adrenergic signaling in heart failure? Circulation research 2003; 93:896-906.

[332] Verma S, McNeill JH: Metformin improves cardiac function in isolated streptozotocin-diabetic rat hearts. The American journal of physiology 1994; 266:H714-719.

[333] Oxborough D, Batterham AM, Shave R, Artis N, Birch KM, Whyte G, Ainslie PN, George KP: Interpretation of two-dimensional and tissue Doppler-derived strain (epsilon) and strain rate data: is there a need to normalize for individual variability in left ventricular morphology? European journal of echocardiography : the journal of the Working Group on Echocardiography of the European Society of Cardiology 2009; 10:677-682.

[334] Modesto KM, Cauduro S, Dispenzieri A, Khandheria B, Belohlavek M, Lysyansky P, Friedman Z, Gertz M, Abraham TP: Two-dimensional acoustic pattern derived strain parameters closely correlate with one-dimensional tissue Doppler derived strain

measurements. European journal of echocardiography : the journal of the Working Group on Echocardiography of the European Society of Cardiology 2006; 7:315-321.

[335] Vandenberg JI, Perry MD, Perrin MJ, Mann SA, Ke Y, Hill AP: hERG K(+) channels: structure, function, and clinical significance. Physiological reviews 2012; 92:1393-1478.

[336] Perrin MJ, Subbiah RN, Vandenberg JI, Hill AP: Human ether-a-go-go related gene (hERG) K+ channels: function and dysfunction. Progress in biophysics and molecular biology 2008; 98:137-148.

[337] Viswanathan PC, Rudy Y: Cellular arrhythmogenic effects of congenital and acquired long-QT syndrome in the heterogeneous myocardium. Circulation 2000; 101:1192-1198.

[338] Choi BR, Burton F, Salama G: Cytosolic Ca2+ triggers early afterdepolarizations and Torsade de Pointes in rabbit hearts with type 2 long QT syndrome. The Journal of physiology 2002; 543:615-631.

[339] Gong Q, Zhang L, Vincent GM, Horne BD, Zhou Z: Nonsense mutations in hERG cause a decrease in mutant mRNA transcripts by nonsense-mediated mRNA decay in human long-QT syndrome. Circulation 2007; 116:17-24.

[340] Hu C, Yan C, Lin J, Liu S, Li Y: Down-regulation of the human ether-a-go-go-related gene in rat cardiac hypertrophy. The American journal of the medical sciences 2011; 341:119-125.

[341] Chu W, Li C, Qu X, Zhao D, Wang X, Yu X, Cai F, Liang H, Zhang Y, Zhao X, Li B, Qiao G, Dong D, Lu Y, Du Z, Yang B: Arsenic-induced interstitial myocardial fibrosis reveals a new insight into drug-induced long QT syndrome. Cardiovascular research 2012; 96:90-98.

[342] Piao L, Li J, McLerie M, Lopatin AN: Transgenic upregulation of IK1 in the mouse heart is proarrhythmic. Basic research in cardiology 2007; 102:416-428.

[343] Bingen BO, Neshati Z, Askar SF, Kazbanov IV, Ypey DL, Panfilov AV, Schalij MJ, de Vries AA, Pijnappels DA: Atrium-Specific Kir3.x Determines Inducibility, Dynamics, and Termination of Fibrillation by Regulating Restitution-Driven Alternans. Circulation 2013; 128:2732-2744.

[344] Niwa N, Nerbonne J: *Myocardial K^+ channels: Primary determinants of action potential repolarisation*. In Billman G, ed: Novel Therapeutic Targets for Antiarrhythmic Drugs, 2010, pp.

[345] Yang ZK, Boyett MR, Janvier NC, McMorn SO, Shui Z, Karim F: Regional differences in the negative inotropic effect of acetylcholine within the canine ventricle. The Journal of physiology 1996; 492 (Pt 3):789-806.

[346] Dobrev D, Graf E, Wettwer E, Himmel HM, Hala O, Doerfel C, Christ T, Schuler S, Ravens U: Molecular basis of downregulation of G-protein-coupled inward rectifying K(+) current (I(K,ACh) in chronic human atrial fibrillation: decrease in GIRK4 mRNA correlates with reduced I(K,ACh) and muscarinic receptor-mediated shortening of action potentials. Circulation 2001; 104:2551-2557.

[347] Barth AS, Tomaselli GF: Cardiac metabolism and arrhythmias. Circulation Arrhythmia and electrophysiology 2009; 2:327-335.

[348] Menick DR, Li MS, Chernysh O, Renaud L, Kimbrough D, Kasiganesan H, Mani SK: Transcriptional pathways and potential therapeutic targets in the regulation of Ncx1 expression in cardiac hypertrophy and failure. Advances in experimental medicine and biology 2013; 961:125-135.

[349] Veglio M, Bruno G, Borra M, Macchia G, Bargero G, D'Errico N, Pagano GF, Cavallo-Perin P: Prevalence of increased QT interval duration and dispersion in type 2 diabetic patients and its relationship with coronary heart disease: a population-based cohort. Journal of internal medicine 2002; 251:317-324.

[350] Jermendy G, Koltai M, Pogátsa G: QT interval prolongation in type 2 (non-insulin-dependent) diabetic patients with cardiac autonomic neuropathy. Acta diabet lat 1990; 27:295-301.

[351] Nomura M, Nakaya Y, Saito K, Kishi F, Miyoshi H, Watanabe K, Ito S, Kubo M, Matsuoka S: Time- and frequency-domain analyses of signal-averaged electrocardiograms in patients with diabetes mellitus. Journal of medicine 1994; 25:271-283.

[352] Yang Q, Kiyoshige K, Fujimoto T, Katayama M, Fujino K, Saito K, Nakaya Y, Mori H: Signal-averaging electrocardiogram in patients with diabetes mellitus. Japanese heart journal 1990; 31:25-33.

[353] Sorgato A, Faggiano P, Simoncelli U, Rusconi C: Prevalence of late potentials in adult aortic stenosis. International journal of cardiology 1996; 53:55-59.

[354] Zhang L, Cannell MB, Phillips AR, Cooper GJ, Ward ML: Altered calcium homeostasis does not explain the contractile deficit of diabetic cardiomyopathy. Diabetes 2008; 57:2158-2166.

[355] Lewis ME, Al-Khalidi AH, Bonser RS, Clutton-Brock T, Morton D, Paterson D, Townend JN, Coote JH: Vagus nerve stimulation decreases left ventricular contractility in vivo in the human and pig heart. The Journal of physiology 2001; 534:547-552.

[356] Casadei B: Vagal control of myocardial contractility in humans. Experimental physiology 2001; 86:817-823.

[357] Boyd AC, Richards DA, Marwick T, Thomas L: Atrial strain rate is a sensitive measure of alterations in atrial phasic function in healthy ageing. Heart 2011; 97:1513-1519.

[358] Ntusi NA, Piechnik SK, Francis JM, Ferreira VM, Rai AB, Matthews PM, Robson MD, Moon J, Wordsworth PB, Neubauer S, Karamitsos TD: Subclinical myocardial inflammation and diffuse fibrosis are common in systemic sclerosis--a clinical study using myocardial T1-mapping and extracellular volume quantification. Journal of cardiovascular magnetic resonance : official journal of the Society for Cardiovascular Magnetic Resonance 2014; 16:21.

[359] Ballo P, Cameli M, Mondillo S, Giacomin E, Lisi M, Padeletti M, Bocelli A, Galderisi M: Impact of diabetes and hypertension on left ventricular longitudinal systolic function. Diabetes research and clinical practice 2010; 90:209-215.

[360] Celotto AM, Chiu WK, Van Voorhies W, Palladino MJ: Modes of metabolic compensation during mitochondrial disease using the Drosophila model of ATP6 dysfunction. PloS one 2011; 6:e25823.

[361] Sethumadhavan S, Vasquez-Vivar J, Migrino RQ, Harmann L, Jacob HJ, Lazar J: Mitochondrial DNA variant for complex I reveals a role in diabetic cardiac remodeling. The Journal of biological chemistry 2012; 287:22174-22182.

[362] Guo LJ, Oshida Y, Fuku N, Takeyasu T, Fujita Y, Kurata M, Sato Y, Ito M, Tanaka M: Mitochondrial genome polymorphisms associated with type-2 diabetes or obesity. Mitochondrion 2005; 5:15-33.

[363] Zaragoza MV, Brandon MC, Diegoli M, Arbustini E, Wallace DC: Mitochondrial cardiomyopathies: how to identify candidate pathogenic mutations by mitochondrial DNA

sequencing, MITOMASTER and phylogeny. European journal of human genetics : EJHG 2011; 19:200-207.

[364] Perin PC, Maule S, Quadri R: Sympathetic nervous system, diabetes, and hypertension. Clinical and experimental hypertension 2001; 23:45-55.

[365] Wickenden AD, Kaprielian R, Kassiri Z, Tsoporis JN, Tsushima R, Fishman GI, Backx PH: The role of action potential prolongation and altered intracellular calcium handling in the pathogenesis of heart failure. Cardiovascular research 1998; 37:312-323.

[366] Sah R, Ramirez RJ, Kaprielian R, Backx PH: Alterations in action potential profile enhance excitation-contraction coupling in rat cardiac myocytes. The Journal of physiology 2001; 533:201-214.

[367] Lacombe VA, Viatchenko-Karpinski S, Terentyev D, Sridhar A, Emani S, Bonagura JD, Feldman DS, Gyorke S, Carnes CA: Mechanisms of impaired calcium handling underlying subclinical diastolic dysfunction in diabetes. American journal of physiology Regulatory, integrative and comparative physiology 2007; 293:R1787-1797.

[368] Han JC, Tran K, Nielsen PM, Taberner AJ, Loiselle DS: Streptozotocin-induced diabetes prolongs twitch duration without affecting the energetics of isolated ventricular trabeculae. Cardiovascular diabetology 2014; 13:79.

11. Appendix

11.1. Presentations

Presentations of data from this study are reproduced below. Some of the data presented was provisional and has subsequently been revised for final presentation in this thesis.

1. **British Cardiac Society Annual Meeting 2012, Heart 2013;99: suppl 2 A12 doi:10.1136/heartjnl-2013-304019.232**

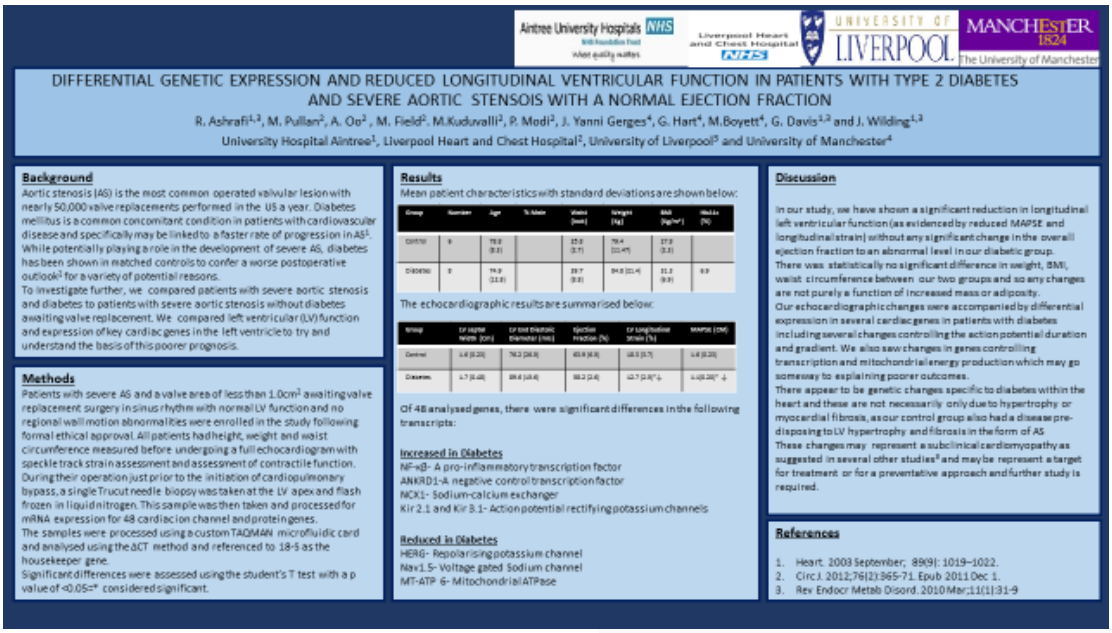

DIFFERENTIAL GENETIC EXPRESSION AND REDUCED LONGITUDINAL VENTRICULAR FUNCTION IN PATIENTS WITH TYPE 2 DIABETES AND SEVERE AORTIC STENSOIS WITH A NORMAL EJECTION FRACTION

R. Ashrafi[1,2], M. Pullan[2], A. Oo[2], M. Field[2], M.Kuduvalli[2], P. Modi[2], J. Yanni Gerges[4], G. Hart[4], M.Boyett[4], G. Davis[1,2] and J. Wilding[1,2]

University Hospital Aintree[1], Liverpool Heart and Chest Hospital[2], University of Liverpool[3] and University of Manchester[4]

Background

Aortic stenosis (AS) is the most common operated valvular lesion with nearly 50,000 valve replacements performed in the US a year. Diabetes mellitus is a common concomitant condition in patients with cardiovascular disease and specifically may be linked to a faster rate of progression in AS[1]. While potentially playing a role in the development of severe AS, diabetes has been shown in matched controls to confer a worse postoperative outlook[2] for a variety of potential reasons.

To investigate further, we compared patients with severe aortic stenosis and diabetes to patients with severe aortic stenosis without diabetes awaiting valve replacement. We compared left ventricular (LV) function and expression of key cardiac genes in the left ventricle to try and understand the basis of this poorer prognosis.

Methods

Patients with severe AS and a valve area of less than 1.0cm² awaiting valve replacement surgery in sinus rhythm with normal LV function and no regional wall motion abnormalities were enrolled in the study following formal ethical approval. All patients had height, weight and waist circumference measured before undergoing a full echocardiogram with speckle track strain assessment and assessment of contractile function. During their operation just prior to the initiation of cardiopulmonary bypass, a single Trucut needle biopsy was taken at the LV apex and flash frozen in liquid nitrogen. This sample was then taken and processed for mRNA expression for 48 cardiac ion channel and protein genes.

The samples were processed using a custom TAQMAN microfluidic card and analysed using the ΔCT method and referenced to 18-S as the housekeeper gene.

Significant differences were assessed using the student's T test with a p value of <0.05=* considered significant.

Results

Mean patient characteristics with standard deviations are shown below:

Group	Number	Age	% Male	Waist (mm)	Weight (kg)	BMI (kg/m²)	HbA1c (%)
CONTROL	9	73.0 (8.2)		97.0 (3.7)	78.4 (11.47)	27.0 (3.3)	
DIABETIC	8	74.0 (11.0)		99.7 (9.0)	84.0 (11.4)	31.2 (4.0)	6.9

The echocardiographic results are summarised below:

Group	LV Septal Width (cm)	LV End Diastolic Diameter (mm)	Ejection Fraction (%)	LV Longitudinal Strain (%)	MAPSE (cm)
Control	1.0 (0.23)	74.0 (10.0)	65.0 (6.0)	18.0 (3.7)	1.0 (0.23)
Diabetic	1.7 (0.48)	69.0 (10.0)	59.2 (5.0)	12.7 (3.0)*↓	0.68 (0.28)* ↓

Of 48 analysed genes, there were significant differences in the following transcripts:

Increased in Diabetes

NF-αβ- A pro-inflammatory transcription factor
ANKRD1-A negative control transcription factor
NCX1- Sodium-calcium exchanger
Kir 2.1 and Kir 3.1- Action potential rectifying potassium channels

Reduced in Diabetes

HERG- Repolarising potassium channel
Nav1.5- Voltage gated Sodium channel
MT-ATP 6- Mitochondrial ATPase

Discussion

In our study, we have shown a significant reduction in longitudinal left ventricular function (as evidenced by reduced MAPSE and longitudinal strain) without any significant change in the overall ejection fraction to an abnormal level in our diabetic group.

There was statistically no significant difference in weight, BMI, waist circumference between our two groups and so any changes are not purely a function of increased mass or adiposity.

Our echocardiographic changes were accompanied by differential expression in several cardiac genes in patients with diabetes including several changes controlling the action potential duration and gradient. We also saw changes in genes controlling transcription and mitochondrial energy production which may go someway to explaining poorer outcomes.

There appear to be genetic changes specific to diabetes within the heart and these are not necessarily only due to hypertrophy or myocardial fibrosis, as our control group also had a disease pre-disposing to LV hypertrophy and fibrosis in the form of AS

These changes may represent a subclinical cardiomyopathy as suggested in several other studies[3] and may be represent a target for treatment or for a preventative approach and further study is required.

References

1. Heart. 2003 September; 89(9): 1019–1022.
2. Circ J. 2012;76(2):365-71. Epub 2011 Dec 1.
3. Rev Endocr Metab Disord. 2010 Mar;11(1):31-9

2. European Congress of Obesity May 2013, **Obes Facts 2013;6(Suppl. 1):49230**

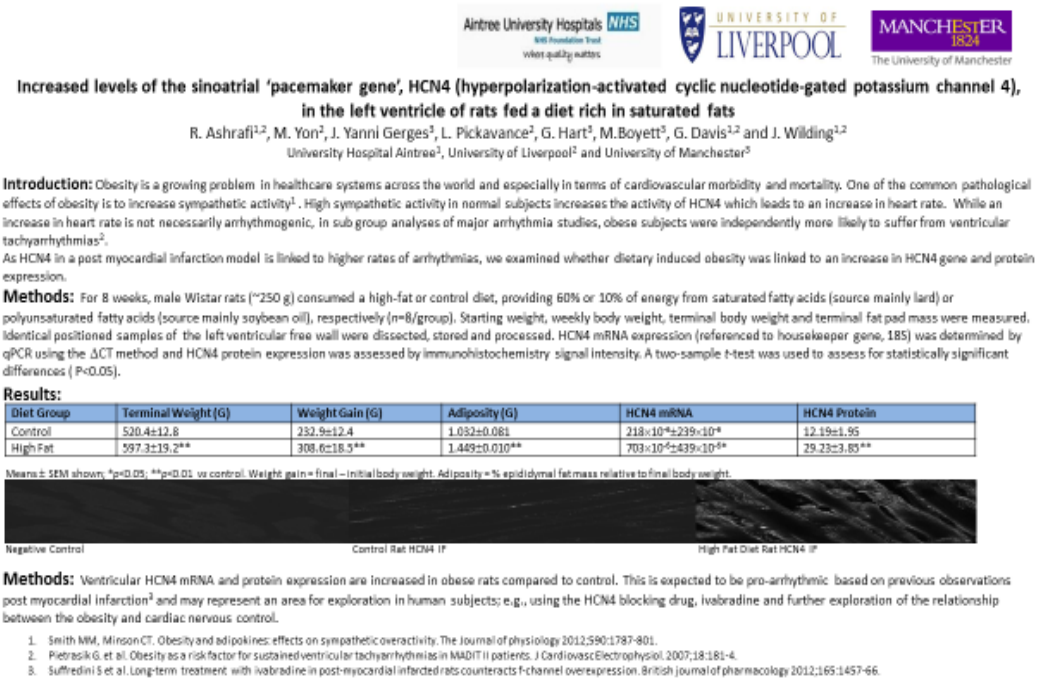

Increased levels of the sinoatrial 'pacemaker gene', HCN4 (hyperpolarization-activated cyclic nucleotide-gated potassium channel 4), in the left ventricle of rats fed a diet rich in saturated fats

R. Ashrafi[1,2], M. Yon[2], J. Yanni Gerges[3], L. Pickavance[2], G. Hart[3], M.Boyett[3], G. Davis[1,2] and J. Wilding[1,2]

University Hospital Aintree[1], University of Liverpool[2] and University of Manchester[3]

Introduction: Obesity is a growing problem in healthcare systems across the world and especially in terms of cardiovascular morbidity and mortality. One of the common pathological effects of obesity is to increase sympathetic activity[1]. High sympathetic activity in normal subjects increases the activity of HCN4 which leads to an increase in heart rate. While an increase in heart rate is not necessarily arrhythmogenic, in sub group analyses of major arrhythmia studies, obese subjects were independently more likely to suffer from ventricular tachyarrhythmias[2].

As HCN4 in a post myocardial infarction model is linked to higher rates of arrhythmias, we examined whether dietary induced obesity was linked to an increase in HCN4 gene and protein expression.

Methods: For 8 weeks, male Wistar rats (~250 g) consumed a high-fat or control diet, providing 60% or 10% of energy from saturated fatty acids (source mainly lard) or polyunsaturated fatty acids (source mainly soybean oil), respectively (n=8/group). Starting weight, weekly body weight, terminal body weight and terminal fat pad mass were measured. Identical positioned samples of the left ventricular free wall were dissected, stored and processed. HCN4 mRNA expression (referenced to housekeeper gene, 18S) was determined by qPCR using the ΔCT method and HCN4 protein expression was assessed by immunohistochemistry signal intensity. A two-sample t-test was used to assess for statistically significant differences (P<0.05).

Results:

Diet Group	Terminal Weight (G)	Weight Gain (G)	Adiposity (G)	HCN4 mRNA	HCN4 Protein
Control	520.4±12.8	232.9±12.4	1.032±0.081	$218\times10^{-6}\pm239\times10^{-6}$	12.19±1.95
High Fat	597.3±19.2**	308.6±18.5**	1.449±0.010**	$703\times10^{-6}\pm439\times10^{-6}$*	29.23±3.85**

Means ± SEM shown; *p<0.05; **p<0.01 vs control. Weight gain = final – initial body weight. Adiposity = % epididymal fat mass relative to final body weight.

Negative Control | Control Rat HCN4 IF | High Fat Diet Rat HCN4 IF

Methods: Ventricular HCN4 mRNA and protein expression are increased in obese rats compared to control. This is expected to be pro-arrhythmic based on previous observations post myocardial infarction[3] and may represent an area for exploration in human subjects; e.g., using the HCN4 blocking drug, ivabradine and further exploration of the relationship between the obesity and cardiac nervous control.

1. Smith MM, Minson CT. Obesity and adipokines: effects on sympathetic overactivity. The Journal of physiology 2012;590:1787-801.
2. Pietrasik G, et al. Obesity as a risk factor for sustained ventricular tachyarrhythmias in MADIT II patients. J CardiovascElectrophysiol. 2007;18:181-4.
3. Suffredini S et al. Long-term treatment with ivabradine in post-myocardial infarcted rats counteracts I-channel overexpression. British journal of pharmacology 2012;165:1457-66.

11.2. Publications

Ashrafi R, Davis G. Cardiomyopathy in diabetics: a review of current opinion on the underlying pathological mechanisms. Advances en Diabetología 2015;31:175-181.